Targeted high-precision radiotherapy
for prostate cancer

Emile van Lin

Targeted high-precision radiotherapy for prostate cancer

Een wetenschappelijke proeve op het gebied van de Medische Wetenschappen

Proefschrift

ter verkrijging van de graad van doctor
aan de Radboud Universiteit Nijmegen
op gezag van de Rector Magnificus prof. dr. C.W.P.M. Blom,
volgens besluit van het College van Decanen
in het openbaar te verdedigen
op woensdag 29 november 2006
om 13.30 uur precies

door
Emmanuel Nicolaas Jozef Theresia van Lin
geboren op 26 December 1963
te Overasselt

Promotor: Prof. dr. J.W.H. Leer
Co-promotor: Dr. A.G. Visser

Manuscriptcommissie:
Prof. dr. J.A. Witjes (voorzitter)
Prof. dr. J.O. Barentsz
Prof. dr. J.J. Battermann (Universiteit Utrecht)
Prof. dr. M. van Herk (Universiteit van Amsterdam)
Dr. J. de Jong

Graphic design: *Communicatie in beeld*, www.communicatieinbeeld.com
met schilderijen van Marian Bax, www.marianbax.nl

Print: Query Exhibition & Conference Services BV, Bloemendaal

Contents

Aan mijn ouders en schoonouders,
dank voor al jullie levenslessen.

1

Introduction and outline

Emile van Lin

INTRODUCTION

Due to the increasing prostate cancer (Pca) awareness and screening on serum prostate-specific antigen (PSA), more than 80 percent of patients with prostate cancer (Pca) present now with clinically localized disease (1). Data, derived from the 2005 Dutch Cancer registration, show 7500 new diagnosed cases of Pca, comprising 20 % of all new male cancer cases. In the Netherlands, one out of 10 men will be confronted with this type of cancer. Patients with localized Pca can choose from a wide range of treatment options; surgery, irradiation (external beam or brachytherapy), hormones or watchful waiting. An excellent review on diagnosis and treatment options for Pca has been published by Peschel *et al.* (2), as part of the "Series on prostate cancer" published in *the Lancet.* Also a full issue of *the Journal of Clinical Oncology* (2005, volume 23, number 23) was dedicated to the management of Pca. Generally spoken, higher dose radiotherapy for intermediate and high risk Pca leads to a longer period of tumor control (3). This is recently confirmed by a large Dutch randomized trail in 664 patients, treated with 68 Gy or 78 Gy (4). But a higher dose also leads to higher late toxicity, mainly rectal bleeding and fecal incontinence, as shown in the same Dutch trial (5). The toxicity rate in radiotherapy is closely related to the irradiated volume of an organ at risk, e.g. the rectal wall, leading to late rectal bleeding (6). So reduction of the irradiated volume, may lead to decreased late toxicity and improved quality of life.

Focusing on external beam radiotherapy for localized Pca, as being the topic of this thesis, technical improvements in radiotherapy treatment preparation and delivery, such as the use of a CT scan in treatment preparation and shielding of normal tissues during treatment (7, 8), patient position verification and correction during daily treatment (9-11), intensity-modulated radiotherapy (IMRT) (12) and incorporation of advanced radiological imaging techniques into the radiotherapy treatment (13, 14) has lead to a more targeted irradiation. In this context, targeted treatment stands for high precision radiotherapy leading to the highest possible tumor control, with lowest as possible radiation-induced toxicity.

In this thesis, the steps are described we took in the past years to improve the Nijmegen radiation treatment for localized Pca. Our first goal was to reduce the irradiated volume of the surrounding normal tissues (e.g. rectum and bladder) by implementing tools for high-precision treatment and to analyze the possible benefits of these additional tools. Next goal was to explore the possibilities of defining a radiotherapy target within the prostatic gland, based on advanced magnetic resonance (MR) techniques, for extra high-dose application locally on tumor-bearing regions. Implementation of IMRT, in which intensity-modulated dose

profiles are applied, rather than flat dose profiles, is opening the possibility of dose painting on a biological target volume, as proposed by Ling *et al.* (15).

OUTLINE

In **chapter 2**, a new method of Pca patient positioning (set-up), at the radiotherapy treatment table, and a patient position verification and correction protocol is described. By reducing the daily position variation during the course of treatment (i.e. 28 - 32 daily treatments on the lineair accelerator), the margin around the prostate, accounting for these variations, could be reduced. As a consequence, the amount of surrounding irradiated tissue could thereby be reduced.

Since 2001, the urologist implants four small gold markers (1 x 7 mm) into the prostate in patients, referred for radiotherapy with curative intent. These markers are well visible on the megavolt images (so-called portal images) that are taken of the pelvic region during the actual radiation treatment. These implanted markers can be used for prostate localization and position verification. In **chapter 3,** the complications and risk factors for toxicity, due to the transrectal gold marker implantation, in 209 consecutive men are presented.

In 2002, we introduced the endorectal balloon (ERB) in clinical practice after promising data, showing benefits in terms of improved prostate immobilization and extra sparing of the rectal wall (Rwall) during radiotherapy (16-18). In **chapter 4**, our first clinical experiences with the ERB are described; patients' tolerance, staff acceptance and workload. The daily prostate position variations, measured on implanted gold markers, were compared in patients treated with and without an ERB, to test its prostate immobilizing capacities.

A full bladder during treatment is recommended, because then a part of the bladder wall will be out of the high dose region and the probability of urinary toxicity will be reduced. A full bladder before daily treatment is also advised, because large variation in bladder filling can cause additional unwanted day-to-day shifts of the prostate, requiring an extra safety margin to be irradiated to account for (19). In **chapter 5**, this issue, using a bladder ultrasound scanner for daily bladder filling checks, is discussed. A biofeedback protocol, aiming at a more constant bladder volume, was developed and tested clinically. Additionally, bladder filling and prostate motion were correlated, using gold marker based portal imaging data.

Gradually, the ERB was introduced into daily practice at our department. So far in literature, three types of ERB were described, having different shapes, volumes and manual handling. In **chapter 6**, a planning study is described, investigating the spatial dose distribution and Rwall sparing effect of these three ERBs for high-dose conformal radiotherapy and IMRT. We have applied more sophisticated graphical displays (20, 21) of the absorbed radiation dose onto the Rwall mucosa, as being one of the most important critical structures in the

development of late rectal toxicity (22). The therapists, being the ones to apply the ERB on a daily basis, evaluated the three ERBs on practical issues. In collaboration with the department of Radiology, a gold-marker based tool was developed to integrate advanced MR imaging techniques (for precise delineation of the prostatic gland and pre-radiotherapy tumor assessment) into our treatment planning procedures (23). Simultaneously, inverse IMRT treatment planning became available for pre-clinical use. In **Chapter 7**, a feasibility planning study is described to incorporate two functional Pca MR imaging techniques into IMRT treatment planning for definition and potential irradiation of a dominant intra-prostatic lesion (DIL). Research work from the Radiology department has shown that is possible to detect this DIL (i.e. the tumor-bearing regions) within the prostatic gland (24, 25). In this planning study, an extra high-dose (a boost) of 90 Gy was applied to the DIL, while the other part of the prostate was planned to receive a moderate dose of 70 Gy. Estimations of the tumor control probability (TCP) and Rwall normal tissue complication probability (NTCP) were calculated to determine the possible gains of this form of targeted biological dose-painting, compared to a more traditional whole prostate irradiation.

One of the a-fore mentioned ERBs has been clinically applied in a cohort of patients and they have been closely followed during and after radiotherapy. Over a period of 3,5 years, 146 rectosigmoidoscopies were performed at the department of Gastroenterology and Hepatology in patients irradiated with and without an ERB. For each patient, the spatial dose distribution over the inner Rwall was calculated and displayed as Rwall surface dose maps. Per patient, multiple endoscopic assessments of the radiation-induced mucosal changes were performed. Acute and late toxicity for both patients groups were scored and compared. The results are described in **chapter 8**

In **chapter 9**, the results and conclusions are summarized. Recommendations and future perspectives on the separate issues, investigated and discussed in this thesis, are given.

REFERENCES

1. Landis SH, Murray T, Bolden S, Wingo PA. Cancer statistics, 1999. CA Cancer J Clin 1999;49:8-31

2. Peschel RE, Colberg JW. Surgery, brachytherapy, and external-beam radiotherapy for early prostate cancer. Lancet Oncol 2003;4:233-41.

3. Pollack A, Zagars GK, Starkschall G, Antolak JA, Lee JJ, Huang E et al. Prostate cancer radiation dose response: results of the M. D. Anderson phase III randomized trial. Int J Radiat Oncol Biol Phys 2002;53:1097-105.

4. Peeters ST, Heemsbergen WD, Koper PC, van Putten WL, Slot A, Dielwart MF et al. Dose-response in radiotherapy for localized prostate cancer: results of the Dutch multicenter randomized phase III trial comparing 68 Gy of radiotherapy with 78 Gy. J Clin Oncol 20061;24:1990-6.

5. Peeters ST, Lebesque JV, Heemsbergen WD, van Putten WL, Slot A, Dielwart MF et al. Localized volume effects for late rectal and anal toxicity after radiotherapy for prostate cancer. Int J Radiat Oncol Biol Phys 2006 ;64:1151-61.

6. Huang EH, Pollack A, Levy L, Starkschall G, Dong L, Rosen I et al. Late rectal toxicity: dose-volume effects of conformal radiotherapy for prostate cancer. Int J Radiat Oncol Biol Phys 2002;54:1314-21.

7. Koper PC, Stroom JC, van Putten WL, Korevaar GA, Heijmen BJ, Wijnmaalen A et al. Acute morbidity reduction using 3DCRT for prostate carcinoma: a randomized study. Int J Radiat Oncol Biol Phys 1999;43:727-34.

8. Koper PC, Jansen P, van PW, van OM, Wijnmaalen AJ, Lebesque JV et al. Gastro-intestinal and genito-urinary morbidity after 3D conformal radiotherapy of prostate cancer: observations of a randomized trial. Radiother Oncol 2004;73:1-9.

9. Bijhold J, Lebesque JV, Hart AA, Vijlbrief RE. Maximizing setup accuracy using portal images as applied to a conformal boost technique for prostatic cancer. Radiother Oncol 1992;24:261-71.

10. de Boer HC, Heijmen BJ. A protocol for the reduction of systematic patient setup errors with minimal portal imaging workload. Int J Radiat Oncol Biol Phys 2001;50:1350-65.

11. Nederveen AJ, Dehnad H, van der Heide UA, van Moorselaar RJ, Hofman P, Lagendijk JJ. Comparison of megavoltage position verification for prostate irradiation based on bony anatomy and implanted fiducials. Radiother Oncol 2003;68:81-8.

12. Zelefsky MJ, Fuks Z, Hunt M, Yamada Y, Marion C, Ling CC et al. High-dose intensity modulated radiation therapy for prostate cancer: early toxicity and biochemical outcome in 772 patients. Int J Radiat Oncol Biol Phys 2002;53:1111-6.

13. Futterer JJ, Heijmink SW, Scheenen TW, Jager GJ, Hulsbergen-Van de Kaa CA, Witjes JA et al. Prostate cancer: local staging at 3-T endorectal MR imaging--early experience. Radiology 2006;238:184-91.

14. Rasch C, Barillot I, Remeijer P, Touw A, Van Herk M, Lebesque JV. Definition of the prostate in CT and MRI: a multi-observer study. Int J Radiat Oncol Biol Phys 1999;43:57-66.

15. Ling CC, Humm J, Larson S, Amols H, Fuks Z, Leibel S et al. Towards multidimensional radiotherapy (MD-CRT): biological imaging and biological conformality. Int J Radiat Oncol Biol Phys 2000;47:551-60.

16. D'Amico AV, Manola J, Loffredo M, Lopes L, Nissen K, O'Farrell DA et al. A practical method to achieve prostate gland immobilization and target verification for daily treatment. Int J Radiat Oncol Biol Phys 2001;51:1431-6.

17. Teh BS, Mai WY, Uhl BM, Augspurger ME, Grant WH3, Lu HH et al. Intensity-modulated radiation therapy (IMRT) for prostate cancer with the use of a rectal balloon for prostate immobilization: acute toxicity and dose-volume analysis. Int J Radiat Oncol Biol Phys 2001;49:705-12.

18. Wachter S, Gerstner N, Dorner D, Goldner G, Colotto A, Wambersie A et al. The influence of a rectal balloon tube as internal immobilization device on variations of volumes and dose-volume histograms during treatment course of conformal radiotherapy for prostate cancer. Int J Radiat Oncol Biol Phys 2002;52:91-100.

19. Lebesque JV, Bruce AM, Kroes AP, Touw A, Shouman RT, Van Herk M. Variation in volumes, dose-volume histograms, and estimated normal tissue complication probabilities of rectum and bladder during conformal radiotherapy of T3 prostate cancer. Int J Radiat Oncol Biol Phys 1995;33:1109-19.

20. Lu Y, Song PY, Li SD, Spelbring DR, Vijayakumar S, Haraf DJ et al. A method of analyzing rectal surface area irradiated and rectal complications in prostate conformal radiotherapy. Int J Radiat Oncol Biol Phys 1995;33:1121-5.

21. Tucker SL, Dong L, Cheung R, Johnson J, Mohan R, Huang EH et al. Comparison of rectal dose-wall histogram versus dose-volume histogram for modeling the incidence of late rectal bleeding after radiotherapy. Int J Radiat Oncol Biol Phys 2004;60:1589-601.

22. O'Brien PC. Radiation injury of the rectum. Radiother Oncol 2001;60:1-14.

23. Huisman HJ, Futterer JJ, van Lin EN, Welmers A, Scheenen TW, van Dalen JA et al. Prostate cancer: precision of integrating functional MR imaging with radiation therapy treatment by using fiducial gold markers. Radiology 2005;236:311-7.

24. Futterer JJ, Engelbrecht MR, Huisman HJ, Jager GJ, Hulsbergen-Van de Kaa CA, Witjes JA et al. Staging prostate cancer with dynamic contrast-enhanced endorectal MR imaging prior to radical prostatectomy: experienced versus less experienced readers. Radiology 2005;237:541-9.

25. van Dorsten FA, van der GM, Engelbrecht MR, van Leenders GJ, Verhofstad A, Rijpkema M et al. Combined quantitative dynamic contrast-enhanced MR imaging and (1)H MR spectroscopic imaging of human prostate cancer. J Magn Reson Imaging 2004;20:279-87.

2

Effectiveness of couch height-based patient set-up and an off-line correction protocol in prostate cancer radiotherapy

Emile N.J.Th. van Lin M.D., Edwin Nijenhuis M.Sc., Henk Huizenga Ph.D., Lisette van der Vight B.Sc., and Andries G. Visser Ph.D.

Department of Radiation Oncology

ABSTRACT

Purpose: To investigate set-up improvement caused by applying a couch height-based patient set-up method in combination with a technologist-driven off-line correction protocol in non-immobilized radiotherapy of prostate patients.

Methods and Materials: A three-dimensional shrinking action level correction protocol is applied in two consecutive patient cohorts with different set-up methods: the traditional "laser set-up" group (n = 43) and the "couch height set-up" group (n = 112). For all directions, left-right, ventro-dorsal and cranio-caudal, random and systematic set-up deviations were measured.

Results: The couch height set-up method improves the patient positioning compared to the laser set-up method. Without application of the correction protocol, both systematic and random errors reduced to 2.2 - 2.4 mm (1 SD) and 1.7 - 2.2 mm (1 SD), respectively. By using the correction protocol, systematic errors reduced further to 1.3 - 1.6 mm (1 SD). One-dimensional deviations were within 5 mm for > 90 % of the measured fractions. The required number of corrections per patient in the off-line correction protocol was reduced significantly during the course of treatment from 1.1 to 0.6 by the couch height set-up method. The treatment time was not prolonged by application of the correction protocol.

Conclusions: The couch height set-up method improves the set-up significantly, especially in the ventro-dorsal direction. Combination of this set-up method with an off-line correction strategy, executed by technologists, reduces the number of set-up corrections required.

INTRODUCTION

Daily accurate patient positioning is one of the prerequisites of radiation oncology. According to ICRU-50/62, the planning target volume (PTV) has to account for internal organ motion and treatment set-up uncertainties in order to ensure adequate coverage of the clinical target volume (CTV). It appeared that patient set-up variations are of the same order (2 - 4 mm (1 SD)) as variations due to internal organ motion (1-3). So, improvement of set-up in prostate radiotherapy could result in reduction of the CTV-PTV margin. Margin reduction is especially important in the ventro-dorsal (VD) direction, where a reduction of the possible overlap of PTV and rectum will result in reduction of the irradiated rectum volume and decreased toxicity.

Set-up errors consist of a systematic component, i.e., the same deviation in the same direction for each fraction throughout the whole treatment course, as well as a random component, i.e., varying from day to day (4). Earlier studies on the set-up accuracy in pelvic irradiation have shown substantial systematic and random deviations (5, 6). Several methods to improve patient set-up have been investigated. Studies using different types of patient immobilization showed controversial results (7-16). With different correction protocols using digital portal images it is possible to reduce set-up errors (17-22). It is well known but hardly reported in literature that standardized patient set-up methods improve patient set-up, for example using the treatment couch height independent from the lateral laser skin mark alignment (23, 24). Patient set-up deviations are dependent on set-up and immobilization procedures specific for each radiation department. Therefore, set-up errors reported by other institutes are an indication but cannot be easily translated into daily practice for one's own patients. It is, therefore, advisable to obtain set-up deviations by repeated portal imaging in each institute (4, 25, 26). The actual accuracy can be compared with the literature and one can decide whether or not to try to improve patient positioning and how. In our institute, after installation of an electronic portal imaging device (EPID), an off-line set-up correction protocol was implemented for prostate irradiation. After installation of carbon-fibre inserts in the treatment couch top, it became possible to standardize our patient set-up by using a "couch height set-up" method for the ventro-dorsal direction. In this method, the (digital) couch height during simulation is applied during the actual treatment (see below).

In the present study, first the extent of the set-up improvement, obtained from applying an off-line correction protocol, has been investigated in a first cohort of prostate patients. In a second cohort, the set-up improvement has been investigated for the "couch height set-up" method in combination with the correction protocol. The magnitude of set-up improvements due to both the off-line correction protocol and the "couch height set-up" method has been investigated. This will enable us to calculate the size of set-up improvement by using the "couch height set-up" method only, e.g. for use at accelerators not yet equipped with an EPID. In this study the additional workload of the used methods is documented as well.

METHODS AND MATERIALS

Patient group and treatment technique

From 1997 to June 2000 155 patients were irradiated for localized prostate cancer and included in this study. After simulation and CT-scanning in treatment position, a beam's-eye-view based conformal treatment plan was performed with individual shielding of normal tissues (Cadplan treatment planning system, Varian). CTV included prostate only or prostate and seminal vesicles. PTV was defined by automatic 10-12 mm 3D expansion of the CTV at the physician's preference (27). An orthogonal four-field isocentric technique was used. If necessary, asymmetric fields were used around the isocenter, marked on the skin during simulation. Doses varied from 63 to 67.5 Gray in 7 to 7.5 weeks, depending on tumor-stage (fractionation four times a week using 2.25 Gray fractions). The investigated patient group was divided in two consecutive cohorts: in cohort 1 patient set-up was performed by laser alignment and controlled with an off-line correction protocol *(n = 43, "laser set-up" group),* in cohort 2 patient set-up was performed with the "couch height set-up" method described below and also controlled with an off-line correction protocol. *(n = 112, "couch height set-up" group).*

Patient immobilization and set-up

During simulation, CT-scanning and the actual treatment, all patients (cohort 1 and 2) were positioned supine on a flat couch that was solely covered with a thin disposable paper sheet. Only a pillow and a foam knee support (Kneefix ™ cushion, Sinmed) were used for relaxed positioning of the head and legs (15). No formal patient immobilization such as a cast or a positioning device was applied (Fig. 1). The patient's skin was marked at the simulator with reference lines, using wall mounted lasers to indicate a tentative center: lateral vertical laser lines to prevent torsion of the patient and rotation of the pelvis, a sagital midline laser line to prevent torsion and to ensure a correct midline position of the patient, and lateral horizontal lines.
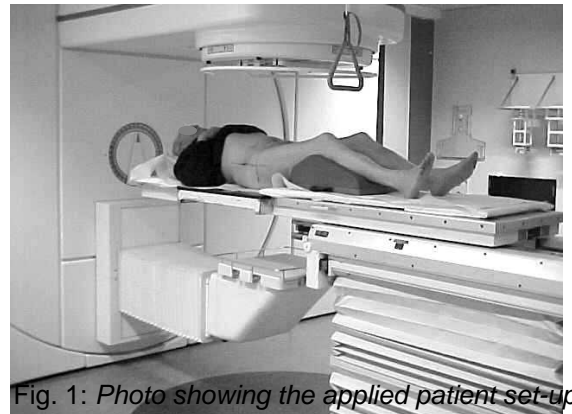
Fig. 1: *Photo showing the applied patient set-up*

At the CT, following simulation, and in the treatment room, the same system of wall mounted alignment lasers was used to match the lines on the patient. No new isocenter was marked on the skin after planning: if necessary, slightly asymmetric fields were used. The patient's skin was marked at the simulator with reference lines, using wall mounted lasers to indicate a tentative center: lateral vertical laser lines to prevent torsion of the patient and rotation of the pelvis, a sagital midline laser line to prevent torsion and to ensure a correct midline position of the patient, and lateral horizontal lines. At the CT, following simulation, and in the treatment room, the same system of wall mounted alignment lasers was used to match the lines on the patient. No new isocenter was marked on the skin after planning: if necessary, slightly asymmetric fields were used.

"Couch height set-up" method

In our institute, before 1997, patients were treated on couch with flexible (mylar) membrane inserts. The sagging of this membrane was 5 – 7 mm in the center depending on patient's weight, leading to a systematic set-up error in the ventro-dorsal direction compared to the simulator couch with

15

a solid wooden top. Since 1997, our accelerator couches (ABB, GE) and CT couch are equipped with carbon-fibre inserts. Measurements showed equal sagging of simulator, treatment and CT couch under a patient's weight (< 2 mm). The accuracy of the (digital) couch-height read-out for all couches was within ± 1 mm. It was, therefore, possible to use the (digital read-out of the) couch height obtained during simulation for more accurate set-up in the ventro-dorsal direction during the actual treatment. In cohort 2, the patients were set up during treatment by alignment of ink skin marks and lasers in the three main directions. In contrast to the laser set-up method (cohort 1), the lateral marks are *only* used to prevent rotation around the longitudinal axis. When this alignment is done, the digital couch-height is noted (for study reasons). Next, the couch is set at the height defined during simulation. The feasibility of this method was tested earlier in a pilot study with 18 patients for whom the set-up was checked by frequent portal imaging (three times a week during the whole treatment). In this pilot study no large set-up errors in the ventro-dorsal direction were seen (data not shown), which led to the set-up of the patients of cohort 2 as described above, referred to as "couch height set-up" method.

Portal image acquisition

Since 1996, a camera-based EPID (Theraview version 1.08) was used at our GE Saturne 42 accelerator. Specific software was developed in-house to draw anatomy templates. Additional software to perform the registration of treatment and reference images was obtained from the B. Verbeeten Institute in Tilburg, The Netherlands (P.H. Vos). A working group, consisting of a radiation technologist, a radiation oncologist and a physicist has been responsible for the introduction of electronic portal imaging. From the beginning, the whole procedure of preparation, image acquisition, analysis and set-up correction was considered as the task of eight radiation technologists (25 % of total technologist group), participating in this study and especially trained for this task. The physicist and/or radiation oncologist were consulted if special problems arose. The simulator film was used as the reference image. After digitizing the reference simulator film, the field shape and an anatomy template consisting of contours of relevant bony structures were drawn. During the actual treatment, portal images were automatically acquired using 2 - 5 monitor units. For analysis the anterior - posterior (AP) and left-lateral (LL) fields were used.

Registration procedure

Measurement of set-up deviations was performed in two steps. First, the imaging system checks automatically the field shape i.e. the position of the field edges, and gives the message 'field shape correct' if reference and portal image completely match. Secondly, the anatomy template is displayed on the screen overlaying the portal image. This template is then manually aligned to the anatomic structures on the portal image using a mouse to obtain the best fit. Image quality of the portal images could be improved by the imaging system. In the registration of the images only translations were considered. Once adequately aligned, the vector coordinates (X, Y and Z) of the measured deviations are displayed on the screen and entered into a spreadsheet. In this study, the X-axis corresponds to the left-right direction, Y-axis to the cranio-caudal direction and Z-axis to the ventro-dorsal direction. All set-up measurements were performed by two trained radiation technologists independently. The results were compared and the average of the two separate deviations was noted. If an inter-observer difference occurred larger than 3 mm for the left-right and cranio-caudal deviation in the AP field, or in the ventro-dorsal deviation in the lateral field or if an inter-observer difference occurred larger than 5 mm for cranio-caudal direction in the lateral field, the

measurements were repeated. Due to overlying bony structures, the matching was more difficult for the lateral images. If the inter-observer differences exceeded these levels in the second round, the two technologists tried to reach consensus by checking each others matching procedures. If no consensus could be achieved, the first two measurements were averaged. Eight percent of all the measurements was repeated by the two observers. The accuracy of this procedure was tested earlier in a pilot study with 100 AP and lateral prostate images of 10 patients. The inter-observer variability for the AP field was slightly smaller than for the lateral field. The registration of the left-lateral field is more difficult than for the AP field due to overlying bony structures (hips, pelvic bones). However, it turned out that all the portal images could be registered and that, due to the procedure followed, the registration procedure *(after consensus)* was adequate within ≈1 mm. The deviation in the X was inferred from the AP field and in the Z from the left lateral field. The set-up deviation in the Y direction was calculated from portal images of the AP and left lateral field, applying a higher weight to the measurement from the AP image, i.e.: $<Y> = [(2*Y\ ap + Y\ left\text{-}lat.\ )/3]$.

Off-line correction protocol

For all patients an off-line verification and correction protocol was used, as described by Bel et al (28), i.e. image analysis and measurement of set-up deviations were performed later on the same day as the treatment to have the results ready prior to the next treatment fraction. The 3D verification procedure uses a shrinking action level protocol [($\alpha/\sqrt{N}$, with α the initial action level (9 mm) and N the number of measurements] and a fixed number of initial measurements (N_{max} = 3). Patient set-up correction is applied only when the vector length of the 3D set-up deviation, averaged over previous fractions, exceeds an action level.

 The protocol consists of two stages.

In the first stage, action levels of size $\alpha/\sqrt{N}$, approximated as 9, 7 and 5 mm, were chosen for the first three initial measurements. Values of α and N_{max} followed from an optimization, using a Monte-Carlo simulation program, aiming to reduce the mean 3D-set-up deviation of each individual patient to within 5 mm at an acceptable workload, i.e. an acceptable number of measurements and set-up corrections (28). If the 3D vector length, averaged over previous measurements, was larger than the action level for that day, a set-up correction was performed, i.e. the patient was repositioned by moving the isocenter over the deviations found in the three directions. If set-up correction was carried out no new lines were drawn on the patient's skin. Correction data were entered in the record and verify system of the accelerator to set a new isocenter. The patient was set-up according to the original lines drawn during simulation and subsequently the couch was shifted according to the magnitude of the correction required. When a component of the required correction was smaller than 2 millimeters, the correction was not applied in that direction. Should set-up correction be mandatory after the first measured fraction (N=1), the applied correction was 2/3 of the 3D vector length to prevent a possible overshoot in the first stage of the verification procedure. After each correction, the calculation of the average 3D-vector was restarted and three measurements, with the corresponding actions levels of 9, 7 and 5 mm (3D-vector), had to be performed again to complete the first stage. The first stage of this protocol was complete when at least 3 (=N_{max}) measurements were done and when the average 3D set-up deviation was below the lowest action level (5 mm).

17

In the next stage, patient positioning was checked by weekly taken digital portal images to deal with set-up deviations that may arise during the course of the treatment, due to possible time-trends (28). The average 3D displacement over the last three measurements was compared with the lowest action level, 5 mm. If the 3D-vector length exceeded this level, the set-up was corrected and the first stage of the verification procedure was restarted, with three set-up measurements and the initial action levels of 9, 7 and 5 mm.

Patient set-up analysis

For all patients, both systematic and random deviations have been studied for the three directions separately. The random variation (denoted as σ) characterizing a patient group is then defined as the SD of the day-to-day set-up positions, averaged over all patients in the group. The systematic variation (denoted as Σ) is defined as the standard deviation of the distribution of average set-up deviations per patient in the group of patients. The overall mean deviation M is the average value over all fractions and all patients. A non-zero M indicates an overall systematic deviation, e.g. a difference in sag or read-out of the couch (4, 17, 29). The overall set-up variation σ_t represents the combination of systematic and random variations for the whole group of patients, given by $\sigma_t = \sqrt{(\sigma^2 + \Sigma^2)}$. The deviations in the three directions for a specific fraction are quadratically combined in one 3D-vector, indicating the 3D set-up deviation. This 3D-vector is used in the off-line correction protocol described above.

In the analysis afterwards, for each individual patient and for the whole group of patients, the random, systematic and overall set-up deviations were calculated. Retrospectively, it was possible to calculate the deviations also as if patients had been irradiated without application of the correction procedure. Furthermore, both the group of *mean* 3D set-up deviations (all patients, one value per patient) has been analyzed as well as the group of *all* 3D set-up deviations (all patients, all measured fractions). It is clear that the first group is more relevant as representing the average displacement during the course of the treatment, and is generally analyzed in literature (17, 18). The latter group represents also the day-to-day variations. In both groups, the fraction of treatments with 3D set-up deviations larger than 5 and 10 mm has been determined.

Workload registration

The workload is obviously very much dependent on organization. The multi-disciplinary approach in our institute facilitated smooth introduction of the involved procedures. Special attention was given to teach the technologists the principles of portal imaging, the definition of set-up deviations, methods of correction and achieved set-up improvements. Before actually performing imaging or image analysis, a technologist was trained by a more experienced colleague. Sets of previously analyzed images were used as training and for two weeks all new measurements done by the trainee were supervised and checked. For all patients, an estimation of additional workload for the radiation technologists was made. Per patient, the extra needed time (for image acquisition and for correction) on the accelerator and time for analysis and administration was noted. For both cohorts of patients, the set-up improvement and the number of corrections needed were registered separately and compared.

RESULTS

In 155 patients, a total of 1562 fractions were analyzed with 6248 measurements in 3124 portal images. An overview of the data obtained is given in table I. The first and third columns show the data related to the "laser set-up" group and "couch height set-up" group respectively, corrected as if no off-line correction protocol was applied. The second and fourth columns show the actual data of those groups.

Systematic variations

In the "laser set-up" group, the off-line correction protocol gave a marked reduction of the systematic set-up variation (Σ) from 2.8 - 4.1 mm down to 1.3 - 1.7 mm (1 SD). The largest improvement is in the ventro-dorsal direction: a reduction of the systematic variation from 4.1 to 1.6 mm. The systematic variations in the "couch height" set-up group (calculated as if no correction protocol was applied) were 2.2 - 2.4 mm (1 SD) compared to 2.8 - 4.1 mm in the "laser set-up" group. Application of the correction protocol in the "couch set-up" group, the actual situation, resulted in further reduction of the systematic variation (table I) down to 1.3 - 1.6 mm (1 SD). The results for the systematic deviations with the correction protocol applied are, thus, similar for both cohorts.

Random variations

Obviously, random set-up variation does not change by application of the off line correction protocol. In the "laser set-up" group, a random variation (σ) of 2 - 2.6 mm (1 SD) was found. In the "couch height set-up" group, the random variations were smaller, i.e. 1.9 - 2.2 mm (1 SD). This indicates that having the couch height closer to the required position during patient set-up, also slightly reduces random set-up deviations.

	Patient cohort 1 "Laser set-up"		Patient cohort 2 "Digital couch height set-up"	
	Without correction	Actual, with correction	Without correction	Actual, with correction
Number of patients	43	43	112	112
Number of measured fractions	439	439	1123	1123
Systematic and random variations				
Σ – systematic variation				
Left-right (mm)	3.3	1.7	2.4	1.6
Cranio-caud (mm)	2.8	1.3	2.3	1.3
Ventro-dors (mm)	4.1	1.6	2.2	1.4
σ – random variation				
Left-right (mm)	2.5	2.5	2.2	2.2
Cranio-caudal (mm)	2.0	2.0	1.7	1.7
Ventro-dorsal (mm)	2.6	2.6	1.9	1.9
σ_t - overall set-up variation				
Left-right (mm)	4.0	3.1	3.4	2.9
Cranio-caudal (mm)	3.4	2.5	3.0	2.2
Ventro-dorsal (mm)	5.0	3.6	3.0	2.5
Mean				
Left-right [mm]	-0.5	-0.4	0.1	0.1
Cranio-caudal [mm]	0.5	0.6	1.3	0.9
Ventro-dorsal [mm]	-1.0	-0.2	0.4	0.2
Off-line correction protocol				
Number of corrections per patient				
Total number (all 3 directions)		1.1		0.6
in left-right direction		0.7		0.4
in cranio-caudal direction		0.6		0.4
in ventro-dorsal direction		0.8		0.4
3D set-up deviations in the group of all fractions. all patients				
$\geq$ 5 mm [%]	42	23	28	12
$\geq$ 10 mm [%]	4	1	0.4	0.1
Mean 3D set-up deviations in the group of all patients				
$\geq$ 5 mm [%]	51	0.0	21	0.0

Table 1: for legends, see next page

Table 1:
Data of both patient cohorts with patient set-up traditionally with the "laser set-up" method and the "couch height set-up" method respectively (see text). In both patient cohorts the set-up variations are given both for the actual treatment and calculated as if no off-line correction protocol has been applied. For the presented quantities see text.

Mean systematic deviation

According to statistics, the mean systematic deviation M averaged over all patients should be of the order of $\Sigma/\sqrt{N_p}$, with N_p the number of patients considered, i.e. of the order of 0.3 - 0.5 mm for all groups considered. This turned out to be true, except for the cranial-caudal direction in the "couch height" set-up group where an unexplained overall systematic deviation of $\approx$ 1 mm was found.

3D set-up deviations

In figure 2, the mean 3D set-up deviations are shown in a cumulative frequency distribution for both cohorts, actual and calculated as if no correction protocol was applied.

Figure 2: *Cumulative frequency distributions of mean 3D set-up deviations for the "laser set-up" group without correction protocol (thin dashed line) and with correction protocol (thick dashed line). and for the "couch height set-up" group without (thin solid line) and with correction protocol (thick solid line) . Vertical axis: percentage of 3D set-up deviations$\geq$ a specific value. Horizontal axis: mean deviations in mm*

Note that figure 2 applies to the group of _mean_ 3D set-up deviations of _each_ patient. In figure 2 is shown that in the "laser set-up" group, without application of the correction protocol, 51% of the patients had a mean 3D set-up deviation of 5 mm or more and 12% even more than 9 mm. In the "laser set-up" group, the percentage of the mean 3D set-up deviation $\geq$ 5 mm was reduced from 51% to zero by using the off-line correction protocol. The use of the "couch height set-up" method alone, without off-line correction protocol, showed remarkably good results: only 21% of the patients has a mean 3D set-up deviation $\geq$ 5 mm, compared to 50% with the "laser set-up" method. Use of the "couch height set-up" method with correction protocol yields slightly better results as use of the "laser set-up" method with the off-line correction protocol: no patients featured a mean 3D set-up deviation larger than or equal to 4 mm.

Instead of the mean 3D set-up deviation per patient, one might consider the group of _all_ 3D set-up deviations (all patients, all fractions), in order to know how often in daily practice deviations occur. As shown in table I, the frequency of the 3D set-up deviations $\geq$ 5 mm and $\geq$10 mm in the "laser set-up" group was reduced from 42% to 23% and from 4% to 1% respectively. In the "couch height set-up" group, the frequency of the 3D set-up deviations $\geq$5 mm is 28 % and is even reduced to 12% with the correction protocol.

Off-line correction protocol characteristics

As shown in Table I, the number of measured fractions in both cohorts was on average 10 per patient, a direct consequence of the chosen values for the parameters in the off-line correction protocol. The number of corrections is significantly lower in the "couch height set-up" group than in the "laser set-up" group: the number of corrections per patient was (on average) 1.1 and 0.6 respectively. The improvement is, as expected, most significant in the ventro-dorsal direction: from 0.8 in the first cohort down to 0.4 corrections per patient in the second cohort.

Ventro-dorsal set-up deviation

It is expected that the "couch height set-up" method gives especially a large improvement in the ventro-dorsal direction. In figure 3, the mean set-up deviations per patient in the ventral-dorsal direction
are shown in a cumulative frequency distribution. In the "laser set-up" group, without application of a correction protocol, 33 % of the measured fractions has a ventro-dorsal deviation of $\geq$ 5 mm. With the "couch height set-up" method, this percentage is decreased to 11 %. With application of the correction protocol, this decreases further to 5 %. It's remarkable that the accuracy of set-up in the ventral-dorsal direction is even better in the "couch height set-up" group without correction protocol than in the "laser set-up" group with correction protocol. For the left-right and cranio-caudal direction, the effect of the "couch height set-up

method" was less pronounced. Combining the "couch height set-up" method with correction protocol resulted in deviations ≥ 5 mm in 7 % and 4 % of the measured fractions respectively (data not shown).
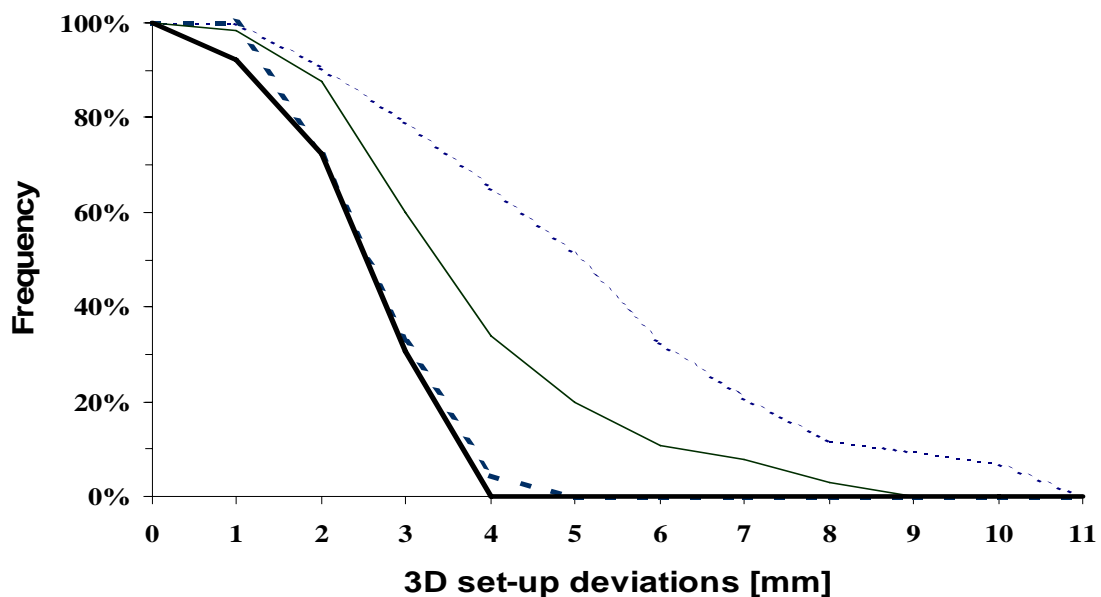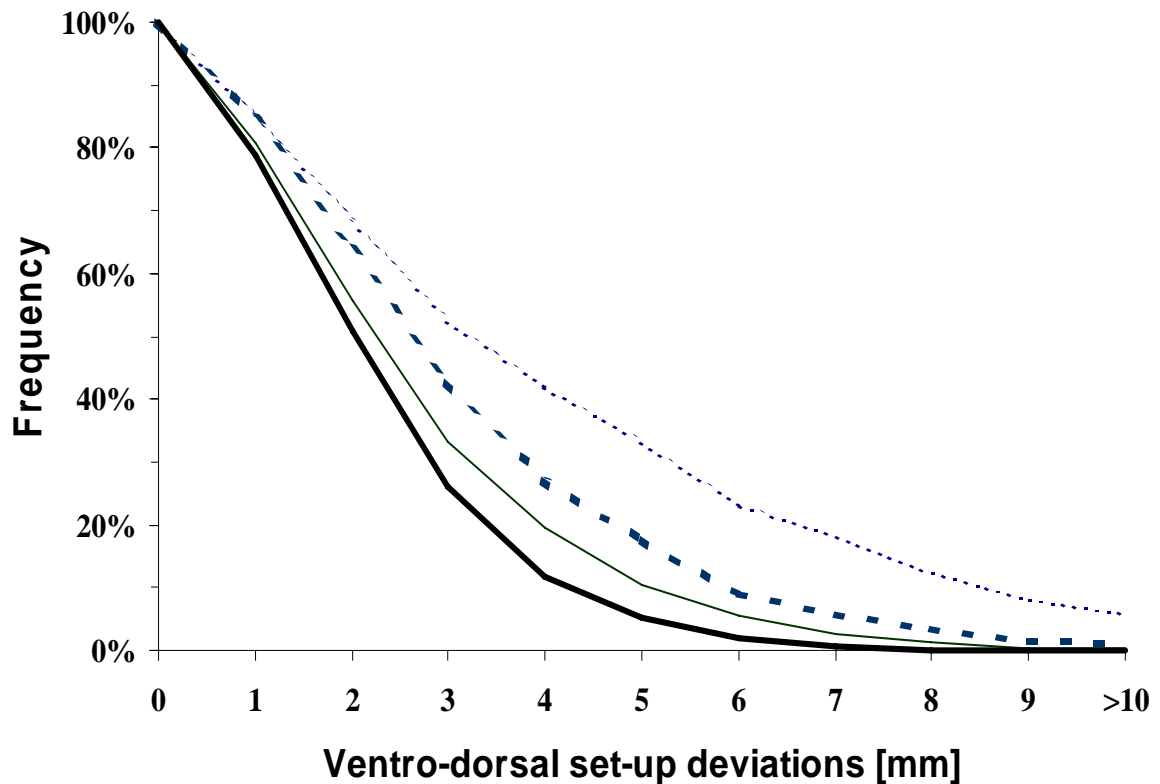

Figure 3: *Cumulative frequency distribution of the ventral-dorsal set-up deviations for the "laser set-up" group without correction protocol (thin dashed line) and with correction protocol (thick dashed line). and for the "couch height set-up" group without (thin solid line) and with correction protocol (thick solid line) . Vertical axis: percentage of set-up deviations ≥ a specific value. Horizontal axis: ventro-dorsal deviations in mm*

Workload

It turned out that during treatment the time of a treatment session (standard time slot 10 minutes for pelvic irradiation) was *not* prolonged due to image acquisition. This is in a situation where, generally, 2 or 3 technologists are executing the patient treatments at one accelerator. Image acquisition, i.e. entering patient data and starting the actual acquisition, is performed by one technologist while the others set up the patient. For each patient, in total about 40 minutes is needed for administrative preparation, verification, and data registration of the whole procedure,

partly the day before the first treatment and partly after each treatment during the day to have corrections ready for the next fraction.

DISCUSSION AND CONCLUSION

This study first confirms again that an off-line correction protocol combined with a "laser set-up" method can reduce the systematic set-up errors significantly without excessive extra workload (17, 18, 20, 21). The results are close to the results of Bel *et al.* and Lebesque *et al.* obtained in a multi-center study in The Netherlands (17, 18). They found that with an average of 0.7 set-up corrections per patients in a shrinking action level protocol, it was possible to reduce the 3D mean set-up deviation > 5 mm from 30 % to less than 2 percent. Our results are similar in terms of improvement of set-up and workload: the mean 3D-set-up deviation $\geq$ 5 mm in the "laser set-up" group was reduced from 51 % to 0 %. Results are for instance also close to Hanley *et al.* (20), who reported systematic set-up variations of 1.3 – 1.9 mm (1 SD) and random set-up variations of 1.7 – 2.0 mm (1 SD); compared to table I.

Secondly, this study clearly shows that use of a "couch height set-up" method improves the set-up in ventro-dorsal significantly. Obviously, a pre-requisite for this result is a similar low sag and accurate read-out of the couches at CT, simulator and accelerator. This large improvement, compared to the "laser set-up" method, can be explained by daily varying motion of the skin during patient set-up in the latter method. It is a significant result that the set-up variation in ventral-dorsal direction is even better for the "couch height set-up" method without correction protocol than for the "laser set-up" method with correction protocol. It's remarkable that also the set-up deviations in the cranial-caudal and left-right direction are reduced when applying the "couch height set-up" method. This might be a side effect of the reduced efforts of the technologists to align the laser lines to the skin lines and, thus, reduces motion of the skin. As a conclusion, this "couch height set-up" method can also be beneficially applied for accelerators without imaging and without correction protocol.

The "couch height set-up" method is not new. We know that some colleagues use this method since carbon-fibre couch inserts and tops became available and "tennis rackets" and mylar couch top inserts were abandoned. In some literature this method is sideways mentioned (5, 14, 24). A similar method as ours was published, however, applied without correction protocol and evaluated only in the ventral-dorsal direction (23). In that study, the height of the isocenter above the couch top was used. In the present study, we use the digital couch height read-out from the simulator, thus including the differences in sag between the couches and the digital read-out inaccuracies. This might be the cause of the slightly lower systematic and random set-up variation in the ventro-dorsal direction found by Greet et al., i.e.

1.3 mm respectively 1.2 mm (1SD) compared to 2.2 mm respectively 1.9 mm (1SD) in our study (see table I - "couch height set-up" method without correction protocol).

Immobilization

In this study, no immobilization was used. In literature, the discussion on immobilization in pelvic irradiation is ongoing. Several groups have investigated this issue with different ways of interpretation, presentation and different conclusions (7-15). We attribute our relatively small random set-up variations, e.g., compared to the results of Mitine *et al.* (7) for their non-immobilized patient group to the stable patient position due to the use of a knee support (see fig.1). Our random set-up variations are also small compared to studies with immobilized patients (7,9). One might imagine that by fitting patients into immobilization devices the skin can move, which introduces additional random variations. So far, immobilization does not seem to yield lower random and systematic variations than the "couch height set-up" method discussed in this paper. This non-immobilized method might even be improved by using a support for the lower legs and ankles (1, 9,10) instead of the universal knee support applied in this study (fig. 1),(16).

CTV - PTV margin

As a result of set-up improvement, the CTV-PTV margin can be reduced. In prostate irradiation, organ motion is an important factor. Prostate position variability has been shown to be larger in the ventro-dorsal direction (2 - 3 mm, 1 SD) and cranial-caudal (2.5 - 4 mm), both due to differences in rectal filling, and less in left-right direction (1 - 2 mm, 1 SD). The seminal vesicles have larger variability in the ventro-dorsal direction (3 - 5 mm, 1 SD) (1-3). Stroom *et al.* and Van Herk *et al.* developed a method for calculation of CTV – PTV margins including organ motion and set-up errors (29, 30).

Their margin rules for CTV - PTV were $2\Sigma + 0.7\sigma$ and $2.5\Sigma + 0.7\sigma$ respectively. Reduction of the systematic set-up error has a major influence on the margin needed. Importing our set-up results into the margin calculations results in a reduction of CTV – PTV margin in the ventral dorsal direction of 3 – 4 mm and for the other directions of 1 – 2 mm. As a result, we have reduced our margins for prostate irradiated patients. Presently, we use a uniform 3D CTV-PTV margin of 8 mm around the prostate and 9 mm around the seminal vesicles in line with Fiorino *et al.* who have also reduced the ventro-dorsal margin from 10 mm to 8 mm as a result of improved set-up by using lower leg immobilization (9).

Implementation of the "couch height set-up" method

Implementation of the "couch-height set-up" method caused changes in the patient positioning methods. Previously, skin marks were used for all three directions. A visual check was performed whether the patient was set-up correctly. With the new method, the lateral

marks are only used to prevent torsion and rotation and the table is set at the prescribed couch height. Initially, this set-up method was rather confusing because a difference between laser lines on the skin and the drawn lateral marks could be present. Acceptance was gained by good communication between the involved disciplines regarding the improvement of set-up accuracy gained during this study.

REFERENCES

1. Van Herk M, Bruce A, Kroes G, et al. Quantification of organ motion during conformal radiotherapy of the prostate by three dimensional image registration. Int J Radiat Oncol Biol Phys 1995;33:1311-1320.

2. Tinger A, Michalski J, Cheng A, et al. A critical evaluation of the planning target volume for 3-D conformal radiotherapy of prostate cancer. Int J Radiat Oncol Biol Phys 1998;42:213-221.

3. Dawson L, Mah K, Franssen E, et al. Target position variability throughout prostate radiotherapy. Int J Radiat Oncol Biol Phys 1998;42:1155-1166.

4. Bijhold J, Lebesque J, Hart A, et al. Maximizing setup accuracy using portal images as applied to a conformal boost technique for prostatic cancer. Radiother Oncol 1992;24:261-271.

5. Creutzberg C, Althof V, de Hoog M, et al. A quality control study of the accuracy of patient positioning in irradiation of pelvic fields. Int J Radiat Oncol Biol Phys 1996;34:697-708.

6. Booth J, Zavgorodni S. Set-up error and organ motion uncertainty: A review. Australas. Phys. Eng. Sci. Med. 1999;22:29-47.

7. Mitine C, Hoornaert M, Dutreix A, et al. Radiotherapy of pelvic malignancies: impact of two types of rigid immobilisation devices on localisation errors. Radiother Oncol 1999;52:19-27.

8. Bentel G, Marks L, Sherouse G, et al. The effectiveness of immobilisation during prostate irradiation. Int J Radiat Oncol Biol Phys 1995;31:143-148.

9. Fiorino C, Reni M, Bolognesi A, et al. Set-up error in supine-positioned patients immobilized with two different modalities during conformal radiotherapy of prostate cancer. Radiother Oncol 1998;49:133-141.

10. Catton C, Lebar L, Warde P, et al. Improvement in total positioning error for lateral prostatic fields using a soft immobilization device. Radiother Oncol 1997;44:265-70.

11. Song P, Washington M, Vaida F, et al. A comparison of four patient immobilization devices in the treatment of prostate cancer patients with three-dimensional conformal radiotherapy. Int J Radiat Oncol Biol Phys 1996;34:213-219.

12. Rosenthal S, Roach M, Goldsmith B, et al. Immobilization improves the reproducibility of patient positioning during six-field conformal radiation therapy for prostate carcinoma. Int J Radiat Oncol Biol Phys 1993;27:921-926.

13. Soffen E, Hanks G, Hwang C, et al. Conformal static field therapy with low-volume low-grade prostate cancer with rigid immobilisation. Int J Radiat Oncol Biol Phys 1991;20:141-146.

14. Bieri S, Miralbell R, Nouet P, et al. Reproducibility of conformal radiation therapy in localized carcinoma of the prostate without rigid immobilisation. Radiother Oncol 1996;38:223-230.

15. Nutting C, khoo V, Walker V, et al. A randomised study of the use of a customised immobilisation system in the treatment of prostate cancer with conformal radiotherapy. Radiother Oncol 2000;54: 1-9.

16. Althof V, Lutjeboer J, Pronk W, et al. Analyis of the use of a simple immobilisation device during prostate radiation (Abstr.) 6th International Workshop on Electronic Portal Imaging. Brussels, Belgium June 2000.

17. Bel A, Vos P, Rodrigus P, et al. High-precision prostate cancer irradiation by clinical application of an off-line patient setup verification procedure using portal imaging. Int J Radiat Oncol Biol Phys 1996;35: 321-332.

18. Lebesque J, Remeijer P, van Riel V, et al. Clinical evaluation of setup verification an correction protocols: results of multicentre studies of the Dutch cooperative EPID group (Abstr.) 5th International Workshop on Electronic Portal Imaging. Phoenix, USA October 1998.

19. De Neve W, De Gersem W, Fortan L, et al. Clinical implementation of electronic portal imaging: correction strategies and set-up errors. Bull Cancer/Radiother 1996;83:401-405.

20. Hanley J, Lumley M, Mageras G, et al. Measurement of patient positioning errors in three-dimensional conformal radiotherapy of the prostate. Int J Radiat Oncol Biol Phys 1997;37:435-444.

21. Mubata C, Bidmead A, Ellingham L, et al. Portal imaging protocol for radical dose-escalated radiotherapy treatment of prostate cancer. Int J Radiat Oncol Biol Phys 199;40:221-231.

22. Stroom J, Olofsen-van Acht M, Quint S, et al. On-line set-up corrections during radiotherapy of patients with gynecologic tumors. Int J Radiat Oncol Biol Phys 2000;46:499-506.

23. Greer P, Mortensen T, Jose C. Comparison of two methods for anterior-posterior isocenter localization in pelvic radiotherapy using electronic portal imaging. Int J Radiat Oncol Biol Phys 1998;41:1193-1199.

24. Vos P. Decision criteria and correction strategies in the clinical use of electronic digital portal imagers (Abstr.) XII th ICCR Meeting, Salt Lake City, USA. May 1997.

25. Denham J, Dally M, Hunter K, et al. Objective decision-making following a portal film: the results of a pilot study. Int J Radiat Oncol Biol Phys 1993;26:869-876.

26. Herman M, Abrams R, Mayer R. Clinical use of on-line portal imaging for daily patient treatment verification. Int J Radiat Oncol Biol Phys 1994;28:1017-1023.

27. Stroom J, Korevaar G, Koper P, et al. Multiple 2D versus 3D PTV definition in treatment planning for conformal radiotherapy. Radiother Oncol 1998;47:297-302.

28. Bel A, van Herk M, Bartelink H, et al. A verification procedure to improve patient setup accuracy using portal image. Radiother Oncol 1993;29:253-260.

29. Stroom J, de Boer H, Huizenga, H, et al. Inclusion of geometrical uncertainties in radiotherapy treatment planning by means of coverage probability. Int J Radiat Oncol Biol Phys 1999;43:905-919.

30. Van Herk M, Remeijer P, Rasch C, et al. The probability of correct target dosage: dose-population histograms for deriving treatment margins in radiotherapy. Int J Radiat Oncol Biol Phys 2000;47:1121-1135.

Ultrasound guided transrectal implantation of gold markers for prostate localization during external radiotherapy: complication rate and risk factors

Johan F. Langenhuijsen, M. D.*, Emile N. J. Th. van Lin, M. D.#,
Lambertus A. Kiemeney,Ph. D.*, Lisette P. van der Vight, B. Sc.#, Andries G. Visser Ph.D.#,
and J. Alfred Witjes, M. D., Ph. D.*

Departments of *Urology and #Radiation Oncology

Submitted

ABSTRACT

Purpose: To report the complication rates and risk factors of transrectally implanted gold markers, used for prostate position verification and correction procedures.

Materials and Methods: In 209 consecutive men with localized prostate cancer four gold markers (1 x 7 mm) were inserted under ultrasound guidance in an outpatient setting and the toxicity was analyzed. All patients received a questionnaire, regarding complications after marker implantation. Complications and risk factors were further evaluated by reviewing the medical charts.

Results: Thirteen patients (6.2 %) had a moderate complication, consisting of pain and fever that resolved after treatment with oral medication. In 1.9 % of the men, minor voiding complaints were observed. Other minor transient complications, defined as hematuria lasting more than 3 days, hematospermia and rectal bleeding occurred in 3.8%, 18.5% and 9.1% of the patients, respectively. These complications were seen more often in patients with higher tumor stage, younger age and shorter duration of hormonal therapy.

Conclusions: Transrectal gold marker implantation as part of the prostate radiotherapy treatment preparation is a safe and well-tolerated procedure. The complications are comparable to or even less than the complications observed in diagnostic prostate biopsies. The proven advantages of marker implantation for high-precision prostate radiotherapy outweigh the minor risks.

INTRODUCTION

Dose escalation in external radiotherapy, for localized prostate cancer improves outcome with a lower PSA-recurrence rate (1, 2). Rectal toxicity is one of the limiting factors and is directly related to the total radiation dose prescribed and the volume of the rectal wall receiving a high dose (3). Prostate motion is considered a source of treatment error, with day-to-day gland displacements between 3-5 mm (4). To account for these prostate movements, treatment margins up to 10-15 mm have to be defined around the gland and result in additional irradiation of the surrounding tissues. To enable margin reduction, radiopaque markers implanted in the prostate are being used as an aid for exact localization of the prostate during the radiotherapy (5-8). Electronic portal imaging systems are widely used for daily prostate position verification and correction procedures (9 - 12). The markers are implanted prior to the acquisition of the planning computer tomography (CT)-scan. Gold markers are well-visible fiducials both in pre-treatment imaging (CT, MR) and in megavolt portal imaging during radiotherapy treatment. Marker migration within the prostate, during the course of radiotherapy is negligible (13). Therefore, implanted gold marker detection is a reliable method for repetitive position verification.
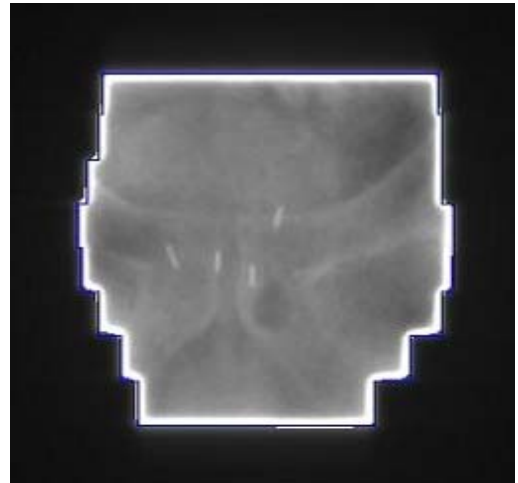
Fig 1 *Portal image of anterior-posterior radiotherapy treatment beam, with four implanted gold markers in situ.*

Although the use of gold markers is increasingly common, complication rates have not been reported in a large patient population. It might be hypothesized, that the complication rates due to marker implantation may be comparable to the complications in patients undergoing diagnostic prostate biopsies. In prostate biopsies few moderate, but frequent minor complications are seen. Analysis was performed by several authors to identify risk factors for complications of prostate biopsies (7, 14-16). The goals of this study are to report on the complication rate in patients with localized prostate cancer in whom gold markers were implanted transrectally and to identify risk factors for complications.

MATERIALS AND METHODS

Patients and gold marker implantation

In all patients referred for radiotherapy on localized prostate cancer (T1-3 N0 M0), the gold marker implantation was performed in the urology outpatient clinic. No preceding enema or anesthesia was used. A prophylactic antibiotic, ciprofloxacin 500 mg. b.i.d. for three days, was given. Anticoagulant medication was stopped 3 to 7 days before marker implantation. Patients were placed in a lateral decubitus position. First, the urologist measured the prostate volume with an ultrasound Kretz Voluson 530D device (GE Kretz, Zipf, Austria) with endorectal transducer. Next, the gold markers were placed, under ultrasound guidance, with a standard 18-gauge prostate biopsy tool (Microvasive Topnotch, Boston Scientific, Natick, MA), mounted onto the endorectal ultrasound transducer (Fig 1a). Fine gold markers of 1 mm diameter and 7 mm length were used (Hospimed International
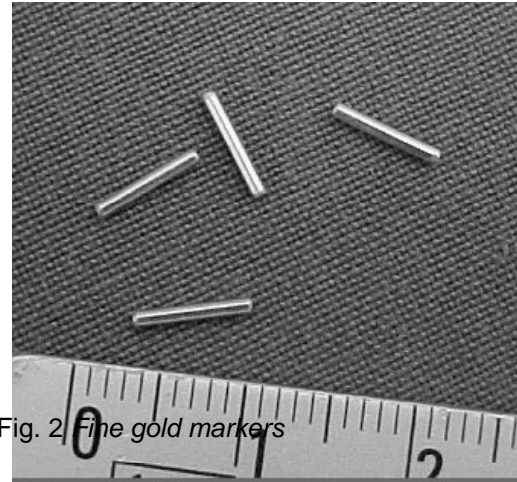
Fig. 2 *Fine gold markers*

B.V., Dalfsen, The Netherlands) (Fig. 1b). The length was chosen for reasons of visibility on the portal images and CT imaging. Two markers were placed left and right at the base, one in the central part next to the urethra and one at the apex of the prostate. After at least one week, to resolve swelling of the gland after implantation, the planning CT-scan (3 mm slice thickness) was obtained. In Fig 1c, an example of a portal image, showing the implanted markers, is displayed.

Complications and risk factors

All patients received a questionnaire, regarding complications after marker implantation. The questionnaire specifically asked for the presence and duration of hematuria, hematospermia, rectal bleeding, fever, and pain. Patients were also asked to report other complaints, symptoms and additional medication taken after the implantation. Pain was scored on a 0 to 10 scale (0=no pain, 10=worst pain imaginable). It was requested to compare the pain, experienced during marker implantation, to the pain at the diagnostic prostate biopsy procedure.

Minor complications, were defined as side effects with transient minimal discomfort, requiring no additional medical intervention. The complications that resulted in moderate discomfort and required additional treatment were considered as moderate complications.

In most cases (184/209) the questionnaires were sent to the patients by mail, after the marker implantation. For this particular retrospective analysis, inconsistencies were verified

with the patient. The notes, made by the urologist or radiation oncologist in the period of marker implantation, were checked retrospectively and all other occurring complications were noted.

Possible risk factors for developing any moderate or any bleeding complications (hematuria, hematospermia or rectal blood loss) were evaluated by reviewing the medical charts: tumor stage, the urologist performing the marker implantation, the use of anticoagulant therapy, previous transurethral resection of prostate (TURP) or prostatitis, the prevalence of diabetes, prednisone use, age, duration of hormonal therapy, and the volume of the prostate. Statistical analysis was performed by T-tests for the comparison of continuous variables and Fisher exact tests (2 $\times$ 2 tables) or Chi-square tests (3 $\times$ 3 tables) for the comparison of categorical variables. To analyze the impact of retrospective analysis, the patients who received the questionnaire directly after the procedure, were evaluated separately and the outcomes were compared with the data obtained retrospectively.

RESULTS

Patients and gold marker implantation

Between January 2001 and September 2005, gold markers were implanted in 236 patients. The mean age was 70 years (range 40-84 years). Twenty-seven patients were lost to follow-up because of death (n=9) or other factors (n=18). In 209 patients the toxicity outcome could be analyzed and results reported concern this group of 209 patients. Of these patients, the tumor was staged as a T1 in 18 cases, T2 in 64 cases and a T3 tumor in 127 cases.

In 8 patients, marker misplacement outside the gland boundaries was observed during the treatment planning CT-scan: 7 times into the bladder, 1 time to the rectum. On average, the whole implantation procedure took 10 minutes. Seventy-nine patients were on anticoagulant therapy: acetylsalicylic acid (n=64), acenocoumarol (n=12) or other (n= 3). Hormonal treatment (HT) was started in 202 patients, mainly before marker implantation, with a mean interval of 7 weeks until the procedure (range 0-40). Prostate volumes ranged from 5 to 136 ml (mean 40 ml). For the retrospective complications analysis, the questionnaire was filled out at a mean time of 90 weeks after marker implantation.

Complications and risk factors

In Table 1 the observed complication rates are shown. No statistically significant differences in any of the complications were found between the patients who filled out the

questionnaire directly after the procedure and the patients who performed this later (data not shown).

Patients	N	%
Minor complications		
Hematuria > 3 days	8	3.8
Hematospermia	15	7.2
Rectal bleeding	19	9.1
Voiding complaints	4	1.9
Moderate complications		
Pain requiring analgesics	6	2.9
Fever	4	1.9
Nausea/vomiting	2	1.0
Allergic reaction antibiotic	1	0.5

Table 1. *Complication rates*

Minor complications

In all cases hematuria was self-limiting within 7 days. Hematospermia, noted by 15 men, was counted only in the 81 patients who reported to have had ejaculations. The average duration of rectal bleeding was 2.5 days. In 13 out of 19 patients, the rectal bleeding lasted for 1 day. One patient reported repeated minor blood loss during 21 days. The voiding complaints consisted of either an increase of previous complaints, or dysuria.

Moderate complications

For the patients with a moderate complication, no admission to the hospital was necessary. Patients with fever got additional antibiotics and the temperature normalized within a few days. The patient with the allergic reaction to ciprofloxacine recovered after termination of this antibiotic.

Pain

The mean pain score was 3.2 (range 0-9). Forty-eight percent of the patients scored 0-2, 37% had a pain score of 3-5 and 15% of the patients scored 6-9. Fifty percent of the patients reported that the marker implantation was less painful than prostate biopsies, while 40% of the patients recorded comparable pain and 10% noted more pain.

Risk factors

Significantly increased bleeding complications were seen in patients with advanced tumor stage, younger age and shorter duration of hormonal treatment (Table 2 and 3). The use of anticoagulants yielded no increased rectal bleeding or other complications rates. None of the investigated risk factors were significantly correlated to any moderate complication.

Risk factor		Bleeding complication % (n)	p	Moderate complication % (n)	p
Tumor stage	T1	5.6 (1/18)	0.026*	0 (0/18)	0.57*
	T2	9.4 (6/64)		6.3 (4/64)	
	T3	22.8 (29/127)		5.5 (7/127)	
Anticoagulant	Yes	20.3 (16/79)	0.45	5.1 (4/79)	1.00
	No	15.4 (20/130)		5.4 (7/130)	
TURP	Yes	3.7 (1/27)	0.054	0 (0/27)	0.37
	No	19.2 (35/182)		6 (11/182)	
Prostatitis	Yes	16.7 (2/12)	1.00	8.3 (1/12)	0.49
	No	17.3 (34/197)		5.1 (10/197)	
Diabetes	Yes	22.2 (4/18)	0.52	0 (0/18)	0.60
	No	16.8 (32/191)		5.8 (11/191)	
Prednisone	Yes	0 (0/1)	1.00	0 (0/1)	1.00
	No	17.3 (36/208)		5.3 (11/208)	

*Key: TURP = transurethral resection of prostate; * = Chi-square test*

Table 2. *Risk factors and complication rates (Fisher exact test)*

Risk factor	Bleeding complication	Mean	p	Major complication	Mean	p
Age	Yes	68.1 years	0.022	Yes	70.6 years	0.85
	No	70.8 years		No	70.3 years	
HT	Yes	4.4 weeks	0.028	Yes	5.1 weeks	0.51
	No	7.2 weeks		No	6.8 weeks	
Prostate volume	Yes	42.8 ml	0.38	Yes	46.2 ml	0.11
	No	39 ml		No	39.2 ml	

Key: HT=hormonal therapy

Table 3. *Risk factors and complication rates (T-test)*

DISCUSSION

In this study, the complications and risk factors were studied after transrectal implantation, under ultrasound guidance, of gold markers for position verification in prostate cancer radiotherapy. This is the first paper reporting the marker-induced toxicity of a large patient group. Minor complications such as hematuria and hematospermia were observed in 3.8% and 18.5% of the patients, respectively. Rectal bleeding was seen in 9.1% of the patients, lasting for an average of 2.5 days. Henry *et al.* reported on twelve patients in whom gold markers were implanted transperineally (17). Three patients noted hematuria, one patient hematospermia and one patient rectal bleeding, which occurred after the marker was most likely implanted through the rectal wall. No infections were seen. The transperineal route is thought to give less rectal bleeding than the transrectal implantation. In this study, the duration of hematuria was not mentioned. Maximally three markers were implanted, which could be a factor in causing less rectal bleeding or hematospermia. The authors reported severe pain during the implantation in three patients and one patient needed analgesics. Comparison with our results is difficult because of the difference in patient numbers. The second study, reporting on implanted marker toxicity, comprises 10 patients and a maximum of three fiducial markers were implanted under ultrasound guidance (7). Three patients reported a transient hematuria the first 24 hours after implantation and seven patients reported an episode of rectal bleeding. Again, comparison to our results is difficult as we reported hematuria longer than 3 days only. Occurrence of hematospermia was not mentioned and no moderate or major complications were observed.

After prostate biopsies 64% - 78% minor complications (i.e. hematuria and hematospermia) are noted (15, 18-20). Moderate complications, mostly infections, are seen infrequently with a maximum of 4% (15, 21). Two studies noted a rate of 23% of hematuria lasting longer than 3 days, 45% hematospermia and 1,7% rectal bleeding (14, 16). We reported less hematuria and hematospermia after marker implantation but more rectal bleeding, although the duration was short. In literature, the percentage of voiding complaints after prostate biopsies varies between 1-12% (16, 20, 22, 23). In our group, only 1.9% of the patients had voiding complaints after the marker implantation. Table 4 shows, for comparison, complication rates after prostate biopsies, as reported in literature and our observed complication rates after marker implantation (depicted in the last line). In some studies, dealing with TRUS and transrectal prostate biopsies, minor or no discomfort is reported in up to 92% of patients and patients' acceptance is high (20, 21).

Authors	Year	Patients (n)	HU >3 days (%)	HS (%)	RB (%)	Voiding (%)	Fever (%)	Adm (%)	Pain/ Analgesics (%)	Patients' acceptance (%)
Clements	1993	80	20*	11.3	7.5	7.5	2.5	1.3	7.5	>70
Rodriguez	1998	127	47	10	10	11.8	1.7	0.8	13	70
Djavan	2001	1051	16.6	10.2	2.4	7.2	2.9	NA	11	89
Collins	1993	89	18	29	37	7	4	NA	22	78
Aus	1993	391	13	9	2.8	NA	2.5	1.8	8	92
Raaijmakers	2002	5802	22.6	50.4	1.3	0.8	3.5	0.5	7.5	NA
Rietbergen	1997	1687	23.6	45.3	1.7	NA	4.2	0.4	7.5	NA
Langenhuijsen	*2006*	*209*	*3.8*	*7.2*	*9.1*	*1.9*	*1.9*	*0*	*2.9*	*85*

*Key: HU = hematuria; HS = hematospermia; RB = rectal bleeding; Adm = admission to hospital; NA = not available; *duration not defined*

Table 4. *Reported complications in prostate biopsies & gold marker implantation*

However, there are also reports in which severe discomfort is mentioned in up to 30% of patients (18). Irani *et al*. evaluated 81 patients undergoing prostate biopsies (24). They found a mean painscore of 3, but 16% had significant discomfort (score>5). We found similar results with a mean painscore of 3.2 and 15% of patients having severe pain during the implantation. Only six patients, reporting pain, needed analgesics. Half of the patients reported that the marker implantation procedure was less painful than the diagnostic biopsies. This might be explained by the fact that only 4 markers are implanted, in contrast to the multiple (6 – 8) biopsies. Furthermore, the uncertainty of the diagnosis during biopsies might play a role in experiencing more pain.

Only 1.9 % of our patients got fever after marker implantation, less than most others reported after prostate biopsies (14, 15, 16, 18, 20-23). It was shown that an antibiotic prescribed for 3 days and started 1 day before the prostate biopsies reduced the number of infectious complications (15). We also started ciprofloxacin one day before marker implantation and continued it for 3 days. Two patients got nausea and vomiting after the implantation. This could be a consequence of the procedure and be a manifestation of bacterimea (23). These patients however did not get fever and the complaints resolved spontaneously.

Anticoagulant medication was stopped 3-7 days before implantation. As a result no extra or longer bleeding complications occurred in this group. We have shown that patients

with higher tumor stage, younger age and with shorter duration of hormonal treatment had significantly more bleeding complications. In these patients, an increased prostatic vascularisation could be an explanation, although this is speculative. It might be advisable to wait with implantation until shortly before radiotherapy, so the hormonal therapy has caused maximal reduction of tumor volume. As we have experienced, a disadvantage of a smaller prostate can be the technical difficulty of the marker implantation. Studies have shown that younger patients experience more pain in prostate biopsies (18, 20). This could not be confirmed for in our study. Raaijmakers *et al.* (16) have identified risk factors for complications after prostate biopsies. An earlier episode of prostatitis was associated with more pain and hospital admission. Prostate volume was as a predictor for urinary retention. In our study, no specific risk factors for complications could be identified and urinary retention did not occur in any of the 209 studied patients.

In each prostate radiotherapy patient referred to our department, gold markers are implanted transrectally. The role of the markers in accurate position verification and correction has been well established (10-12, 25). Recently, the first clinical data have been published of a new type of implantable radiofrequency emitting device, measuring continuously the position of the prostate during treatment (26). Implantation under ultrasound guidance of these markers, in size comparable to the gold markers, yielded also no severe complications. Apart from verification purposes, we have been using the gold markers for high precision magnetic resonance imaging (MRI) – CT fusion and prostate delineation during the treatment planning process (27).

CONCLUSIONS

Transrectal gold marker implantation for prostate position verification is safe and appears to be a well-tolerated procedure. In only 1.9 % of the studied patients, minor voiding complaints were observed. Other minor transient complications, defined as hematuria lasting more than 3 days, hematospermia and rectal bleeding occurred in 3.8%, 18.5% and 9.1% of the implanted patients. These minor bleeding complications were more frequently seen in patients with higher tumor stage, younger age and shorter duration of hormonal therapy. Moderate complications were rare (6.2%) and consisted mainly of pain and fever. These were treated with oral medication, which resolved the complaints quickly. The complications after gold marker implantation were comparable to or even less than in diagnostic prostate biopsies. The proven advantages of marker implantation for high-precision prostate radiotherapy outweigh the minor risks.

REFERENCES

1. Peeters ST, Heemsbergen WD, Koper PC, *et al.* Dose-response in radiotherapy for localized prostate cancer: results of the Dutch multicenter randomized phase III trial comparing 68 Gy of radiotherapy with 78 Gy. *J Clin Oncol* 2006;24:1990-1996

2. Zietman AL, DeSilvio ML, Slater JD, *et al.* Comparison of conventional-dose vs high-dose conformal radiation therapy in clinically localized adenocarcinoma of the prostate: a randomized controlled trial. *JAMA* 2005;294:1233-1239

3. Pollack A, Zagars GK, Starkschall G, *et al.* Prostate cancer radiation dose response: results of the M. D. Anderson phase III randomized trial. *Int J Radiat Oncol Biol Phys* 2002;53:1097-1105

4. Langen KM, Jones DT. Organ motion and its management. *Int J Radiat Oncol Biol Phys* 2001;50:265-278

5. Balter JM, Sandler HM, Lam K, *et al.* Measurement of prostate movement over de course of routine radiotherapy using implanted markers. *Int J Radiat Oncol Biol Phys* 1995;31:113-118

6. Vigneault E, Pouliot J, Laverdiere J, *et al.* Electronic portal imaging device detection of radioopaque markers for the evaluation of prostate position during megavoltage irradiation: a clinical study. *Int J Radiat Oncol Biol Phys* 1997;37:205-212

7. Dehnad H, Nederveen AJ, van der Heide UA, *et al.* Clinical feasibility study for the use of implanted gold seeds in the prostate as reliable positioning markers during megavoltage irradiation. *Radiother Oncol* 2003;67:295-302

8. Litzenberg D, Dawson LA, Sandler H, *et al.* Daily prostate targeting using implanted radiopaque markers. *Int J Radiat Oncol Biol Phys* 2002;52:699-703

9. Wu J, Haycocks T, Alasti H, *et al.* Positioning errors and prostate motion during conformal prostate radiotherapy using on-line isocenter set-up verification and implanted prostate markers. *Radiother Oncol* 2001;61:127-133

10. Schallenkamp JM, Herman MG, Kruse JJ, *et al.* Prostate position relative to pelvic bony anatomy based on intraprostatic gold markers and electronic portal imaging. *Int J Radiat Oncol Biol Phys* 2005;63:800-811

11. Van Lin EN, van der Vight LP, Witjes JA, *et al.* The effect of an endorectal balloon and off-line correction on the interfraction systematic and random prostate position variations: a comparative study. *Int J Radiat Oncol Biol Phys* 2005;61:278-288

12. Van den Heuvel F, Fugazzi J, Seppi E, *et al.* Clinical application of a repositioning scheme, using gold markers and portal imaging. *Radiother Oncol* 2006;79:94-100

13. Pouliot J, Aubin M, Langen KM, *et al.* (Non)-migration of radiopaque markers used for on-line localization of the prostate with an electronic portal imaging device. *Int J Radiat Oncol Biol Phys* 2003;56:862-866

14. Rietbergen, JB, Kruger AE, Kranse R, *et al.* Complications of transrectal ultrasound-guided systematic sextant biopsies of the prostate: evaluation of complication rates and risk factors within a population-based screening program. *Urology* 1997;49:875-880

15. Norberg M, Holmberg L, Häggman M, *et al.* Determinants of complications after multiple transrectal core biopsies of the prostate. *Eur Radiol* 1996;6:457-461

16. Raaijmakers R, Kirkels WJ, Roobol MJ, *et al.* Complication rates and risk factors of 5802 transrectal ultrasound-guided sextant biopsies of the prostate within a population-based screening program. *Urology* 2002;60:826-830

17. Henry AM, Wilkinson C, Wylie JP, *et al.* Trans-perineal implantation of radio-opaque treatment verification markers into the prostate: an assessment of procedure related morbidity, patient acceptability and accuracy. *Radiother Oncol* 2004;73;57-59

18. Rodriguez LV, Terris MK Risks and complications of transrectal ultrasound guided prostate needle biopsy: a prospective study and review of the literature. *J Urol* 1998;160:2115-2120

19. Gustafsson O, Norming U, Nyman CR, *et al.* Complications following combined transrectal aspiration and core biopsy of the prostate. *Scand J Urol Nephrol* 1990;24:249-251

20. Djavan B, Waldert M, Zlotta A, *et al.* Safety and morbidity of first and repeat transrectal ultrasound guided prostate needle biopsies: results of a prospective European prostate cancer detection study. *J Urol* 2001;166:856-860

21. Aus G, Hermansson CG, Hugosson J, *et al.* Transrectal ultrasound examination of the prostate: complications and acceptance by patients. *Br J Urol* 1993;71:457459

22. Clements R, Aideyan OU, Griffiths GJ, *et al.* Side effects and patient acceptability of transrectal biopsy of the prostate. *Clin Radiol* 1993;47:125-126

23. Collins GN, Lloyd SN, Hehir M, *ET AL.* Multiple transrectal ultrasound-guided prostatic biopsies-true morbidity and patient acceptance. *Br J Urol* 1993;71:460-463

24. Irani J, Fournier F, Bon D, *et al.* Patient tolerance of transrectal ultrasound-guided biopsy of the prostate. *Br J Urol* 1997;79:608-610

25. Scrabrough TJ, Golden NM, Ting JY, *et al.* Comparison of ultrasound and implanted seed marker prostate localization methods: Implication of image-guided radiotherapy. *Int J Radiat Oncol Biol Phys* 2006;65:378-387

26. Willoughby TR, Kupelian PA, Pouliot J, *et al.* Target localization and real-time tracking using the Calypso 4D localized prostate cancer. *Int J Radiat Oncol Biol Phys* 2006;65:528-534

27. Huisman HJ, Fütterer JJ, van Lin EN, *et al.* Prostate cancer: precision of integrating functional MR imaging with radiation therapy treatment by using gold markers. *Radiology* 2005;236:311-317

4

The effect of an endorectal balloon and off-line correction on the interfraction systematic and random prostate position variations: a comparative study

Emile N.J.Th van Lin, M.D.[#], Lisette P. van der Vight, B.Sc.[#], J.Alfred Witjes, M.D., Ph.D.[*], HenkJan J. Huisman, Ph.D.[¶], Jan Willem Leer, M.D. Ph.D.[#], and Andries G. Visser, Ph.D.[#]

Departments of [#]Radiation Oncology, [¶]Radiology and [*]Urology

ABSTRACT

Purpose: To investigate the effect of an endorectal balloon (ERB) and an off-line correction protocol on the day-to-day, interfraction prostate gland motion, in patients receiving external beam radiotherapy for prostate cancer.

Methods and materials: In 22 patients, irradiated with an ERB in situ ("ERB group") and in 30 patients without an ERB ("No-ERB group"), prostate displacements were measured daily in three orthogonal directions with portal images. Implanted gold markers and an off-line electronic portal imaging correction protocol were used for prostate position verification and correction. Movie loops were analyzed to evaluate prostate motion and rectal filling variations.

Results: The off–line correction protocol reduced the systematic prostate displacements, equally for the ERB and No-ERB group, to 1.3 – 1.8 mm (1 SD). The mean 3D displacement was reduced to 2.8 mm and 2.4 mm for the ERB and No-ERB group, respectively. The random interfraction displacements, relative to the treatment isocenter, were not reduced by the ERB and remained nearly unchanged in all three directions: 3.1 mm (1SD) left-right, 2.6 mm (1SD) superior-inferior and 4.7 mm (1SD) for the anterior-posterior direction, respectively. These day-to-day prostate position variations can be explained by the presence of gas and stool besides the ERB.

Conclusions: The off-line corrections on the fiducial markers are effective in reducing the systematic prostate displacements. The investigated ERB does not reduce the interfraction prostate motion. Although the overall mean displacement is low, the day-to-day interfraction motion, especially in anterior-posterior direction, remains high compared to the systematic displacements.

INTRODUCTION

The prostate moves over the course of a radiation treatment. The interfraction motion in anterior-posterior (AP) direction, ranging from 1.5 – 4.5 mm, 1 Standard Deviation (1 SD), appears to be larger than in superior-inferior (SI), (ranging from 0.9 – 3.9 mm (1 SD)), and in left-right (LR) directions (ranging from 0.7 – 1.9 mm (1 SD)). (See overview by Langen *et al.* (1). According to the ICRU definitions, the CTV (clinical target volume) – PTV (planning treatment volume) margin accounts for organ motion. For prostate treatment, the largest CTV - PTV margin should be towards the rectum, usually 8 – 15 mm. The AP motion is mainly correlated with variations in rectal filling (2). Controlling the prostate motion may enable margin reduction, and consequently reduction of irradiated rectal wall volume. Rectal toxicity is one of the limiting factors in dose escalation and is directly related to the total radiation dose prescribed and the volume of the rectal wall receiving a high dose (3). One of the challenges in prostate radiation therapy is elevating dose without increasing rectal toxicity.

Two different methods have been investigated to control prostate motion: daily beam position adjustment and prostate gland immobilization. To localize and correct for the prostate displacement by adjustment of the beam positions, repetitive CT scanning (4), radiopaque markers, detectable on portal imaging systems (5-10), and ultra-sound systems have been used (11). Several investigators tested an endorectal balloon (ERB) for gland immobilization and rectal wall sparing (12-17).

The advantages of the ERB may be threefold. First, the ERB is expected to immobilize the prostate gland by giving a constant rectal filling that pushes the prostate towards the pubic bone. Second, the ERB pushes the dorsal rectal wall away from the high dose region, resulting in rectal wall sparing and reduced rectal toxicity (15-17). Third, Teh *et al.* (15) showed that the air-filled ERB could give additional reduction of rectal wall dose at the air-tissue interface.

To date, no comparative study has been conducted evaluating the systematic (i.e. same deviation present throughout the whole treatment) and random (i.e. deviation varying from day to day) variation in prostate position in patients irradiated with and without an ERB during the whole course of the treatment. The first goal of this study was to evaluate the interfraction prostate gland motion in patients treated with and without an ERB. The second goal was to distinguish between systematic and random prostate position variations, because they have a different impact on the magnitude of the CTV-PTV margins (18,19).

MATERIALS AND METHODS

Patient preparation and treatment

Fifty-two patients were irradiated for localized prostate cancer (T1-3N0M0) and, after informed consent was given, included in this study. No exclusion criteria were applied, and patients were assigned to either patient group: treatment with or without ERB, over a period of twelve months, i.c. the year 2002. All patients received three to six months neo-adjuvant hormonal therapy. Four fine gold markers (1mm diameter, 7 mm length) were inserted under trans-rectal ultrasound guidance by a urologist. Two gold markers were inserted in the base, one at the apex and one in the central part (next to urethra) of the prostate gland. A standard 18-gauge prostate biopsy tool was used (Micro-vasive topnotch, Boston Scientific, USA.*)* and prophylactic antibiotics were given (ciprofloxacin 500 mg, BID, for 3 days). To ensure proper localization of the gold markers, orthogonal pelvic X-rays were made, one hour after the marker placement.

After at least one week, to resolve swelling of the gland after marker implantation, a planning CT-scan was obtained at 3mm slice thickness (AcQsim spiral CT, Philips Medical Systems). Prior to CT scanning and daily treatments patients were advised to use a laxative diet and, if necessary a laxans, and have a full bladder by drinking 500 ml of water. A beams-eye-view based 3D-conformal treatment plan was designed, with individual shielding of normal tissues (Cadplan treatment planning system, Varian). The CTV included prostate only or prostate and seminal vesicles. The PTV was defined by automatic 10 mm 3D expansion of the CTV. An orthogonal four-field isocentric technique was used. Doses varied from 63 to 67.5 Gy, in 7 to 7.5 weeks, depending on tumor-stage (fractionation four times a week using 2.25 Gy fractions). The investigated patient group was divided in two cohorts: patients treated without an ERB (n = 30, "No-ERB" group), and patients treated with a daily ERB in situ (n = 22, "ERB" group).

The investigated ERB, originally designed as an endorectal coil for magnetic resonance (MR) imaging, was supplied by Medrad (Medrad, Pittsburgh, PA). This ERB has a specific anatomical concave shape to conform to the prostate gland-rectal interface (13). Deflated, the ERB has a diameter of 15 mm. The ERB was inflated with 80 cc of air (standard amount of air used for MR imaging) and had a length of 90 mm and a diameter of 45 mm (Fig. 1a). For every treatment fraction, the radiation therapist placed a new ERB. Special attention was given to correct placement of the ERB, i.e. concavity of the balloon directed towards the prostate, and the ERB was gently pulled towards the anal sphincter, to ensure a proper position in relation to the prostate (Fig. 1b).
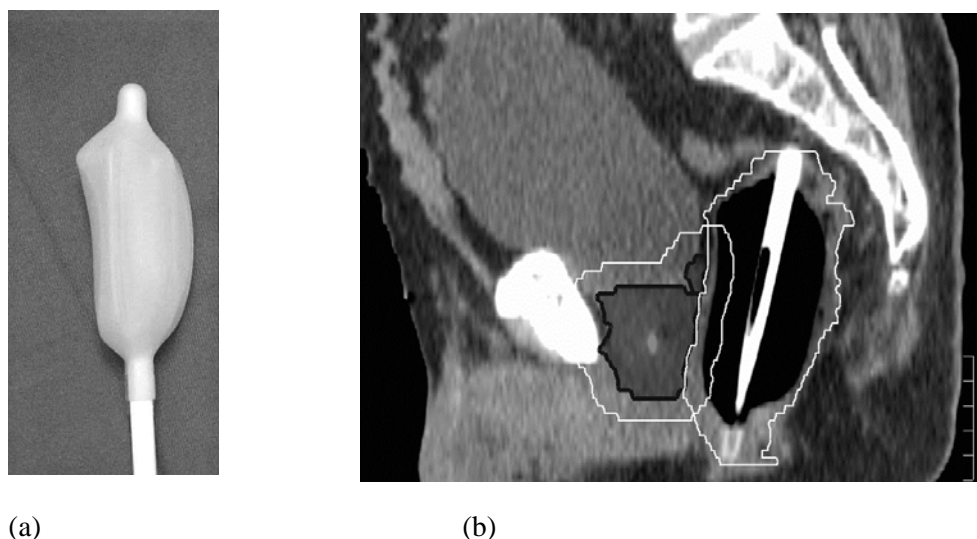
(a)   (b)

Fig. 1.
Lateral view of ERB, inflated with 80 cc of air (a) and a saggital planning CT scan reconstruction, with endorectal balloon (ERB) inserted and prostate and seminal vesicles highlighted, surrounded by the PTV (b)

During CT-scanning and all treatment fractions, patients were positioned supine on a flat couch that was covered with a thin disposable paper sheet. Only a pillow and a foam knee support (Kneefix ™ cushion, Sinmed, Reeuwijk, The Netherlands) were used for relaxed positioning of the head and legs, respectively. For patient positioning, a system of wall-mounted alignment lasers was used. The digital read-out of the treatment couch height, obtained during CT-scanning, was used for more accurate set-up during the actual treatment, as described earlier (20).

Portal Imaging and registration procedures

Daily portal images were acquired using a commercial camera-based electronic portal imaging device (EPID), equipped with a CCD camera (Theraview NT, Cablon Medical B.V., Leusden, The Netherlands) mounted at our GE Saturne 42 accelerator. The digitally reconstructed radiograph (DRR) derived from the planning CT-scan was used as the reference image. The field shape, an anatomy template consisting of contours of relevant bony structures and the contours of the four gold markers were delineated on the DRR. During the actual treatment, daily portal images were acquired using the first 30 monitor units of the orthogonal (anterior - posterior (AP) and left-lateral (LL)) treatment beams (Fig. 2).
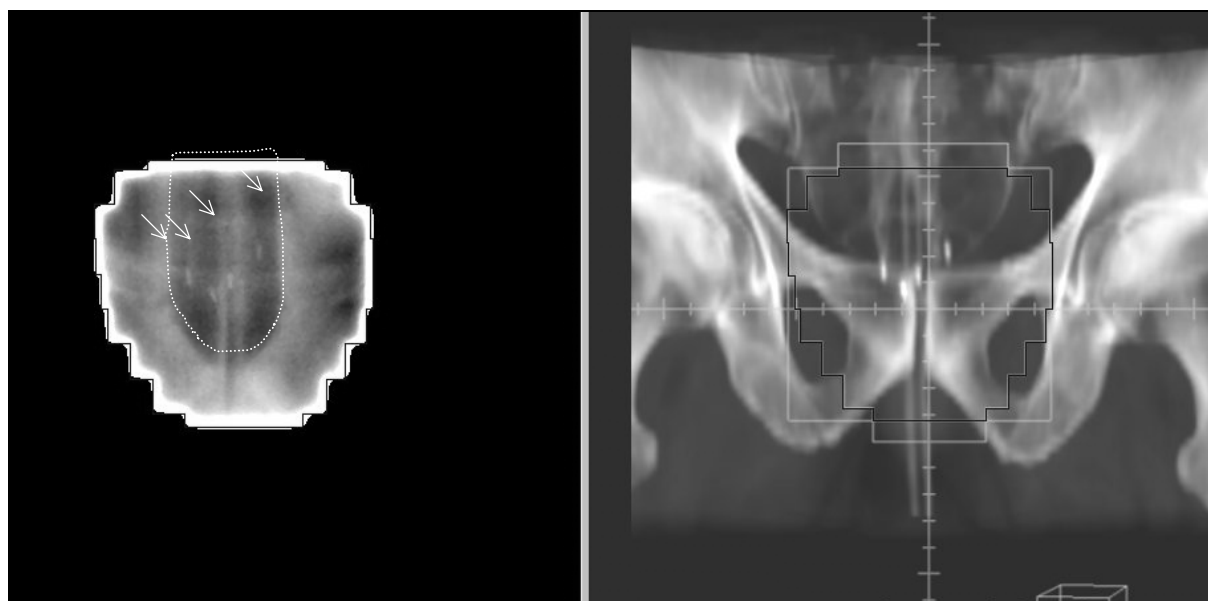
(a)
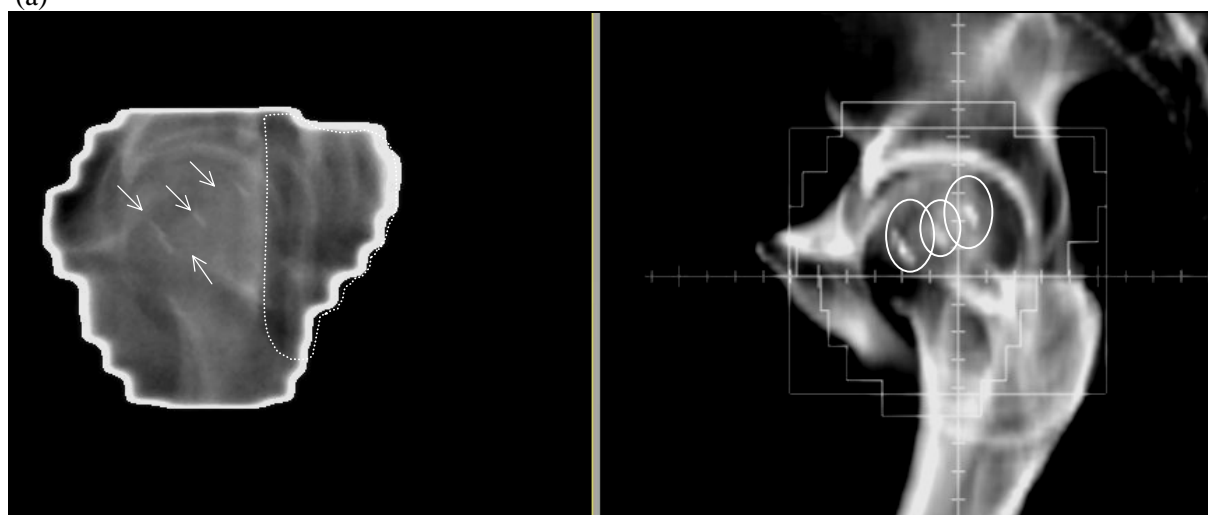
(b)

Fig. 2.
EPID computer screen and reference images (right side) of anterior (a) and left lateral (b) portal images (left side). The four implanted gold markers and the contours of the endorectal balloon are indicated.

The prostate position is measured both relative to the treatment isocenter (denoted as pr-iso) and relative to the bony structures (denoted as pr-bo) to evaluate the internal motion of the prostate, independent of the patient set-up variations. To analyze both the daily patient and prostate position variations, the bony anatomy template and the marker contours derived from the DRR, were displayed overlaying the portal image, and were manually aligned to obtain the best fit. The vector co-ordinates (X for left-right, Y for superior-inferior and Z for anterior-posterior) of the measured patient (i.e. bony structures) and prostate (i.e. markers) displacements, as well as the in-plane rotations in the frontal and saggital plane were displayed on the screen and recorded.

In thirteen randomly chosen patients the position of the four individual markers were measured and compared to the geometric center of the four markers on the DRR, to investigate possible marker migration within the prostate gland during treatment. For four patients, treated with ERB, loops of all treatment fractions were made, i.e., all the consecutive portal images (AP and LL) were displayed as a movie loop.

Patient set-up and prostate position analysis

For each patient, the systematic and random gland translations were calculated for the three orthogonal directions separately. Also systematic and random prostate rotations were measured. The definitions for systematic and random errors, introduced by Bijhold *et al.* (21), were used and calculated for the "No-ERB " and "ERB" group. The standard deviation of the random prostate position variations (denoted as σ_{pr}), derived from the gold markers, is defined as the SD of the day-to-day variations, averaged over all patients in the group. The distribution of systematic prostate deviations is characterized by Σ_{pr}, defined as the standard deviation of the distribution of average prostate deviations per patient. The overall mean prostate deviation, M_{pr}, is the average prostate deviation in one direction over all measured fractions and all patients. The random, systematic and overall mean prostate position relative to the treatment isocenter (denoted as $\sigma_{pr\text{-}iso}$, $\Sigma_{pr\text{-}iso}$ and $M_{pr\text{-}iso}$ respectively) and relative to the bony structures (denoted as $\sigma_{pr\text{-}bo}$, $\Sigma_{pr\text{-}bo}$ and $M_{pr\text{-}bo}$ respectively) were measured. The analysis of the prostate motion relative to the bones is necessary to evaluate the possible immobilizing effect of the ERB.

Off-line EPID-based correction protocol

For interfraction prostate position verification and correction, the so-called No Action Level (NAL) off-line correction protocol was used, as described by de Boer *et al.* (22). With this type of correction protocol systematic errors can be reduced, with a minimum of extra workload and no extra treatment time necessary on the accelerators (20).

For the correction protocol, each patient was positioned and imaged during the first three fractions without setup correction, unless an unexpected large (> 10 mm) prostate deviation was found. Next, the systematic prostate positioning error was estimated from the mean error of these three fractions, and the correction was applied from fraction 4 onwards. A patient set-up correction was performed by moving the couch according to the deviations found in the three orthogonal directions. Due to limitations in table parameters readout, corrections were rounded to integer millimeters. A correction of 1 mm in any one direction (1D) was considered not relevant, and therefore not applied. After each correction, a set of portal images was made to check the executed correction.

From the second week on, the prostate positioning was checked weekly by digital portal images to deal with deviations that may arise during the course of the treatment, due to possible time trends (e.g. due to rectal and bladder irritation). Now, a correction was applied if the 3D vector length (averaged over 3 measurements) exceeded an action level of 5 mm. In this 3D vector, the measured 1D deviations in the three orthogonal directions are quadratically combined ($3D = \sqrt{(SI^2 + AP^2 + LR^2)}$) (6).

For the analysis, the prostate position variations (including both set-up variations and internal prostate motion) were calculated for each individual patient and for the whole group of patients. Retrospectively, it was also possible to calculate these deviations with the corrections undone, i.e. as if patients had been irradiated without application of the correction procedure. To evaluate the effect of the correction protocol, the mean 3D prostate gland deviation was calculated (one value for each patient) as the average of the 3D vector lengths of the deviations over all measured fractions with corrections and with corrections undone.

The random and systematic variations were compared applying t-tests and F-tests, respectively. Analysis of variance (ANOVA) tests were applied to analyze the influence of different factors (presence of endorectal balloon, application of corrections). For the statistical analysis the Stata package was used (release 8, Stata Corporation, College Station, Texas, USA).

Workload, personnel and patient experiences

For both patient groups an estimation of additional workload was made. Per patient the extra time needed (balloon handling, image acquisition and set-up correction) on the accelerator and time for analysis and administration was recorded. Also specific experiences from patients treated with an ERB, and the attending therapists were collected.

RESULTS

Gold markers: toxicity, visibility and migration

The implantation of the gold markers was performed by one experienced urologist (J.W.). Since 2001, beside this study, approximately 180 patients have undergone this procedure without significant problems. The procedure takes five minutes per patient. Insertion of gold markers in the reviewed 53 patients caused no major acute complications. Ten patients observed transient haematuria, five transient heamatospermia and twenty-nine patients suffered from slight rectal bleeding on the day of implantation. In two patients, one gold marker was not visible on the pelvic X-ray image and was lost by insertion of the marker in the urethra or urinary bladder, and excreted by urinary miction. All portal images could be registered for both bony

landmarks and gold markers (Fig. 2). In total 1397 treatment fractions (2794 portal images) were evaluated, i.e. a mean of 27 measurements per patient.

In a randomly chosen subset of 13 patients, intraprostatic marker migration, over the whole treatment, was investigated. The position of each implanted marker was matched to the corresponding marker on the reference image for each fraction. From these data, the displacement of an individual marker, relative to the geometric centre of all markers, could be derived. The average vector length of the displacement of an individual marker was 1.0 ± 0.6 mm. The standard deviation (SD) of a marker position, relative to the geometric centre, over all fractions, averaged over the 13 patients, was 0.4, 0.5, and 0.8 mm (1SD) in the LR, SI and AP directions, respectively. These measured displacements have to be corrected for the localization precision for the individual markers. The localization precision could be estimated from the interobserver variation for matching the marker position to the reference image. This variation was relatively small: 0.3 mm in the LR-direction, 0.4 mm in both the SI- and AP-direction. With this correction by quadratic subtraction, for the localization accuracy, it can be stated that the migration of markers, during the observed 7 weeks of treatment, was less than 1 mm and hence considered to be negligible.

Prostate displacement relative to the pelvic bones: internal motion

As displayed in Table 1, the internal prostate motion, measured relative to the bony structures, appeared to be comparable for both patient groups, irrespective of the use of an ERB. The systematic deviation (Σ_{pr-bo}) ranged from 0.7 – 2.8 mm (1 SD) for the No-ERB group, and 1.0 – 3.0 mm (1 SD) for the ERB group.

	Σ_{pr-bo} Systematic (1 SD)	σ_{pr-bo} Random (1 SD)	M_{pr-bo} **Mean**	Σ_{pr-bo} Systematic (1 SD)	σ_{pr-bo} Random (1 SD)	M_{pr-bo} Mean
	No ERB (N=30)			**ERB (N=22)**		
x (left - right)	0.7 mm	1.3 mm	- 0.6 mm	1.0 mm *(p= 0.07)*	1.5 mm *(p=0.19)*	- 0.5 mm
y (sup - inf)	2.8 mm	1.9 mm	0.3 mm	3.0 mm *(p= 0.71)*	1.8 mm *(p= 0.41)*	0.7 mm
z (ant - pos)	2.2 mm	2.5 mm	-1.3 mm	2.5 mm *(p=0.51)*	2.8 mm *(p=0.39)*	- 0.7 mm

Table 1.
Internal gland motion: prostate displacements relative to bony structures, without balloon (No-ERB) and with balloon (ERB).
Abbreviations: Σ_{pr-bo} = systematic deviation; σ_{pr-bo} = random, day to day, deviation; M_{pr-bo} = overall mean deviation

The random day-to-day prostate position variation (σ_{pr-bo}) ranged from 1.3 – 2.5 mm (1 SD) for the No-ERB group and 1.5 – 2.8 mm (1 SD) for the ERB group. The day-to-day variation was largest in the anterior-posterior direction (i.e. towards the rectum): 2.5 mm and 2.8 mm for the No-ERB and ERB group, respectively. Application of statistical tests indicates no significant difference between the ERB and No-ERB groups: the p-values listed in Table 1 do not reach significance, neither for systematic deviations (Σ_{pr-bo}) nor for random variations (σ_{pr-bo}).

The overall mean deviation of the prostate position relative to bone ($_{pr-bo}$) was ≤ 1 mm, except in the AP direction for the No-ERB group (1.3 mm). In Fig. 3, all the measured prostate displacements in the sagittal plane (i.e. superior-inferior and anterior-posterior direction), with and without ERB are displayed.
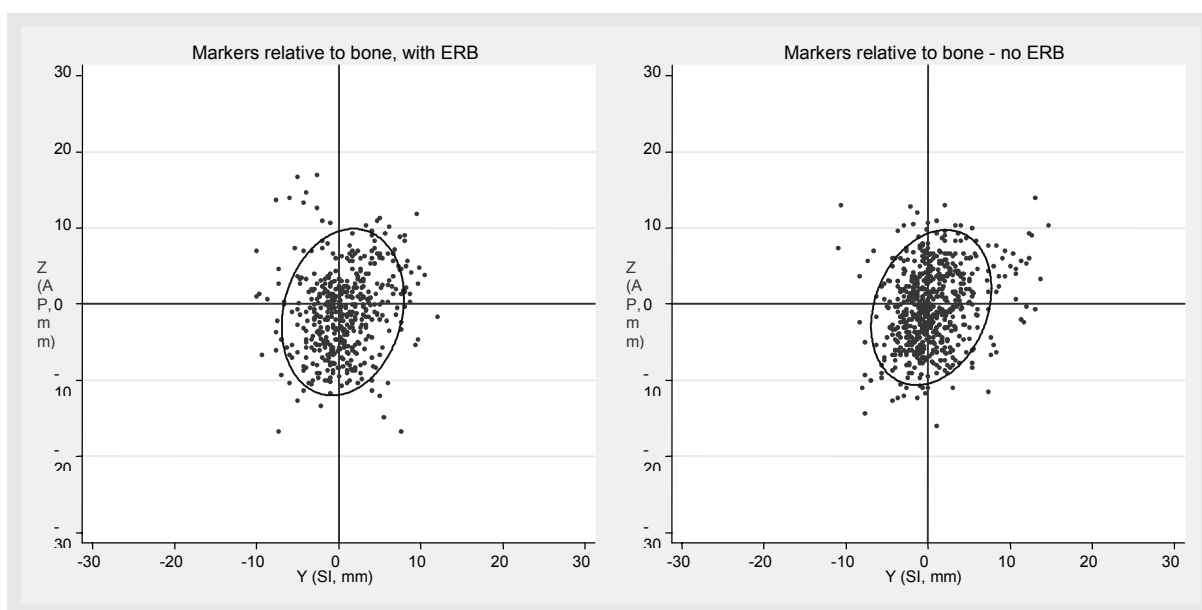
Fig. 3.
Scatter plot of the internal prostate displacements, relative to the bony structures, in the sagittal plane, with ERB (left) and without ERB (right). Each point represents the displacement measured during a treatment fraction, after correction. The superimposed ellipse indicates the 95 % confidence region of the marker displacements (solid line).

Also this representation of the results, as indicated by the 95 % confidence region calculated from the data, indicates that there is no difference in the geometrical variations between the No-ERB and ERB group.

Prostate displacement relative to the treatment isocenter

In Table 2, the remaining prostate position variations, after correction, relative to the treatment isocenter are displayed.

After Off-line Correction	$\Sigma_{\text{pr-iso}}$ Systematic (1 SD)	$\sigma_{\text{pr-iso}}$ Random (1 SD)	$M_{\text{pr-iso}}$ **Mean**	$\Sigma_{\text{pr-iso}}$ Systematic (1 SD)	$\sigma_{\text{pr-iso}}$ Random (1 SD)	$M_{\text{pr-iso}}$ Mean
	No ERB (N=30)			**ERB** (N=22)		
x (left -right)	1.6 mm (p= 0.02)	2.8 mm	- 0.3 mm	1.3 mm (p= 0.005)	3.1 mm	0.0 mm
y (sup -inf)	1.3 mm (p< 10^{-4})	2.3 mm	0.2 mm	1.8 mm (p= 0.003)	2.6 mm	1.3 mm
z (ant - pos)	1.5 mm (p< 10^{-4})	4.3 mm	-0.6 mm	1.8 mm (p= 0.0001)	4.7 mm	- 0.4 mm

Table 2.
Prostate displacements relative to treatment isocenter, without balloon (No-ERB) and with balloon (ERB), after correction (a). Retrospectively calculated systematic deviations for both groups, with corrections undone (b). The p-values given for the systematic displacements are the results of F-tests comparing the deviations with and without corrections.
Abbreviations: $\Sigma_{\text{pr-iso}}$ = systematic deviation; $\sigma_{\text{pr-iso}}$ = random, day to day, deviation; $M_{\text{pr-iso}}$ = overall mean deviation

Here, the systematic and random prostate deviations were comparable for both patients groups as well. The systematic deviation ($\Sigma_{\text{pr-iso}}$) ranged from 1.3 – 1.6 mm (1 SD) for the No-ERB group and 1.3 – 1.8 mm (1 SD) for the ERB group. The random day-to-day prostate deviation ($\sigma_{\text{pr-iso}}$) ranged from 2.3 – 4.3 mm (1 SD) for the No-ERB group and 2.6 – 4.7 (1 SD) mm for the ERB group. In the ERB and No-ERB group, both systematic and random variations were largest in the anterior-posterior direction. The overall mean prostate position relative to the treatment isocenter ($M_{\text{pr-iso}}$) was $\leq$ 1 mm, except for the superior-inferior direction (1.3 mm) in the ERB group. Application of an F-test to compare the systematic variations after corrections and with the corrections undone shows that that the effect of the corrections is highly significant, for both the No-ERB and ERB group and for all directions.

In Fig. 4, the means and the standard deviations of the prostate position relative to the treatment isocenter are displayed for both groups per patient.
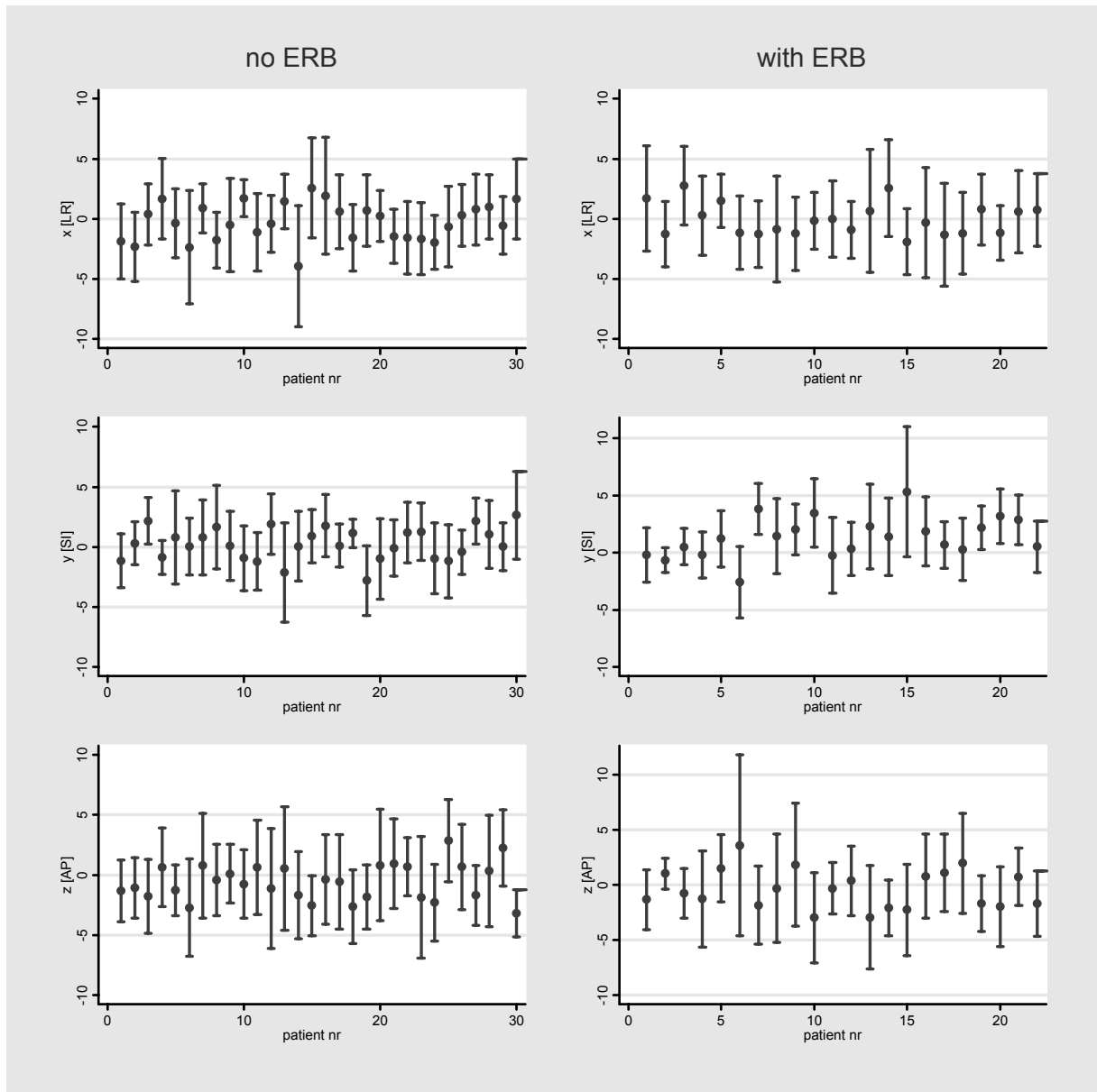
Fig. 4.
Mean prostate displacements per patient in the three axial directions, after off-line correction, without (No-ERB) and with endorectal balloon (ERB). The error bars represent the standard deviations (1SD), i.e. the random, day-to-day, interfractional prostate gland motion.

The standard deviations represent the random variations for each patient. With or without balloon, there was no overall difference in the day-to-day position of the prostate gland. Within each group there were patients with relative large and small random deviations in the individual directions, ranging from ≈ 1 mm up to > 5 mm, irrespective of the presence or absence of the ERB. Rotations around the AP axis are practically absent. The respective

random and systematic rotations around the LR axis appear to be 0.4 and 0.9 degrees and 0.7 and 1.3 degrees for the No-ERB and ERB group, respectively.

Evaluation of daily portal images and movie loops

Evaluation of the daily portal images clearly showed presence of transient and passing gas in the rectum in both patient groups, resulting in deformations of the outer rectal wall contour. For the ERB group, it appeared that the position of the balloon varied throughout the treatment (i.e. depth of insertion) and gas bubbles could be observed beside the balloon, giving an extra extension of the rectum and displacement of the prostate. In both groups, in 10 – 20 % of all daily treatment fractions the portal images showed passing gas and air bubbles in the rectum. As an example, the measured prostate deviations, relative to the bony structures, for one patient with ERB (Fig. 5a), and four portal images are displayed (Fig. 5b-e). Although a correction was performed, from fraction four on, there was still a large interfraction day-to-day prostate position variation throughout the next treatment fractions. In fraction number five, the portal images (Fig. 5b and 5d) showed evidently the presence of a gas bubble around the ERB. This probably caused the large deviations, mainly in the LR (5 mm) and AP (3 mm) directions. In fraction 9, no gas bubble, beside the ERB, was present (Fig. 5c and 5e). Here the deviations were relatively small ($\leq$ 1 mm) .
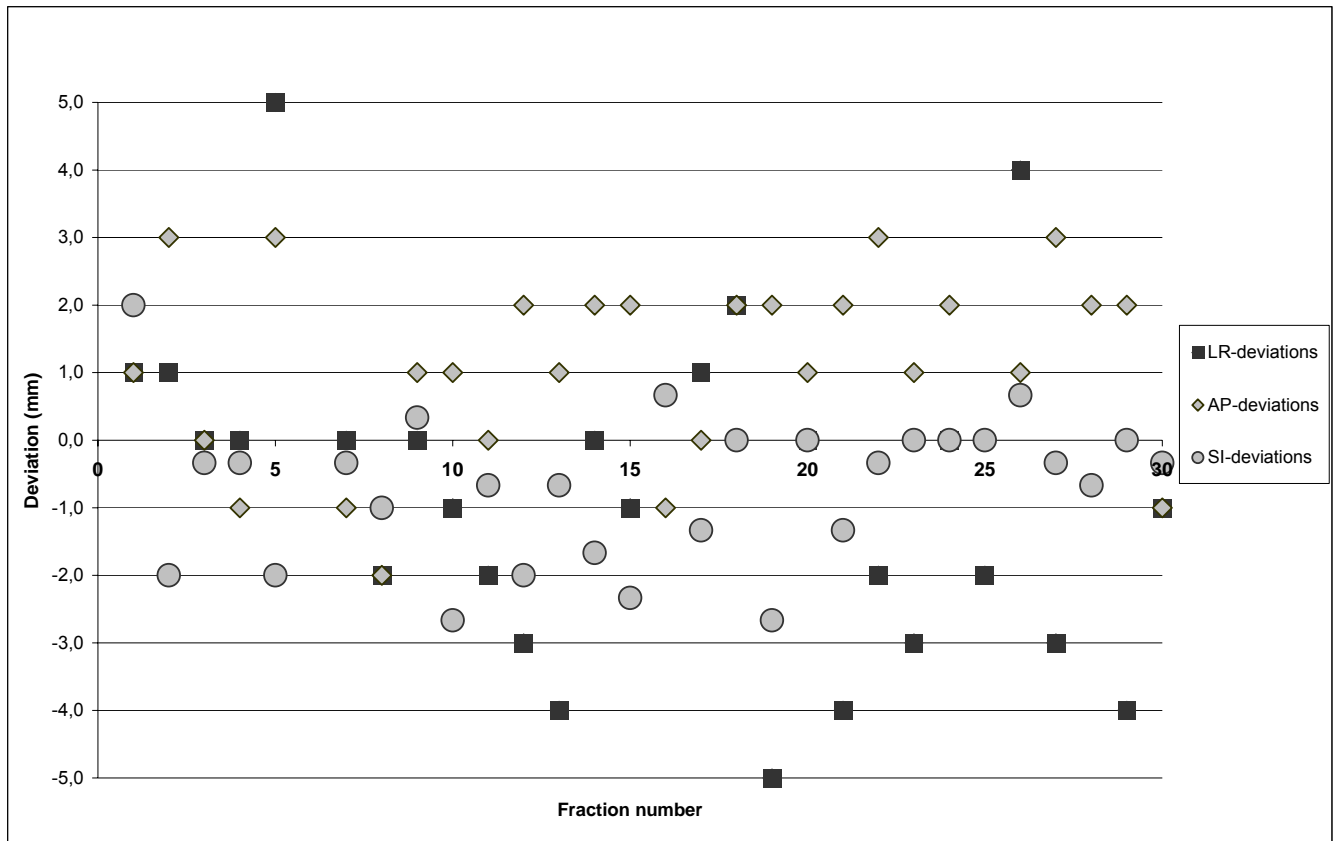
(a)
Fig. 5.
Measured prostate position deviations, relative to the bony structures, in the LR, SI and AP direction for all treatment fractions, for one patient, treated with an endorectal balloon. The measured deviations for these fractions are indicated (a). Portal images for fraction number 5 (b, c), fraction number 9 (b, d) are displayed. The endorectal balloon and surrounding air are indicated, as one contour (dashed line).

(b)

(c)

Fraction 5

Fig 5 (d)

Fraction 9
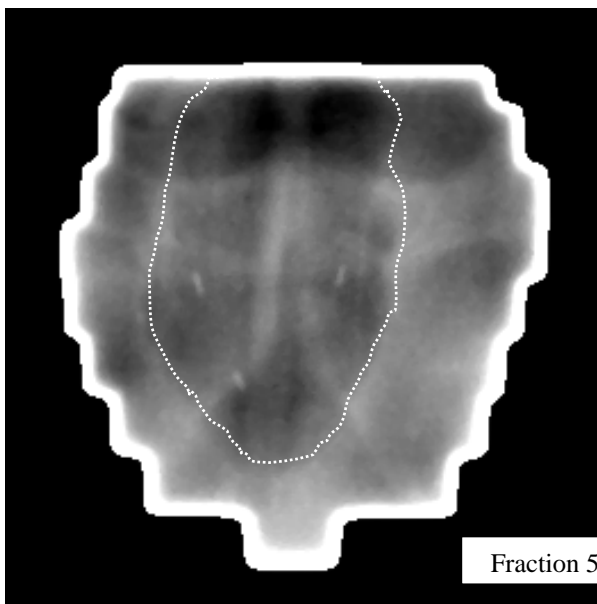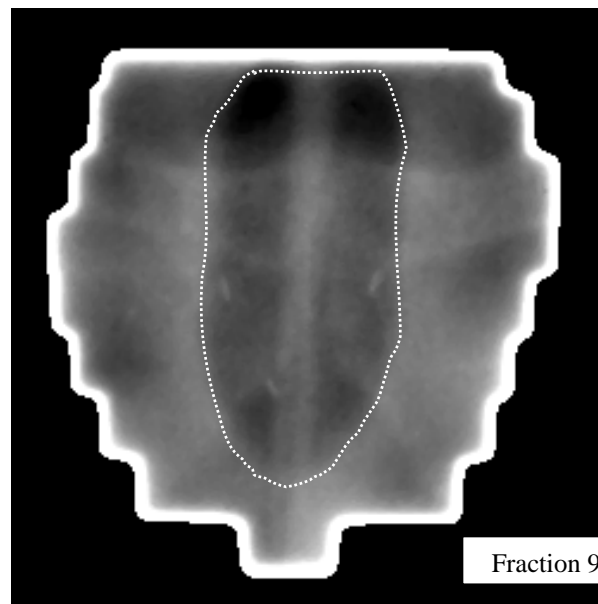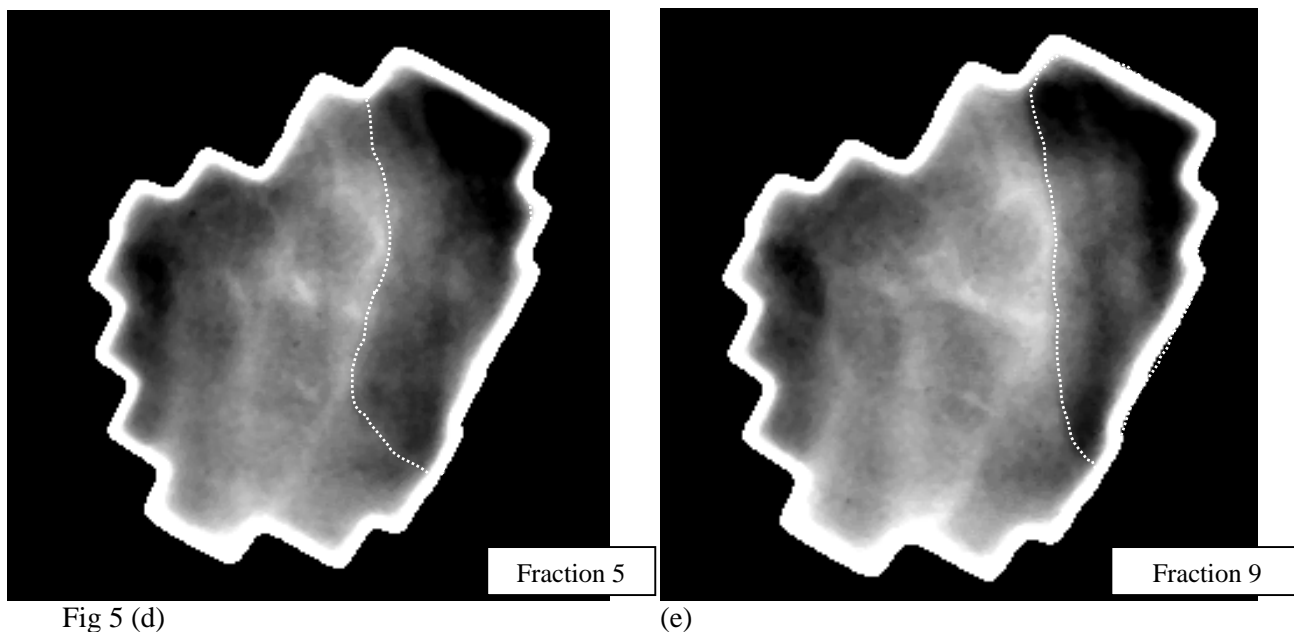
(e)
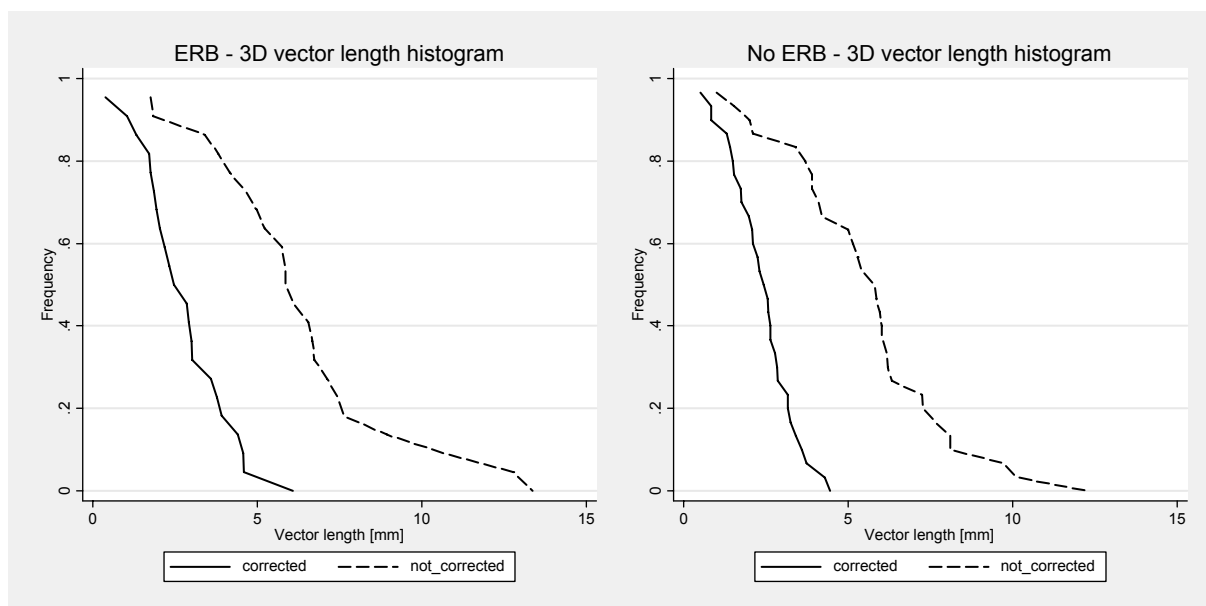
Fig. 6.
Cumulative frequency distributions of mean 3D prostate displacements (vector lengths), for ERB group (left) and the No-ERB group (right). The solid curves represent the distribution of vector lengths after (offline) position correction; the dotted curves are the distributions of vector lengths without correction.

Effect of off-line correction on prostate position

Application of the No Action Level off-line correction protocol reduced the systematic prostate deviations. The average number of corrections per patient throughout the treatment, according to the described off-line protocol, was nearly equal for the No-ERB and the ERB group; 1.6 and 1.8, respectively. Retrospectively, the systematic prostate displacements, relative to the isocenter were calculated for both groups, with the corrections undone (Table

3b). In comparison with the data from Table 3a, there is a reduction of fifty percent in the systematic interfraction prostate deviation due to the correction protocol, for all orthogonal directions and in both investigated patient groups. For example, in the anterior-posterior direction the resulting systematic prostate deviation is reduced for the no-ERB group from 3.9 mm to 1.5 mm (1 SD), and for the ERB group from 4.5 mm to 1.8 mm (1 SD). In Fig. 6, the mean 3D displacements are displayed in a cumulative frequency distribution, for the ERB and No-ERB groups. The applied correction strategy had a comparable effect in both groups. The overall mean 3D deviation (vector length) was reduced from 6.4 mm to 2.8 mm for the ERB group and from 5.2 mm to 2.4 mm for the No-ERB group, respectively. After correction, the percentage of patients, having a mean 3D deviation ≥ 5 mm, was reduced from 68 % to 5 % for the ERB group, and from 67 % to 0 % for the No-ERB group. There was, as expected, no reduction of random deviations due to this off-line protocol.

The effectiveness of the off-line corrections in reducing the systematic prostate position variations and the lack of effect of the endorectal balloon was confirmed by ANOVA tests. The off-line corrections in the LR and SI directions proved to be significant at $p = 0.02$ and $p = 0.0002$, respectively. The higher p-value ($p = 0.07$, not statistically significant) in the AP-direction might be caused by the fact that the random variations (due to prostate motion) are highest in this direction. The presence of the balloon was not significant in the LR and AP directions and had a p-value of 0.027 in the SI-direction, associated with a somewhat higher value of $\Sigma_{pr\text{-}iso}$ in the ERB group.

Workload, personnel and patient experiences

The application and removal of the ERB was performed by trained therapists. Every day a new ERB was used and lubrication facilitated a smooth rectal introduction. Overall patients' acceptance of the ERB was good. Extra time was taken to explain the background of the ERB to the individual patient. Eighteen of the 22 ERB patients experienced more local anal irritation, grade 1 or higher, compared to the No-ERB group. This resolved within 3 weeks after treatment, in all patients. In two cases lidocaine cream was prescribed and scored as grade 2 anal irritation. One patient, with hemorrhoids, stopped using the ERB, due to excessive anal irritation and hemorrhoid bleeding and was scored as grade 3 irritation. This patient was excluded from the analysis. For this patient, a new CT-scan, without ERB, and treatment plan were made and patient resumed treatment within two days. Since then, painful and bleeding hemorrhoids were considered to be a contra-indication for the ERB.

On the accelerator, an extra three minutes per treatment fraction were necessary for the ERB procedure. For a No-ERB prostate treatment, a standard time slot of 10 min is booked. For the ERB prostate treatment, we now book 15 min per fraction. As described

earlier, the off-line portal imaging and correction protocol did not prolong our treatment time on the accelerator. For the correction procedure, in total about 40 min per patient is needed for administrative preparation, verification, and data registration (20).

DISCUSSION

In this study, the interfraction prostate gland position variations were followed on a daily basis by registration of fiducial gold markers, in patients treated with and without an ERB. In a review paper by Langen *et al* (1), a summary is given of known prostate motion data. The SDs for prostate motion, relative to the bony structures are given, but no separate data are given for the systematic and random organ displacements. In the present study, both random and systematic prostate gland displacements were calculated, because of the different impact on the choice of correction strategy and the impact on choice of treatment margins. Stroom *et al.* (18) and Van Herk *et al.* (19) proposed recipes for calculation of the CTV – PTV margins to account for both systematic (Σ) and random errors (σ). Their margin rules were $2\Sigma + 0.7\sigma$ and $2.5\Sigma + 0.7\sigma$, respectively. Thus, reduction of the systematic prostate displacement has the largest influence on the margin required.

Fiducial gold markers

To evaluate the daily prostate motion, fiducial gold markers were implanted in the prostate gland. This has been proven to be a safe and reliable method (5-10). We encountered no serious complications so far in over 180 patients. The insertion can be performed in about five minutes by an experienced urologist. One of the major concerns was if the markers would migrate over the course of treatment. Like other investigators, we found no significant marker migration (23;24). The gold markers are well visible on the portal images and trained therapists can execute quickly and accurately the image registration.

Endorectal balloon and internal prostate motion

Other groups have reported previously about the clinical benefits of different types of ERB's, in terms of patients acceptance and reduced rectal toxicity (12-17;25). Teh *et al.* (14 ;15) investigated the combination of IMRT and an ERB. The procedure was feasible and produced favorable acute toxicity profiles. Data derived from McGary *et al.* (12) showed, in 10 patients with a rectal balloon in situ, an internal prostate motion, measured by CT-CT image fusion and relative to the bony anatomy, for the superior-inferior direction with an overall mean of 0.43 mm and a standard deviation of 3.54 mm, representing the systematic error. Motion in the AP and LR direction was minimal, on the order of the measurement uncertainty ($\approx$ 1 mm). No specific data were given on the distribution of the systematic and random errors for the

separate directions (12). Patel *et al.* (17) demonstrated the clinical feasibility and the rectal wall sparing effect of an ERB. In seven patients, the prostate motion, relative to the pelvic bones was measured. The mean standard deviations, representing the systematic errors, were 2.6 and 3.1 mm in the AP and SI directions, respectively. The LR deviation was 1 mm (1 SD) (17). These data are comparable to our data (see Table 1). Also here, no data were presented on the random, day-to-day variation. D'Amico *et al.* (13) found a reduction of <u>intra</u>fractional prostate motion, during a measured 2-min time interval, by an ERB. The maximum displacement, for any direction, was reduced from 4 to 1 mm during the 2-min time interval, by applying an ERB. The mean displacement was reduced from 1.8 to 1.3 mm. No data of interfraction motion were presented (13). The group of Wachter *et al.* (16) in Vienna has a large experience in the use of an ERB for daily prostate treatment. With the use of their balloon, the maximum displacement larger than 5 mm, in the AP direction, was reduced from 8/10 patients to 2/10 patients. Displacements in other directions could not be measured (16).

Effect of endorectal balloon and correction protocol

In our study, we analyzed the effect of an ERB on the systematic and random, day-to-day, interfraction prostate gland displacements, for all three directions in combination with an EPID-based correction protocol. The effect of the ERB on the position of the seminal vesicles could not be determined. To evaluate this, markers should be implanted into the seminal vesicles or repeated daily CT scans should be obtained.

It was expected that introduction of the ERB could in addition reduce the internal prostate motion, mainly by reducing the random day-to-day variation. First, it was expected that motion could be reduced by fixation of the prostate gland between the pubic bone and the air-filled balloon, as seen in Fig. 1b. Secondly, the filling of the rectum by the balloon with a fixed amount of air, should eliminate the prostate motion due to variable rectum volume, e.g. by stool and or gas. However, our data show that the random day-to-day variation of the prostate position relative to the bony structures is <u>not</u> reduced with a balloon (Table 1). Especially for the AP direction, the random error is still relatively high, 2.8 mm (1 SD), compared to 1.5 mm and 1.8 mm for the LR and SI directions, respectively. For both groups, with or without an ERB, the overall mean internal organ motion, determined over all measured fractions, is low (0.5 – 1.5 mm). With balloon, for all directions, the overall mean displacement is less than 1 mm, comparable to the data of McGary *et al.* (12) and Teh *et al.*(15). This means that, although the overall prostate displacement is low, the interfraction displacements can be considerably high, as demonstrated in this study.

The movie loops of all daily portal images of the investigated patients showed in 10 – 20 % of the treatment fractions clearly the presence of gas bubbles, equally in both groups, (Fig. 5). So, the assumption that an ERB gives a constant rectal filling, and therefore

immobilizes the prostate gland, could not be confirmed in this study. The day-to-day interfraction prostate motion is still present, mainly in the direction towards the rectum. This is in agreement with observations form Husband *et al.* (26). In their study, the ERB used for MR imaging did not reduce or prevent significant rectal activity, causing prostate motion. So also the presence of an ERB may cause rectal wall activity and possibly pelvic muscle tension alterations, causing prostate motion.

For the prostate position, relative to the treatment isocenter (Table 2), the systematic errors with or without balloon are reduced to less than 2 mm (1 SD), due to the NAL off-line correction protocol. With a minimum of extra workload and less than 2 corrections per patients, it was possible to reduce the systematic organ displacement by a factor two, to 1.3 – 1.6 mm (1 SD) (Table 2). This is in line with data from Nederveen *et al* (8). Because the corrections are applied on the fiducial markers, Σ_{pr-iso} appears to be smaller than Σ_{pr-bo}. The random, day-to-day displacements remain relatively large; 3.1 mm, 2.6 mm and 4.7 mm (1 SD) for the LR, SI and AP directions, respectively. That σ_{pr-iso} comes out somewhat larger than σ_{pro-bo} can be understood from the fact that the former contains both the set-up variations and the variations due to internal prostate motion. Again, the day-to-day variation for the AP direction, towards the rectum, is the largest. A treatment planning study has shown that prostate motion in this direction can cause a significant reduction of dose to the CTV (27). Fig. 3 and 4 also show no marked differences between the group with and without rectal balloon. Also rotations did not differ in both groups. In Fig. 4, the individual mean and random displacements for all three directions are displayed; in both groups there are great inter-individual differences in organ motion.

The investigated ERB, originally designed for MR imaging, was not developed for specific prostate immobilization during radiotherapy. Modification of shape (i.e. more anatomic conformation or greater length), amount of air inflated, or ERB in combination of medication to reduce bowel movements, may be opportunities to reduce the presence of gas and extra bowel motion to reduce the day-to-day prostate motion. This should be topic of further investigation.

As shown in the present study, an off-line correction protocol is not suitable to correct for random (day to day) prostate displacements, observed with this ERB. On-line correction, with organ position verification and correction prior to the actual treatment, is apparently the only way to reduce these random prostate position variations. Daily prostate localization by the so-called BAT ultrasound system (NOMOS corporation, Sewickley, PA), is widely used for on-line non-invasive prostate verification and correction (11). Recently, van den Heuvel *et al.* assessed the efficacy and accuracy of this system. They concluded that the ultrasound-based

adjustment showed only significant improvement in the superior-inferior direction, but not for the other two directions (28).

Increasingly, implanted fiducial gold markers in combination with daily portal imaging are used for verification and correction strategies. On-line correction strategies, daily executed, have been tested in clinical practice and have shown to be effective in reducing the positioning variations (6). In Nijmegen we have initiated such an on-line marker-based correction protocol. Reliable automated marker detection systems have been developed and are helpful to reduce the workload of these daily online procedures (29).

Although the ERB appeared not to be effective in immobilizing the prostate or reducing position variations, it can play an important role in the further development of radiation treatment of prostate cancer as it may still be an effective tool in reducing rectal toxicity by pushing the dorsal rectal wall away from the PTV (30). These possible positive effects of the ERB will be a topic of future studies.

CONCLUSIONS

This study investigated the effect of an ERB on the daily prostate motion. Implanted gold markers and an off-line EPID-based correction protocol were used to verify and correct the prostate gland position in a group of patients treated with an ERB and a group irradiated without an ERB. The correction protocol reduced effectively the systematic errors to less than 2 mm (1 SD). Although the overall mean prostate position deviation was less than 1 mm, large random, interfraction prostate displacements, were observed, even with an ERB inserted. These large variations can be partly explained by the presence of gas and stool in the rectum besides the balloon. The largest day-to-day displacement was in the anterior-posterior direction, towards the rectum: up to 4.7 mm (1 SD). These random deviations in this direction are high in relation to the post-correction systematic prostate position deviations.

REFERENCES

1. Langen KM, Jones DT. Organ motion and its management. Int J Radiat Oncol Biol Phys 2001;50(1):265-78.

2. Van Herk M, Bruce A, Kroes AP, Shouman T, Touw A, Lebesque JV. Quantification of organ motion during conformal radiotherapy of the prostate by three dimensional image registration. Int J Radiat Oncol Biol Phys 1995;33(5):1311-20.

3. Storey MR, Pollack A, Zagars G, Smith L, Antolak J, Rosen I. Complications from radiotherapy dose escalation in prostate cancer: preliminary results of a randomized trial. Int J Radiat Oncol Biol Phys 2000;48(3):635-42.

4. Lattanzi J, McNeely S, Hanlon A, Das I, Schultheiss TE, Hanks GE. Daily CT localization for correcting portal errors in the treatment of prostate cancer. Int J Radiat Oncol Biol Phys 1998;41(5):1079-86.

5. Dehnad H, Nederveen AJ, van der Heide UA, van Moorselaar RJ, Hofman P, Lagendijk JJ. Clinical feasibility study for the use of implanted gold seeds in the prostate as reliable positioning markers during megavoltage irradiation. Radiother.Oncol. 2003;67(3):295-302.

6. Herman MG, Pisansky TM, Kruse JJ, Prisciandaro JI, Davis BJ, King BF. Technical aspects of daily online positioning of the prostate for three-dimensional conformal radiotherapy using an electronic portal imaging device. Int J Radiat Oncol Biol Phys 2003;57(4):1131-40.

7. Litzenberg D, Dawson LA, Sandler H, Sanda MG, McShan DL, Ten Haken RK et al. Daily prostate targeting using implanted radiopaque markers. Int J Radiat Oncol Biol Phys 2002;52(3):699-703.

8. Nederveen AJ, Dehnad H, van der Heide UA, van Moorselaar RJ, Hofman P, Lagendijk JJ. Comparison of megavoltage position verification for prostate irradiation based on bony anatomy and implanted fiducials. Radiother Oncol 2003;68(1):81-8.

9. Vigneault E, Pouliot J, Laverdiere J, Roy J, Dorion M. Electronic portal imaging device detection of radioopaque markers for the evaluation of prostate position during megavoltage irradiation: a clinical study. Int J Radiat Oncol Biol Phys 1997;37(1):205-12.

10. Alasti H, Petric MP, Catton CN, Warde PR. Portal imaging for evaluation of daily on-line setup errors and off-line organ motion during conformal irradiation of carcinoma of the prostate. Int J Radiat Oncol Biol Phys 2001;49(3):869-84.

11. Chandra A, Dong L, Huang E, Kuban DA, O'Neill L, Rosen I et al. Experience of ultrasound-based daily prostate localization. Int J Radiat Oncol Biol Phys 2003;56(2):436-47.

12. McGary JE, Teh BS, Butler EB, Grant W3. Prostate immobilization using a rectal balloon. J Appl Clin Med Phys 2002;3(1):6-11.

13. D'Amico AV, Manola J, Loffredo M, Lopes L, Nissen K, O'Farrell DA et al. A practical method to achieve prostate gland immobilization and target verification for daily treatment. Int J Radiat Oncol Biol Phys 2001;51(5):1431-6.

14. Teh BS, Mai WY, Uhl BM, Augspurger ME, Grant WH3, Lu HH et al. Intensity-modulated radiation therapy (IMRT) for prostate cancer with the use of a rectal balloon for prostate immobilization: acute toxicity and dose-volume analysis. Int J Radiat Oncol Biol Phys 2001;49(3):705-12.

15. Teh BS, McGary JE, Dong L, Mai WY, Carpenter LS, Lu HH et al. The use of rectal balloon during the delivery of intensity modulated radiotherapy (IMRT) for prostate cancer: more than just a prostate gland immobilization device? Cancer J 2002;8(6):476-83.

16. Wachter S, Gerstner N, Dorner D, Goldner G, Colotto A, Wambersie A et al. The influence of a rectal balloon tube as internal immobilization device on variations of volumes and dose-volume histograms during treatment course of conformal radiotherapy for prostate cancer. Int J Radiat Oncol Biol Phys 2002;52(1):91-100.

17. Patel RR, Orton N, Tome WA, Chappell R, Ritter MA. Rectal dose sparing with a balloon catheter and ultrasound localization in conformal radiation therapy for prostate cancer. Radiother.Oncol. 2003;67(3):285-94.

18. Stroom JC, de Boer HC, Huizenga H, Visser AG. Inclusion of geometrical uncertainties in radiotherapy treatment planning by means of coverage probability. Int J Radiat Oncol Biol Phys 1999;43(4):905-19.

19. Van Herk M, Remeijer P, Rasch C, Lebesque JV. The probability of correct target dosage: dose-population histograms for deriving treatment margins in radiotherapy. Int J Radiat Oncol Biol Phys 2000;47(4):1121-35.

20. van Lin EN, Nijenhuis E, Huizenga H, van der Vight L, Visser A. Effectiveness of couch height-based patient set-up and an off-line correction protocol in prostate cancer radiotherapy. Int J Radiat Oncol Biol Phys 2001;50(2):569-77.

21. Bijhold J, Lebesque JV, Hart AA, Vijlbrief RE. Maximizing setup accuracy using portal images as applied to a conformal boost technique for prostatic cancer. Radiother Oncol 1992;24(4):261-71.

22. de Boer HC, Heijmen BJ. A protocol for the reduction of systematic patient setup errors with minimal portal imaging workload. Int J Radiat Oncol Biol Phys 2001;50(5):1350-65.

23. Poggi MM, Gant DA, Sewchand W, Warlick WB. Marker seed migration in prostate localization. Int J Radiat Oncol Biol Phys 2003;56(5):1248-51.

24. Pouliot J, Aubin M, Langen KM, Liu YM, Pickett B, Shinohara K et al. (Non)-migration of radiopaque markers used for on-line localization of the prostate with an electronic portal imaging device. Int.J.Radiat.Oncol.Biol.Phys. 2003;56(3):862-6.

25. Ciernik IF, Baumert BG, Egli P, Glanzmann C, Lutolf UM. On-line correction of beam portals in the treatment of prostate cancer using an endorectal balloon device. Radiother Oncol 2002;65(1):39-45.

26. Husband JE, Padhani AR, MacVicar AD, Revell P. Magnetic resonance imaging of prostate cancer: comparison of image quality using endorectal and pelvic phased array coils. Clin.Radiol. 1998;53(9):673-81.

27. Happersett L, Mageras GS, Zelefsky MJ, Burman CM, Leibel SA, Chui C et al. A study of the effects of internal organ motion on dose escalation in conformal prostate treatments. Radiother.Oncol. 2003;66(3):263-70.

28. Van den HF, Powell T, Seppi E, Littrupp P, Khan M, Wang Y et al. Independent verification of ultrasound based image-guided radiation treatment, using electronic portal imaging and implanted gold markers. Med.Phys. 2003;30(11):2878-87.

29. Aubin S, Beaulieu L, Pouliot S, Pouliot J, Roy R, Girouard LM et al. Robustness and precision of an automatic marker detection algorithm for online prostate daily targeting using a standard V-EPID. Med Phys 2003;30(7):1825-32.

30. Nutting CM, Corbishley CM, Sanchez-Nieto B, Cosgrove VP, Webb S, Dearnaley DP. Potential improvements in the therapeutic ratio of prostate cancer irradiation: dose escalation of pathologically identified tumour nodules using intensity modulated radiotherapy. Br J Radiol 2002;75(890):151-61.

Bladder filling variation during radiation treatment of prostate cancer: can the use of a bladder ultrasound scanner and biofeedback optimize bladder filling?

Marcel R. Stam, M.D., Emile N.J.Th van Lin, M.D., Lisette P. van der Vight, B.Sc., Johannes H.A.M. Kaanders, M.D. Ph.D. and Andries G. Visser, Ph.D.

Department of Radiation Oncology

ABSTRACT

Purpose: To investigate the use of a bladder ultrasound scanner in achieving a better reproducible bladder filling during irradiation of pelvic tumors, specifically prostate cancer.

Methods and Materials: First, the accuracy of the bladder ultrasound scanner relative to CT was validated in a group of 26 patients. Next, daily bladder volume variation was evaluated in a group of 18 patients. Another 16 patients participated in a biofeedback protocol, aiming at a more constant bladder volume. The last objective was to study correlations between prostate motion and bladder filling, by using EPID data on implanted gold markers.

Results: A strong correlation between bladder scanner volume and CT volume (R = 0.95) was found. Daily bladder volume variation was very high (1 SD = 47.2%). Bladder filling and daily variation did not significantly differ between the control and the feedback group (47.2% and 40.1% respectively). Furthermore no linear correlations between bladder volume variation and prostate motion were found.

Conclusions: This study shows large variations in daily bladder volume. The use of a biofeedback protocol yields little reduction in bladder volume variation. Even so, the bladder scanner is an easy to use and accurate tool to register these variations.

INTRODUCTION

In most pelvic cancers, better local control is achieved with a higher radiation dose (1-3), however this is limited by the tolerance of the normal tissues (4-9). One way of achieving better local control, without increasing normal tissue damage, is by escalating the dose while conforming the dose distribution and gradient to the target volume. Dose-escalated three-dimensional conformal radiotherapy (3D-CRT) has shown to be effective (9-11) and intensity modulated radiotherapy (IMRT) is very promising (12, 13) in achieving these goals.

Another way of limiting toxicity is by controlling the internal anatomy, e.g. irradiation with a full bladder. With bladder filling part of the bladder moves away from the target volume resulting in a smaller irradiated bladder volume. This has been shown for irradiation of bladder cancer and prostate cancer (14-16). Because a dose-volume relation for bladder toxicity exists, one can increase the prescribed dose while maintaining the same bladder toxicity probability (4, 5, 13, 14). Furthermore, a full bladder moves the small intestine out of the irradiation field (17, 18). As a result of the strong dose-volume relation for small bowel toxicity, this also leads to a decrease of intestinal toxicity, e.g. chronic diarrhea (4, 8). For these reasons, patients, who have to be irradiated for a pelvic tumor, are asked to have a full bladder during irradiation. However, large variations in bladder volume throughout a treatment period have been found (14, 15, 19-22). The observed variations cause a problem for the estimation of dose volume histogram based toxicity probabilities, because this assessment is only based on one measurement. (14, 15). Furthermore, large bladder volume variations also increase interfraction motion of organs like the prostate and the uterus (19-21, 23-26).

To date, no reports about bladder volume variation measured on a daily basis have been published. Nor have there been studies striving to achieve a more constant bladder filling, by using biofeedback. The main goal of this study was to quantitate bladder filling variation on a day by day basis during irradiation, using a portable ultra-sound based bladder volume scanner (BS). This machine was originally developed and validated for the measurement of bladder residue after micturition. Therefore the first objective was to validate the BS for larger bladder volumes. The next objective was to evaluate the usefulness of a biofeedback protocol, in achieving a more constant full bladder. Results of this protocol were compared to results from patients that were treated without biofeedback. In order to have a homogeneous patient population, a cohort of prostate cancer patients was chosen. The last goal was to evaluate the relationship between bladder filling variation and prostate displacement.

METHODS AND MATERIALS

Patients

From April 2003 until August 2005, 60 prostate cancer (T1-3N0M0) patients were included in the study. From all patients informed consent was obtained. In the BS validation phase 26 patients were enrolled. These patients were selected if curative (primary or salvage) radiotherapy was planned. The remaining 34 patients (Table 1) participated in the intervention phase of the study. Patients were specifically selected on their ability to maintain a full bladder.

	Control group *No. (%)*	Feedback group *No. (%)*
Gleason grade		
4-6	11 (61)	8 (50)
7	4 (22)	5 (31)
8-10	3 (17)	3 (19)
cT- Stage (TNM 6th ed.)		
1	3 (17)	3 (19)
2	8 (44)	4 (25)
3	7 (39)	9 (56)
PSA		
0-10	8 (44)	7 (44)
10-20	8 (44)	3 (19)
>20	2 (11)	6 (38)
Acute toxicity (RTOG/EORTC(28))		
GU		
0	3 (17)	3 (19)
1	13 (72)	10 (62)
2	2 (11)	3 (19)
GI		
0	5 (28)	2 (13)
1	7 (39)	9 (56)
2	6 (33)	5 (31)
Age mean (range)	70.7 (58-78)	70.0 (56-78)

Table 1
Patient characteristics for the control and feedback group. With respect to these characteristics, no significant differences between both groups were found.

Main exclusion criteria were disorders possibly interfering with correct bladder scanning (Table 2). Of these 34 patients, 16 were given daily feedback. The results of this group were compared to those of the 18 patients who did not receive feedback. Assignment to a group was done on a consecutive basis before the patient was asked to participate.

Inclusion	Exclusion
Prostate carcinoma	Micturition frequency > 1/h
Primary curative radiotherapy	Nycturia >4x
Gold marker insertion possible	Urinary incontinence
Informed consent	Median laparotomy scar interfering with bladder scanning
	Aberrant bladder form (e.g. diverticula)
	Lymfocele interfering with bladder scanning
	Social or psychological problems interfering with protocol compliance

Table 2
Inclusion and exclusion criteria.

Patient preparation and treatment

All patients received three to six months neo-adjuvant hormonal therapy. Under transrectal ultrasound guidance, four fine gold markers (1 mm diameter, 7 mm length) were inserted into the prostate by an urologist. After at least one week, to resolve swelling of the gland as a result of marker implantation, a planning CT scan (AcQsim® spiral CT; Philips medical systems, Bothell, WA, USA) was obtained at 3 mm slice thickness. According to protocol (as in many other centers in the Netherlands) patients were advised to have a comfortably full bladder prior to CT scanning and daily treatment. A "comfortably full" bladder is described by the physicians as having definite but easily tolerable micturition urge. CT scanning and radiation treatment were performed with patients in a supine position. For more details on patient positioning en treatment setup see van Lin *et al.* (27). A beams-eye-view based 3D-conformal treatment plan (orthogonal 4-field technique) was designed. Treatment planning was done with Pinnacle3® version 6.2b (Philips medical systems, Andover, MA, USA). The planning target volume consisted of the prostate only or prostate and seminal vesicles with a 7 mm 3D margin. Prescribed dose was 67.5 Gy to the isocentre, in 30 fractions (four times a week). Patients were seen weekly by the radiation oncologist, and acute urinary and rectal toxicity was scored using the RTOG / EORTC scale (28).

Bladderscan measurement validity

For bladder volume measurements, a portable automated ultrasound based urinary bladder volume scanner (BS) was used (BVI 3000 BladderScan®; Diagnostic Ultrasound Europe B.V., IJsselstein, The Netherlands). This device is equipped with a digital display screen and a handheld scanning head. The scanning head is positioned at the midline above the pubic symphysis (Fig. 1). When activated, the 2-MHz   Fig. 1 *Photograph of the bladderscan*

.transducer rotates automatically by 15° increments and provides 12 cross-sectional areas. From these cross-sectional areas the bladder volume is calculated automatically. This machine was originally developed to measure bladder residue after micturition. Therefore, we first tested the accuracy of the bladder scanner in our patient population (with a larger variation in bladder volume). As the gold standard the bladder volume derived from the planning CT scan (denoted as VCT) was used. Delineation of the bladder on the CT scan was performed by the attending physician and checked by one observer (M.S.).

BS measurements were made at most ten minutes before the planning CT scan. Two trained technologists each performed three BS measurements. The mean of these measurements will be denoted as $V_{bl\text{-}scan}$. For evaluating the correlation between $V_{bl\text{-}scan}$ and V_{CT}, linear regression analysis was performed. Bladderscan interobserver variability (denoted as $\mathbf{\Delta}_{inter}$) was defined as the absolute value of (A-B)/C*100%. Where A and B are the mean of the measurements of respectively technologist A and technologist B for one patient. C is the mean of measurements A and B. BS intra-observer variability (denoted as $\mathbf{\sigma}_{intra}$) was defined as $SD_{measurements}/Mean_{measurements}*100\%$ for one observer and one patient.

Bladder volume measurement during treatment

In the intervention phase of this study, daily variation of the bladder volume during irradiation was investigated. Directly before the start of every treatment session, specially trained technologists performed three BS measurements. The mean of all measurements of a patient, performed during the treatment period is denoted as $V_{treatm\text{-}tot}$. $V_{treatm\text{-}rel}$ is then defined as $V_{treatm\text{-}tot}$ relative to V_{CT}. As measure of daily variation of bladder filling the SD of $V_{treatm\text{-}tot}$ (denoted as $\mathbf{\sigma}_{bl}$) is used, whereas $\mathbf{\sigma}_{bl\text{-}rel}$ is defined as $\mathbf{\sigma}_{bl}$ relative to $V_{treatm\text{-}tot}$.

We also evaluated whether patients could accurately predict their bladder filling. A four point scale for micturition urge was used (Table 3). Patients were asked to score micturition urge at the same moment as bladder scanning was performed.

Biofeedback protocol

A biofeedback protocol, aimed at achieving a more constant bladder volume, was tested in a group of 16 patients. The goal of giving feedback was to improve the patients ability to distinguish between an almost empty.and moderately full bladder.

Score	Description
1	"Just urinated / no urge whatsoever"
2	"Maybe some urge"
3	"Easily tolerable but definite urge"
4	"Barely tolerable urge"

Table 3 *Micturition urge score*

The feedback consisted of telling the patient his daily bladder volume together with a drinking advice. The advice to drink more was given when the daily volume was < 80% of $V_{bl-scan}$. When patients had a bladder volume ranging from 80 to 120% of $V_{bl-scan}$ they should drink the same amount the next day. When the measurement was >120% of $V_{bl-scan}$ patients were advised to drink less. This feedback was given, every treatment day, by the technologists, directly after measuring the bladder volume.

Prostate motion and relation to bladder filling

During the intervention phase the relation between changes in bladder filling and prostate displacement was studied. Prostate motion data were derived from our standard used prostate position verification and correction protocol. This gold marker and electronic portal imaging device (EPID) based correction protocol has been described earlier in detail (29). In short, this protocol uses digitally reconstructed radiographs (DRR) derived from the planning CT scan as reference images. EPID images made during treatment are registered to the DRR's, using the intraprostatic markers as fiducials. The registration measures the deviation of the prostate relative to the DRR in the three orthogonal directions. For correction the so-called No Action Level (NAL) off-line correction protocol is applied, as described by de Boer *et al* (30). This protocol strives to minimize systematic errors, with the use of as few EPID measurements as possible.

As measure of systematic prostate deviation, we have used the mean of all EPID measurements (in one direction) during treatment of one patient (denoted as M_{prost}). Because the

NAL protocol minimizes the systematic prostate deviation, all calculations of $\textbf{\textit{M}}_{prost}$ were performed with the corrections undone. As measure of systematic change in bladder filling the difference between $V_{treatm-tot}$ en V_{CT} (denoted as $\Delta_{treatm-tot}$) was used. Linear regression analysis was performed to study the relation between these values. To describe the random prostate motion, the SD of $\textbf{\textit{M}}_{prost}$ was used (denoted as $\boldsymbol{\sigma}_{prost}$). In order to arrive at the most accurate estimate of random prostate deviation error, $\boldsymbol{\sigma}_{prost}$ was also calculated with the corrections undone (30, 31). For random variation in bladder filling, values of $\boldsymbol{\sigma}_{bl}$ were taken. To find any relation between $\boldsymbol{\sigma}_{prost}$ and $\boldsymbol{\sigma}_{bl}$, linear regression analysis was performed.

Workload, personnel and patient experiences

The time needed to train the technologists in the use of the BS was recorded. Furthermore an estimation of the additional workload was made. Per patient the extra time needed on the accelerator for bladder scanning and administration was recorded. Also specific experiences from patients in both groups, and the attending technologists were collected.

Statistical Analysis

Mean volumes and SD's were compared by applying the t-test. If F-testing showed a significant difference in variance or Kolmogorov-Smirnov testing showed a non-Gaussian distribution the Mann-Whitney U test was used. Linear regression analysis was performed to quantitate correlations between various variables. In the analysis of contingency tables Fischer's exact test was applied. Differences were considered significant if two-tailed p-values were lower than 0.05. For statistical analysis SPSS® version 12 (SPSS inc., Chicago, Illinois, USA) was used.

RESULTS

Bladderscan measurement validity

Using the data of the first 26 (5 postoperative) patients BS test characteristics were determined. Based on a total of 156 BS measurements, values of mean Δ_{inter} and mean $\boldsymbol{\sigma}_{intra}$ were 11.3% and 6.3% respectively. Interobserver difference in delineation of the bladder on CT never exceeded 10 ml. Furthermore a strong correlation (R = 0,95) between V_{CT} and $V_{bl-scan}$ was found, indicating a high accuracy of the BS (Fig. 2).
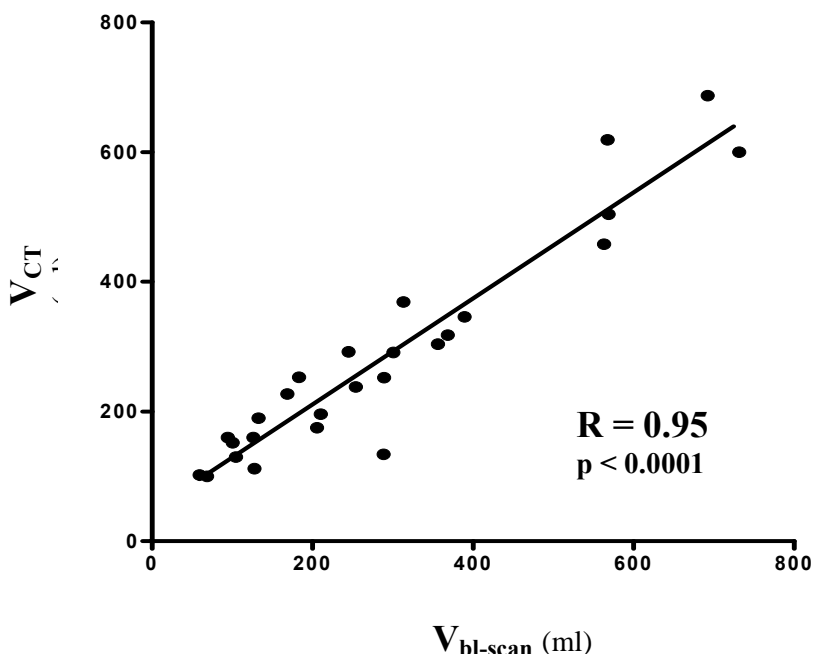
Fig. 2
Linear correlation graph showing $V_{bl\text{-}scan}$ (bladder volume measured with the bladderscan) vs. V_{CT} (bladder volume derived from the CT scan).

Bladder volume measurement during treatment and effects of the biofeedback protocol

On average bladder filling during treatment ($V_{treatm\text{-}tot}$) was better in the feedback group relative to the control group. Also, it approached the values measured on the planning CT scans more closely ($V_{treatm\text{-}rel}$). Furthermore, daily bladder volume variations ($\sigma_{bl\text{-}rel}$) were somewhat smaller in the feedback group. These improvements were, however, not statistically significant. A summary of these measurements is shown in Table 4. Besides only about 1 in every 4 patients could participate in the intervention phase, because of the in- and exclusion criteria.

	n	$V_{treatm\text{-}tot}$ (ml) mean (1SD)	V_{CT} (ml) mean (1SD)	$V_{treatm\text{-}rel}$ (%) mean (1SD)	$\sigma_{bl\text{-}rel}$ (%) mean (1SD)
feedback group	16	313 (156)	367 (202)	94.6 (25.3)	40.1 (16.1)
control group	18	250 (149)	348 (237)	83.2 (43.8)	47.2 (15.6)
p-value		0.24	0.81	0.38	0.20

Table 4
Summary of bladder volume measurements during treatment. P-values are derived from t-testing of the differences between the control and feedback group.
Abbreviations: $V_{treatm\text{-}tot}$ = the mean of all bladderscan measurements during treatment; V_{CT} = the bladder volume derived from the CT-scan.; $V_{treatm\text{-}rel}$ = $V_{treatm\text{-}tot}$ relative to V_{CT}.; $\sigma_{bl\text{-}rel}$ = the SD of $V_{treatm\text{-}tot}$ relative to $V_{treatm\text{-}tot}$.

A weak but significant correlation (R = 0.31) between subjective urge score and bladder volume was found, although a large intra- and inter-patient variance in prediction of bladder volume was seen (Fig. 3). There was no indication that patients in the feedback group performed better in this respect (data not shown).
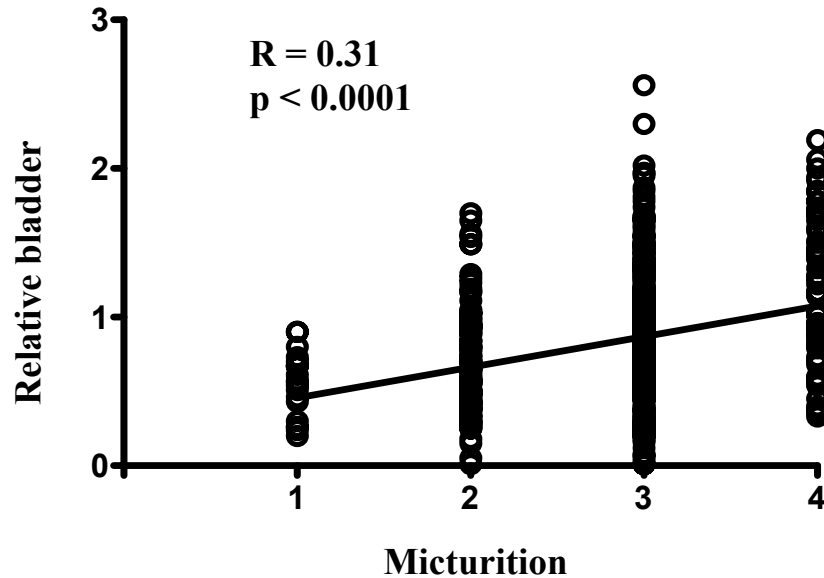
Fig. 3 *Linear correlation graph showing micturition urge score versus relative bladder volume. Relative bladder volume was calculated by dividing the volume measured with the bladder scanner by the volume measured on CT (V_{CT}).*

A negative time trend for bladder volume during irradiation was found. This time trend amounts to 31% bladder volume decrease (control group) during the whole treatment period. The decrease of bladder volume was less pronounced in the feedback group than in the control group (19% vs. 31%) but not significantly different (Fig. 4).

Table 4

Summary of bladder volume measurements during treatment. P-values are derived from t-testing of the differences between the control and feedback group.

Abbreviations: $V_{treatm-tot}$ = the mean of all bladderscan measurements during treatment; V_{CT} = the bladder volume derived from the CT-scan.; $V_{treatm-rel}$ = $V_{treatm-tot}$ relative to V_{CT}.; σ_{bl-rel} = the SD of $V_{treatm-tot}$ relative to $V_{treatm-tot}$.

Prostate motion and relation to bladder filling

The difference ($\Delta_{treatm-tot}$) in bladder filling during the treatment period ($V_{treatm-tot}$) and the CT scan (V_{CT}) did not correlate with systematic prostate position deviation (M_{prost}). For linear regression graphs see Fig. 5a-c. Furthermore no linear correlation between daily variation in bladder volume (σ_{bl}) and random prostate motion (σ_{prost}) was found (data are not shown). The highest correlation coefficient (R) found in these analyses was 0.22, indicating that only 5% (R square) of variance in prostate position is caused by changes in bladder filling.

(a)

(b)

(c)
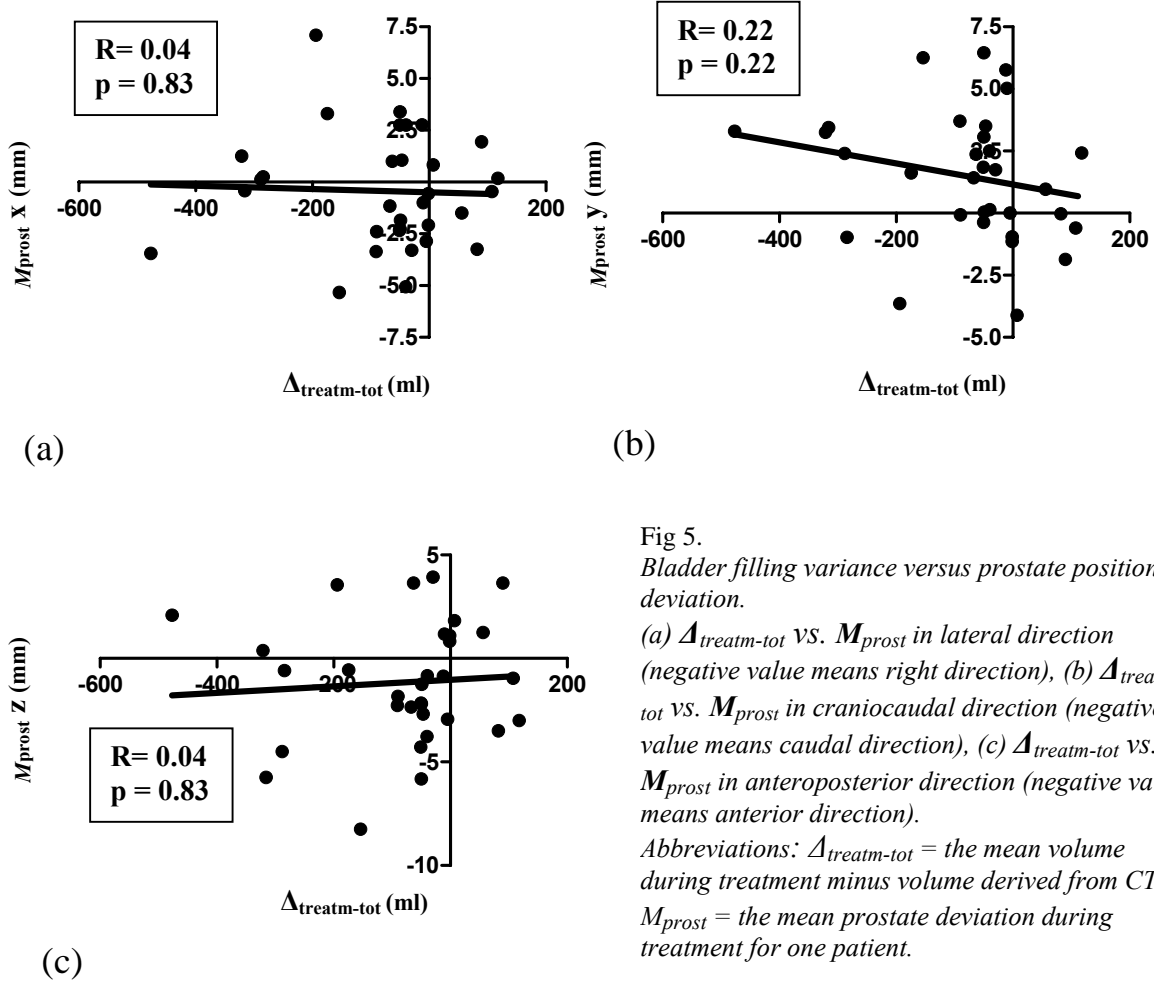
Fig 5.
Bladder filling variance versus prostate position deviation.
(a) $\Delta_{treatm-tot}$ vs. M_{prost} in lateral direction (negative value means right direction), (b) $\Delta_{treatm-tot}$ vs. M_{prost} in craniocaudal direction (negative value means caudal direction), (c) $\Delta_{treatm-tot}$ vs. M_{prost} in anteroposterior direction (negative value means anterior direction).
Abbreviations: $\Delta_{treatm-tot}$ = the mean volume during treatment minus volume derived from CT.; M_{prost} = the mean prostate deviation during treatment for one patient.

Workload, personnel, and patient experiences

Bladder scanner measurements were performed by trained technologists. Learning to use the bladder scanner usually took about 15 minutes. On the accelerator three minutes extra time were needed for three BS measurements. Overall acceptance and participation of the patients was good. In the feedback group some patients were so enthusiastic, that they had to be tempered not to become obsessed with attaining the "optimal" bladder volume. Acute toxicity was generally mild (no grade III toxicity). There was no difference in GU nor in GI toxicity between both groups (Table 1).

DISCUSSION

Bladderscan measurement validity

In order to establish the accuracy of the bladder scanner in the whole range of bladder volumes, we tested the BS in 26 patients. We found the BS measurements to be very accurate in assessing bladder volume, and inter- and intraobserver variability were low. Our findings were comparable to other studies in which mostly relative small bladder volumes were used to validate the bladder scanner for other purposes (32, 33).

Bladder volume during treatment

To date, there have been no reports about bladder volume variation measured on a daily basis. In the current study daily bladder volume measurements were made in a cohort of 18 prostate cancer patients. We found daily bladder volume variation to be very high (1SD = 47.2% for the control group). Furthermore, patients had a significant decrease of bladder volume during the irradiation period of about 30%. Other authors investigated changes in bladder volume using (at most once weekly) consecutive CT scans (see Table 5).

Although bladder filling variations found in this study were high, they are comparable to values found by others (14, 15, 19-22). These authors report bladder filling variations ranging from 30 to 50%. Also a trend towards decreased bladder filling over time was noted in several of these studies (14, 15, 22).

Biofeedback protocol

In this study, a protocol, meant to achieve a more constant full bladder by means of giving simple biofeedback, was tested. On average, bladder filling during treatment ($V_{treatm-tot}$) was better in the feedback group, relative to the control group. Also, it approached the values measured on the planning CT scans more closely ($V_{treatm-rel}$). Furthermore, daily bladder volume variations (σ_{bl-rel}) were somewhat smaller in the feedback group. These improvements were, however, not statistically significant. Since the data hints at just a small improvement by the biofeedback protocol and only 1 in every 4 patients could be included, the beneficial effect of the biofeedback was deemed not clinically relevant in this

Author	No. of patients	No. of scans	Bladder filling variation	Bladder volume decrease over time
This study	18	daily	47% (1SD)	31%
Lebesque et al. (14)	11	3	33% (1SD)	28%
Roeske et al. (21)	10	weekly	30% (1SD)	50% of patients increase 50% of patients decrease
Melian et al. (20)	8	4	"large" (no specific data were mentioned)	-
Antolak et al. (22)	17	4	"large" (no specific data were mentioned)	16%
Zellars et al. (19)	24	2	51%	-
Fiorino et al. (15)	9	weekly	ratio smallest to largest volume = 3.8	47%

Table 5 *Bladder filling variation as reported in the literature.*

specific subset of patients (i.e. prostate cancer patients) and recruitment of patients was ended. The absence of a statistically significant effect of the biofeedback protocol could be due to the relative small number of patients. Another cause may be the baseline micturition problems most prostate cancer patients have. Although only patients with no, or minor micturition complaints were selected in an attempt to avoid this confounder. Also acute urinary and rectal toxicity could impair the ability of patients to maintain a constant full bladder. Whether this was truly a disturbing factor is questionable, because acute toxicity was limited to at most grade II and did not differ significantly between groups. The lack of improvement by the feedback protocol might also be the result of its subjective nature. Indeed, we did find a significant relation between the micturition urge score and bladder filling, but this relation was weak. Together with the extreme variance between and within patients, such a score then seems quite useless.

Based on these findings, only asking a patient to have a full bladder during irradiation will not result in a constant bladder filling. More objective protocols, prescribing a certain amount of fluids to be drunk before irradiation, or minimum time between last micturition and irradiation, have reported comparable large variances in bladder volume (14, 15, 20).

With the absence of effective protocols to ensure a full bladder, one can only screen patients for large bladder filling variations. One could make weekly or daily CT scans, but the use of the bladder scanner as a screening tool would be a lot easier and more cost-effective. This way only patients with large differences between bladder volume during treatment and during simulation could be identified for a repeat CT scan. From this CT scan, more accurate treatment plans and toxicity probabilities could be derived. Alternatively the bladder scanner could be used in a more directive protocol. Such a protocol would start for example by booking several patients together in one large time slot. The patient with the best bladder volume would be irradiated first. Patients with inadequate bladder filling could then drink extra fluids to increase their bladder volume.

Prostate motion and correlation with bladder filling

Prostate motion as measured with our EPID protocol is in the same range as reported in the literature (21-24). In this study, the difference between mean treatment bladder volume and CT volume did not correlate significantly with mean prostate deviation. Furthermore no significant correlation between daily variation in bladder filling and random prostate motion was found. These findings seem to contradict reports of other authors, which find at least weak correlations between bladder filling variation and prostate position (19, 21, 23-26). One reason could be that, in our correlation analysis, mean values and SD's of prostate position and bladder volume changes over the entire treatment were used. As the NAL protocol only yields limited prostate position data (i.e. not daily EPID measurements), we have chosen to use mean values. Compared to correlating daily bladder volume with daily prostate position deviation, this is quite a coarse method, and could have easily obscured the relation between prostate motion and changes in bladder filling. Authors using values measured on the same day did indeed find a weak correlation between prostate motion and changes in bladder filling (19, 21, 23-26). Many authors also report far stronger correlations between rectal filling changes and prostate motion (19, 21-26). Because rectal filling was not evaluated in this study, no estimation of the confounding effect of rectal filling on prostate position deviation can be made.

CONCLUSION

This study shows bladder volume variation to be very high (1SD = 47.2%). Using the bladder scanner in a simple biofeedback protocol does not yield a significant decrease in bladder filling variation (1SD = 40.1%). This underlines the shortcomings of a protocol, in which patients are only asked to have a full bladder during irradiation. Even so, the bladder scanner is an easy to use and accurate tool to register bladder volume variations. One could use it as a screenings tool to identify patients with large bladder filling variations for which then repeat CT scans and treatment plans could be made.

REFERENCES

1. Pollack A, Zagars GK, Starkschall G, et al. Prostate cancer radiation dose response: results of the M. D. Anderson phase III randomized trial. Int J Radiat Oncol Biol Phys 2002;53:1097-1105.

2. Sengelov L, von der Maase H. Radiotherapy in bladder cancer. Radiother Oncol 1999;52:1-14.

3. Glimelius B, Isacsson U, Jung B, et al. Radiotherapy in addition to radical surgery in rectal cancer: evidence for a dose-response effect favoring preoperative treatment. Int J Radiat Oncol Biol Phys 1997;37:281-287.

4. Emami B, Lyman J, Brown A, et al. Tolerance of normal tissue to therapeutic irradiation. Int J Radiat Oncol Biol Phys 1991;21:109-122.

5. Marks LB, Carroll PR, Dugan TC, et al. The response of the urinary bladder, urethra, and ureter to radiation and chemotherapy. Int J Radiat Oncol Biol Phys 1995;31:1257-1280.

6. Perez CA, Breaux S, Bedwinek JM, et al. Radiation therapy alone in the treatment of carcinoma of the uterine cervix. II. Analysis of complications. Cancer 1984;54:235-246.

7. Perez CA, Grigsby PW, Lockett MA, et al. Radiation therapy morbidity in carcinoma of the uterine cervix: dosimetric and clinical correlation. Int J Radiat Oncol Biol Phys 1999;44:855-866.

8. Coia LR, Myerson RJ, Tepper JE. Late effects of radiation therapy on the gastrointestinal tract. Int J Radiat Oncol Biol Phys 1995;31:1213-1236.

9. Zelefsky MJ, Cowen D, Fuks Z, et al. Long term tolerance of high dose three-dimensional conformal radiotherapy in patients with localized prostate carcinoma. Cancer 1999;85:2460-2468.

10. Dearnaley DP, Khoo VS, Norman AR, et al. Comparison of radiation side-effects of conformal and conventional radiotherapy in prostate cancer: a randomised trial. Lancet 1999;353:267-272.

11. Morris DE, Emami B, Mauch PM, et al. Evidence-based review of three-dimensional conformal radiotherapy for localized prostate cancer: an ASTRO outcomes initiative. Int J Radiat Oncol Biol Phys 2005;62:3-19.

12. Zelefsky MJ, Fuks Z, Hunt M, et al. High-dose intensity modulated radiation therapy for prostate cancer: early toxicity and biochemical outcome in 772 patients. Int J Radiat Oncol Biol Phys 2002;53:1111-1116.

13. Mundt AJ, Roeske JC, Lujan AE, et al. Initial clinical experience with intensity-modulated whole-pelvis radiation therapy in women with gynecologic malignancies. Gynecol Oncol 2001;82:456-463.

14. Lebesque JV, Bruce AM, Kroes AP, et al. Variation in volumes, dose-volume histograms, and estimated normal tissue complication probabilities of rectum and bladder during conformal radiotherapy of T3 prostate cancer. Int J Radiat Oncol Biol Phys 1995;33:1109-1119.

15. Fiorino C, Foppiano F, Franzone P, et al. Rectal and bladder motion during conformal radiotherapy after radical prostatectomy. Radiother Oncol 2005;74:187-195.

16. Fokdal L, Honore H, Hoyer M, et al. Impact of changes in bladder and rectal filling volume on organ motion and dose distribution of the bladder in radiotherapy for urinary bladder cancer. Int J Radiat Oncol Biol Phys 2004;59:436-444.

17. Brierley JD, Cummings BJ, Wong CS, et al. The variation of small bowel volume within the pelvis before and during adjuvant radiation for rectal cancer. Radiother Oncol 1994;31:110-116.

18. Kim TH, Chie EK, Kim DY, et al. Comparison of the belly board device method and the distended bladder method for reducing irradiated small bowel volumes in preoperative radiotherapy of rectal cancer patients. Int J Radiat Oncol Biol Phys 2005;62:769-775.

19. Zellars RC, Roberson PL, Strawderman M, et al. Prostate position late in the course of external beam therapy: patterns and predictors. Int J Radiat Oncol Biol Phys 2000;47:655-660.

20. Melian E, Mageras GS, Fuks Z, et al. Variation in prostate position quantitation and implications for three-dimensional conformal treatment planning. Int J Radiat Oncol Biol Phys 1997;38:73-81.

21. Roeske JC, Forman JD, Mesina CF, et al. Evaluation of changes in the size and location of the prostate, seminal vesicles, bladder, and rectum during a course of external beam radiation therapy. Int J Radiat Oncol Biol Phys 1995;33:1321-1329.

22. Antolak JA, Rosen, II, Childress CH, et al. Prostate target volume variations during a course of radiotherapy. Int J Radiat Oncol Biol Phys 1998;42:661-672.

23. Langen KM, Jones DT. Organ motion and its management. Int J Radiat Oncol Biol Phys 2001;50:265-278.

24. Crook JM, Raymond Y, Salhani D, et al. Prostate motion during standard radiotherapy as assessed by fiducial markers. Radiother Oncol 1995;37:35-42.

25. Ten Haken RK, Forman JD, Heimburger DK, et al. Treatment planning issues related to prostate movement in response to differential filling of the rectum and bladder. Int J Radiat Oncol Biol Phys 1991;20:1317-1324.

26. Schild SE, Casale HE, Bellefontaine LP. Movements of the prostate due to rectal and bladder distension: implications for radiotherapy. Med Dosim 1993;18:13-15.

27. van Lin EN, Nijenhuis E, Huizenga H, et al. Effectiveness of couch height-based patient set-up and an off-line correction protocol in prostate cancer radiotherapy. Int J Radiat Oncol Biol Phys 2001;50:569-577.

28. Cox JD, Stetz J, Pajak TF. Toxicity criteria of the Radiation Therapy Oncology Group (RTOG) and the European Organization for Research and Treatment of Cancer (EORTC). Int J Radiat Oncol Biol Phys 1995;31:1341-1346.

29. van Lin EN, van der Vight LP, Witjes JA, et al. The effect of an endorectal balloon and off-line correction on the interfraction systematic and random prostate position variations: a comparative study. Int J Radiat Oncol Biol Phys 2005;61:278-288.

30. de Boer HC, Heijmen BJ. A protocol for the reduction of systematic patient setup errors with minimal portal imaging workload. Int J Radiat Oncol Biol Phys 2001;50:1350-1365.

31. Bijhold J, Lebesque JV, Hart AA, et al. Maximizing setup accuracy using portal images as applied to a conformal boost technique for prostatic cancer. Radiother Oncol 1992;24:261-271.

32. Huang YH, Bih LI, Chen SL, et al. The accuracy of ultrasonic estimation of bladder volume: a comparison of portable and stationary equipment. Arch Phys Med Rehabil 2004;85:138-141.

33. Byun SS, Kim HH, Lee E, et al. Accuracy of bladder volume determinations by ultrasonography: are they accurate over entire bladder volume range? Urology 2003;62:656-660.

6

Rectal wall sparing effect of three different endorectal balloons in 3D conformal and IMRT prostate radiotherapy

Emile N.J.Th van Lin, M.D., Aswin L. Hoffmann M.Sc., Peter van Kollenburg B.Sc.,
Jan Willem Leer, M.D. Ph.D., and Andries G. Visser, Ph.D.

Department of Radiation Oncology

ABSTRACT

Purpose: To investigate the dosimetric consequences and rectal wall (Rwall) sparing effect of three different endorectal balloons (ERBs) for 3-dimensional conformal radiotherapy (3D-CRT) and intensity-modulated radiotherapy (IMRT) for prostate cancer.

Methods and materials: In 20 patients, four planning CT-scans were made, one without ERB and three with ERB1, 2 or 3 inserted. Two different planning target volumes (PTV) were defined: prostate only (PTV-P) and prostate plus seminal vesicles (PTV-PSV). 3D-CRT and IMRT planning techniques were used and the prescription dose was 78 Gy. In 284 treatment plans, the Rwall mean dose, the Rwall NTCP, and the absolute Rwall volumes exposed to ≥50 Gy (V_{50}) and ≥70 Gy (V_{70}) were calculated. For spatial dose distribution analysis, inner rectal wall dose maps and dose surface histograms (DSH) were generated.

Results: Each ERB was tolerated well. In case of 3D-CRT, each ERB showed a statistically significant reduction all of the measured parameters. ERB2 and ERB3 performed better than ERB1. In IMRT, a statistically significant reduction in the Rwall dose parameters could not be demonstrated for any of the ERBs. For 3D-CRT and IMRT, due to the rectal dilation, ranging from 8 to 20 cm in circumference, the ERBs resulted in reduction of the relative inner Rwall surface exposed to intermediate and high-doses.

Conclusions: In 3D-CRT, any ERB showed a significant rectal wall sparing effect. ERB2 and ERB3 were superior to ERB1. For both 3D-CRT and IMRT, a reduction of the relative inner Rwall surface exposed to intermediate and high-doses was found, which may lead to reduced late rectal toxicity. Development of user- and patient-friendly ERBs is warranted to increase their acceptability.

INTRODUCTION

Dose escalation in prostate radiotherapy can improve treatment outcome, especially for intermediate- and high-risk patients (1). Rectal toxicity is the major limiting factor in prostate dose escalation and it is related to the total radiation dose prescribed and the volume of the rectal wall receiving a high dose (2-4). One of the challenges in radiation therapy of the prostate is elevating dose without increasing rectal toxicity. Nowadays, three-dimensional conformal radiotherapy (3D-CRT) is widely available and allows to deliver high doses to the prostate only (P) or to the prostate and seminal vesicles (PSV) while sparing the surrounding normal tissues, such as bladder and rectum, resulting in favorable toxicity profiles as compared to conventional radiotherapy (5). Further improvement of dose conformality can be achieved by intensity-modulated radiation therapy (IMRT). This technique opened the way to more aggressive dose escalation in prostate cancer, while maintaining the same risk of developing severe rectal toxicity (6). Nevertheless, implementation and actual treatment using IMRT, on a daily basis, is complex and therefore not yet available in every treatment center (7).

It is known that the majority of cancer foci is located in the peripheral zone of the prostate, adjacent to the anterior rectal wall (8). Consequently, this part of the rectal wall will inevitably be in the high dose region. It has been demonstrated that the lateral and dorsal part of the rectal wall can be pushed away from the high dose region by insertion of an inflatable endorectal balloon (ERB). Three types of air-filled ERBs have been investigated, separately, for their rectal wall sparing effect in 3D-CRT and IMRT. Treatment planning studies and clinical studies of individual ERBs have shown that the use of an ERB can be advantageous (9-15).

To date, no planning study has been performed to compare the potential rectal wall sparing effect for these types of ERBs in one patient group. The goal of this study was to investigate the dosimetric consequences and the rectal wall sparing effect of each ERB, for both 3D-CRT and IMRT treatment techniques using two target volumes, P and PSV, and to compare them to treatment plans without an ERB.

MATERIALS AND METHODS

Patient selection and preparation

Twenty patients, who were referred to our department for irradiation of localized prostate cancer (T1-3N0M0), were included in this study, after informed consent was given. Besides apparent pre-existing anal irritation and hemorrhoids, no further exclusion criteria were applied. Prior to CT scanning, patients used a laxative diet and a laxans (Microlax clysma 5 mL, Pharmacia B.V. Woerden, The Netherlands), and were intended to have a full bladder by drinking 500 ml of water.

Endorectal balloons

The first ERB (ERB1) is a flexible rectal balloon tube made of soft rubber, commonly used in diagnostic radiology for barium enema procedures. It is a 30-cm-long two-way rectal tube with silkolatex coating and a silkolatex balloon (Nordmann®, Rüsch AG, Kernen, Germany). Deflated, the ERB has a diameter of 8 mm. The dimensions of the balloon, filled with 40 cc of air, are 5.0 cm in length and 4.5 cm in diameter, as described earlier by *Wachter et al.* (14, 16-18) (Fig. 1a).

The second ERB (ERB2) was originally designed as an endorectal coil for magnetic resonance (MR) imaging (Medrad, Pittsburgh, PA). The latex balloon is fixed on a slightly flexible PVC shaft with a length of 33 cm. This ERB has a specific anatomical concave shape to conform to the prostate gland-rectal interface (9, 19). Deflated, the ERB has a diameter of 10 mm. The ERB was inflated with 80 cc of air and had a length of 90 mm and a diameter of 45 mm (Fig. 1b). This amount of air chosen was in accordance with the amount when used for MR imaging. ERB1 and ERB2 originate from radiological procedures and are open-air systems with a direct connection between the rectal lumen and the outer air. As described by others, in clinical practice, ERB1 en ERB2 are covered by a condom prior to daily insertion in order to prevent rectal content leakage during irradiation (13, 14). For hygienic reasons, we used no condoms but closed the open-air connection of these ERBs with clamps.

The third ERB (ERB3) also originates from diagnostic radiology. It is a rectal balloon catheter consisting of a non-latex retention cuff on a rigid 15 cm shaft (EZ-EM, Westbury, NY). Deflated, the ERB has a diameter of 15 mm. This ERB was inflated with 100 cc of air, the same amount as used by the Baylor College group (11, 12, 20) and had a length of 45 mm and a diameter of 60 mm) (Fig. 1c).
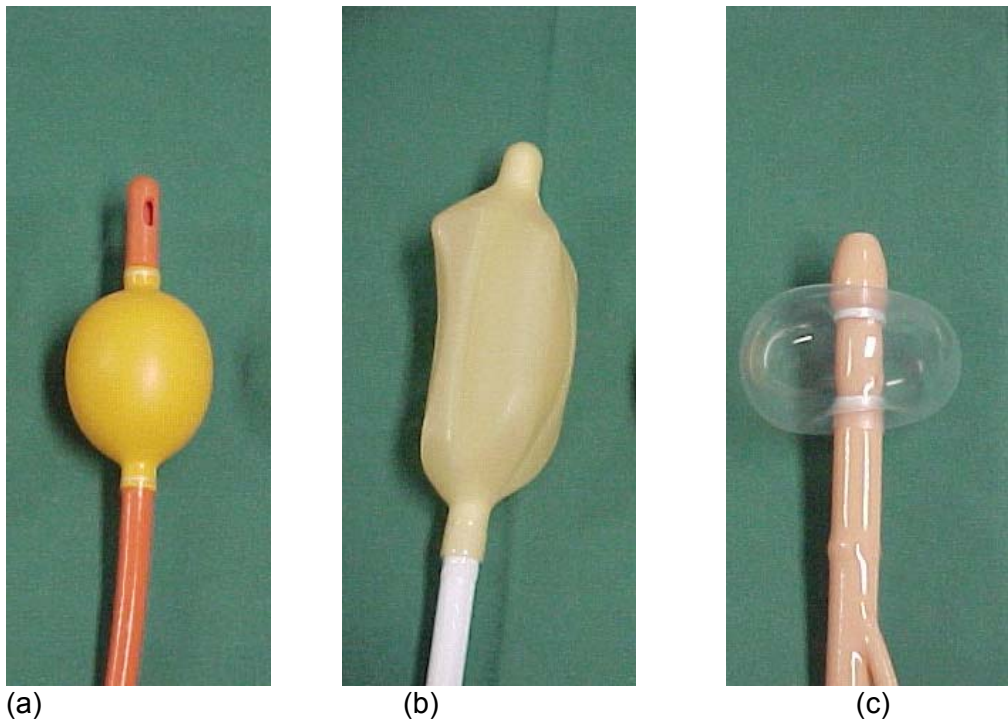
Fig 1
The endorectal balloons: (a) ERB1, (b) ERB2 and (c) ERB3

In all patients, the order of CT scanning was the same, according to increasing volume of ERBs: No-ERB, ERB1, ERB2 and ERB3 (Fig. 2). The same person (EVL) inserted all balloons while patients were turned on their left side. Insertion was facilitated by lubrication gel (K-Y gel, Johnson & Johnson, Arlington, TX). After inflation the ERB was gently pulled towards the anal sphincter to ensure a proper position in relation to the prostate. Within 20 minutes, four planning CT-scans (one without and three with ERB in situ) were obtained at 3mm slice thickness, resulting in 80 CT-scans (AcQsim spriral CT, Philips Medical Systems, Bothell, WA). Patients were positioned supine during acquisition of the CT images.
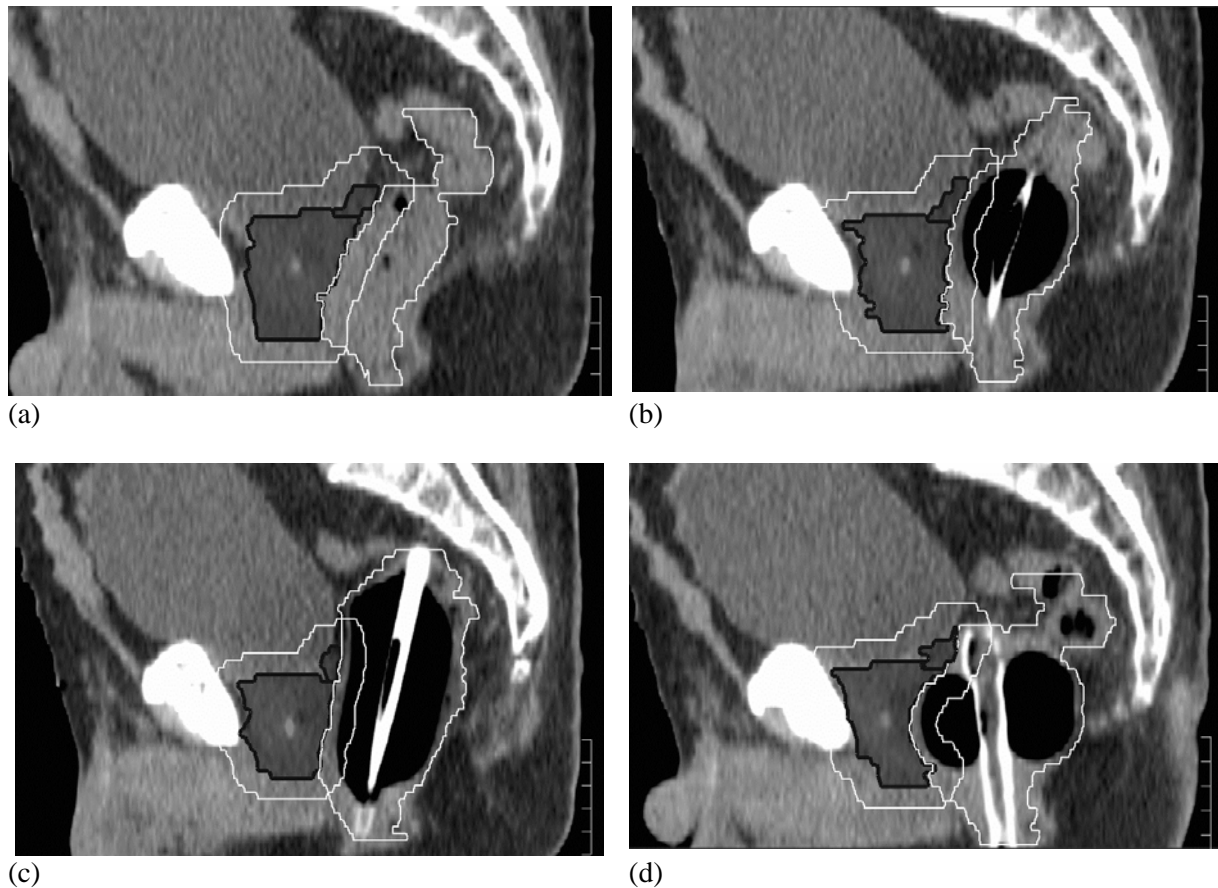
Fig. 2.
Sagittal CT images of a patient with (a) No ERB, (b) ERB1, (c) ERB2 and (d) ERB 3 inserted. Prostate, seminal vesicles and rectal outer contours are highlighted. The planning treatment volume surrounds the prostate and seminal vesicles.

Organ delineation and treatment planning

The images of all 80 CT scans were imported into the Pinnacle[3] treatment planning system (Philips Medical Systems, Andover, MA) for 3D-CRT and IMRT treatment planning. The prostate gland only (P) and the prostate and seminal vesicles (PSV) were contoured in all CT scans and defined as clinical target volumes (CTV). In every CT-scan the outside contour of the ERB was delineated to determine the total volume of the ERB (amount of air plus the volume of the device itself). On each slice the following surrounding normal structures were outlined: bladder, femoral heads, and rectal wall. The rectal wall (Rwall) representing the rectal wall organ volume was defined as the difference between the inner and the outer rectal wall contour (4, 14). Rwall was delineated from the ischial tuberosities up to the rectosigmoid flexure. For each patient, delineation was done over the same length to obtain the same Rwall volume per patient and allow intercomparison. Two independent observers performed the delineation of the rectal inner and outer wall contours. For 3 randomly chosen patients, the rectum contours for each of the 4 CT scans were delineated 5 times by each of the observers,

to assess the intra- and inter-observer delineation variations. These variations were expressed as the coefficient of variation ($\pm$ 1 SD relative to the mean).

For every CT-scan, two planning target volumes (PTVs) were defined: a PTV for prostate only (PTV-P) and a PTV for prostate and seminal vesicles (PTV-PSV). To generate these PTVs, a 3D CTV-PTV margin of 10 mm was used for the 3D-CRT plans. For the IMRT plans, a CTV-PTV margin of 7 mm was used, as it was assumed that departments using IMRT for daily practice also use specific position verification and correction protocols, resulting in reduced margins (7).

A dose of 78 Gray (Gy) was prescribed in 39 daily fractions of 2 Gy, derived from the M.D. Anderson randomized trial (1). For evaluation of the rectal wall sparing effect, first, the normal tissue complication probability (NTCP) of the Rwall, for each individual patient over the different ERBs, were compared. For the NTCP calculations the Lyman-Kutcher-Burman (LKB) model with Emami parameters (n=0.12, m=0.15 and TD_{50}=80 Gy) was used (21-23).

Secondly, the mean dose of the Rwall was derived from the planning system and compared for all treatment plans (4, 24). From the Rwall dose volume histogram (DVH) the absolute Rwall volume (cc) receiving 50 Gray or more (V_{50}) and the absolute Rwall volume (cc) receiving 70 Gray or more (V_{70}) were derived (3, 25). The different diameters and lengths of the three ERBs resulted in different inner rectal wall surfaces. Therefore, the spatial dose distribution over the inner rectal wall mucosa was visualized by generating rectum dose surface maps (4) and dose surface histograms (DSH) (26).

3D-CRT treatment planning technique

Four coplanar beams were used, consisting of four orthogonal, equally weighted 18 MV photon fields (Anterior-Posterior, Posterior-Anterior, Left-Lateral and Right-Lateral). A beams-eye-view based 3D-conformal treatment plan was designed, with individual shielding of normal tissue, utilizing a multileaf collimator (MLC), and a dose level of 78 Gy at the International Commission of Radiation units and Measurements (ICRU) reference point.

IMRT treatment planning technique

An inverse planned step-and-shoot IMRT-plan was made for every patient, consisting of 5 coplanar, equidistant, non-opposing 10 MV photon energy beams. One beam was oriented posterior-anterior (PA) while the other 4 beams were equally spaced around the isocenter. The inverse planning system tried to meet as good as possible the objectives displayed in Table 1. The maximum allowable dose outside the delineated structures was 38 Gy (weight factor 1).

ROI	Objective	Dose level (Gy)	Volume (%)	Weight
CTV	Uniformity	78	100	10
CTV	Max Dose	82	100	8
PTV	Min Dose	74	100	10
PTV	Max Dose	78	100	8
PTV	Uniformity	78	100	1
PTV	Min DVH	74	99	10
Rectal Wall	Max Dose	75	100	50
Rectal Wall	Max DVH	60	10	20
Rectal Wall	Max DVH	50	20	10
Rectal Wall	Max DVH	40	30	10
Bladder	Max DVH	74	2	3
Bladder	Max DVH	60	15	2
Left Femur	Max Dose	50	100	1
Right Femur	Max Dose	50	100	1

Table 1.
IMRT treatment planning objectives and weight factors

Abbreviations:
ROI = region of interest, CTV = clinical target volume, PTV = planning target volume, Max Dose = maximum allowable dose, Min Dose = minimal allowable dose, DVH = dose volume histogram

Statistical analysis

The Analyse-it® software (Analyse-it Software Ltd, Leeds, England) add-in for Microsoft Excel was used for statistical calculations. The Wilcoxon signed rank test was used to for paired comparison of the three measured quantities (NTCP, V_{70}, V_{50}) in the same subjects for any two different ERBs. Differences were considered significant for two-tailed p values less than 0.05.

Patient experiences and ERB positioning

After each CT-scanning session, each patient was asked for his experiences regarding the introduction of the different balloons, i.e. the complaints during the procedure. On the CT scan, the position of the ERB was evaluate.

RESULTS

Patient characteristics

The patients investigated represented a broad range of prostate and seminal vesicles volumes. The mean volume ($\pm$ 1 SD) for the prostate was 69 cc ($\pm$ 35 cc) ranging from 37 to 187 cc. The mean volume ($\pm$ 1 SD) for the seminal vesicles was 17 cc ($\pm$ 5 cc) ranging from 7 to 28 cc.

Rectal wall delineation and ERB characteristics

Overall, the Rwall was delineated over a mean length of 11.5 cm (median 11.4 cm, ranging from 10.2 to 13.5 cm). The median volumes of the delineated Rwall per patient, compared for each of the four CT-scans, for the No-ERB, ERB1, ERB2 and ERB3, were 57.0 cc, 58.6 cc, 48.4 cc and 55.5 cc respectively and did not significantly differ (p = 0.81). The Rwall delineation inter-observer co-efficient of variation was 4.4 % $\pm$ 1.6%. The Rwall delineation intra-observer co-efficient of variation was 4.2 % $\pm$ 1.8 %. The intra-observer variance was not statistically different from that found between the observers.

The mean total volume ($\pm$ 1 SD) of the inserted ERB was 58 cc ($\pm$ 7 cc) for ERB1, 108 cc ($\pm$ 6 cc) for ERB2 and 117 cc ($\pm$ 11 cc) for ERB3. Insertion of the different ERBs resulted in an increase of the total rectal volume (Rwall outside encompasses Rwall plus rectal content). Without the ERB, the mean Rwall outside ($\pm$ 1 SD) was 83cc ($\pm$ 16 cc), 138 cc ($\pm$ 18 cc) when ERB1 was inserted and inflated, 185 cc ($\pm$ 18 cc) for ERB2 and 189 cc ($\pm$ 21 cc) for ERB3. When evaluating the CT-scans with ERB in situ, it appeared that, despite laxation, gas and faecal material was present and extended the rectum, as found in our previous study (19). For this reason, one patient was excluded from further analysis. In this patient the Rwall outside volume without ERB was 138 cc. With the ERBs, the Rwall outside volume ranged from 200 to 250 cc. For three patients, one of 4 CT scans was excluded because of large rectum extension due to gas and faecal material. These were the CT-scans with ERB1, No-ERB and ERB3, for these three patients, respectively. In total, 71 CT-scans and 284 treatment plans were used for the definitive analysis.

Rectal wall sparing effect of the ERBs in 3D-CRT

The 3D-CRT planning technique resulted in a good PTV coverage for all four CT-scans; the mean dose ($\pm$ 1 SD) for the PTV-P and PTV-PSV was 76.5 Gy ($\pm$ 0.6 Gy) and 77.1 Gy ($\pm$ 0.5 Gy), respectively. Examples of typical dose distributions for the 3D-CRT plans, with and without an ERB, are given in Fig. 3 a-b.
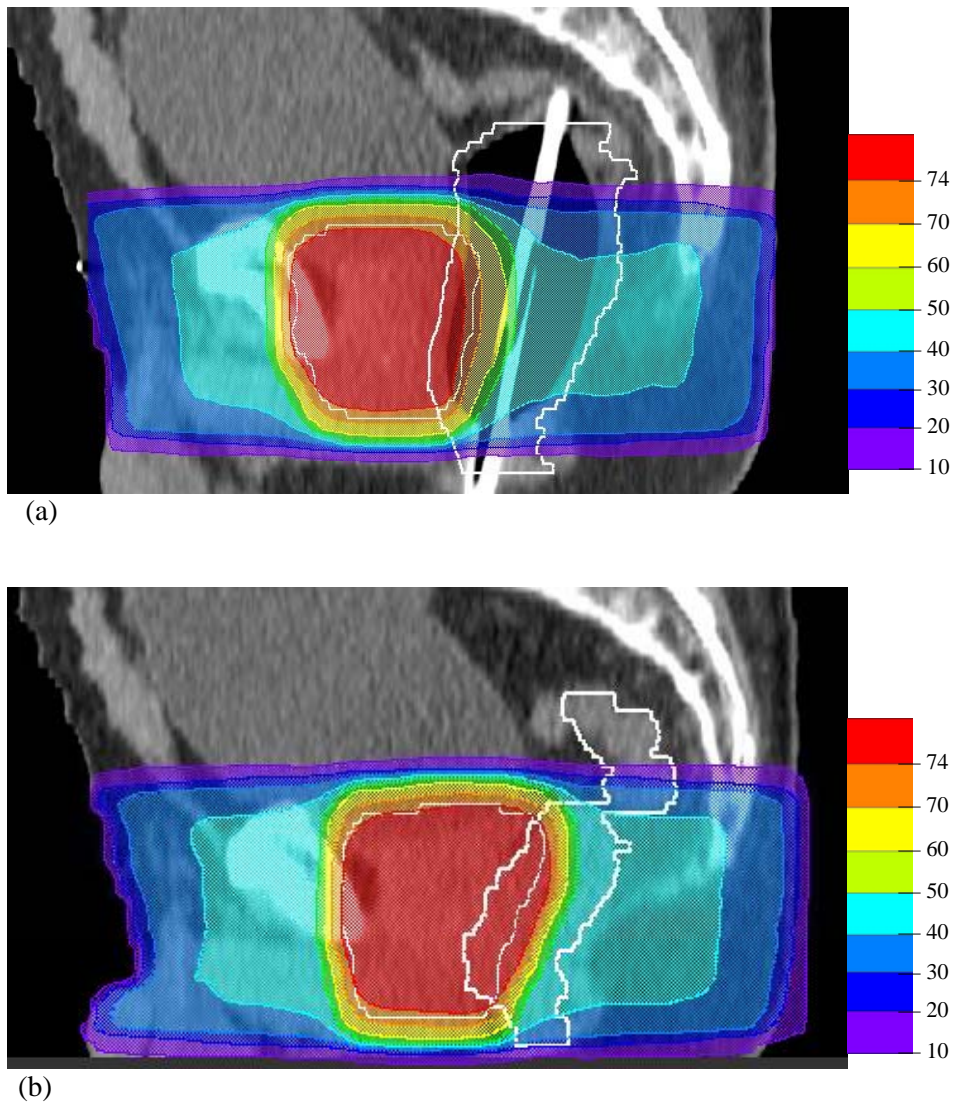
Fig. 3.
Sagittal CT images with dose distribution, in Gy, for 3D-CRT PTV-P, for (a) No-ERB and (b) ERB2. PTV (prostate + 10 mm margin) and rectal outer contour are highlighted (white lines).

The *mean Rwall dose* was reduced significantly for both PTV-P and PTV-PSV by using any of the ERBs (Table 2).

	3D-CRT				IMRT			
	PTV-PSV		PTV-P		PTV-PSV		PTV-P	
	Mean Rwall Dose (Gy)	p value	Mean Rwall dose (Gy)	p value	Mean Rwall dose(Gy)	p value	Mean Rwall dose(Gy)	p value
No-ERB	60.7		48.8		40.6		35.6	
ERB 1	56.6	*0.002*	44.9	*0.001*	41.0	*0.14*	34.8	*0.28*
ERB 2	54.4	*0.003*	44.2	*0.002*	41.5	*0.67*	34.4	*0.49*
ERB 3	56.0	*0.001*	45.3	*0.002*	40.9	*0.15*	32.6	*0.40*

Table 2.
Mean rectal wall (Rwall) dose for the 3D-CRT and IMRT treatment techniques and for the two different PTVs. The p values, given for ERB1, 2 and 3, resulted from the Wilcoxon signed ranks test comparing the mean Rwall dose for the respective ERBs against No-ERB.
Abbreviations: PTV-PSV = planning treatment volume for prostate and seminal vesicles; PTV-P = planning treatment volume for prostate only.

In case of PTV-P there was no significant difference between ERB1, 2 or 3 (p values ranged from 0.33 to 0.89). In case of the PTV-PSV, ERB2 gave a small, but statistically significant reduction of mean Rwall dose compared to ERB1 (p = 0.001) and to ERB3 (p = 0.01).

With respect to *NTCP* of the Rectal Wall in PTV-PSV, any type of ERB gave a significant reduction compared to the treatment plan without ERB (Table 3). Both ERB2 and 3 do also give a small, but significant NTCP reduction compared to ERB1 with p values of < 0.0001 and 0.0027, respectively. In case of PTV-P, any of the ERBs gave a significant reduction of the NTCP Rwall compared to irradiation without an ERB (Table 3). ERB3, the one with the largest diameter, was performing statistically better than ERB1 (p = 0.03) and ERB2 (p = 0.03), although the absolute differences in NTCP were small.

(a)
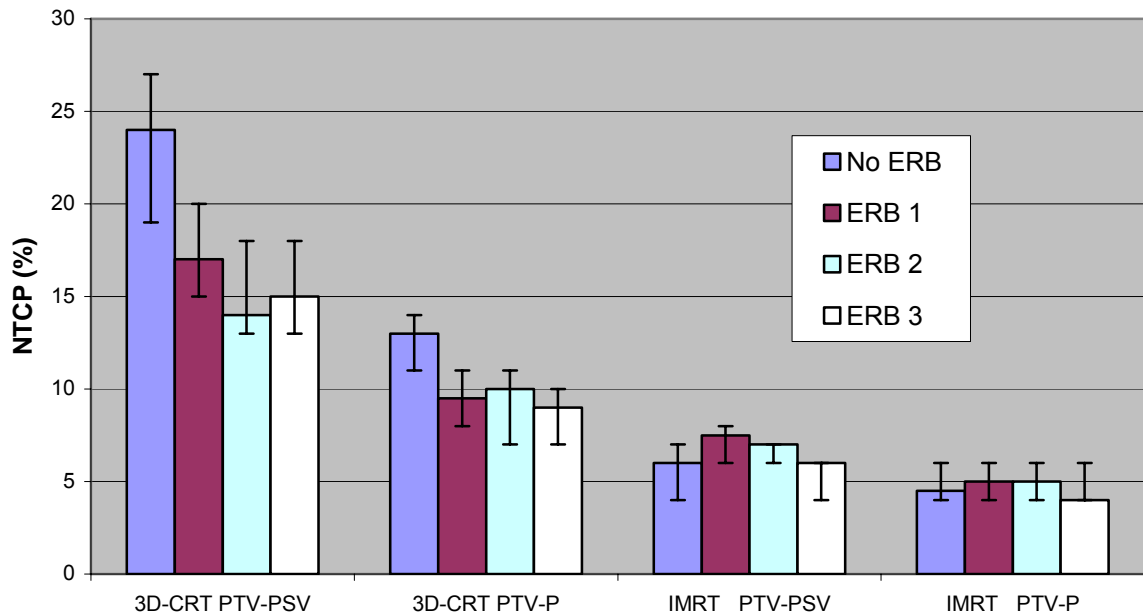
	3D-CRT				IMRT			
	PTV-PSV		PTV-P		PTV-PSV		PTV-P	
	NTCP (%)	p value	NTCP (%)	p value	NTCP (%)	p value	NTCP (%)	p value
No-ERB	24.0		13.0		6.0		4.5	
ERB 1	17.0	*0.0005*	9.5	*< 0.0001*	7.5	*0.0003*	5.0	*0.51*
ERB 2	14.0	*< 0.0001*	10.0	*< 0.0001*	7.0	*0.0001*	5.0	*0.33*
ERB 3	15.0	*< 0.0001*	9.0	*< 0.0001*	6.0	*0.0001*	4.0	*1.0*

(b)

Table 3.
(a) NTCP of the rectal wall, in median values, for the 3D-CRT and IMRT treatment techniques and for the two different PTVs. The median values are shown with the 95% confidence interval.
(b) The p values, given for ERB1, 2 and 3, resulted from the Wilcoxon signed ranks test comparing the NTCP for the respective ERBs against No-ERB.
Abbreviations: PTV-PSV = planning treatment volume for prostate and seminal vesicles; PTV-P = planning treatment volume for prostate; NTCP = normal tissue complication probability

The amount of Rwall volume, irradiated to a dose level of 50 Gy or more, the so-called V_{50} was significantly reduced by the use of any type of ERB in case of PTV-PSV (Table 4). Both ERB2 and 3 gave a larger reduction of V_{50} in than ERB1, with p-values of 0.002 and 0.005 respectively. There was no statistical difference between ERB2 and 3 (p = 0.63). For PTV-P, also all three types of ERBs gave a significant reduction in V_{50} compared to No-ERB.

ERB3 gave a significant reduction compared to ERB1 and 2, with p values of 0.0004 and 0.01, respectively. ERB1 and 2 did not differ (p = 0.45) significantly.

(a)

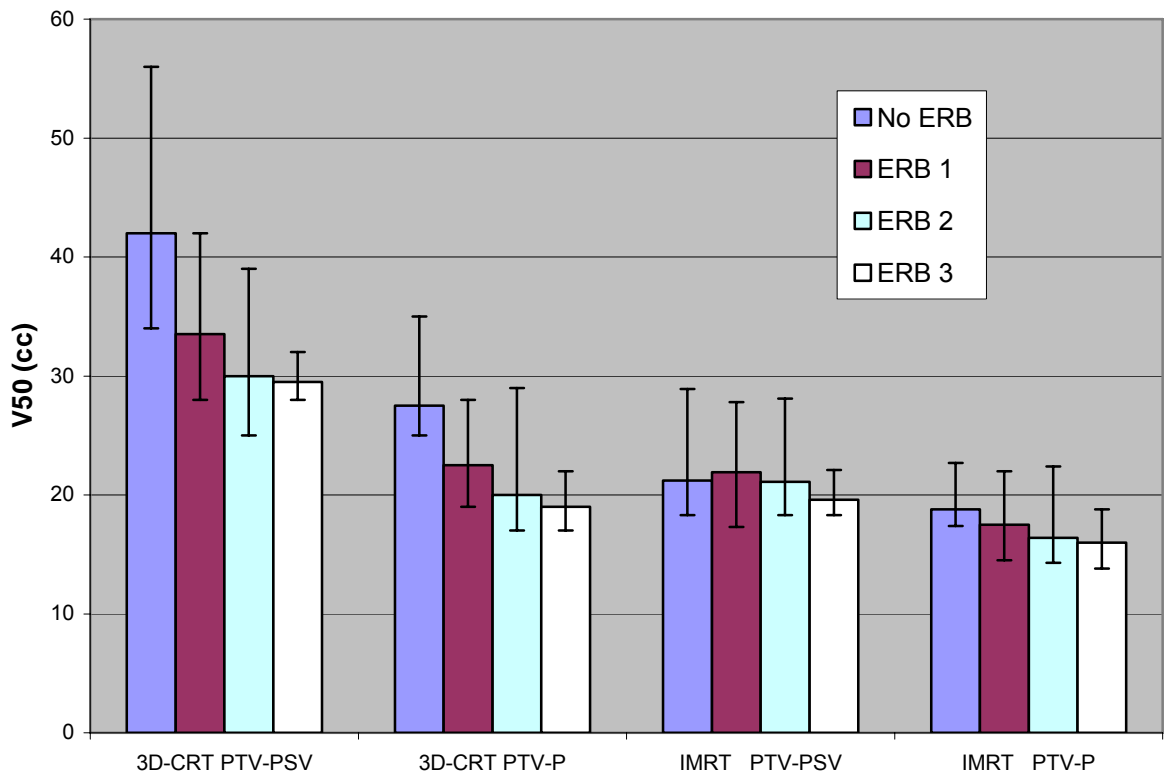|	3D-CRT				IMRT			
	PTV-PSV		PTV-P		PTV-PSV		PTV-P	
	V50 (cc)	p value	V50 (cc)	p value	V50 (cc)	p value	V50 (cc)	p value
No-ERB	42.0		27.5		21.2		18.8	
ERB 1	33.5	*0.0003*	22.5	*< 0.0001*	21.9	*0.93*	17.5	*0.05*
ERB 2	30.0	*0.0002*	20.0	*0.0001*	21.1	*0.80*	16.4	*0.04*
ERB 3	29.5	*0.0004*	19.0	*< 0.0001*	19.6	*0.10*	16.0	*0.01*

(b)

Table 4.
(a) V50 (cc) of the rectal wall for the 3D-CRT and IMRT treatment techniques and for the two different PTVs. The median values are shown with the 95% confidence interval. (b) The p values, given for ERB1, 2 and 3, resulted from the Wilcoxon signed ranks test comparing the V50 for the respective ERBs against No-ERB.
Abbreviations: PTV-PSV = planning treatment volume for prostate and seminal vesicles; PTV-P = planning treatment volume for prostate; V50 = rectal wall volume receiving $\geq$ 50 Gy in cc.

The V_{70} was, in case of PTV-PSV, significantly reduced by using any type of ERB (Table 5). ERB2 en 3 gave a larger reduction than ERB1, with p-values of 0.004 and 0.003, respectively. There was no statistical difference between ERB2 and 3 (p = 0.60). For PTV-P,

all three types of ERBs gave a significant reduction of V_{70}, compared to No-ERB. ERB3 gave more reduction than ERB1 and 2, with p-values of 0.0051 and 0.0319, respectively. There was no significant difference between ERB1 and 2 (p = 0.5416).

(a)

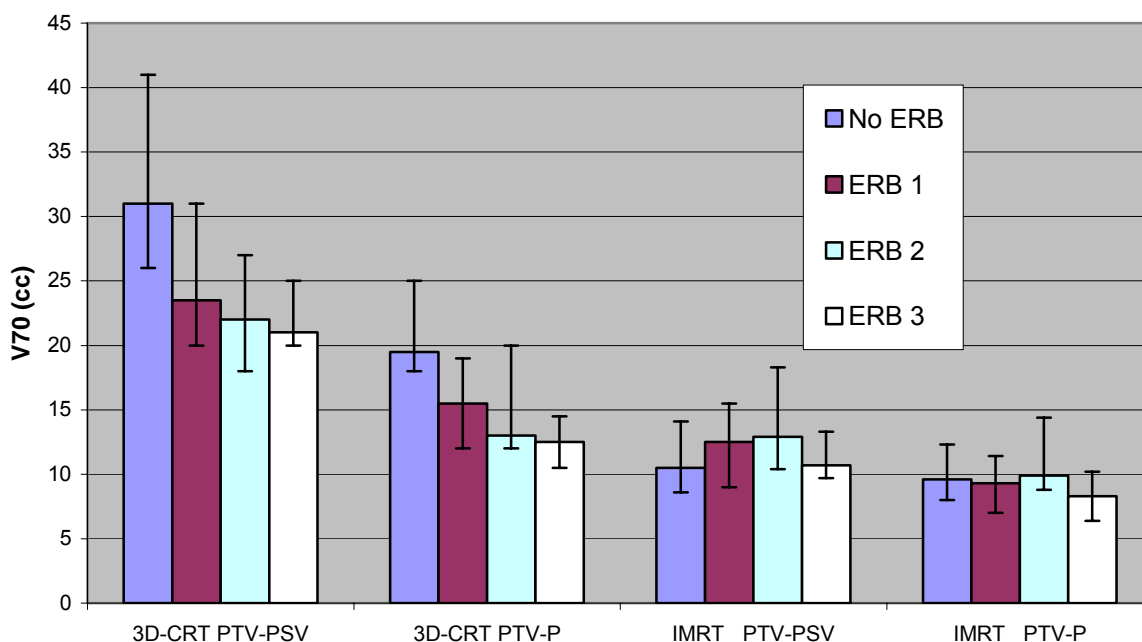|	3D-CRT				IMRT			
	PTV-PSV		PTV-P		PTV-PSV		PTV-P	
	V70 (cc)	p value	V70 (cc)	p value	V70 (cc)	p value	V70 (cc)	p value
No ERB	31.0		19.5		10.5		9.6	
ERB 1	23.5	0.0005	15.5	0.0003	12.5	< 0.0001	9.3	0.43
ERB 2	22.0	< 0.0001	13.0	0.0008	12.9	< 0.0001	9.9	0.20
ERB 3	21.0	0.0003	12.5	< 0.0001	10.7	0.0021	8.3	0.19

(b)

Table 5.
(a) V70 (cc) of the rectal wall for the 3D-CRT and IMRT treatment techniques and for the two different PTVs. The median values are shown with the 95% confidence interval (b) The p values, given for ERB1, 2 and 3, resulted from the Wilcoxon signed ranks test comparing the V70 for the respective ERBs against No-ERB.
Abbreviations: PTV-PSV = planning treatment volume for prostate and seminal vesicles; PTV-P = planning treatment volume for prostate; V70 = rectal wall volume receiving ≥ 70 Gy in cc.

Rectal wall sparing effect of the ERBs in IMRT

The inverse IMRT planning technique resulted in a good PTV coverage for all four CT-scans; the mean dose ($\pm$ 1 SD) for the PTV-P and PTV-PSV was 76.5 Gy ($\pm$ 0.1 Gy) for both target volumes.

Examples of typical dose distributions for the IMRT plans, with and without ERB, are given in Fig. 4 a-b.
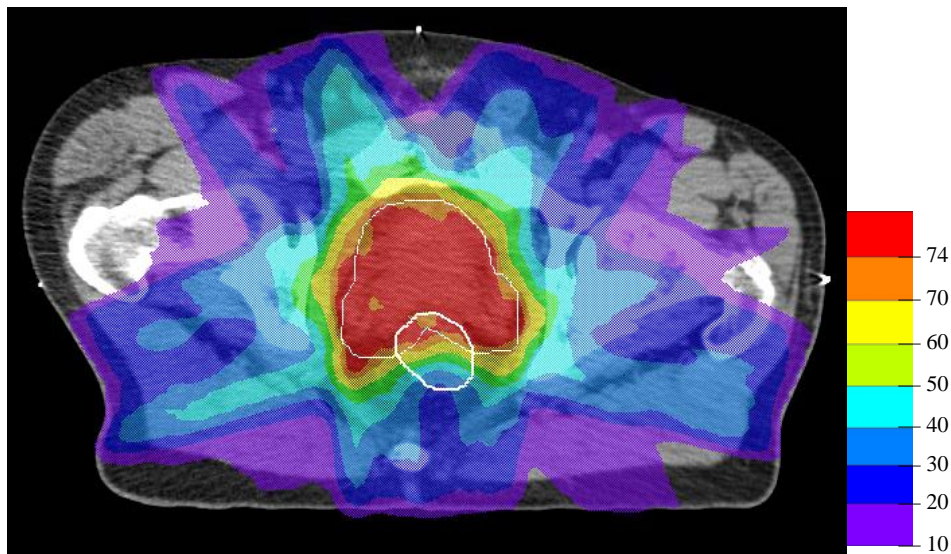
(a)
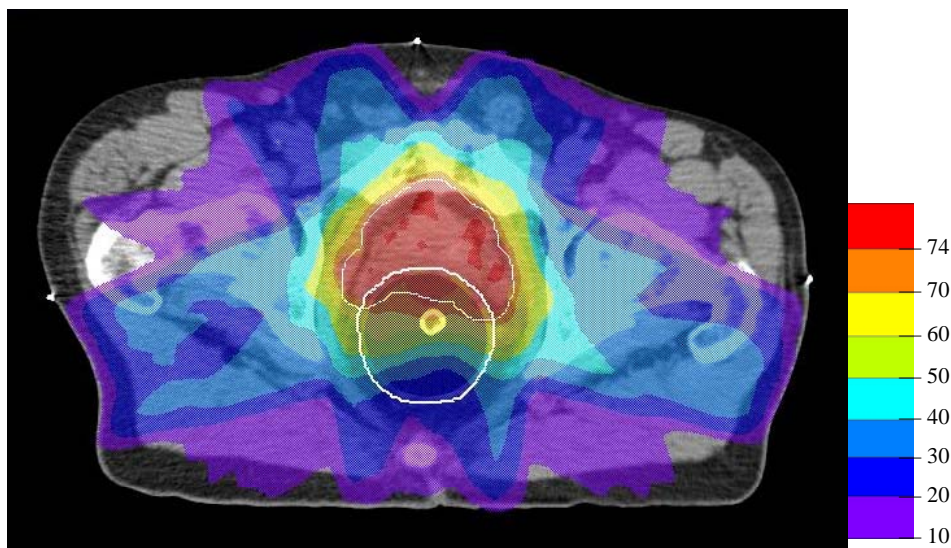
(b)

Fig. 4.
Transversal CT images with dose distribution, in Gy, for IMRT PTV-PSV, for (a) No-ERB and (b) ERB3. PTV (prostate and seminal vesicles + 7 mm margin) and rectal outer contour are highlighted (white lines).

The *mean Rwall dose* was not reduced significantly for both PTV-P and PTV-PSV by any of the ERBs (Table 2). A statistically significant difference in mean Rwall dose between the different types of ERB could not be demonstrated.

In case of PTV-PSV, the *NTCP Rwall* increased slightly, but statistically significant, by applying any type of ERB (Table 3). Between the different types of ERBs there was no significant difference (p values ranged from 0.16 to 0.46). For PTV-P, the NTCP Rwall did not significantly change by the use of any type of ERB. There was no statistically significant difference between the investigated ERBs (p values ranged from 0.33 to 0.51).

The V_{50} of the Rwall (Table 4), in case of PTV-PSV, was not reduced by any type of ERB, compared to the V_{50} of the IMRT plan without ERB. When comparing the V_{50} between the three ERBs, it showed that V_{50} for ERB3 was slightly, but significantly lower than for ERB1 (p = 0.005) and ERB2 (p = 0.02). There was no difference between ERB1 and 2 (p = 0.42). For PTV-P, ERB2 and 3 slightly, but significantly, reduced V_{50}. The V_{50} in ERB3 was significantly lower than for ERB1 (p = 0.0003). There was no difference between ERB2 and 3 (p = 0.21).

The V_{70} of the Rwall, in case of PTV-PSV, was slightly, but significantly increased by any of the three ERBs, compared to the planning without ERB (Table 5). Within the group of ERBs there were differences: ERB1 and 3 had significantly lower V_{70} than ERB2, with p-values of 0.007 and 0.0001, respectively. There was no significant difference between ERB1 and 3 (p = 0.27). For PTV-P, no difference was found for ERB1, 2 or 3, compared to No-ERB. Within the group of ERBs, only for ERB3, compared to ERB2, the V_{70} was significantly lower (p = 0.04). There was no difference between ERB1 and 2 (p = 0.64) or between ERB1 and 3 (p = 0.13).

Rectal wall dose maps and dose surface histograms

Dose maps (displayed by virtual rectum unfolding) and dose surface histograms (DSH) of the inner rectal wall showed, in case of 3D-CRT, a clear sparing effect of the ERBs compared to the treatment plan without ERB. As an example, the inner rectal wall dose surface maps (Fig. 5 a-d) and DSH (Fig. 5 e) of PTV-PSV treatment plans are displayed. Note the differences in rectal wall dilation by the different ERBs, yielding different maximum inner rectal wall circumferences of 8 cm, 13 cm, 14 cm and 20 cm for No-ERB, ERB1, 2 and 3, respectively (Fig. 6 a-d). For the treatment plan without an ERB, over a length of 7 cm (4 – 11 cm ab ano) the whole circumferential area of the inner rectal wall is exposed to a dose of 50 Gy and more (Fig. 5 a). In case of ERB2, this area is limited to the ventral rectal wall (Fig. 5 c). The two shorter ERBs (ERB1 and 3) do not dilate the rectum on the level of the seminal vesicles (11 cm ab ano) and here the high dose area reached the dorsal rectal mucosa (Fig. 5 b, d). From the DSH, it can be understood that the mucosal area exposed to doses over 40 Gy is reduced by the ERB (Fig. 5 e). For example, the fractional inner rectal wall area, irradiated > 60 Gy is reduced from 68% without ERB to 38% with ERB3 inserted.

Fig. 5.
Inner rectal wall dose surface maps for 3D-CRT PTV-PSV treatment plans for (a) No-ERB, (b) ERB1, (c) ERB2 and (d) ERB3. The dose distribution, of the inner rectal wall circumference, in Gray, is displayed on an unfolded rectum (i.c. the rectum is cut open at the posterior wall). On the horizontal axis the circumferential distance from anterior to posterior is displayed. On the vertical axis the distance from the most caudal delineated CT-slice is shown.
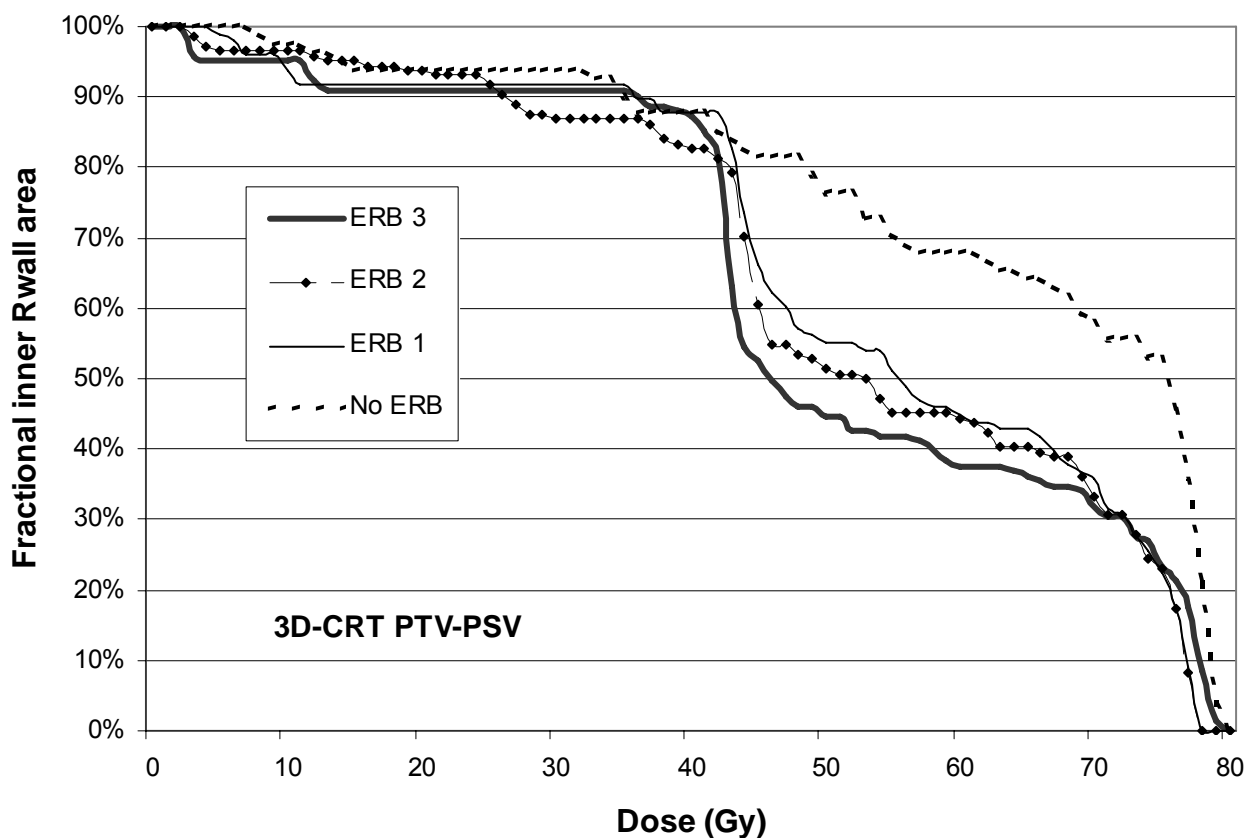
(e)

Fig. 5e.
Inner Rectal Wall dose surface histogram for 3DCRT PTV-PSV treatment plans for No-ERB, ERB1, ERB2 and ERB3.

As an example of a representative IMRT treatment plan, the inner rectal wall dose maps (Fig. 6 a-d) and the DSHs for IMRT PTV-P are displayed. The absolute surface area, irradiated to doses over 60 Gy is not evidently different between the 4 dose maps, as displayed in Fig 6 a-d. But due to the dilatation of the inner rectal wall, the fractional area of the inner rectal wall irradiated > 60 Gy is reduced from 31 % (No-ERB) to 17 – 20 % for ERB1-3 (Fig. 6 e).

(a)   (b)

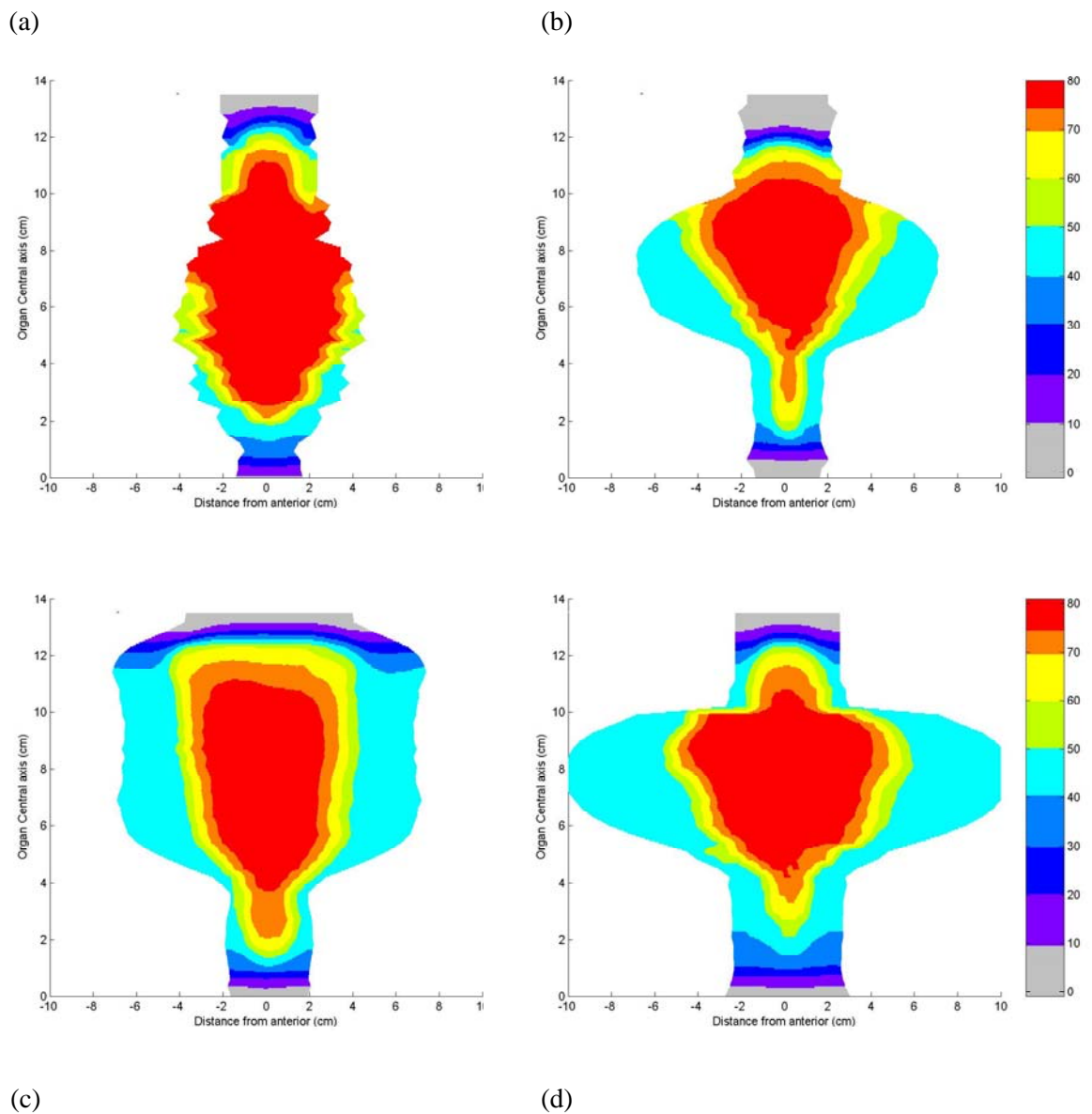

(c)   (d)
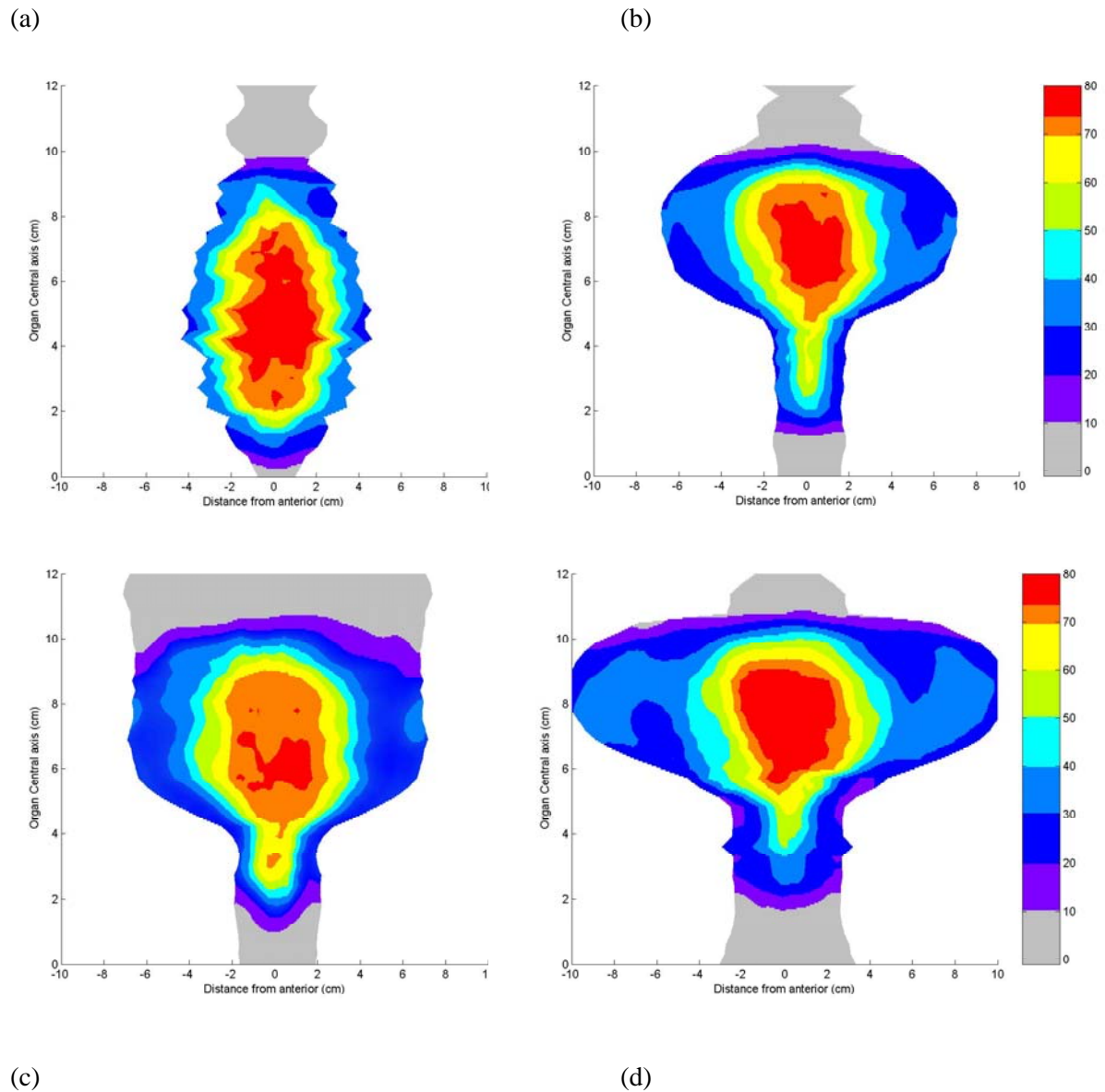
Fig. 6.

Inner rectal wall dose surface maps for IMRT PTV-P treatment plans for (a) No-ERB, (b) ERB1, (c) ERB2 and (d) ERB3. The dose distribution of the inner rectal wall circumference is displayed on an unfolded rectum (i.c. the rectum is cut open in the posterior wall). On the horizontal axis the circumferential distance from anterior to posterior is displayed. On the vertical axis the distance from the most caudal delineated CT-slice is shown.
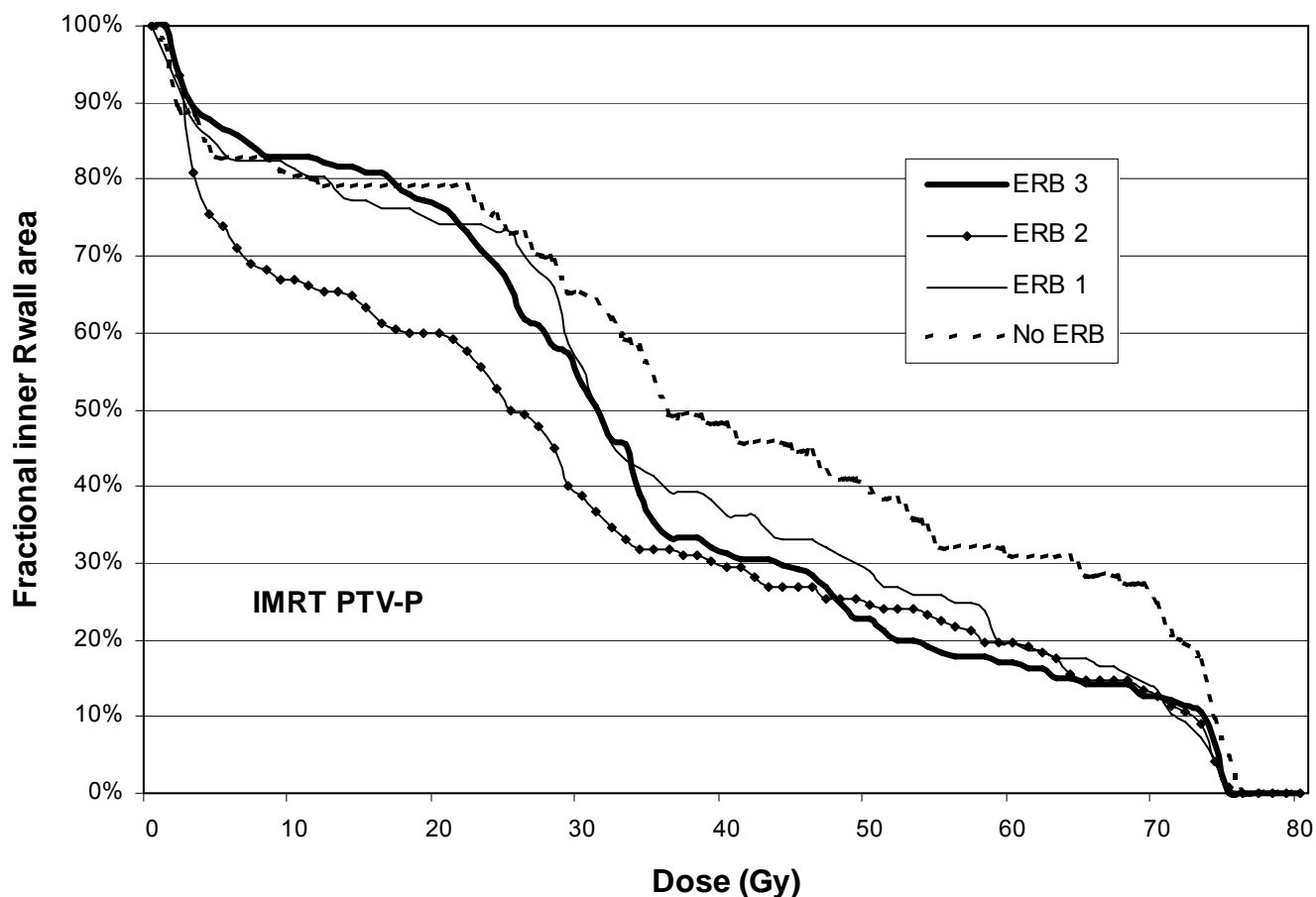
Fig 6 e.
Inner Rectal Wall dose surface histogram for IMRT PTV-P treatment plans for No-ERB, ERB1, ERB2 and ERB3.

ERB positioning and patient tolerance

No serious events, i.e rectal bleeding or severe anal irritation, occurred during the introduction of the ERBs and CT scanning session. The insertion of ERB1 was very easy due to its flexibility and small size. After inflation, patients noticed no extra pressure on the rectal wall or bladder. On CT scan, the position of the ERB1 was good, except for one case, where the ERB pointed towards the ventral anterior wall (Fig 7 a). ERB2 was slightly flexible and had the longest balloon (90 mm). All patients experienced some pressure on the rectal wall and bladder. The positioning was good in all cases. The long shaft was very helpful for the

introduction and positioning of the ERB. For ERB3, the balloon with the largest diameter, the inflation was painful in 5 patients: they experienced a local high pressure onto the rectal wall. This feeling disappeared within 1 minute. Insertion and positioning was complicated, due to the very rigid short shaft. In one patient, the ERB pointed too far to the ventral side and impressed the ventral rectal wall (Fig 7 b). Although no formal scoring system was used, patients experienced ERB1 (the smallest) to be favorite. For the personnel, ERB2 was the easiest to handle and to insert also because of the closed air system.
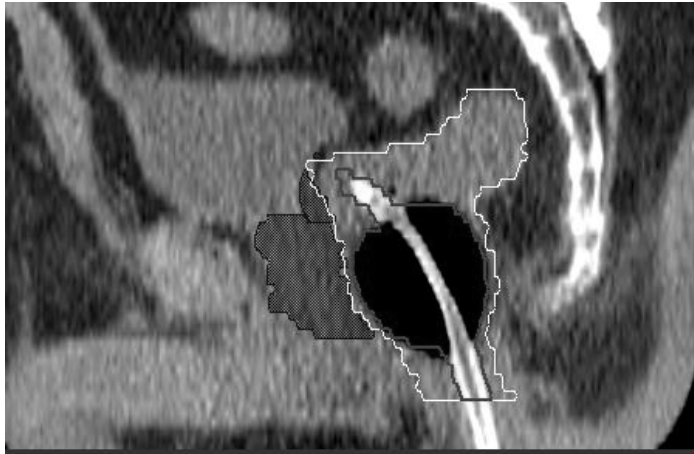
(a)
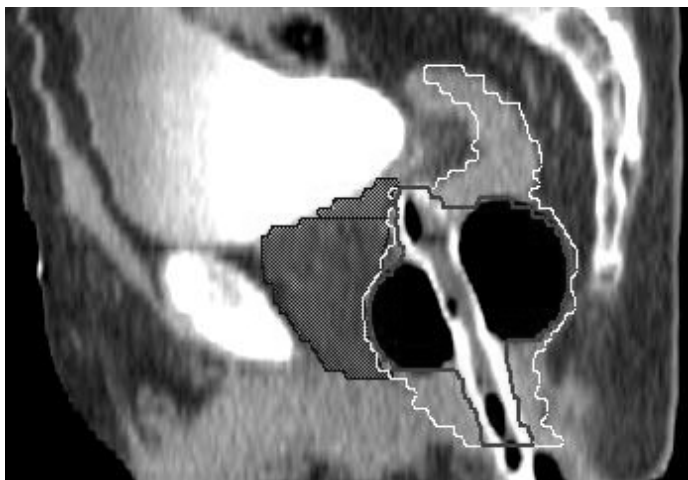
(b)

Fig. 7.
Example of incorrect positioning, in two different patients, of (a) ERB1 and (b)ERB3.
Prostate and seminal vesicles are highlighted in dark grey. The outer contours of the ERB and the rectal outer contour are highlighted.

DISCUSSION

In this prostate cancer radiotherapy treatment planning study, the dosimetric consequences and rectal wall sparing effect of three different ERBs were investigated for two different treatment techniques and two different PTVs. It appeared that, depending on the PTV and treatment technique (either 3D-CRT or IMRT), there were significant differences in the rectal wall sparing effect between the three types of ERBs, which could be correlated to the specific shape and size of the ERBs.

3D-CRT

The combination of 3D-CRT and any type of investigated ERB significantly reduced the mean dose, NTCP, V_{50} and V_{70} for the rectal wall. In case of irradiating the prostate only (PTV-P) it appeared that ERB3, the balloon having the largest diameter, performed the best. This can be explained by the greater prostate – posterior rectal wall distance. When the seminal vesicles are included into the PTV (PTV-PSV), ERB1 was inferior to the larger ERB2 and 3; ERB1 is not long and voluminous enough to separate the posterior rectal wall from the seminal vesicles, as clearly visible from Fig 5 b.

IMRT

Application of any ERB in combination with IMRT treatment planning did not result in a statistically significant reduction in NTCP or in mean dose of the rectal wall. Nevertheless, there were differences between the ERBs. In irradiation of the prostate only (PTV-P), the V_{50} and V_{70} of ERB3 were lower than for ERB1 and 2, again due to its largest inner rectal wall circumference. In case of PTV-PSV, NTCP and V_{70} were slightly increased by any of the ERBs. Evaluation of the CT-scans showed that with ERB, the anterior rectal wall is pushed towards the prostatic gland and even between the seminal vesicles, resulting in a larger rectal wall volume being exposed to high doses, compared to the situation without ERB. This effect was most clear for ERB2, the longest ERB, resulting in a higher V_{70}.

So far, two groups have reported on their first clinical results of the ERB (10, 11, 14). The group of Wachter *et al.* in Vienna investigated the type of ERB referred as ERB1 in our study. In 10 patients four planning CT-scans were made. A four-field box technique was used. The PTV consisted of prostate only or prostate + seminal vesicles surrounded by a 10 mm margin, and a dose of 66 Gy was prescribed. In case of PTV-P, they found a significant dose reduction to the rectal wall, mainly at the posterior wall, as a result of the increased distance between prostate and posterior rectal wall. In case of PTV-PSV, this advantage was lost. At the level of the seminal vesicles, this small-sized ERB does not dilate the rectum, and the

seminal vesicles can curl around the rectum, thereby decreasing the distance between the PTV and posterior rectal wall (14). This is confirmed in the present study (Fig. 5b). The Baylor college group reported their clinical experiences in 100 patients on the combination of IMRT (mean dose 76 Gy) and ERB3. A favorable acute toxicity profile was found, and dose escalation with an ERB seemed feasible (10, 11). Patel *et al.* conducted a treatment planning study in five patients and compared 3D-CRT with IMRT, also with PTV-P and PTV-PSV (13). The prescription dose was 76 Gy. ERB3 was inserted and filled with only 60 cc of air, in contrast to 100 cc of air, as propagated by the Baylor College group and as used in our present investigation. A treatment plan with an inflated ERB was compared against a plan with a deflated ERB. They concluded that application of this ERB gave as much rectal sparing as highly conformal IMRT, which is comparable to our NTCP data (Table 3). IMRT plus an ERB produced further rectal sparing, and this type of ERB was considered to be helpful for dose escalation (13). In contrast to our results, they found a decrease of the V_{70} Rwall. This can be explained by the smaller amount of air present in the ERB. It should be noted that the comparison was made with a CT scan with a deflated ERB inserted. As stated before, the diameter of the deflated ERB2 is still 15 mm. The CTV-PTV margin chosen by Patel *et al* for IMRT planning was 5 mm. The deflated ERB pushes the posterior rectal wall 15 mm away from the prostate gland, and with the steep dose gradient of an IMRT plan, even a slight rectal filling (caused by this ERB shaft) might cause a rectal wall sparing effect. Also we have shown in our study that introduction of an ERB can cause an artificial rectal wall shift (Fig. 7).

In clinical practice, any type of ERB is well accepted by the patients. For ERB3, 58 percent of the patients tolerated it without problems, while the remainder experienced it to be uncomfortable, but tolerable. In 2/116 patients the volume of air had to be reduced from 100 to 50 cc because of rectal discomfort (12). Also, ERB1 en ERB2 have proven to be clinically well tolerable. In 4/107 patients the application of ERB1 had to be stopped because of proctitis (14). In a group of 22 patients irradiated with ERB2, 2 patients developed transient Grade 2 anal irritation. Painful and bleeding hemorrhoids are considered to be a contraindication for ERB insertion (19). In this study, the 3 ERBs were tolerated well and insertion posed no great problems, although in the literature it was reported that in up to one-third of the assessed patients the ERB positioning was suboptimal (15). Daily ERB position verification is mandatory. Apart from results of the dosimetric study, the patients favored ERB1. In terms of accurate positioning of the ERB, ERB2 was considered favorite. For hygienic reasons we would not use condoms for daily application, as is necessary for the present design of ERB1 and 3. In a previous study we used a new ERB2 for every treatment fraction, and this was well accepted by our therapists (19).

The ERB has often been referred to as a prostate immobilizer (9, 12-15). We have investigated this issue and measured the prostate motion in patients with the ERB2 daily

inserted and compared it to a No-ERB group. With ERB, the day-to-day interfraction prostate displacements remained nearly unchanged, up to 4.7 mm (1 SD) for the anterior-posterior direction. This was caused by the presence of gas and stool besides the ERB (19). Also in this study it was shown on CT-scans that any ERB, even after rigorous laxation, could not prevent the presence of gas and stool, causing extra filling of the rectum and so a possible shift of the prostatic gland. Therefore, it should be advised to use any ERB in combination with daily prostate position verification and correction procedures.

In this present study, we evaluated the rectal wall sparing effect based on the dose distribution to the Rwall instead of the dose distribution for the entire rectum, including contents, as suggested by Tucker *et al* (4). It has become clear that, apart from the high Rwall doses (50 – 70 Gy) (2, 3, 25), also lower doses, up to 32 Gy may affect the risk of developing rectal bleeding (4, 24, 27, 28). Skwarchuk *et al.* (28) reported that, if the 50 % isodose curve (35 – 38 Gy) encompasses the outer rectal contour, the risk of rectal bleeding was increased. Tucker *et al.* (4) found that if 80 % or more of the Rwall surface was exposed to doses > 32 Gy, the risk of late rectal bleeding was increased by 50 %. It was suggested that these low dose areas play an important role in the rectal mucosal regeneration of the adjacent high dose regions (28, 29). In other words, small areas of high-dose exposed rectal wall are believed to regenerate faster if surrounded by areas of low dose. Inner Rwall dose surface histograms, showed, also in case of IMRT, a clear reduction of relative Inner Rwall exposed to intermediate and high-doses by the ERBs (Fig. 5e, Fig. 6e) which may contribute to reduce late rectal toxicity. Further exploration and more frequent usage of Rwall DSHs can give insight in this matter and can help to develop better NTCP models (4, 23). From the data presented it can be concluded that the use of an ERB is advantageous in combination with prostate 4 field 3D-CRT, a treatment modality still used more frequently than IMRT techniques (7). The intermediate to high-dose (45 – 75 Gy) areas were significantly reduced, resulting in a lower NTCP of the Rwall. Although we were not able to demonstrate a clear advantage in terms of NTCP, mean dose, V_{50} and V_{70} reduction, the definitive role of an ERB in prostate IMRT has to be determined in large comparative clinical studies. The first clinical experiences in primary prostate cancer radiotherapy and post-prostatectomy irradiation are promising, with favorable acute and late rectal toxicity profiles (10, 11, 30).

We have demonstrated that the use of a relatively large ERB (such as ERB2 and 3) in IMRT causes an improvement in the ratio between low and high-dose exposed surface areas, which may be advantageous in reducing rectal toxicity. Furthermore, the use of an air-filled ERB has shown to give an additional Rwall dose reduction of 15 % at the air-tissue interface (10). These two issues together with further improvement in IMRT treatment optimization (including Rwall constraints for low doses) and treatment delivery, including on-line position verification and correction procedures, are topics of future investigation to define the definitive

role of the ERB. As a result of this study, we are now in the process of developing a dedicated single-use ERB for daily insertion.

CONCLUSION

This study investigated the rectal wall (Rwall) sparing effect of three clinically applied ERBs for 3D-CRT and IMRT prostate cancer radiotherapy treatment techniques. Two different treatment volumes, prostate only (PTV-P) and prostate plus seminal vesicles (PTV-PSV), were defined. Each ERB was tolerated well, but incorrect positioning occurred in some cases and regular verification verification is therefore mandatory. The NTCP, mean dose, V_{50} and V_{70} of the Rwall were calculated in 284 treatment plans. For 3D-CRT, each ERB showed a clear Rwall sparing effect, by reducing of all the measured parameters. The larger type ERB2 and ERB3 performed better than the smaller sized ERB1. No statistically significant reduction of the parameters could be demonstrated for the combination of IMRT with any of the ERBs. Nevertheless, the different dilatation of the inner rectal wall, ranging from 8 to 20 cm, caused a shift in the ratio between high dose and low dose exposed surface areas. This might have a positive influence on the mucosal regeneration (28, 29), and thereby reduce the risk of rectal bleeding. Therefore, more clinical data and longer follow up are necessary to define the precise role of the ERB in combination with prostate IMRT. Development of patient- and therapist-friendly ERBs is warranted to increase their acceptability.

REFERENCES

1. Pollack A, Zagars GK, Starkschall G, et al. Prostate cancer radiation dose response: results of the M. D. Anderson phase III randomized trial. Int J Radiat Oncol Biol Phys 2002;53(5):1097-1105.

2. Storey MR, Pollack A, Zagars G, et al. Complications from radiotherapy dose escalation in prostate cancer: preliminary results of a randomized trial. Int J Radiat Oncol Biol Phys 2000;48(3):635-642.

3. Kupelian PA, Reddy CA, Klein EA, et al. Short-course intensity-modulated radiotherapy (70 GY at 2.5 GY per fraction) for localized prostate cancer: preliminary results on late toxicity and quality of life. Int J Radiat Oncol Biol Phys 2001;51(4):988-993.

4. Tucker SL, Dong L, Cheung R, et al. Comparison of rectal dose-wall histogram versus dose-volume histogram for modeling the incidence of late rectal bleeding after radiotherapy. Int J Radiat Oncol Biol Phys 2004;60(5):1589-1601.

5. Dearnaley DP, Khoo VS, Norman AR, et al. Comparison of radiation side-effects of conformal and conventional radiotherapy in prostate cancer: a randomised trial. Lancet 1999;353(9149):267-272.

6. Zelefsky MJ, Fuks Z, Hunt M, et al. High-dose intensity modulated radiation therapy for prostate cancer: early toxicity and biochemical outcome in 772 patients. Int J Radiat Oncol Biol Phys 2002;53(5):1111-1116.

7. Galvin JM, Ezzell G, Eisbrauch A, Yu C, et al. Implementing IMRT in clinical practice: a joint document of the American Society for Therapeutic Radiology and Oncology and the American Association of Physicists in Medicine. Int J Radiat Oncol Biol Phys 2004;58(5):1616-1634.

8. Chen ME, Johnston DA, Tang K, et al. Detailed mapping of prostate carcinoma foci: biopsy strategy implications. Cancer 2000;89(8):1800-1809.

9. D'Amico AV, Manola J, Loffredo M, et al. A practical method to achieve prostate gland immobilization and target verification for daily treatment. Int J Radiat Oncol Biol Phys 2001;51(5):1431-1436.

10. Teh BS, Dong L, McGary JE, et al. Rectal wall sparing by dosimetric effect of rectal balloon used during Intensity-Modulated Radiation Therapy (IMRT) for prostate cancer. Med Dosim 2005;30(1):25-30.

11. Teh BS, Mai WY, Uhl BM, et al. Intensity-modulated radiation therapy (IMRT) for prostate cancer with the use of a rectal balloon for prostate immobilization: acute toxicity and dose-volume analysis. Int J Radiat Oncol Biol Phys 2001;49(3):705-712.

12. Teh BS, Woo SY, Mai WY, et al. Clinical experience with intensity-modulated radiation therapy (IMRT) for prostate cancer with the use of rectal balloon for prostate immobilization. Med Dosim 2002;27(2):105-113.

13. Patel RR, Orton N, Tome WA, et al. Rectal dose sparing with a balloon catheter and ultrasound localization in conformal radiation therapy for prostate cancer. Radiother Oncol 2003;67(3):285-294.

14. Wachter S, Gerstner N, Dorner D, et al. The influence of a rectal balloon tube as internal immobilization device on variations of volumes and dose-volume histograms during treatment course of conformal radiotherapy for prostate cancer. Int J Radiat Oncol Biol Phys 2002;52(1):91-100.

15. Miralbell R, Molla M, Arnalte R, et al. Target repositioning optimization in prostate cancer: is intensity-modulated radiotherapy under stereotactic conditions feasible? Int J Radiat Oncol Biol Phys 2004;59(2):366-371.

16. Wachter S, Gerstner N, Goldner G, et al. Rectal sequelae after conformal radiotherapy of prostate cancer: dose-volume histograms as predictive factors. Radiother Oncol 2001;59(1):65-70.

17. Wachter-Gerstner N, Wachter S, Goldner G, et al. Biochemical response after 3-d conformal radiotherapy of localized prostate cancer to a total dose of 66 gy 4-year results. Strahlenther Onkol 2002;178(10):542-547.

18. Wachter S, Gerstner N, Goldner G, et al. Endoscopic scoring of late rectal mucosal damage after conformal radiotherapy for prostatic carcinoma. Radiother Oncol 2000;54(1):11-19.

19. van Lin EN, van der Vight LP, Witjes JA, et al. The effect of an endorectal balloon and off-line correction on the interfraction systematic and random prostate position variations: A comparative study. Int J Radiat Oncol Biol Phys 2005;61(1):278-288.

20. Teh BS, McGary JE, Dong L, et al. The use of rectal balloon during the delivery of intensity modulated radiotherapy (IMRT) for prostate cancer: more than just a prostate gland immobilization device? Cancer J 2002;8(6):476-483.

21. Lyman JT. Complication probability as assessed from dose-volume histograms. Radiat Res 1985;104(Suppl):13-19.

22. Kutcher GJ, Burman C. Calculation of complication probability factors for non-uniform normal tissue irradiation: the effective volume method. Int J Radiat Oncol Biol Phys 1989;16 (6):1623-1630

23. Emami B, Lyman J, Brown A, et al. Tolerance of normal tissue to therapeutic irradiation. Int J Radiat Oncol Biol Phys 1991;21(1):109-122.

24. Zapatero A, Garcia-Vicente F, Modolell I, et al. Impact of mean rectal dose on late rectal bleeding after conformal radiotherapy for prostate cancer: dose-volume effect. Int J Radiat Oncol Biol Phys 2004;59(5):1343-1351.

25. Huang EH, Pollack A, Levy L, et al. Late rectal toxicity: dose-volume effects of conformal radiotherapy for prostate cancer. Int J Radiat Oncol Biol Phys 2002;54(5):1314-1321.

26. Lu Y, Song PY, Li SD, et al. A method of analyzing rectal surface area irradiated and rectal complications in prostate conformal radiotherapy. Int J Radiat Oncol Biol Phys 1995;33(5):1121-1125.

27. Jackson A, Skwarchuk MW, Zelefsky MJ, et al. Late rectal bleeding after conformal radiotherapy of prostate cancer. II. Volume effects and dose-volume histograms. Int J Radiat Oncol Biol Phys 2001;49(3):685-698.

28. Skwarchuk MW, Jackson A, Zelefsky MJ, et al. Late rectal toxicity after conformal radiotherapy of prostate cancer (I): multivariate analysis and dose-response. Int J Radiat Oncol Biol Phys 2000;47(1):103-113.

29. Skwarchuk MW, Travis EL. Volume effects and epithelial regeneration in irradiated mouse colorectum. Radiat Res 1998;149(1):1-10.

30. Teh BS, Mai WY, Augspurger ME, et al. Intensity modulated radiation therapy (IMRT) following prostatectomy: more favorable acute genitourinary toxicity profile compared to primary IMRT for prostate cancer. Int J Radiat Oncol Biol Phys 2001;49(2):465-472.

IMRT boost dose planning on dominant intra-prostatic lesions: gold marker based 3D fusion of CT with dynamic contrast-enhanced and ¹H-spectroscopic MR imaging

Emile N.J.Th van Lin, M.D.[#], Jurgen J. Fütterer M.D.[¶], Stijn W.T.P.J. Heijmink M.D.[¶], Lisette P. van der Vight, B.Sc.[#], Aswin L. Hoffmann, M.Sc.[#], Peter van Kollenburg, B.Sc.[#], HenkJan J. Huisman, Ph.D.[¶], Tom W.J. Scheenen, Ph.D.[¶], J.Alfred Witjes, M.D., Ph.D. , Jan Willem Leer, M.D. Ph.D.[#], Jelle O. Barentsz , M.D. Ph.D.[¶], and Andries G. Visser, Ph.D.[#]

Departments of [#]Radiation Oncology, [¶]Radiology and Urology, Radboud University Nijmegen Medical Centre, Nijmegen, The Netherlands

ABSTRACT

Purpose: To demonstrate the theoretical feasibility of integrating two functional prostate MR imaging techniques (dynamic contrast-enhanced MR imaging (DCE-MRI) and [1]H-MR spectroscopic imaging (MRSI)), into inverse treatment planning for definition and potential irradiation of a dominant intra-prostatic lesion (DIL) as a biological target volume for high-dose intra-prostatic boosting with IMRT (DIL-IMRT).

Methods and materials: In five patients, four gold markers were implanted. An endorectal balloon was inserted for both CT scanning and MR imaging. A DIL volume was defined by DCE-MRI and MRSI using different prostate cancer specific physiologic (DCE-MRI) and metabolic (MRSI) parameters. The CT-MR image registration was performed automatically by matching 3D gold marker surface models with the iterative closest point method. DIL-IMRT plans, consisting of whole prostate irradiation to 70 Gy and a DIL boost to 90 Gy, and standard IMRT plans, where the whole prostate was irradiated to 78 Gy (IMRT-78) were generated. The tumor control probability (TCP) and rectal wall normal tissue complication probability (Rwall NTCP) were calculated and compared between the two IMRT approaches.

Results: Combined DCE-MRI and MRSI yielded a clearly defined single DIL volume (range 1.1 – 6.5 cc) in all patients. In this small, selected patient population no differences in TCP were found. A decrease in Rwall NTCP was observed in favor of the DIL-IMRT plan, as compared to the IMRT-78 plan.

Conclusions: Combined DCE-MRI and MRSI functional image-guided high-dose intra-prostatic DIL IMRT planned as a boost to 90 Gy is theoretically feasible. Preliminary results indicate that DIL-IMRT may improve the therapeutic ratio by decreasing the NTCP with unchanged TCP. A larger patient population, with more variation of the number, size and localization of the DIL, and a feasible mechanism for treatment implementation has to be studied to extend these preliminary tumor control and toxicity estimates.

INTRODUCTION

The use of defining a biological target volume (BTV) and intensity-modulated radiotherapy (IMRT) for advanced "dose painting", as proposed by Ling *et al.* (1) is gradually introduced into clinical practice. This has been made possible by advanced imaging techniques. Prostate magnetic resonance (MR) imaging techniques can be fused with planning computed tomography (CT)-scans and this has been shown to enable improved target delineation (2,3). Functional MR imaging techniques have developed over the years. Dynamic contrast-enhanced MR imaging (DCE-MRI) can visualize prostate cancer (neo)vascularity (4,5). [1]H-MR spectroscopic imaging (MRSI) has been shown to provide a high specificity for prostate cancer (6,7). These techniques can lead to a more accurate staging and localization of prostate cancer (8-12) and are valid methods for early evaluation of radiotherapy effect (13).

The "classical" whole-prostate dose escalation has improved treatment outcome (14-16). Nevertheless, intra-prostatic failures do occur and can be detected by MR imaging (17). Cellini *et al.* (18) performed an MR-based analysis of intra-prostatic failure and concluded that, in all their observed cases, local recurrence originates within the initial tumor volume. Strategies, mainly for brachytherapy and low-size (< 50 cc) prostates, have been tested to detect the so-called "Dominant Intra-prostatic Lesion" (DIL) by MRSI and have been given an extra boost dose to this DIL, to thereby increase the therapeutic ratio (19-23). To acquire high-resolution anatomical MR data an endorectal coil is usually inserted causing deformation of the prostate gland. Consequently, accurate image registration with the initial planning CT scan (without endorectal coil) is often difficult. The CT-MR matching can be done by mutual information based automatic registration (24) or manually, by visual approximation (19,22). To overcome the difficulties in registration, we developed a gold marker based 3D CT-MR fusion protocol (25) where an endorectal balloon (ERB) is used during CT-scanning and treatment that has the same dimensions as the MR endorectal coil (26). ERBs are also used in prostate radiotherapy for their rectal wall sparing effect (27-29). In our daily practice, fiducial gold markers are used for position verification and correction procedures (30-32). These markers are clearly visible on both CT and T_2*-weighted MR images. Reliable and accurate image fusion is feasible using above-mentioned conditions (25,33).

To date, the combination of two functional MR imaging techniques (DCE-MRI and MRSI), gold markers and an ERB for biological image-guided external beam radiotherapy has not been described elsewhere. The purpose of this study was to demonstrate the feasibility of the fusion of these functional MR imaging techniques with CT, using gold markers as fiducials, and to integrate these images into inverse treatment planning to define a BTV for high-dose intra-prostatic DIL boosting with IMRT. The next goal was to make an estimation of the

potential gains, in terms of tumor control probability (TCP) and rectal toxicity, by analyzing normal tissue complication probability (NTCP).

MATERIALS AND METHODS

This pilot study was performed over a period of 6 months, until December 2004. Patients with biopsy proven prostate cancer were selected for our study. At the start of this study, only patients with uni-lateral prostate cancer were selected. Patient exclusion criteria were: previous hormonal therapy, positive lymphadenectomy, contraindications to MR imaging (e.g., cardiac pacemakers, intracranial clips) and contraindications to endorectal coil insertion (e.g., anorectal surgery, inflammatory bowel disease). Finally, five patients were enrolled in this study, after informed consent was given.

In each patient, four fine gold markers (1-mm diameter, 7-mm length) were implanted in the prostate through trans-rectal ultrasound guidance by an experienced urologist (J.A.W.) (Fig. 1a). Two markers were inserted in the base, one in the apex and one in the central part (next to the urethra) of the prostate gland. A standard 18-gauge prostate biopsy tool was used (Micro-invasive topnotch, Boston Scientific, Natick, MA, US.*)* (Fig. 1b) and prophylactic antibiotics were given (ciprofloxacin 500 mg, BID, for 3 days).
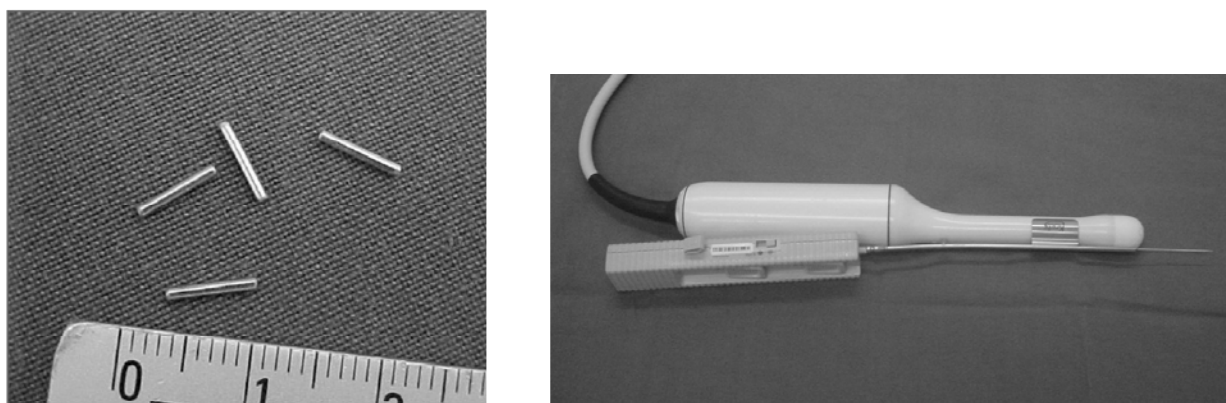
Fig.1. *(a) Fine gold fiducial prostate markers. (b) Prostate biopsy tool used for marker implantation, mounted on ultrasound probe.*

After at least 1 week, to resolve swelling of the gland after marker implantation, patients underwent both CT and MR imaging on the same day, within 4 hours. Patient positioning during both CT and MR examinations was identical to that during treatment: supine on a flat couch that was covered with a thin disposable paper sheet. Only a pillow and a foam

knee support were used for relaxed positioning of the head and legs, respectively. Prior to the imaging sessions, patients used a laxative diet and a laxans (Microlax clysma 5 mL, Pharmacia B.V. Woerden, The Netherlands), and were intended to have a full bladder by drinking 500 ml of water.

CT and MR imaging protocol

The planning CT scan was obtained at 3-mm slice thickness with a multi-slice CT scanner (150 mA, 140 kV, feed 12.5 mm, rotation 0.5s) (AcQsim spiral CT; Philips Medical Systems, Bothell, WA). An ERB was inserted and inflated with 80 cc of air to mimic MR imaging conditions and reduce prostate deformation differences. The ERB used during CT imaging is a modified MR endorectal balloon without the coil wiring and has the same dimensions and shape as the MR endorectal coil (MedRad, Indianola, PA, US) (26,29) (Fig. 2a).

MR imaging was performed using a 1.5T MR scanner (Magnetom Sonata, Siemens, Erlangen, Germany). Patients were imaged in supine position. Integrated endorectal phased-array coils were used (Medrad, Indianola, PA, US). After digital rectal examination the endorectal coil was inserted and inflated with 80 cc of air. Peristalsis was suppressed by an intramuscular injection of 1 mg glucagon (Glucagen; Novo Nordisk A/S, Denmark) prior to the examination. Localizing images were acquired for anatomical orientation and to confirm coil positioning. The three-part scanning protocol is listed in order of acquisition in Table 1. Firstly, for anatomical information, T_2-weighted fast spin echo (FSE) images were acquired in three planes (Fig. 2b). A transversal T_2*-weighted gradient echo sequence (MEDIC) provided clear visualization of the gold markers (Fig. 2c). Secondly, MRSI was obtained using a 3D chemical shift imaging (3D-CSI) sequence. Thirdly, DCE-MRI was performed using one intermediate weighted and repeated T_1-weighted imaging during 2 minutes. A dose of 0.2 mmol/kg gadolinium-DTPA (Magnevist, Schering, Berlin, Germany) was injected using a power injector (Spectris, Medrad, Indianola, PA, US) with saline flush.
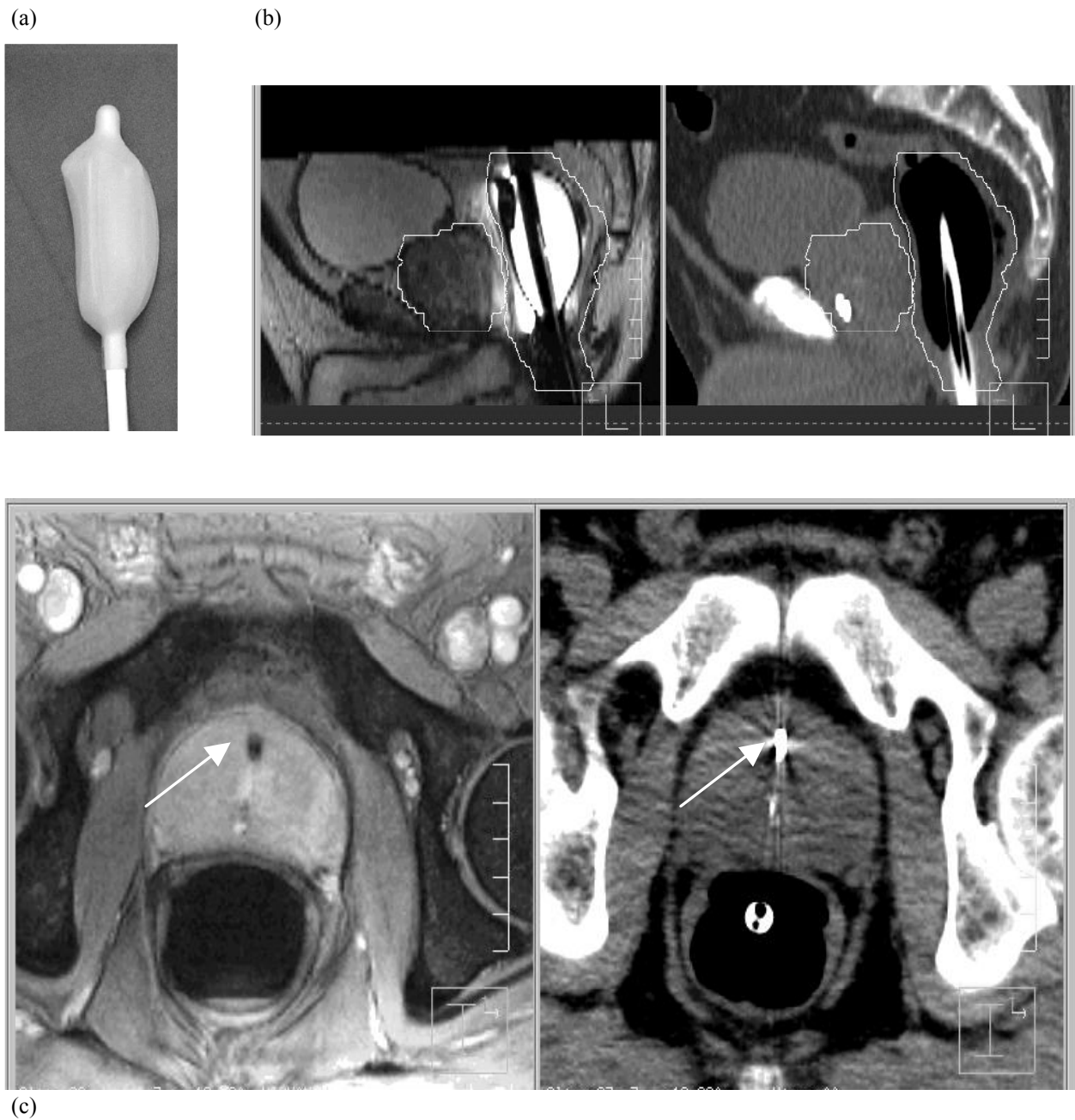
(a)

(b)

(c)

Fig. 2.
(a) Endoretal balloon used during CT and MR imaging.
(b) Sagittal MR T_2-weighted image (FSE) (left panel) and CT image (right panel) with endorectal balloon inserted. Prostate and outer rectal wall are highlighted.
(c) Transverse MR T_2*-weighted (MEDIC) image (left panel) and CT (right panel) image, gold marker is indicated (arrow)

Sequence	TR (ms)	TE (ms)	α (°)	slice thickness (nr of slices)	FOV (mm)	matrix	in plane voxelsize
FSE	4100	119	180	4.0 (15)	280	512 x 256	0.35 x 0.35
MEDIC	700	18	30	3 (22)	285	512x448	0.56 x 0.56
3D-MRSI (interpolated)	640	120	PRESS	4.3 (12)	84	14 x 14	4.3 x 4.3
turboFLASH (pre)	800	1.61	8	4.0 (10)	280	192 x 256	1.09 x 1.09
turboFLASH (post)	34	1.61	10	4.0 (10)	280	192 x 256	1.09 x 1.09

Pre = pre-contrast; post = post-contrast

Table 1.
Magnetic Resonance Imaging Protocol; Scanning Parameters

Imaging registration

CT and MR imaging sets were aligned by registering the MEDIC MR volume to the CT volume, using an in-house developed application as described by Huisman *et al.* (25). In summary, the markers, displayed on T_2*-weighted (MEDIC) MR and CT, were semi-automatically segmented and converted into 3D surface models (Fig. 3a, b). The 3D surface models from both datasets were then registered by minimizing the root-mean-square distance between the surfaces using the iterative closest point (ICP) method (25). The registration was visually verified by observing the fused CT and MEDIC MR images. The MR marker surface model was depicted in green while the CT marker surface model was overlaid in red with CT window and level set to reveal only the markers (Fig. 3c). In case the fused display demonstrated clearly visible mis-registrations the registration procedure was reiterated.

DIL delineation

The radiologist (J.F.), performing the DIL delineation, was unaware of the tumor characteristics (local staging by digital rectal examination, PSA or Gleason score) during the evaluation of the images. Post-processing entailed two stages. First, the acquired DCE-MRI and MRSI data were processed to extract functional feature images. The DCE-MRI dataset, to identify regions of neo-vascularity, was analyzed based on multiple physiologic parameters, such as the K_{cp}, quantifying the permeability
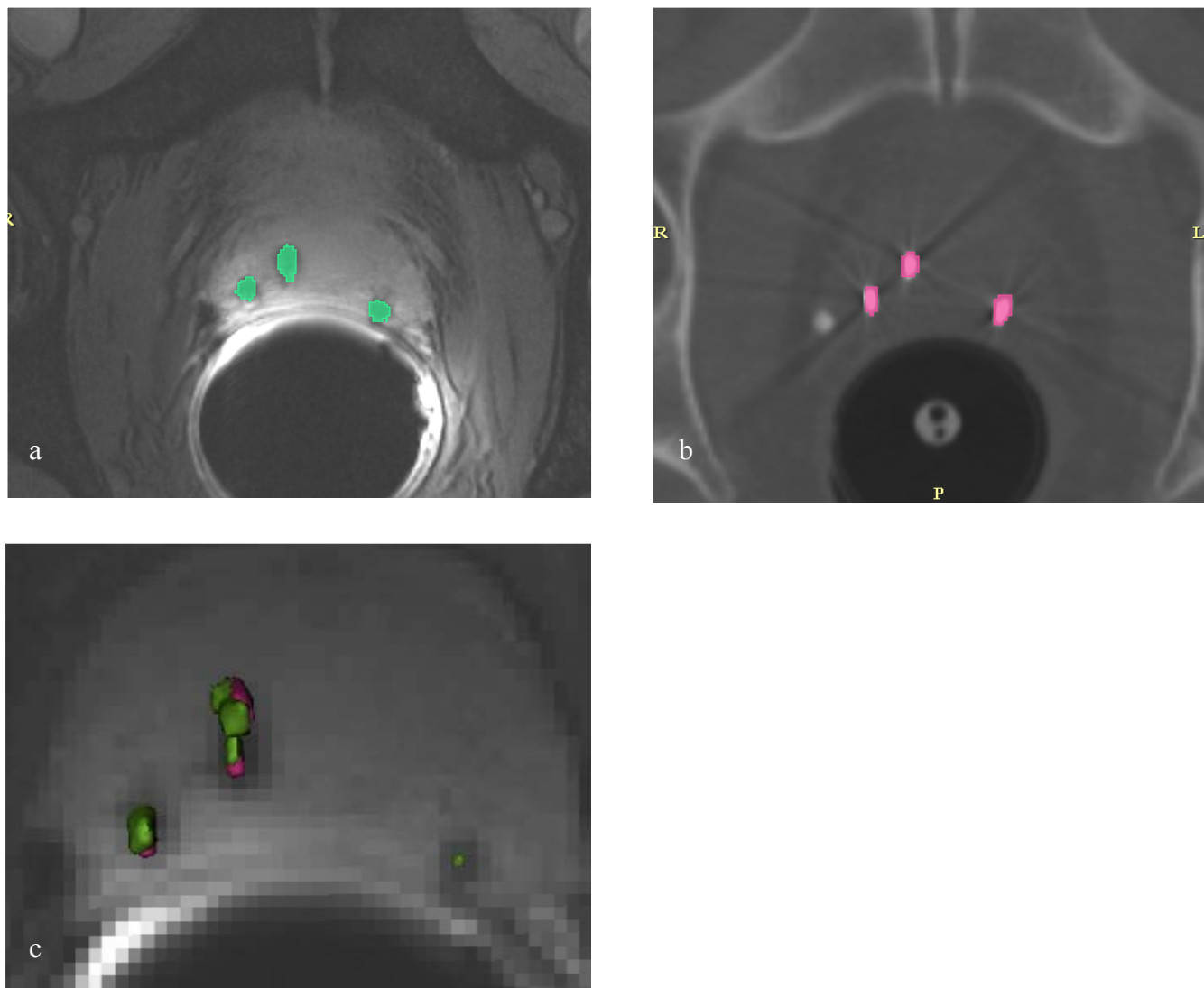
Fig. 3.

Marker registration by iterative closest point (ICP) method. Markers are semi-automatically segmented on (a) T2*-weighted MR image (MEDIC) and on (b) CT image. (c) MR (green) and CT (red) marker surface models registered by minimizing the root-mean-square distance of the separate models.

surface area, K_{trans}, defined as the volume transfer constant and ECV, for quantification of the extracellular volume (5,9). Then, based on these findings, the MRSI dataset was evaluated to make the final diagnosis of prostate cancer or normal prostate tissue, by analyzing the separate [1]H-MR spectra of the prostate gland voxels. A choline + creatine/citrate ratio > 0.9 was considered to be positive for prostate cancer (6,7,9,10).

In the second post-processing stage, these DCE-MRI and MRSI feature images and the T_2-weighted prostate images were fused; the functional images were overlaid in

transparent colors on T_2-weighted MR images in three perpendicular planes. A 3-D editor, build within the registration application, was used to delineate the boundary of the DIL (Fig. 4a). During the editing process of the DIL, the radiologist was able to switch between the DCE-MRI and MRSI feature images and the T_2-weighted MR images with the cross-section of the resulting tumor model visible in all planes. The definitive tumor model was then saved as a binary DIL volume. The registration parameters that aligned the MEDIC MR data and the CT data were used to align the DIL volume with the CT data. The aligned DIL volume, together with the MEDIC MR images and the T_2-weighted MR images were then transferred and imported into the radiotherapy treatment planning system. An illustrated case example is described in the *Results* section.

IMRT treatment planning

The radiation oncologist (E.V.L.) and the radiologist (J.F.) reviewed the MEDIC MR images, the T_2-weighted MR images and the aligned DIL volume. Together they delineated the prostate gland in the MEDIC and the T_2-weighted MR images. The resulting contours were automatically transferred to the corresponding CT slices and defined as the prostate clinical target volume (CTV). The registered DIL volume in the image fusion window of the Pinnacle[3] treatment planning system (Philips Medical Systems, Andover, MA) was reviewed and the DIL CTV was defined (Fig. 4b). On each CT slice the normal surrounding structures were outlined: bladder, urethra, femoral heads and rectal wall. The rectal wall (Rwall) was defined as the difference between the inner and outer rectal wall contour (34). The Rwall was delineated from the ischial tuberosities up to the rectosigmoid flexure.
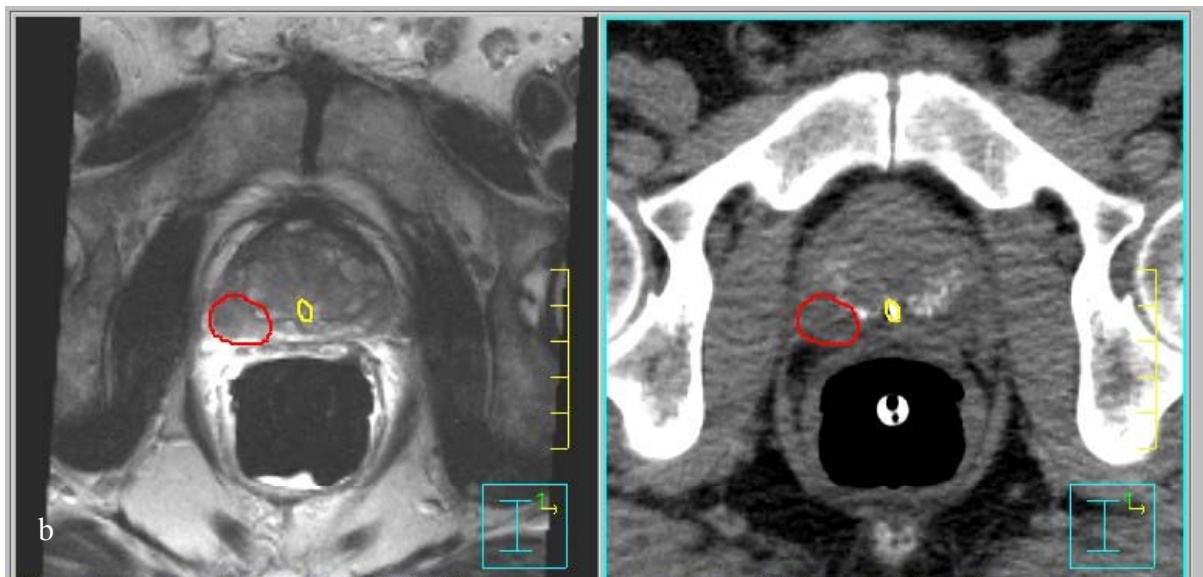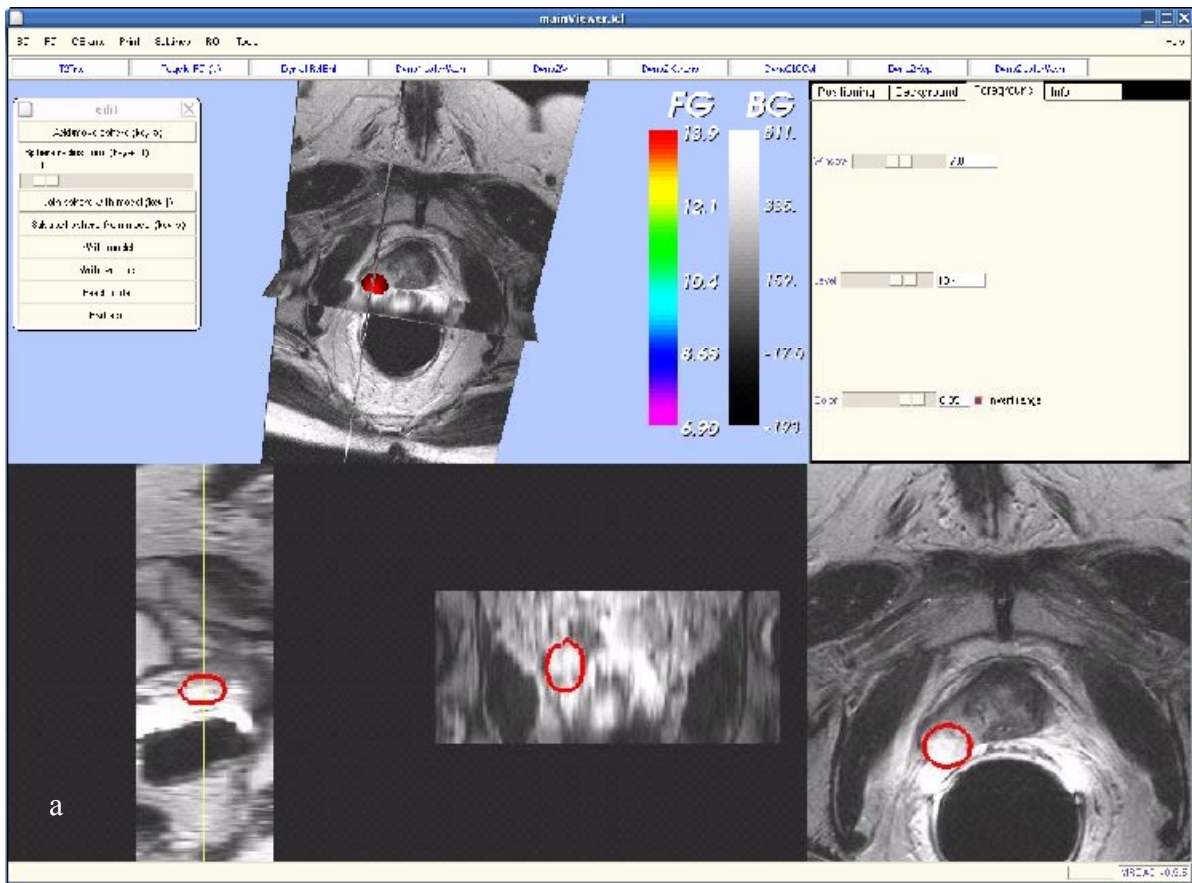
Fig. 4
(a) 3D editor for delineation of the DIL volume. DIL is highlighted in red
(b) DIL volume (highlighted in red) is transferred into treatment planning system and displayed on a transversal MR T_2-weighted image (left panel) and on a CT image (right panel). In yellow the central gold marker is indicated.

For each patient, two IMRT treatment plans were made to compare the tumor control probability (TCP) and predicted rectal toxicity, as estimated by the NTCP. First, the DIL-IMRT plan was identified, irradiating a PTV_{70} and a PTV_{90}. The PTV_{70} was defined as the prostate gland + 7 mm isotropic margin (prescription dose 70 Gy). The PTV_{90} consisted of the DIL + 5 mm isotropic margin (prescription dose 90 Gy). Next, a more standard IMRT plan (IMRT-78) was constructed, in which PTV_{78} consisted of the prostate gland + 7 mm isotropic margin. For this plan the prescription dose was 78 Gy (14). For both plans, the dose per fraction was 2 Gy for the prostate. In the DIL-IMRT plan, the dose per fraction for the DIL was 2.57 Gy.

For both plans, the step-and-shoot IMRT plan consisted of seven coplanar, non-opposing 10 MV photon energy beams. One beam was oriented posterior-anterior (PA) while the other six beams were configured with equidistant gantry angles.

For both plans, equal DVH and maximum dose objectives for the normal tissues were defined (Table 2). In addition, the maximum allowable dose outside the delineated structures was set to 38 Gy (weight factor = 1). For the DIL-IMRT plan and IMRT-78 plan the following target volume objectives were defined. In brackets the weight factor (W) for the corresponding objective is noted. Objectives regarding the CTV were: minimal allowable dose of 90 % of the prescription dose (W=10), maximum allowable dose 110 % of the prescription dose (W=10). Objectives for the PTV were: minimum dose 90 % (W=2), maximum dose 110 % (W 5) and dose uniformity (W 1). For the PTV, also DVH objectives are defined: > 99 % of the PTV volume should receive a minimal dose of 95 % of the prescription dose (W=10). For the DIL-IMRT plan, the maximum allowable dose within the DIL was set on 94 Gy (W=1).

For comparison of the IMRT-78 and the DIL-IMRT plans, the mean doses for the prostate and DIL were calculated. For the Rwall, the NTCP for serious ($\geq$ grade 3 rectal toxicity) was computed, applying the Lyman-Kutcher-Burman model with Emami parameters (n=0.12, m=0.15 and TD_{50}=80 Gy) (35-37). The resulting spatial dose distribution over the inner surface of the rectal wall, representing the rectal wall mucosa, was visualized by generating inner rectal wall dose surface maps (38).

For TCP calculations, the Poisson-based model of Webb and Nahum was used, taking the interpatient variation in radiosensitivity over a representative cohort of patients into account (39). The model parameters used were taken from Nahum *et al.* (40): a mean $\pm$ standard deviation radiosensitivity (α_{mean} and σ_{α}, respectively) of 0.26 ± 0.06 Gy^{-1} and an α/β-ratio of 8.3 Gy were used. Furthermore, it was assumed that the initial clonogenic cell density for the DIL was 10^7 cells/cc, and for the rest of the prostate was 10^5 cells/cc. Proliferation effects were ignored in the calculations.

ROI	Objective	Dose level (Gy)	Volume (%)	Weight factor
Rectal Wall	Max Dose	75	100	50
Rectal Wall	Max DVH	60	10	20
Rectal Wall	Max DVH	50	20	10
Rectal Wall	Max DVH	40	30	10
Bladder	Max DVH	70	2	3
Bladder	Max DVH	60	15	2
Urethra	Max DVH	80	50	1
Urethra	Max Dose	85	100	1
Left Femur	Max Dose	50	100	1
Right Femur	Max Dose	50	100	1

Table 2.

IMRT treatment planning objectives and planning weight factors for the normal tissues.

Abbreviations: ROI = region of interest, Max Dose = maximum allowable dose, DVH = dose volume histogram

RESULTS

Imaging and post-processing

The marker implantation posed no problems. This procedure took five minutes per patient on the urology outpatient clinic. The ERB was tolerated well and no problems arose during the imaging procedures. The planning CT-scan took 15 minutes totally, while the MR imaging at the radiology department took one hour (10 minutes patient preparation and 50 minutes imaging), which was rather strenuous for this elderly patient population. In one patient the MR imaging was interrupted due to lower back pain, but eventually the MR procedure could be finished. The post-processing was performed by an experienced radiologist in 40 minutes; DCE-MRI evaluation 10 minutes, MRSI evaluation 20 minutes, DIL delineation five minutes and files preparation for transmission to the radiotherapy department five minutes. The next day, the radiation oncologist and the radiologist reviewed the images. The target volumes and normal tissues were delineated in 60 minutes. The inverse DIL-IMRT and IMRT-78 treatment planning were performed in 1.5 – 2 hours.

Pat. No.	PSA (ng/ml)	Gleason score	Stage	Prostate vol. (cc)	DIL vol. (cc)	DIL Loc.	DIL-IMRT 70-90 Gy				IMRT-78 Gy		
							Mean Dose (Gy)				Mean Dose Prostate (Gy)		
							DIL	Prostate	NTCP Rwall (%)	TCP (%)		NTCP Rwall (%)	TCP (%)
1	7.8	7	T1c	79	1.1	R-PZ	90.0	71.3	2	89	77.7	4	88
2	8.2	6	T2a	106	1.8	L-PZ	91.2	71.6	3	85	77.8	6	85
3	7.7	5	T2a	74	6.5	R-PZ	90.5	71.5	6	86	78.4	6	83
4	5.8	7	T2a	41	2.2	R-PZ	90.8	71.4	5	89	78.1	6	87
5	7.0	8	T2a	51	1.8	L-PZ	90.7	71.5	3	88	78.6	6	87

Table 3
Patient characteristics, and DIL-IMRT and IMRT-78 treatment planning results.

*Abbreviations: DIL Loc. = DIL localization, NTCP = normal tissue complication probability, TCP = tumor control probability, DIL = dominant intra-prostatic lesion, L-PZ = left peripheral zone, R-PZ = right peripheral zon*e

Intra-prostatic IMRT boosting with DCE-MRI and MRS image guidance

In all 5 patients a DIL could be determined by the combined functional MR imaging techniques. The initial PSA level ranged from 5.8 to 8.2 ng/ml and the prostate volume ranged from 41 to 106 cc (Table 3). The DIL volumes ranged from 1.1 to 6.5 cc and all were localized in the right or left peripheral zone.

An example of a comprehensive MR examination and DIL volume delineation procedure of a 71-year-old prostate cancer patient (Pat. no. 4 from Table 3) is shown in Fig. 5. The patient presented with a PSA of 5.8 ng/ml and a palpable tumor in the right prostate lobe, staged on digital rectal and ultrasound examination as T2. A total of eight ultrasound-guided biopsies were taken, four from the left and four from the right prostatic lobe. Two right peripheral biopsies revealed a Gleason sum seven adenocarcinoma. The T_2-weighted MR images showed a decrease of signal intensity in the right peripheral zone, without capsular invasion (Fig. 5a). Evaluation of the DCE-MR imaging showed contrast kinetic parameters, suggesting malignancy on the right side (Fig. 5b-c). MRSI confirmed the previous findings. An increased choline+creatine/citrate ratio in eight voxels was found in the right peripheral zone (Fig. 5d-e), and a choline+creatine/citrate map was constructed to visualize the MRSI based tumor nodule (Fig. 4f). Based on the combined DCE-MRI and MRSI data, this prostate tumor was staged as T2a located in the right peripheral zone. The DIL volume was delineated within the 3D editor and transferred to the treatment planning system. The DIL volume was 2.2 cc and a 3D margin of 5 mm was drawn for PTV_{90}. The prostate gland measured 41 cc and a 3D margin of 7 mm was drawn for PTV_{70} (Fig. 6). The DIL-IMRT planning resulted in a dose

distribution as displayed in Fig. 7a. For this plan a TCP of 89% was estimated and an NTCP Rwall of 5%. The IMRT-78 treatment plan (Fig. 7b) yielded a TCP of 87% and an NTCP Rwall of 6%.
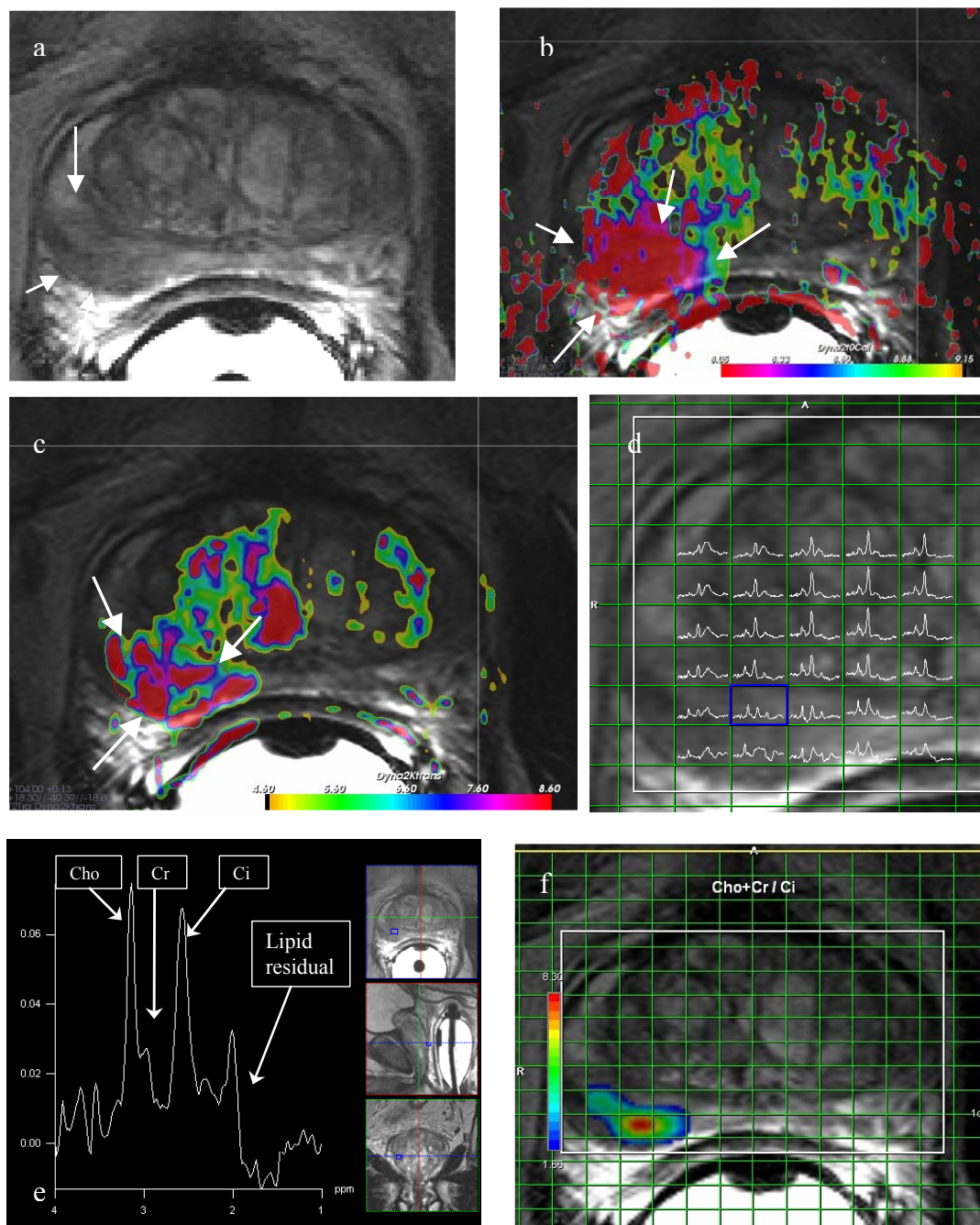
Fig. 5 DCE-MRI and MRSI results of patient no. 4.

(a) Axial T_2-weighted MR image with decreased signal intensity in the right peripheral zone (arrows), without evidence of capsular invasion. DCE-MRI results are displayed in b-c.

(b) The start-of-enhancement parameter demonstrated an earlier enhancement in part of the low-signal-intensity lesion (arrows) compared to the left peripheral zone.

(c) The volume transfer constant (K_{trans}) was elevated in the low-signal intensity lesion (arrows) indicating tumor tissue.

(d) MRSI detected elevated choline and low citrate peaks in 7 voxels. The blue box indicates the voxel, of which the spectrum, as displayed in Fig. 5e, originates from.

(e) ^{1}H-MR spectrum from a voxel in the right peripheral zone. An increased choline+creatine/citrate ratio indicates prostate cancer. Cho = choline, Cr = creatine and Ci = citrate.

(f) A strongly interpolated (choline + creatine over/ citrate map was used to visualize the MRSI-based tumor nodule.
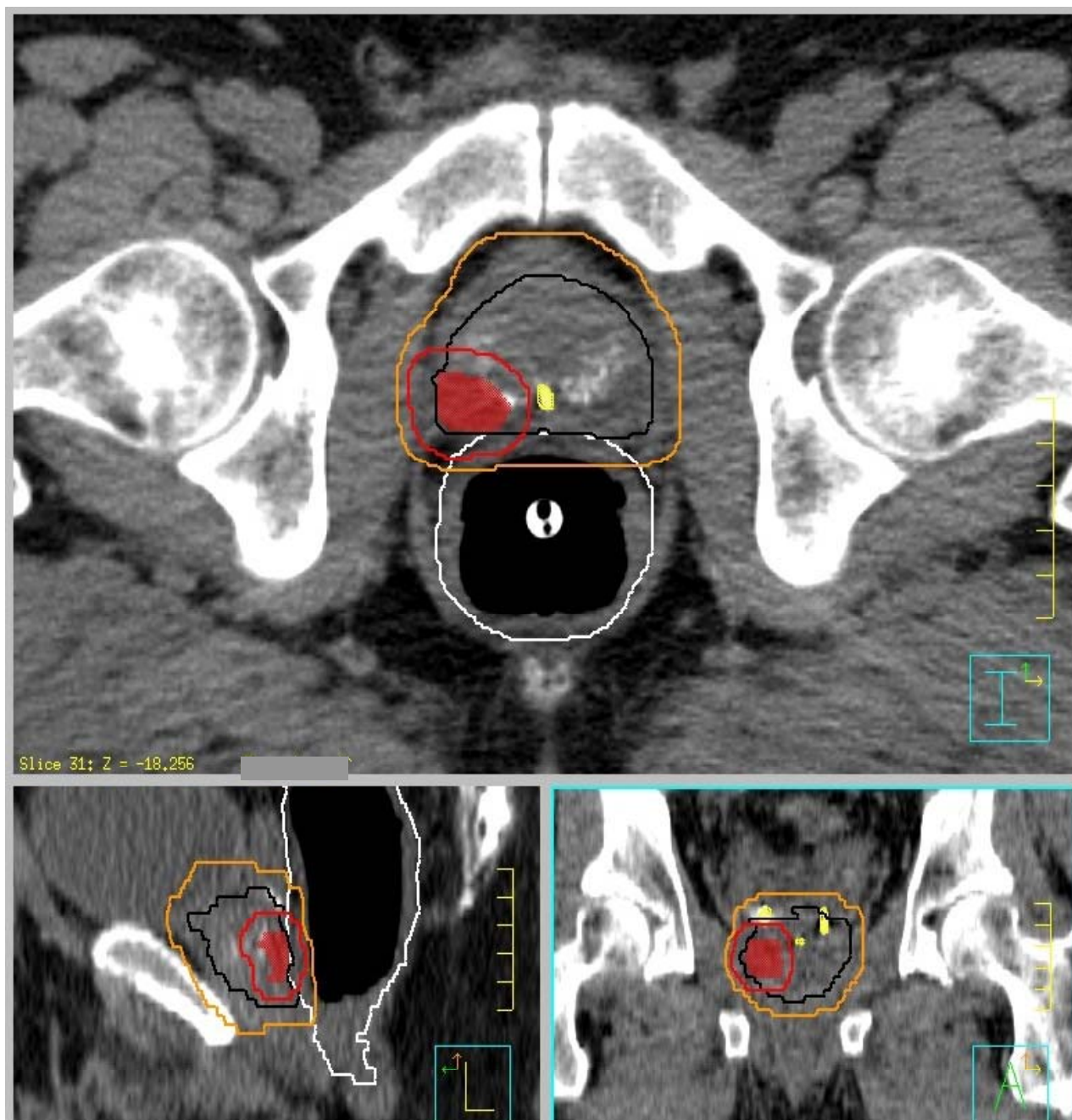
Fig 6.
DIL-IMRT treatment volumes of patient no. 4.
3 panel (transversal, saggital en coronal view) CT treatment planning image: the DIL volume (red colorwash) and prostate (black line) were delineated with a margin of 5 and 7 mm, for PTV$_{90}$ (red line) and PTV$_{70}$ (orange line), respectively. In yellow the central gold marker is indicated.

A summary of the comparison of DIL-IMRT and IMRT-78 data for the investigated patients is given in Table 3. Overall, in this small selected number of patients, the TCPs, ranging from 83% to 89% did not differ between the two IMRT plans. But in four out of five patients, DIL-IMRT reduced the NTCP Rwall, ranging from 1 to 3%. For every individual patient, the therapeutic (TCP/NTCP) ratio was increased by the DIL-IMRT plan. An example of

the different dose distribution pattern of the inner rectal wall surface for the two treatment plans is displayed in Fig. 7c-d. The combination of DIL-IMRT and a daily inserted ERB, which dilates the rectal wall, gives a different dose distribution over the inner rectal wall (Fig. 7c), compared to the IMRT-78 plan and ERB (Fig. 7d). In case of DIL-IMRT, a smaller area is exposed to a dose > 80 Gy, surrounded by a larger area of about 70 Gy and the dorsal rectal wall is exposed to doses < 40 Gy**.**
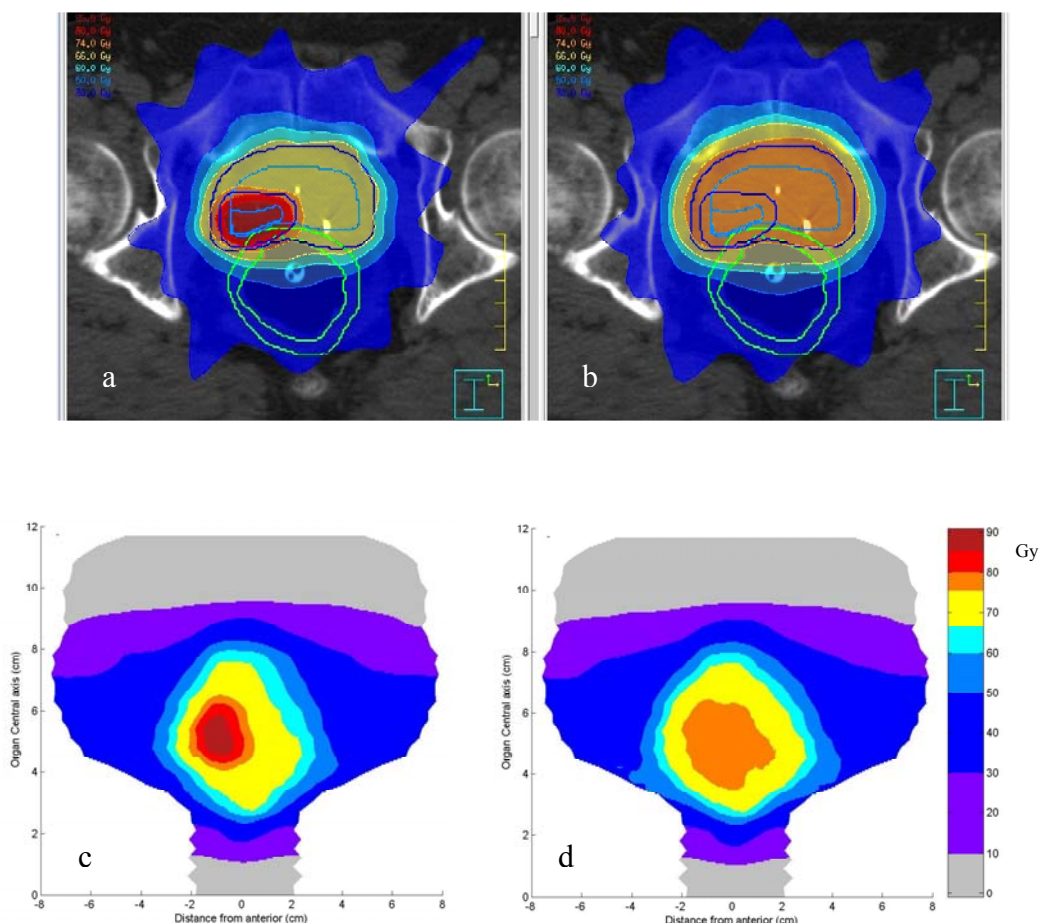
Fig 7.
Transversal dose distribution: for (a) DIL-IMRT 70-90 and (b) IMRT-78 plan of patient no. 4.
Inner rectal wall dose surface maps resulted from the (c) DIL-IMRT plan and from (d) the IMRT-78 plan.
The dose distribution of the inner rectal wall surface is displayed by virtual rectum unfolding (i.c. the
rectum is virtually cut open along the posterior wall). On the horizontal axis the distance from anterior
(towards the prostate and seminal vesicles) is displayed. On the vertical axis the distance from the most
caudal delineated CT-scan is given.

DISCUSSION

In this study, we have shown the feasibility of using combined functional imaging techniques of the prostate gland to integrate them into inverse treatment planning and to define a biological target volume (BTV) (1) for high dose intra-prostatic IMRT boosting. This MR-based BTV was then superimposed onto a treatment planning CT with a CT-MR gold marker-based fusion protocol. With two different IMRT plans and commonly used TCP and NTCP models, preliminary data were produced to investigative the potential gains of the DIL-IMRT concept.

Pickett *et al.* (21) were the first to report on the possible advantages of incorporating MR imaging, both anatomical and functional, into a static field prostate IMRT plan. In their case report the feasibility of treating a single lobe to 90 Gy, by MRSI guidance, was demonstrated. Previous investigations have shown that using anatomical MR images for more accurate prostate delineation resulted in 30 % reduction of prostate volume and a reduction of the proportion of irradiated rectal wall (2,3). This is demonstrated in Fig. 6, where, as a result of the MR, a sharp delineation of the ventral part of the gland tissue on the CT can be made. Integration of anatomical prostate MR imaging with the described CT-MR marker-based fusion method is now implemented into our daily clinical practice.

Due to the increasing availability and improvements in MR imaging, its role in prostate radiotherapy has developed rapidly over the past years. With high sensitivity and specificity, both DCE-MRI and MRSI can provide accurate tumor staging (4,5, 8-12). MRSI has shown to provide a high specificity for prostate cancer (7,41). This technique has proven to be capable of accurately detecting prostate cancer in the peripheral zone (9,10,12). However, the availability of this imaging modality is still limited. Only a few institutions have the opportunity and the experience to use MRSI clinically. Experience with DCE-MRI in breast and bladder cancer indicates that, due to neo-vascularization, malignant lesions demonstrate an earlier and faster enhancement compared with that of benign lesions (42,43). This technique is widely available and is capable of detecting regions of prostate cancer in both the peripheral and the central prostate gland zone (4,5,9,10). In summary, DCE-MRI can identify regions of neo-vascularity, suggestive for prostate cancer, while MRSI can detect malignant tumor nodules on voxel-size with high specificity.

Functional prostate MRS imaging can also help to assess local tumor control in early stage prostate cases (13). MR-based analysis in 118 prostate cancer patients, irradiated to a dose of 65 – 70 Gy, revealed that all twelve observed intra-prostatic recurrences originated within the initial tumor (18). This supports the concept of intra-prostatic boosting, with a dose higher than 70 Gy, while maintaining the dose to the remainder of the prostate at an intermediate dose level (around 65 – 70 Gy). The concept of a BTV for prostate cancer means

detection and localization of dominant tumor nodules with higher tumor cell density, the so-called DIL, in contrast to non-DIL prostate tissue where the tumor cell density is lower and therefore a lower irradiation dose may be sufficient. Based on that hypothesis, we tested the DIL-IMRT 70-90 Gy treatment planning in a small selected patient population and compared it with a more standard whole-prostate IMRT 78 Gy plan. Our data suggest a comparable high TCP, ranging from 83% to 89%, for both IMRT plans. The DIL-IMRT plan produced in 4 out of 5 patients a lower Rwall NTCP, as compared to the IMRT-78 plan and in all patients the therapeutic (TCP/NTCP) ratio was increased.

Nutting *et al.* (20) performed an IMRT planning study in six patients in which the DIL volume and localization were derived from prostatectomy specimens that were projected into planning CT scans. An IMRT plan (70 Gy whole prostate + 20 Gy boost on DIL) was compared with a whole homogeneous irradiated prostate with IMRT to 70 Gy. With the DIL boosting the estimated TCP increased from 64.4% to 95.6%. Instead of 70 Gy we choose for 78 Gy, as a result of the positive MD Anderson randomized trial (14). Nutting *et al.* (20) observed a 1.8% increase of the rectal NTCP, to a mean value of 7.7% for the DIL-boost plan. The rectal volume was delineated as the rectal wall plus content, so a direct comparison with our NTCP data is difficult. With our DIL-IMRT plan the estimated Rwall NTCP decreased for the individual patients with 1 – 3 %, to a mean NTCP of 4 %. In our study the CTV-PTV margins were smaller (7 and 5 mm), while Nutting *et al.* (20) applied 10 mm margins, which also can explain the differences in NTCP.

The TCP/NTCP ratio, as observed by Nutting *et al.* (20), was very dependent on the localization of the DIL: anteriorly in the prostate or posteriorly, close to the anterior rectal wall. In our pilot study, we detected the DILs in the posterior part of the peripheral zone of the prostate in all five patients. According to extensive pathological examinations, this is also the localization where the highest portion (74 %) of the cancer foci is located (44). Nevertheless, we have to expand our patient population to obtain more variation of DIL localization and different DIL volumes to further investigate the impact on the TCP/NTCP ratio. Currently, we are enrolling more patients for this study. Also the effect of this novel approach on other surrounding radiosensitive structures, such as the neurovascular bundle, penile bulb and urethra has to be investigated. This will be topic of future investigations.

In prostate brachytherapy, the MR image-guided DIL boosting concept has been tested for patients with a prostate gland volume < 50 cc (19,22,23). Only MRSI was used for DIL detection and localization. Zaider *et al.*(23) registered MRSI and ultrasound images for boosting of the intra-prostatic tumor regions. In a single patient, three different DIL volumes (1.36 – 3.71 cc) were defined: one from actual MRSI information and two hypothetically constructed. Depending on the size of the DIL, the image-guided boost yielded TCP values ranging from 94.3% to 96.5%, without increasing the maximum urethral dose. In comparison,

standard brachytherapy treatment resulted in TCP values ranging from 64.9% to 76.1%. An endorectal probe, filled with 100 cc of air, was used for MRSI, causing gland deformation and therefore difficulties arose with the registration procedure. They have developed an algorithm to overcome this problem and achieved absolute 3D-positional errors of 2.2 mm   1.2 (mean   1SD) (24). Dibiase *et al.*(19) and Pouliot *et al.*(22) encountered similar problems with precise MR-CT registration due to gland deformation by the endorectal coil. MRSI defined prostate boost volumes were manually entered into the planning system and the gland distortion was only addressed visually. In our study, we used an endorectal balloon (ERB) filled with 80 cc of air, identical to the MR endorectal coil, for CT-scanning. This resulted in almost equal deformation of the prostate gland in MR and CT scanning, resulting in an accurate DIL projection onto the CT scan. The ICP method, in which the gold marker surface models are automatically registered, was used (25). This yielded an MR-CT fusion precision of 1.1 mm in a dataset of 21 patients, using five operators.

ERBs are used in prostate radiotherapy for their rectal wall sparing effect and are well tolerated by most patients (27-29,38). Since two years, the ERB, as mentioned in this study, has been used in our department and no severe ERB-related toxicity, apart from local anal irritation, has been reported. The ERB is applied and removed by the therapists and per treatment fraction an extra three minutes is added for the whole ERB procedures (26). The ERB is often referred to as a prostate immobilizer, but due to presence of gas and stool surrounding the ERB, the day-to-day interfraction prostate displacements can be high, up to 4.7 mm (1 SD) for the anterior-posterior direction (26). Therefore, we now use the ERB in combination with a gold marker based portal imaging verification and correction protocol (26,30-32). As reported earlier, to increase their acceptability, development of user- and patient-friendly ERBs is warranted (38).

The presented DIL-IMRT plan, in combination with a daily inserted ERB, which dilates the rectal wall, gives an interesting dose distribution over the inner rectal mucosa (Fig. 7c). A relatively small area is exposed to high doses (> 80 Gy), surrounded by a larger area of intermediate doses and a low dose over the dorsal rectal wall. Recent data have shown that this type of spatial dose distribution and also the amount of rectal wall surface irradiated to low doses may further reduce the Rwall NTCP (34). Therefore, in treated DIL-IMRT patients, the actual Rwall late toxicity may even be lower than the estimations calculated in this study, based on the Lyman-Kutcher-Burman model with Emami parameters (35-37). Execution of the DIL-IMRT concept and thorough follow-up may also provide us with additional information to construct more accurate Rwall NTCP models.

Regarding the TCP calculations, it should be remarked that there is still an ongoing debate in the literature on the LQ parameter values especially whether the α/β ratio is low, i.e. in the range typical for late responding tumors (44-46). For the TCP calculations we have

applied parameters comparable to those applied by Nutting et al (20), i.e. an α/β value typical of early responding tissues (as applied by Nahum et al (40)) and further assuming a heterogeneous distribution of radiation sensitivities ( ) and assuming a ratio of 100 in the clonogen densities between DIL (10^7 cells/cm^3) and the rest of the prostate (10^5 cells/cm^3). An extensive comparison of different TCP models is beyond the scope of this paper. However, we have verified that choosing lower α/β TCP models does not alter the conclusions. If parameters proposed by Wang *et al.* (45) were used (i.e. α/β = 3.1 Gy, α = 0.15 ± 0.04 Gy^{-1}, T_{pot} = 42 days and number of clonogens is in the range 10^6-10^7) or those as proposed by Fowler *et al.* (46) (i.e. α/β= 1.5 Gy, α = 0.0391 ± 0.0098 Gy^{-1}) the absolute TCP values changed, but the *relative* values for the DIL-IMRT and IMRT-78 plans were comparable and did not differ.

The issue of multi-focality of prostate cancer is not addressed in this technical feasibility study. In a large pathology study, 83% of the prostatectomy specimens had more than one cancer focus (47). For this feasibility study we selected patients with uni-lateral palpable, ultrasound detected and biopsy-proven tumors. This was done to avoid possible extra difficulties in interpreting and executing the implementation of the described CT-MR fusion and DIL-IMRT planning. Pouliot *et al.* (22) have reported on multiple DIL volumes and it was possible to deliver separate boost volumes on these tumor nodules with MRS-guided brachytherapy, without compromising the surrounding normal tissues**.** In another study, a multiple boost implant in one patient with four tumor foci was impractical to perform (19). For all other patients an MRSI-guided brachytherapy boost was given successfully with toxicity comparable to conventional treatment. The goal of our study was to demonstrate the feasibility of incorporating two MR imaging techniques in a (single) external beam DIL-IMRT concept for a wide range of prostate gland volumes (41-106 cc). The next step will be to include more patients, also with more than one DIL and to investigate the possible advantages or disadvantages, in terms of tumor control probability and toxicity. Xia *et al.* (48) have already demonstrated the feasibility of planning two DILs up to 90 Gy with IMRT on a selected patient case, but their DIL volumes were derived from MRSI only and, due to ERB induced gland deformation in the MRS study, the MR-CT image fusion was a visual approximate process. The DIL-IMRT concept may not be applicable in the case of more than two or three DILs localized near the rectal wall or urethra, due to unacceptably high estimated toxicity scores. Currently, we are also enrolling bi-lateral prostate tumors with multiple DILs and we are further evaluating the presented intra-prostatic IMRT boosting under DCE-MRI and MRSI guidance.

CONCLUSION

In this study, the feasibility was demonstrated to integrate two functional prostate MR imaging techniques into inverse treatment planning, for the definition of a dominant intra-prostatic lesion (DIL) for high-dose intra-prostatic boosting with IMRT (DIL-IMRT). In all patients the combination of DCE-MRI, identifying regions of neo-vascularity, suggestive for prostate cancer, and MRSI, detecting tumor nodules with high specificity, yielded a clearly defined single DIL volume. This DIL volume could be accurately transferred to the radiotherapy treatment planning system, by CT-MR image registration based on matching 3D gold marker surface models and usage of the same type of ERB for CT and MR imaging. Compared to the IMRT-78 plan, the DIL-IMRT plan estimated a similar TCP, but a decreased Rwall NTCP. This resulted in an increase of the therapeutic (TCP/NTCP) ratio, in favor of the DIL-IMRT plan. Also the typical Rwall spatial dose distribution, as a result of the DIL boosting, may indicate a further reduced actual rectal toxicity.

Before bringing DIL-IMRT into clinical practice, a larger patient population, with more variation in the number and localization of the DIL, has to be studied, additionally including the preliminary tumor control probabilities and toxicity estimates.

REFERENCES

1. Ling CC, Humm J, Larson S, et al. Towards multidimensional radiotherapy (MD-CRT): biological imaging and biological conformality. Int J Radiat Oncol Biol Phys 2000;47(3):551-560.

2. Rasch C, Barillot I, Remeijer P, et al. Definition of the prostate in CT and MRI: a multi-observer study. Int J Radiat Oncol Biol Phys 1999;43(1):57-66.

3. Roach M, III, Faillace-Akazawa P, Malfatti C, et al. Prostate volumes defined by magnetic resonance imaging and computerized tomographic scans for three-dimensional conformal radiotherapy. Int J Radiat Oncol Biol Phys 1996;35(5):1011-1018.

4. Engelbrecht MR, Huisman HJ, Laheij RJ, et al. Discrimination of prostate cancer from normal peripheral zone and central gland tissue by using dynamic contrast-enhanced MR imaging. Radiology 2003;229(1):248-254.

5. Huisman HJ, Engelbrecht MR, Barentsz JO. Accurate estimation of pharmacokinetic contrast-enhanced dynamic MRI parameters of the prostate. J.Magn Reson.Imaging 2001;13(4):607-14.

6. Heerschap A, Jager GJ, van der Graaf M, et al. In vivo proton MR spectroscopy reveals altered metabolite content in malignant prostate tissue. Anticancer Res 1997;17(3A):1455-1460.

7. Scheidler J, Hricak H, Vigneron DB, et al. Prostate cancer: localization with three-dimensional proton MR spectroscopic imaging--clinicopathologic study. Radiology 1999;213(2):473-480.

8. Futterer JJ, Scheenen TW, Huisman HJ, et al. Initial experience of 3 tesla endorectal coil magnetic resonance imaging and 1H-spectroscopic imaging of the prostate. Invest Radiol 2004;39(11):671-680.

9. Noworolski SM, Henry RG, Vigneron DB, et al. Dynamic contrast-enhanced MRI in normal and abnormal prostate tissues as defined by biopsy, MRI, and 3D MRSI. Magn Reson Med 2005;53(2):249-255.

10. van Dorsten FA, van der Graaf M, Engelbrecht MR, et al. Combined quantitative dynamic contrast-enhanced MR imaging and (1)H MR spectroscopic imaging of human prostate cancer. J Magn Reson Imaging 2004;20(2):279-287.

11. Fütterer JJ, Engelbrecht MR, Huisman HJ, et al. Dynamic contrast-enhanced endorectal MR imaging in staging prostate cancer prior to radical prostatectomy – experienced versus less experienced readers. Radiology 2005 in press.

12. Coakley FV, Kurhanewicz J, Lu Y, et al. Prostate cancer tumor volume: measurement with endorectal MR and MR spectroscopic imaging. Radiology 2002;223(1):91-97.

13. Pickett B, Kurhanewicz J, Coakley F, et al. Use of MRI and spectroscopy in evaluation of external beam radiotherapy for prostate cancer. Int J Radiat Oncol Biol Phys 2004;60(4):1047-1055.

14. Pollack A, Zagars GK, Starkschall G, et al. Prostate cancer radiation dose response: results of the M.D. Anderson phase III randomized trial. Int J Radiat Oncol Biol Phys 2002;53(5):1097-1105.

15. Pollack A, Hanlon AL, Horwitz EM, et al. Prostate cancer radiotherapy dose response: an update of the fox chase experience. J Urol 2004;171(3):1132-1136.

16. Zelefsky MJ, Fuks Z, Hunt M, et al. High-dose intensity modulated radiation therapy for prostate cancer: early toxicity and biochemical outcome in 772 patients. Int J Radiat Oncol Biol Phys 2002;53(5):1111-1116.

17. Coakley FV, Teh HS, Qayyum A, et al. Endorectal MR imaging and MR spectroscopic imaging for locally recurrent prostate cancer after external beam radiation therapy: preliminary experience. Radiology 2004;233(2):441-448.

18. Cellini N, Morganti AG, Mattiucci GC, et al. Analysis of intraprostatic failures in patients treated with hormonal therapy and radiotherapy: implications for conformal therapy planning. Int J Radiat Oncol Biol Phys 2002;53(3):595-599.

19. Dibiase SJ, Hosseinzadeh K, Gullapalli RP, et al. Magnetic resonance spectroscopic imaging-guided brachytherapy for localized prostate cancer. Int J Radiat Oncol Biol Phys 2002;52(2):429-438.

20. Nutting CM, Corbishley CM, Sanchez-Nieto B, et al. Potential improvements in the therapeutic ratio of prostate cancer irradiation: dose escalation of pathologically identified tumour nodules using intensity modulated radiotherapy. Br J Radiol 2002;75(890):151-161.

21. Pickett B, Vigneault E, Kurhanewicz J, et al. Static field intensity modulation to treat a dominant intra-prostatic lesion to 90 Gy compared to seven field 3-dimensional radiotherapy. Int J Radiat Oncol Biol Phys 1999;44(4):921-929.

22. Pouliot J, Kim Y, Lessard E, et al. Inverse planning for HDR prostate brachytherapy used to boost dominant intraprostatic lesions defined by magnetic resonance spectroscopy imaging. Int J Radiat Oncol Biol Phys 2004;59(4):1196-1207.

23. Zaider M, Zelefsky MJ, Lee EK, et al. Treatment planning for prostate implants using magnetic-resonance spectroscopy imaging. Int J Radiat Oncol Biol Phys 2000;47(4):1085-1096.

24. Mizowaki T, Cohen GN, Fung AY, et al. Towards integrating functional imaging in the treatment of prostate cancer with radiation: the registration of the MR spectroscopy imaging to ultrasound/CT images and its implementation in treatment planning. Int J Radiat Oncol Biol Phys 2002;54(5):1558-1564.

25. Huisman HJ, Fütterer JJ, van Lin EN, et al. Precision of integrating functional magnetic resonance in radiotherapy treatment of prostate cancer using fiducial gold markers registration methods. Radiology 2005;236:311-317.

26. van Lin EN, van der Vight LP, Witjes JA, et al. The effect of an endorectal balloon and off-line correction on the interfraction systematic and random prostate position variations: A comparative study. Int J Radiat Oncol Biol Phys 2005;61(1):278-288.

27. Teh BS, McGary JE, Dong L, et al. The use of rectal balloon during the delivery of intensity modulated radiotherapy (IMRT) for prostate cancer: more than just a prostate gland immobilization device? Cancer J 2002;8(6):476-483.

28. Wachter S, Gerstner N, Dorner D, et al. The influence of a rectal balloon tube as internal immobilization device on variations of volumes and dose-volume histograms during treatment course of conformal radiotherapy for prostate cancer. Int J Radiat Oncol Biol Phys 2002;52(1):91-100.

29. Woel R, Beard C, Chen MH, et al. Acute gastrointestinal, genitourinary, and demotological toxicity during dose-escalated 3D-conformal radiation therapy (3DCRT) using an intrarectal balloon for prostate gland localization and immobilization. Int J Radiat Oncol Biol Phys 2005;62(2):392-396.

30. Herman MG, Abrams RA, Mayer RR. Clinical use of on-line portal imaging for daily patient treatment verification. Int J Radiat Oncol Biol Phys 1994;28(4):1017-1023.

31. Litzenberg D, Dawson LA, Sandler H, et al. Daily prostate targeting using implanted radiopaque markers. Int J Radiat Oncol Biol Phys 2002;52(3):699-703.

32. Vigneault E, Pouliot J, Laverdiere J, et al. Electronic portal imaging device detection of radio opaque markers for the evaluation of prostate position during megavoltage irradiation: a clinical study. Int J Radiat Oncol Biol Phys 1997;37(1):205-212.

33. Parker CC, Damyanovich A, Haycocks T, et al. Magnetic resonance imaging in the radiation treatment planning of localized prostate cancer using intra-prostatic fiducial markers for computed tomography co-registration. Radiother Oncol 2003;66(2):217-224.

34. Tucker SL, Dong L, Cheung R, et al. Comparison of rectal dose-wall histogram versus dose-volume histogram for modeling the incidence of late rectal bleeding after radiotherapy. Int J Radiat Oncol Biol Phys 2004;60(5):1589-1601.

35. Lyman JT. Complication probability as assessed from dose-volume histograms. Radiat Res 1985;104(suppl):13-19.

36. Kutcher GJ, Burman C. Calculation of complication probability factors for non-uniform normal tissue irradiation: the effective volume method. Int J Radiat Oncol Biol Phys 1989;16(6):1623-1630.

37. Emami B, Lyman JT, Brown A, et al. Tolerance of normal tissue to therapeutic irradiation. Int J Radiat Oncol Biol Phys 1991;21(1):109-122.

38. van Lin EN, Hoffmann, AL, van Kollenburg, P, et al. Rectal wall sparing effect of three different endorectal balloons in 3D conformal and IMRT prostate radiotherapy. Int J Radiat Oncol Biol Phys 2005;63(2):565-576.

39. Webb S, Nahum AE. A model for calculating tumour control probability in radiotherapy including effects of inhomogeneous distributions of dose and clonogenic cell density. Phys Med Biol 1993;38:653-666.

40. Nahum AE, Movsas B, Horwitz EM, et al. Incorporating clinical measures of hypoxia into tumour local control modelling of prostate cancer: Implications for the α/β ratio. Int J Radiat Oncol Biol Phys 2003;57(2):391-401.

41. Kurhanewicz J, Vigneron DB, Nelson SJ, et al. Citrate as an in vivo marker to discriminate prostate cancer from benign prostatic hyperplasia and normal prostate peripheral zone: detection via localized proton spectroscopy. Urology 1995;45(3):459-466.

42. Barentsz JO, Jager GJ, van Vierzen PB, et al. Staging urinary bladder cancer after transurethral biopsy: value of fast dynamic contrast-enhanced MR imaging. Radiology 1996;201(1):185-193.

43. Boetes C, Barentsz JO, Mus RD, et al. MR characterization of suspicious breast lesions with a gadolinium-enhanced TurboFLASH subtraction technique. Radiology 1994;193(3):777-781.

44. Brenner DJ, Hall EJ. Fractionation and protraction for radiotherapy of prostate carcinoma. Int J Radiat Oncol Biol Phys 1999;43:1095-1101.

45. Wang JZ, Guerrero M, Li XA. How low is the a/b ratio for prostate cancer. Int J Radiat Oncol Biol Phys 2003;55:194-203.

46. Fowler J, Chappell R, Ritter M. Is a/b ratio for prostate really low? Int J Radiat Oncol Biol Phys 2001;50:1021-1031.

47. Chen ME, Johnston DA, Tang K, et al. Detailed mapping of prostate carcinoma foci: biopsy strategy implications. Cancer 2000;89(8):1800-1809.

48. Xia P, Pickett B, Vigneault E, et al. Forward or inversely planned segmental multileaf collimator IMRT and sequential tomotherapy to treat multiple dominant intraprostatic lesions of prostate cancer to 90 Gy. Int J Radiat Oncol Biol Phys 2001;51(1):244-254.

8

Reduced late rectal mucosal changes after prostate three-dimensional conformal radiotherapy with endorectal balloon, as observed in repeated endoscopy

Emile N.J.Th van Lin, M.D.,∗ Jón Kristinsson, M.D.,# Mariëlle E.P. Philippens M.D.,∗ Dirk J. de Jong, M.D., Ph.D.,# Lisette P. van der Vight, B.Sc., ∗ Johannes H.A.M. Kaanders M.D. Ph.D.,∗ Jan Willem Leer, M.D. Ph.D.,∗ and Andries G. Visser, Ph.D.∗

Department of Radiation Oncology∗
Department of Gastroenterology and Hepatology#

ABSTRACT

Purpose: To investigate prospectively the rectal wall (Rwall) spatial dose distribution, toxicity and mucosal changes after prostate cancer radiotherapy with or without an endorectal balloon (ERB).

Methods and materials: 24 patients with ERB and 24 without ERB (No-ERB) were treated with three-dimensional conformal radiotherapy (3D-CRT) to a dose of 67.5 Gy. The Rwall was divided into 16 mucosal areas and Rwall dose surface maps were constructed. After three months, six months, one year and two years a rectosigmoidoscopy was performed and each mucosal area was scored on telangiectasia, congestion, ulceration, stricture and necrosis. Late rectal toxicity was correlated to the endoscopic findings.

Results: The ERB significantly reduced the Rwall volume exposed to doses > 40 Gy. Late rectal toxicity (grade $\geq$ 1) was reduced significantly in the ERB group. 146 scopies and 2336 mucosal areas were analyzed. Telangiectases were most frequently seen and appeared after six months. At one and two years, significantly less high-grade telangiectasia (T 2-3) was observed in the ERB group at the lateral and posterior part of the Rwall. In mucosal areas exposed to doses > 40 Gy, less high-grade telangiectases (T 2-3) were seen in the ERB group compared to the No-ERB group.

Conclusions: An ERB reduced the Rwall volume exposed to doses > 40 Gy, resulting in reduction of late rectal mucosal changes and reduced late rectal toxicity. Although further analysis is needed, these data suggest an ERB-induced increased tolerance for late Rwall damage.

INTRODUCTION

Numerous studies have investigated the relationship between the delivered dose distribution to the rectum and the risk of late rectal toxicity in prostate cancer radiotherapy. Exposure to high dose (> 60 Gy) (1-4) as well as intermediate doses (32 – 50 Gy) is associated with higher risk of late rectal bleeding (5-8). Perhaps more important is the pattern of the spatial dose distribution over the inner rectal wall (Rwall), as seen on Rwall dose maps. Cluster model analysis indicated that the size of Rwall mucosa, exposed to doses between 27 and 43 Gy, was significantly associated with late rectal toxicity (5). Therefore, to prevent increasing late toxicity rates in dose escalation, one should not only focus on the high doses but also on the intermediate Rwall doses and on the spatial dose distribution. Endorectal balloons (ERB) have been tested to reduce toxicity by decreasing the Rwall volume being irradiated (9-17). This Rwall sparing effect has been evaluated for three different ERBs by construction of inner Rwall dose maps that revealed an advantageous spatial dose distribution (14). The ERB reduced the Rwall surface exposed to intermediate and high doses, by pushing the lateral and posterior Rwall away from the high-dose region. An air-filled ERB may cause an additional dose reduction to the superficial anterior rectal mucosa due to the dose build-up effect, without underdosing the prostate gland (12). Clinical studies in patients irradiated with an ERB have shown a favorable low late rectal toxicity rate (9, 12).

Late rectal, radiation induced, mucosal changes (i.e. telangiectasia, mucosal congestion and ulceration), as being the pathologic cause of late rectal bleeding (18) have been evaluated by endoscopy (19, 20). The incidence and evolution of these mucosal radiation effects were studied in both symptomatic ("bleeders") and a-symptomatic ("non-bleeders") patients. First, a strong correlation was observed between the presence and severity of telangiectases and the radiation dose administered to the Rwall mucosa (19, 20). Secondly, patients with more severe high-grade telangiectasia had a higher probability (66 – 80 %) of developing late rectal bleeding. Therefore, high-grade mucosal changes were assumed to be predictive for late rectal bleeding, many years after completion of the treatment (18).

In patients irradiated with or without an ERB no comparative study has yet been conducted to prospectively investigate late rectal mucosal changes and to correlate these findings to a detailed Rwall dose distribution. The first goal of this study was to display and analyze the differences in geographical dose distributions over the inner Rwall mucosa. The second goal was to compare the rectal mucosal changes, as observed by periodical standardized endoscopy, and to correlate these to the Rwall dose distributions and to the commonly used late toxicity grading scales.

MATERIALS AND METHODS

Patient preparation and treatment

Forty-eight patients were irradiated for localized prostate cancer (T1-3N0M0) and, after informed consent was given, included in this study. Apparent pre-existing anal irritation, an active inflammatory bowel disease or hemorrhoids, were exclusion criteria. Patients were randomly assigned to receive a treatment with ("ERB group", n = 24) or without ERB ("No-ERB group", n = 24) over a period of twelve months, i.e. the year 2002. Details on preparation and treatment have been described earlier (21). In brief, four fine gold markers were inserted under ultrasound guidance for prostate position verification and correction (Hospimed International B.V., Dalfsen, The Netherlands). A planning CT-scan was obtained at 3mm slice thickness (AcQsim spiral CT; Philips Medical Systems, Bothell, WA). The planning target volume (PTV) was defined as the prostate plus seminal vesicles, both expanded with a 9 mm 3D margin. The rectum was delineated from the ischial tuberosities up to the rectosigmoid flexure; both the inner and outer Rwall contours were outlined (6, 16). A beams-eye-view based 3D-conformal treatment plan was designed, with individual shielding of normal tissues (Pinnacle[3] treatment planning system; Philips Medical Systems, Andover, MA). With an orthogonal, equally weighted, 18 MV photons four-field isocentric technique, a dose of 67.5 Gy was delivered in 7.5 weeks (four fractions per week), applying 2.25 Gy daily fractions (Fig. 1).

The ERB was inflated with 80 cc of air and had a length of 90 mm and a diameter of 45 mm (22) (Medrad, Indianola, PA). Before every treatment fraction, a new ERB was inserted by the attending radiation therapist. Patients were positioned supine, on a flat couch and a foam knee support. A correction protocol (21) was applied during treatment, to reduce systematic positioning errors using a camera-based electronic portal imaging device (Theraview NT, Cablon Medical B.V., Leusden, The Netherlands).

All patients were seen weekly during the treatment period and every three months afterwards. Acute and late urinary and rectal toxicity items were scored during each visit, according to the Radiation Therapy Oncology Group and the Fox Chase Modified Late Effects Normal Tissue Task force radiation morbidity scales (4). Late toxicity was evaluated over the period of the first 30 months after completion of the radiotherapy.

(a)
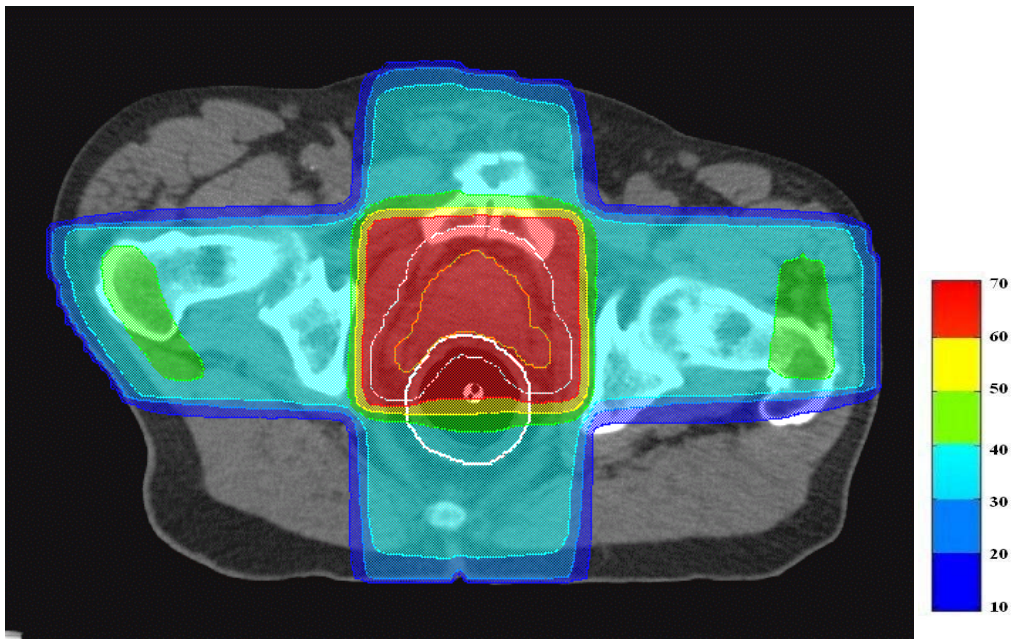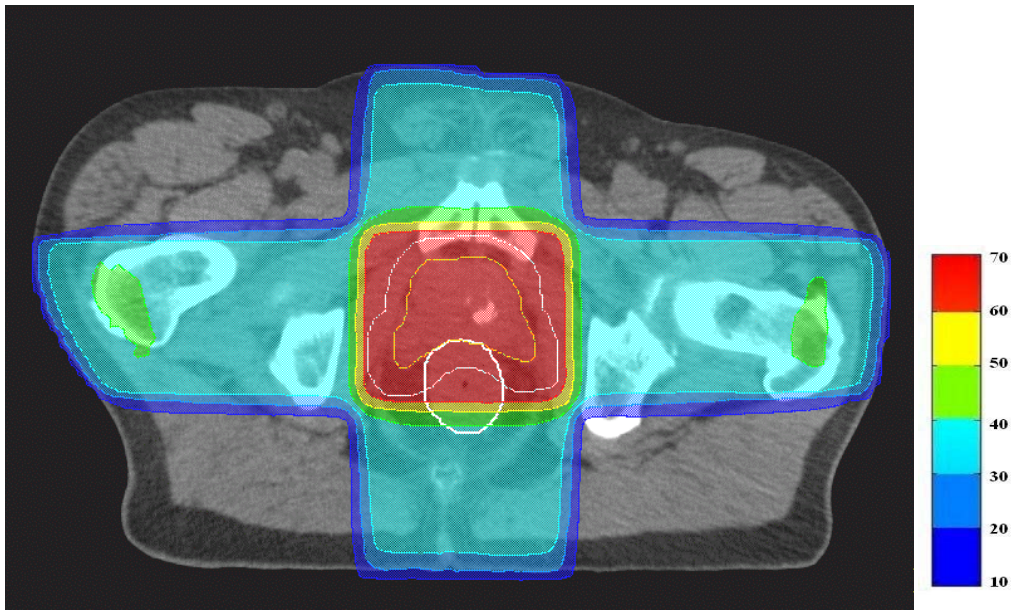
(b)

Fig. 1.
Transversal CT images with dose distribution, in Gy, for (a) No-ERB and (b) ERB patient.
Prostate and seminal vesicles (yellow lines), Planning target volume: prostate and seminal vesicles + 9
mm margin (thin white lines) and rectal outer contour (thick white lines) are highlighted.

Endoscopy and mucosal scoring system

All patients underwent a standardized rectosigmoidoscopy by a trained and experienced endoscopist, three months, six months, one year and two years after completion of the radiation treatment. A sodium-phosphate enema 133 ml (Tramedico B.V., Weesp, The Netherlands) was given 20 minutes before the examination. A mucosal mapping and scoring system, as described by Wachter *et al.*, was used (20). The inner Rwall mucosa was divided into four distance levels in caudo-cranial direction, as measured from the anus; 0 - 4 cm, 4 – 8 cm, 8 – 12 cm and 12 – 16 cm. At each level, four mucosal areas (anterior, left-lateral, right-lateral and posterior) were defined, resulting in 16 mucosal areas to be evaluated per patient. Each mucosal area was scored on five distinct endoscopic items; the presence and grading of telangiectasia (grade 0 – 4), mucosal congestion (grade 0 – 3), ulceration (grade 0 - 4), stricture (grade 0 – 4) and necrosis (grade 0 –1), according to an internationally accepted scoring system for radiation induced proctitis (20).

The different grades of telangiectasia are abbreviated as "T 0" up to "T 3" (Table 1). Low-grade telangiectasia was defined as the presence of T 1. High-grade telangiectasia, predictive for late rectal bleeding (19, 20), was defined as the presence of T 2 or T 3, and is abbreviated in the text as T 2-3.

Grading	Telangiectasia	Abbreviation
0	none	T 0
1	a single telangiectasis	T 1
2	multiple non-confluent telangiectases	T 2
3	multiple confluent telangiectas	T 3

Table 1. *Grading system used for telangiectasia per mucosal area*

The endoscopist was unaware if the patient was irradiated with or without an ERB and how long ago the treatment was completed. The grading scores were noted on a scoring list and transferred to the radiotherapy department for further evaluation. Thus the endoscopist was also not informed about the scoring data of previous investigations.

In both groups, patients who experienced any form of late (> 3 months after end of treatment) rectal bleeding, ranging from slight rectal blood loss to bleeding needing medical intervention, were identified as "bleeders". The highest observed telangiectasia scores (max mucosal Rwall T score), as observed over the course of all endoscopies were correlated to late rectal bleeding and compared with the "non-bleeders".

Rectal wall dose surface maps and EUD

After the definitive treatment plan was made, the spatial dose distribution over the inner Rwall mucosa was visualized by generating Rwall dose surface maps (5, 14). The dose distribution on the inner Rwall surface was displayed by means of virtual rectum "unfolding". Corresponding with the division of the inner Rwall into mucosal areas for the endoscopic evaluation, the Rwall dose surface map was divided into16 areas. To correlate the endoscopic findings to the radiation dose of that area, the generalized equivalent uniform dose (EUD) for every separate mucosal area was computed. The generalized EUD represents the uniform dose, which leads to the same probability of injury as the corresponding inhomogeneous dose distribution of each mucosal area. For calculation of the Rwall EUD, the value $\alpha = 6$ was chosen for the normal tissue-specific parameter that describes the dose-volume effect, according to Wu *et al.* (23). Illustrated case examples are described in the *Results* section. Each mucosal area was assigned to a EUD bin (0 - 20, 20 – 40, 40 – 60 and > 60 Gy) and the incidences of the separate dose bins were computed for both the No-ERB and ERB group. To demonstrate the overall differences in spatial dose distribution over the inner Rwall mucosal areas for each treatment group, two patient group mean EUD mucosal area maps were constructed. Finally, for each separate mucosal area, assigned to a EUD dose bin, the presence of high-grade telangiectasia (T 2–3) was counted and compared between the No-ERB and ERB patients.

Statistical analysis

Differences in the observed toxicity scores were analyzed by chi-square tests or Fisher exact tests. The association between EUD and toxicity was analyzed by means of contingency tables for the mucosal areas in specific EUD bins (0 - 20, 20 – 40, 40 – 60 and > 60 Gy). Differences were considered significant for two-tailed p-values less than 0.05. For the statistical analysis the Stata package was used (Stata Corporation, College Station, Texas, USA).

RESULTS

Patient tolerance and toxicity

As described earlier, the transrectal implantation of the gold markers was a safe and simple procedure and the ERB was tolerated well by the patients (21).

The acute urinary and rectal toxicity scores were similar for the No-ERB (n=24) and ERB group (n=24). Grade 1 urinary toxicity was scored in 19 cases and grade 2 in 4 cases in the No-ERB group and in 13 and 7 patients in the ERB group, respectively. No grade 3 acute urinary toxicity was observed in both groups. The main complaints were increased urinary frequency, and in two patients of each group a temporary catheterization was necessary. In the No-ERB group, acute grade 1 rectal toxicity was scored in 12 cases and grade 2 in 7 cases and in the ERB group in 11 and 7 patients, respectively. The main complaints were increased defecation frequency, and slight mucous discharge. In the ERB group, in two out of the seven patients with grade 2 toxicity, mild rectal bleeding occurred, which resolved within two weeks after radiotherapy. No grade 3 acute gastro-intestinal toxicity was observed in both groups.

After 30 months of follow-up, the late urinary toxicity in both groups was mild (no grade 3 or 4) and comparable for both groups; grade 1 and 2 was scored for the No-ERB group in 8 and 3 cases, respectively and for the ERB group in 3 and 3 cases, respectively. Main complaints were increased frequency and nocturia more than twice baseline. One ERB patient experienced minor hematuria after two years, which resolved spontaneously after two months (no confirmative cystoscopy was performed).

The observed late rectal toxicity (grade 1 or higher) was significantly lower for the ERB group (p = 0.003). Grade 1 was experienced in 14 patients in the No-ERB group and in 5 patients in the ERB-group. Grade 2 rectal bleeding occurred in one patient in the No-ERB group. In one patient from the No-ERB group a grade 3 rectal bleeding, resulted in two blood transfusions and five laser coagulations. In the ERB group no grade 2 or 3 rectal toxicity occurred.

"Bleeders" and "non-bleeders"

In the No-ERB group, 8 patients (33 %) experienced some form of late rectal bleeding ("bleeders") (Table 2).

Max. T score	No-ERB			ERB		
	Non-bleeders	Bleeders	Total	Non-bleeders	Bleeders	Total
T 0	1	0	1	0	0	0
T 1	2	0	2	2	0	2
T 2	9	4	13	14	2	16
T 3	4	4	8	5	1	6
Total	16	8		21	3	

Table 2.
 Number of non-bleeders and bleeders per treatment group, stratified by maximum telangiectasia score (Max. T score) of the mucosal Rwall on endoscopy.

The onset was between 9 and 24 months (median 18) after radiotherapy. The patient with grade 2 bleeding needed two laser coagulations after which the bleeding resolved completely. The patient with grade 3 rectal toxicity needed five coagulations and two transfusions, but after 30 months of follow-up, this patient still experienced intermittent (once per month) minor rectal bleeding. Five patients experienced occasional (once per few days to once a week) blood; this all resolved spontaneously after 5 to 20 months. One patient has had every two or three days blood spots on his stool, since 13 months post-irradiation.

In the ERB group, 3 patients (13 %) were identified as bleeders (Table 2), starting 10, 23 and 29 months after radiotherapy; in two patients, bloody discharge appeared once a week, which resolved completely. In one patient only once a month some blood spots appeared on the stool.

Due to the limited size of the two groups, the difference in late rectal bleeding was not statistically significant (p = 0.17)

Endoscopic findings

A total of 146 rectosigmoidoscopies were performed. The average duration of each procedure was 10 minutes and no complications occurred. The distribution of the number of endoscopies was as follows: after three months: 18 and 13, after six months: 11 and 18, after one year: 21 and 23 and after two years: 22 and 20, for the ERB and No-ERB group,

respectively. A total of 2336 mucosal areas was inspected and graded for the five endoscopic scoring items.

In none of the patients mucosal stricture or necrosis was observed. In nine mucosal areas of five patients (three ERB and two No-ERB), grade 1 superficial micro-ulcerations (< 1 cm^2) were detected. All but one resolved spontaneously. Mucosal congestion of the analyzed mucosal areas was equally often observed in the ERB (9 %) and No-ERB (10 %) group. In four patients (two ERB and two No-ERB), grade 3 congestion (diffuse confluent reddening and edematous mucosa) was scored. In three patients this congestion was resolved at the next endoscopy. Overall, no differences were observed between the two groups in the presence of mucosal congestion (data not shown).

Telangiectasia (grade 1 – 3) was seen in 29 % (No-ERB) and 20 % (ERB) of the mucosal areas. The evolution over time is displayed separately for low-grade T 1 (Fig. 2a) and high-grade T 2-3 (Fig. 2b). In both patient groups the low- and high-grade telangiectasia became apparent after 6 months and reached a peak at one year. For T 1 the incidences in both groups decreased after one year. For the high grade T 2-3 the peak incidence was also reached after one year, but after two years no evident decrease could be observed in both groups. At 6 months a higher incidence in T 1 (p = 0.09) was seen in the ERB group. One year after radiotherapy, significantly less T 1 (p = 0.045) and T 2-3 scores (p = 0.0003) were apparent in the ERB group. At two years, the incidence of T 2-3 was still lower in the ERB-group (p = 0.0003), but for T 1 the difference was no longer statistically significant (p = 0.15).

(a)
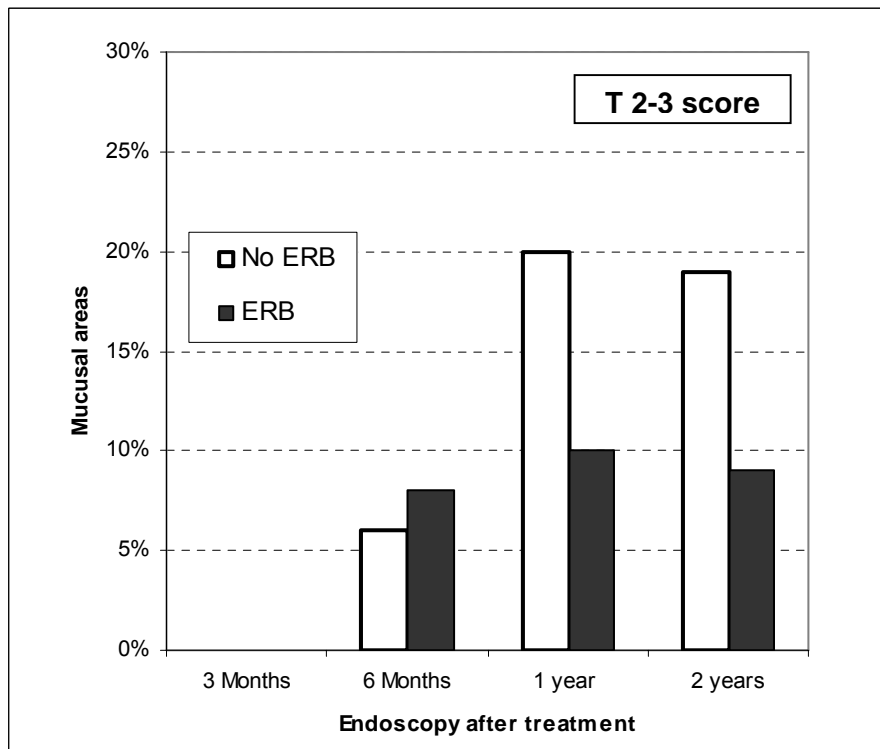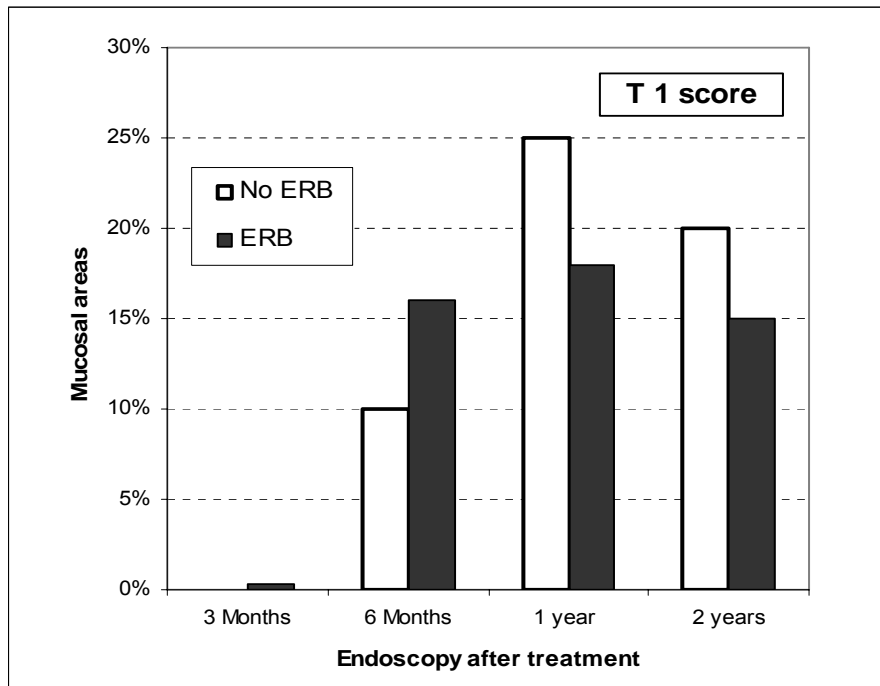
(b)

Fig. 2.
Percentage of mucosal areas scored with (a) low-grade (T 1 score) or (b) high-grade (T 2-3 score) telangiectasia at endoscopy after radiotherapy.

The two years scores, after full expression of the telangiectases, were used to analyze the spatial distribution of T 1 (Fig. 3a) and T 2-3 (Fig. 3b) over the anterior, lateral and posterior Rwall. T 1 telangiectasis was not only seen at the anterior or lateral Rwall, but also at the posterior wall in both groups. The differences between the No-ERB and ERB group were not statistically significant. For T 2-3, a significant reduction was seen at the lateral Rwall ($p = 0.007$) and posterior Rwall ($p = 0.05$), in favor of the ERB group (Fig. 3b). For the anterior wall, there was also a difference, but did not reach statistical significance ($p = 0.07$).

Correlation endoscopic findings and late rectal bleeding

In the No-ERB and ERB group, all patients that experienced rectal bleeding, had one or more mucosal areas with high-grade T2-3 telangiectasia (Table 2). In the two patients who needed laser coagulations extensive confluent T 3 telangiectases in multiple areas were observed.

Overall, there was no statistically significant difference in the occurrence of the maximum mucosal Rwall score of T 2-3 between the two groups (21 vs. 22, $p = 1.00$). T 0-1 scores never led to late rectal bleeding, T 2-3 scores did in 38 % of the No-ERB patients and in 14 % of the ERB patients. So, although there was no difference in T 2-3 scores between the two groups, a trend was noticeable (not yet statistically significant $p = 0.088$) of less late rectal bleeding for patients with T 2-3 in the ERB group.

The presence of mucosal congestion or superficial micro-ulcerations could not be related to late rectal bleeding (data not shown).

(a)
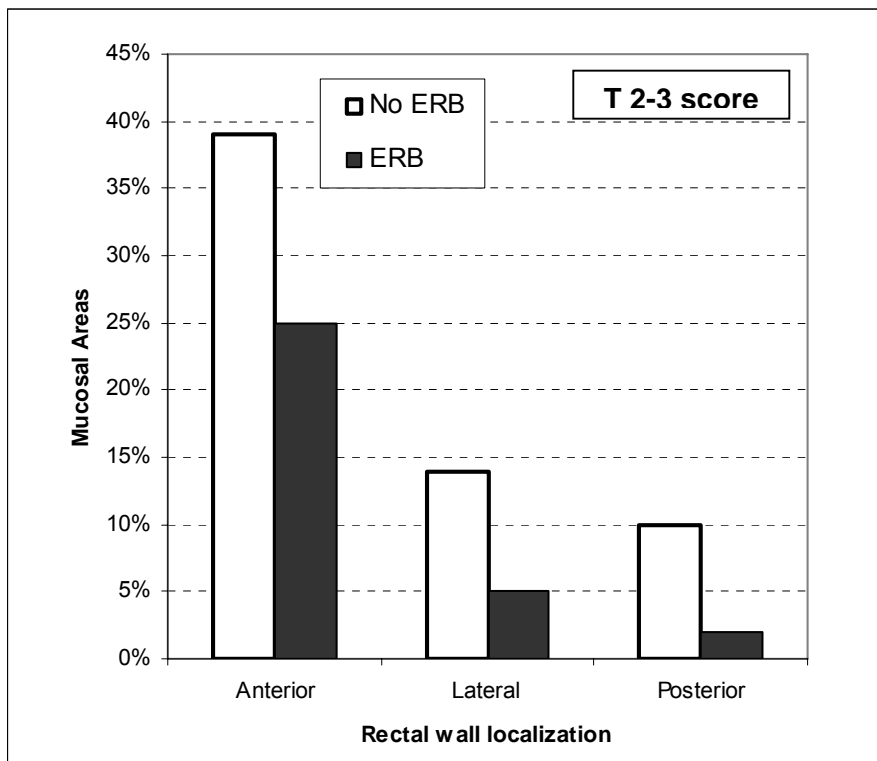
(b)

Fig. 3.
Percentage of anterior, lateral and posterior mucosal areas scored with (a) low-grade (T 1 score) or (b) high-grade (T 2-3 score) telangiectasia at two years after radiotherapy.
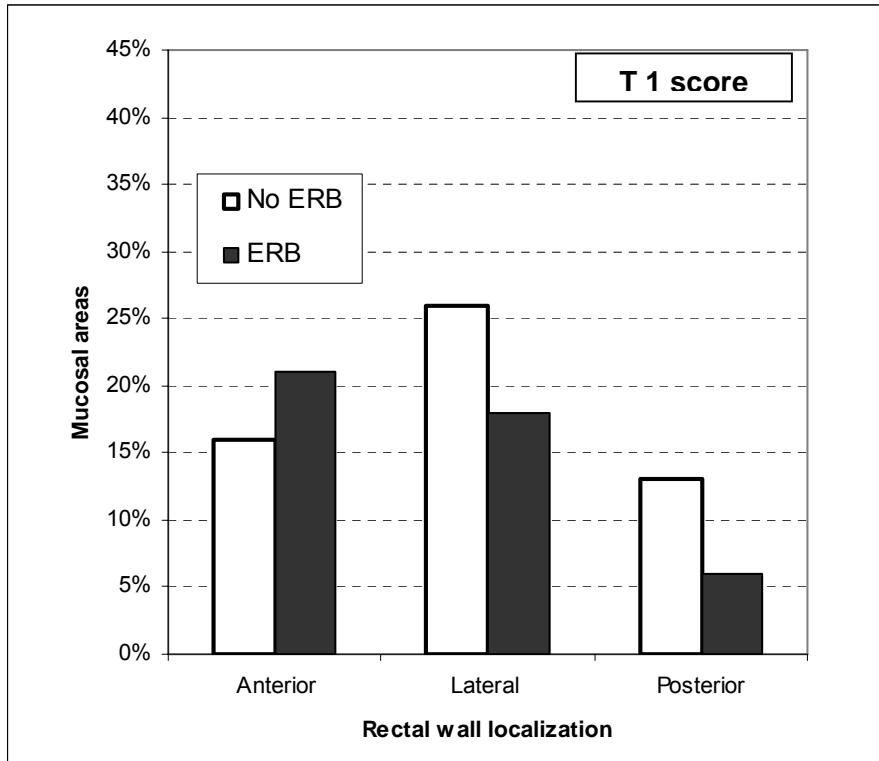
Rectal wall dose surface maps and EUD

Examples of the projected dose distribution on the Rwall in beams eye view and dose surface maps, for a No-ERB and an ERB patient, are displayed in Fig. 4a and Fig. 5a, respectively. Next, the dose grid, displayed over the unfolded inner Rwall, is presented (Fig. 4b and Fig. 5b). This individual dose grid was used to compute the EUD in each of the 16 mucosal areas, resulting in a Rwall EUD map for each patient (Fig. 4c and Fig. 5c). In Fig. 4d and 5d, the endoscopy telangiectasia scores, at one and two years, are displayed. For good comparison with the dose maps, the EUD and T score of the posterior mucosal areas are presented in duplicate. The No-ERB patient (Fig. 4) had a EUD of the anterior and lateral Rwall mucosal areas (0 – 8 cm) of 59 – 67 Gy and the posterior Rwall (0 – 8 cm) was exposed to 47 – 49 Gy. At one year, T 1 and T 2 telangiectases were seen on the anterior and lateral Rwall (0 – 8 cm). After two years, circumferential high-grade T 2 was scored. Clinically, this patient experienced grade 2 rectal bleeding. In the ERB patient example (Fig. 5), the Rwall EUD map revealed a high dose irradiation to the anterior Rwall (59 – 67 Gy), an intermediate dose to the lateral Rwall (44 – 56 Gy) and a low dose (30 - 35 Gy) for the posterior Rwall mucosal areas. At the one-year mucosal assessment, the anterior Rwall areas were scored as T 1 and T 2 (Fig. 5 d, upper panel). Up to 8 cm, the lateral and posterior areas were scored as T1. At two years, the telangiectases at the lateral and posterior Rwall areas were resolved. On the anterior side, one mucosal area was scored as T 2 and two areas as T 1. In 30 months of follow-up, this patient developed no rectal bleeding.

a

b

c

d

Fig. 4.
Patient treated without endorectal balloon (No-ERB).
(a) Rectal wall (Rwall) left-lateral beams eye view dose projection (left panel) and unfolded inner Rwall dose surface map (right panel).
(b) Inner Rwall calculated dose grid.
(c) Rwall equivalent uniform dose (EUD) mucosal dose map.
(d) Telangiectasia score (T score) per mucosal area at one year (upper panel) and at two years (lower panel).
Abbreviations: R-POST = right posterior Rwall; L-POST = left posterior Rwall; R-LAT = right lateral Rwall; L-LAT = left lateral Rwall; ANT = anterior Rwall.

Patient with ERB — Inner Rectal Wall Localization

	R-POST			R-LAT						ANT						L-LAT						L-POS		
	0	0	0	0	0	0	0	0	0	0	0	0	0	0	0	0	0	0	0	0	0	0	0	0
14	0	0	0	0	0	0	0	0	0	0	0	0	0	0	0	0	0	0	0	0	0	0	0	0
13	0	0	0	0	0	0	0	0	0	0	0	0	0	0	0	0	0	0	0	0	0	0	0	0
12	2	2	2	2	2	2	2	2	2	2	2	2	2	2	2	2	2	2	2	2	2	2	2	2
11	4	4	4	4	4	4	5	5	5	5	5	5	5	5	5	5	5	5	4	4	4	4	4	4
10	21	21	21	21	22	23	27	35	43	45	46	46	46	46	45	44	39	29	24	22	22	21	21	21
9	33	33	33	33	33	33	39	53	62	64	64	65	64	64	64	63	59	47	36	33	33	33	33	33
8	35	35	34	34	34	35	39	50	62	66	66	67	67	67	66	66	64	52	40	35	34	34	34	35
7	35	35	35	35	35	35	39	48	61	66	67	67	67	67	67	66	64	56	43	37	35	35	35	35
6	35	35	35	35	35	36	43	59	65	66	67	67	67	67	67	66	62	46	37	35	35	35	35	35
5	35	35	35	35	35	35	37	45	60	66	67	67	67	67	67	67	66	59	42	36	35	35	35	35
4	35	35	35	35	35	38	47	56	63	66	67	67	67	67	67	66	60	47	41	36	35	35	35	35
3	35	35	35	35	35	36	40	54	64	66	66	67	67	66	67	66	59	44	37	36	35	35	35	35
2	35	35	35	35	35	36	39	44	54	61	65	66	66	66	66	66	65	62	56	50	41	37	36	35
1	34	34	34	34	35	35	35	36	38	42	48	53	57	56	55	52	46	42	37	36	35	35	34	34
0	32	32	32	32	33	33	33	34	34	34	34	34	34	33	33	33	32	32	32	32	32	32	32	32

(a)

Patient with ERB — EUD

EUD	R-P	R-L	A	L-L	L-P
12-16 cm	2	2	2	2	2
8-12 cm	32	44	59	48	30
4-8 cm	35	50	67	56	35
0-4 cm	35	44	60	53	34

(c)

Patient with ERB — T score 1 year

	R-P	R-L	A	L-L	L-P
12-16 cm	0	0	0	0	0
8-12 cm	0	0	1	0	0
4-8 cm	1	1	2	1	1
0-4 cm	1	1	2	1	1

(b)

T score 2 years

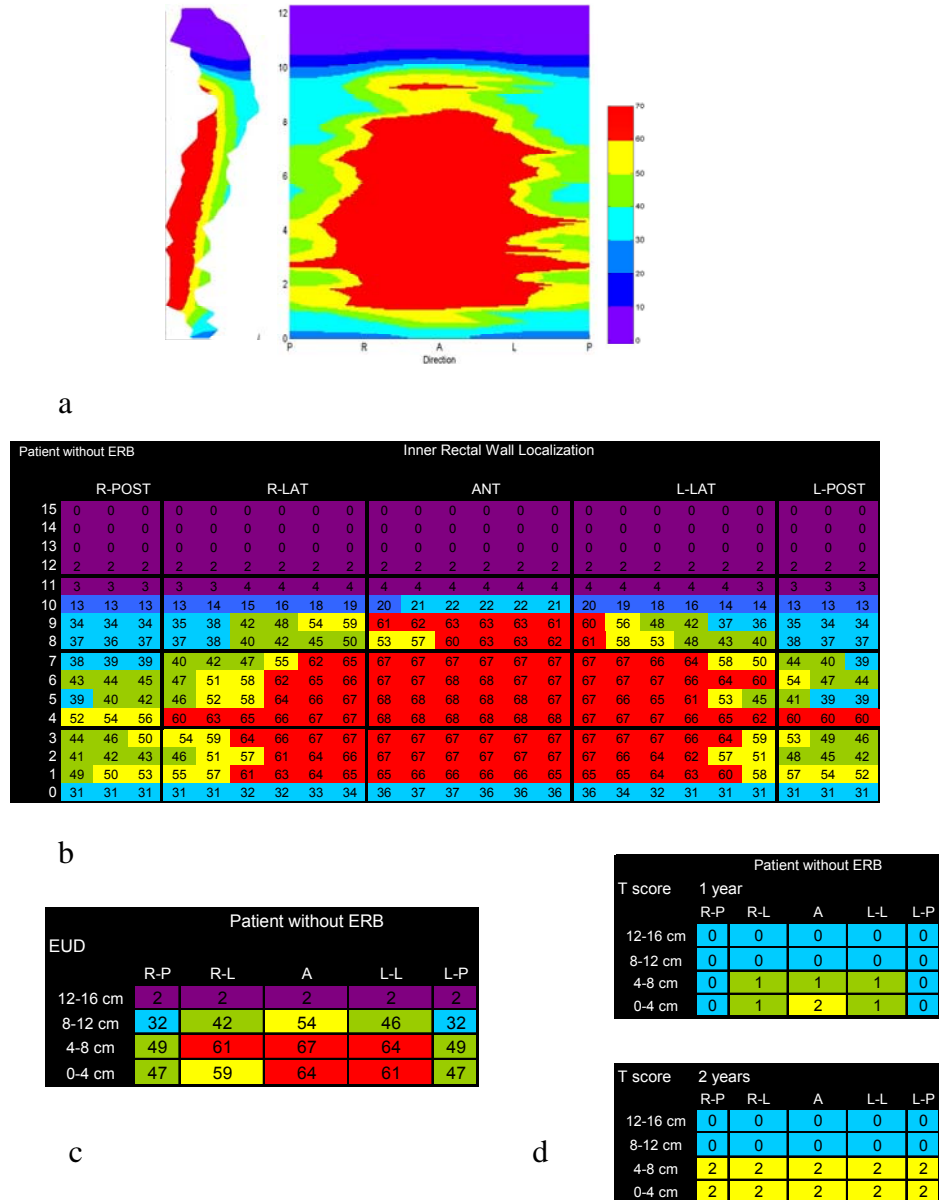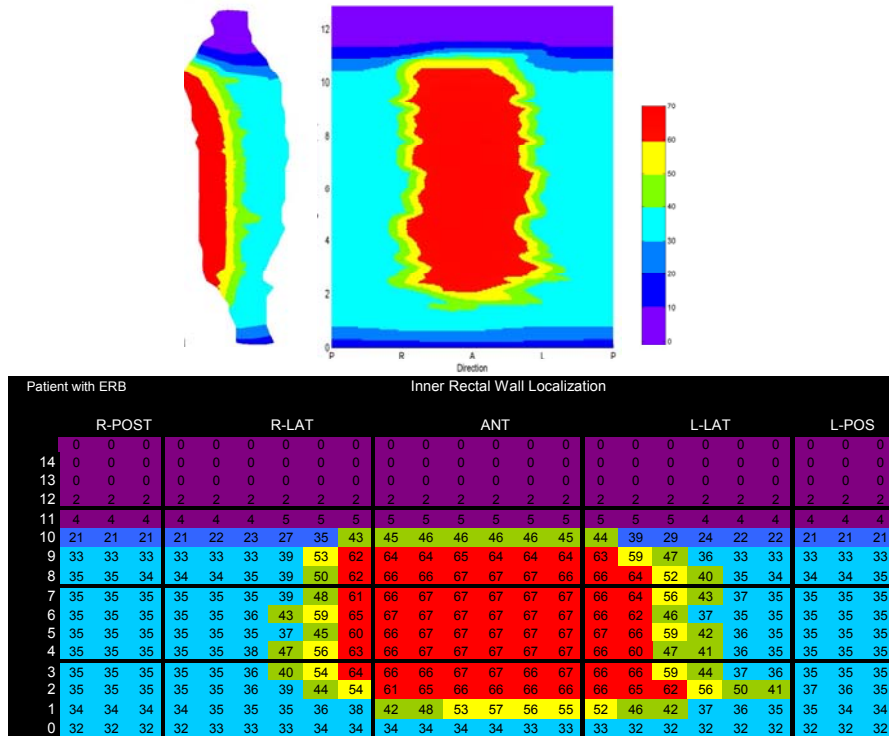|	R-P	R-L	A	L-L	L-P
12-16 cm	0	0	0	0	0
8-12 cm	0	0	1	0	0
4-8 cm	0	0	1	0	0
0-4 cm	0	0	2	0	0

(d)

Fig. 5.
Patient treated with endorectal balloon (ERB)
(a) Rectal wall (Rwall) left-lateral beams eye view dose projection (left panel) and unfolded inner Rwall dose surface map (right panel).
(b) Inner Rwall calculated dose grid.
(c) Rwall equivalent uniform dose (EUD) mucosal dose map.
(d) Telangiectasia score (T score) per mucosal area at one year (upper panel) and at two years (lower panel).
Abbreviations: R-POST = right posterior Rwall; L-POST = left posterior Rwall; R-LAT = right lateral Rwall; L-LAT = left lateral Rwall; ANT = anterior Rwall.
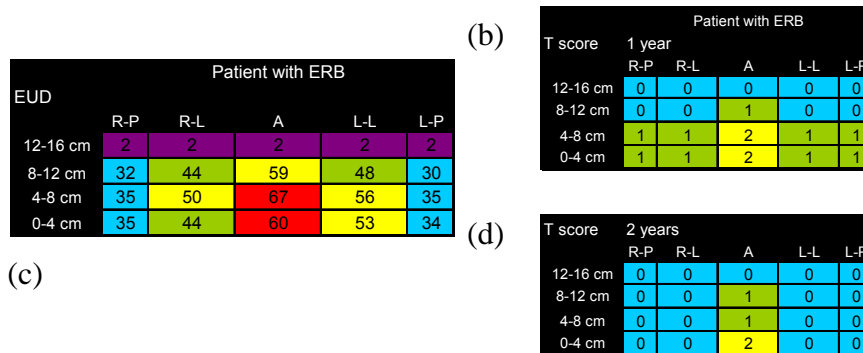
In the ERB group, a significantly higher proportion of the Rwall mucosal areas were exposed to lower doses in comparison to the No-ERB group (Fig. 6); for 0 - 20 Gy (p = 0.03) and for the 20 – 40 Gy (p = 0.014). The percentages of mucosal areas exposed to higher doses were significantly lower, in favor of the ERB group: 40 – 60 Gy (p = 0.048), 60 - 68 Gy (p = 0.043). The maximum observed EUD did not exceed 68 Gy.
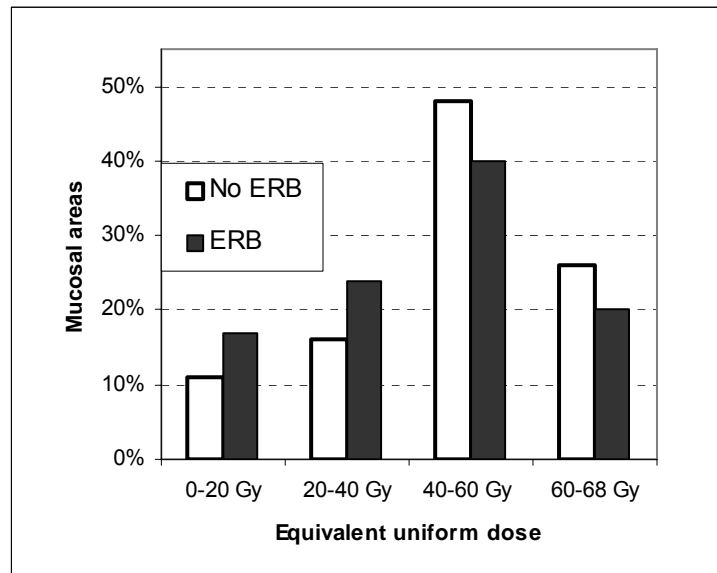

Fig. 6.
Percentage of rectal wall mucosal areas exposed to irradiation dose, for patients treated without endorectal balloon (No-ERB) and with endorectal balloon (ERB).

The patient group mean EUD mucosal area maps are displayed in Fig. 7. For the ERB-group, the rectal distension by the ERB resulted in mean lower doses, less than 40 Gy, over all the posterior mucosal areas. For the anterior mucosal areas, the mean EUDs, at the level of the prostate (0 – 8 cm ab anum) were not different between the ERB and No-ERB group. At the level of the seminal vesicles (8-12 cm, anterior and lat) the mean doses are higher for the ERB group. At that level, the anterior Rwall is being pushed towards the seminal vesicles explaining the higher Rwall dose there.

T 2-3 score			
1 year			
EUD (Gy)	No-ERB	ERB	p-value
0 - 20	4%	0%	0.12
20 - 40	6%	5%	0.69
40 - 60	23%	11%	0.017
60 - 68	48%	33%	0.13
2 years			
EUD (Gy)	No-ERB	ERB	p-value
0 - 20	0%	0%	
20 - 40	11%	5%	0.41
40 - 60	30%	14%	0.02
60 - 68	52%	28%	0.03

Table 3. *Mucosal areas exposed to different dose levels,with high-grade telangiectasis score (T 2-3)at one and two year's endoscopy assessment. Abbreviations: EUD = equivalent uniform dose.*

Correlation endoscopic findings and dose per mucosal area

As displayed in Table 3, after one and two years the intermediate dose (40 – 60 Gy) exposed mucosal areas for the ERB group showed significantly less high-grade telangiectasia. The incidence of T 2–3 was reduced to approximately half, compared to the No-ERB group. For the high-dose (60 – 68 Gy) exposed areas, the percentage of areas showing T 2-3 at two years was also significantly reduced in favor of the ERB group. After one year this difference did not reach statistical significance. For the lower dose exposed mucosal areas (0 - 20 Gy and 20 – 40 Gy), the incidence of T 2–3 was low (< 10 %) and not statistically different between the two patient groups.

No ERB group					
Mean EUD					
	R-P	R-L	A	L-L	L-P
12-16 cm	2	2	2	2	2
8-12 cm	29	36	43	37	29
4-8 cm	49	60	67	61	49
0-4 cm	46	54	60	56	46

ERB group					
Mean EUD					
	R-P	R-L	A	L-L	L-P
12-16 cm	2	2	2	2	2
8-12 cm	30	46	55	49	30
4-8 cm	37	57	67	60	37
0-4 cm	35	46	58	50	35

Fig. 7.
Patient group mean EUD mucosal area maps for (a) the No-ERB group and (b) ERB group
Abbreviations: EUD = equivalent uniform dose; ERB = endorectal balloon; A = anterior Rwall; L-L = left lateral Rwall; R-L = right lateral Rwall; L-P = left posterior Rwall; R-P = right posterior Rwall.

DISCUSSION

In this study, the late rectal mucosal changes, induced by 3D conformal radiotherapy (3D-CRT) for prostate cancer, have been prospectively followed by regular endoscopies in patients irradiated with and without an ERB. As expected, telangiectasia was seen most frequently after two years. The development and severity of telangiectasia in the irradiated rectal mucosa is considered to be the major pathologic change resulting in late rectal bleeding causing, among other anorectal symptoms, a severe reduction of quality of life (18, 24). The relation between the high dose delivered to the Rwall and the observed late rectal toxicity is well known (1-4). Also, it has been suggested that intermediate doses (6-8), especially the spatial dose distribution of dose areas below 45 Gy, to the Rwall play an important role in this phenomena (5). Earlier, we have demonstrated the Rwall sparing effect of different ERBs by reduction of the Rwall volumes exposed to high and intermediate doses, for both 3D-CRT and intensity-modulated radiotherapy (IMRT) (14). One of these ERBs we have been using clinically for the present study. After being instructed by the physician, the attending therapists were capable to apply the single-use ERB and, with some experience, this procedure adds two minutes to the daily treatment time. This ERB could not reduce the day-to-day interfraction prostate displacements (21) and now we use the prostate ERB in combination with a daily on-line gold-marker based portal imaging protocol. The ERB was also shown to be of value for CT-MR image fusion in image-guided radiotherapy (25).

Previously, others have reported that the ERB is well tolerated, and the related acute toxicity resolved quickly with standard interventions (10-13, 16, 17, 21). This is in line with the present observations, where no grade 3 acute toxicity was observed.

Late toxicity data for radiotherapy with the use of an ERB are now coming available. The Baylor College group irradiated 116 men with IMRT (mean dose 76 Gy) and a daily-applied 100 cc ERB (12). After a median follow-up of 31 months, they reported a grade 2 and 3 late rectal toxicity rate of 6.9% and 1.7%, respectively. D'Amico *et al.* reported a 10%

estimate of grade 3 rectal bleeding, after two years, in 57 men treated with four-field 3D-CRT (dose 75.6 Gy) and a 60 cc ERB, applied in 15 of the 40 radiation treatments (9). Both authors reported a reduction of the volume of the rectum receiving 70 Gy or more, due to the ERB (9, 12). No statements were made about reduction of Rwall dose exposure in lower dose regions and no endoscopic assessment has been reported yet. Although it is recognized that the patient population in the present study is smaller and the prescribed dose is lower than the afore-mentioned two studies, the late rectal toxicity rate (Grade 1 or higher) after 30 months was significantly lower for the ERB group. In the ERB-group no rectal bleeding requiring medical interventions occurred. Longer follow-up is necessary before definitive conclusions can be drawn, because the onset of late anorectal symptoms can extend beyond two or three years after completion of radiotherapy (1, 5, 18, 24, 26-29).

To our knowledge, this is the first comparative prospective analysis of late rectal mucosal changes in two patients groups, No-ERB and ERB, by periodical standardized rectosigmoidoscopy, independent of the existence of radiation related symptoms. Zelefsky *et al.* (27) reported endoscopic findings in 57 patients presenting with late rectal bleeding after high-dose 3D-CRT, up to 81 Gy. Exact numbers were not provided, but most patients had telangiectases of the anterior wall and only patients reporting severe grade 3 rectal toxicity had rectal ulceration. At our endoscopic assessments, performed up to two years and with a maximum Rwall dose of 68 Gy, no rectal ulcerations have been observed yet. Wachter *et al.* (20) performed a single sigmoidoscopy in 44 patients irradiated with a dose of 66 Gy, four-field 3D-CRT, and a 40 cc air-filled ERB at a median of 29 months after treatment. In contrast to our study, no individual Rwall dose surface maps were used for dose-response analysis. Further, the Rwall dose exposure per mucosal area was not a calculation from the treatment planning system, but an estimation derived from the lateral beam's-eye view. Corresponding to our data, a good correlation was observed between the endoscopic findings and the estimated Rwall dose; the occurrence of grade 3 telangiectasia was strictly limited to high-dose (> 60 Gy) regions at the anterior wall, while grade 1 and 2 telangiectasia were observed at the whole

circumference, corresponding to the medium (30 – 60 Gy) and low-dose (< 30 Gy) regions. Also a good correlation between clinically apparent symptoms and the endoscopy scores was found. Nine patients (20%) experienced late rectal bleeding. In 66% of these patients grade 2-3 telangiectasia were observed compared to 15% in the non-bleeders. On the other hand, in five patients without rectal bleeding, grade 2-3 telangiectasia were seen. These findings correspond to those of the present study. It was postulated that, not only the high dose regions at the anterior rectal wall but also the dose distribution of the whole circumference is relevant in the development of late rectal bleeding (20).

The importance of reducing high dose exposure to the posterior Rwall has been recognized previously (30) and interventions such as lateral rectal shielding have reduced late rectal morbidity (31). The present study has shown that the ERB reduced the dose to the posterior and lateral Rwall mucosa, while maintaining a high dose to the anterior mucosa (Fig. 1b, 5, 7). This resulted in a significant reduction of T 2-3 after one and two years (Fig. 2b) and attributed to a reduced late rectal toxicity in the ERB group. This reduction of severe late rectal changes was mainly seen, as expected, in the lateral and posterior Rwall mucosal areas (Fig. 3b).

The observed onset of bleeding symptoms correlated well with larger studies, where rectal bleeding appeared most often between 12 and 30 months of follow-up (1, 3, 27-29). This is in line with the presented endoscopic findings, where T 2-3 developed in the first year after treatment and reached a peak at the one-year assessment (Fig. 2b). In another prospective analysis, in 20 prostate cancer patients (65 Gy, four-field box technique, without ERB), every 6 months up to 3 years after treatment, rectosigmoidoscopies were planned (19). A statistically significant correlation was found between multiple telangiectases, rectal bleeding and mucosal discharge. In line with our observations, the development of telangiectasis evolved at a rate parallel to the development of rectal bleeding. Eighty percent of the patients, who developed T 2-3, experienced late rectal bleeding. In five patients with telangiectasia spontaneous mucosal improvement was seen. Detailed data on localization, spatial dose distribution and the

estimated dose on these mucosal areas were not provided. As concluded by the authors, this improvement may be an explanation for the observation that rectal bleeding resolves in patients with mild symptoms after radiotherapy. We also saw improvement of mucosal changes during follow-up (Fig. 5e) and relief of late rectal bleeding. One can hypothesize that the probability of regeneration of rectal mucosa, and thus amelioration of rectal bleeding after time, may depend first, on the size and the severity of Rwall damage and secondly, on the dose distribution in surrounding areas. We will, therefore, continue to perform endoscopies to gain more insight in the development and evolution of mucosal changes in relation to rectal bleeding and other anorectal symptoms, such as fecal frequency and incontinence.

This mucosal recovery phenomena can then be studied more in detail, e.g. by means of cluster model analysis, as proposed by Tucker *et al.* (5). In their case-control study, a two-dimensional cluster model of late rectal toxicity was tested. In this model, the probability of rectal complications does not only depend on the dose-wall histogram, but also on the spatial distribution of radiation damage. It was concluded that a dose range of 27 to 43 Gy (median 32 Gy) might be associated most significantly to grade ≥2 rectal toxicity. We have shown that the ERB, in combination with the applied 67.5 Gy four-field 3D-CRT, yielded a dose reduction of the posterior Rwall (0-8 cm) from 48 Gy (No-ERB) to 36 Gy (ERB) (Fig. 7). With reduction of treatment margins or improvement of dose delivery (e.g. IMRT) the dose delivered to the posterior and lateral Rwall may even further be reduced, well below the recommended 32 Gy (5).

Finally, surprising differences were observed in Rwall dose-effect relationships between the two groups. In both groups, all bleeders had mucosal areas with T 2-3 scores. But in the ERB group, only 14% of the patients with T 2 or T 3 scores developed late rectal bleeding, while in the No-ERB group this was 38% (Table 2). This difference could not be fully explained by the difference in spatial dose distribution or volumetric Rwall reduction of the ERB. In the ERB group, in Rwall mucosal areas exposed to intermediate (40 – 60 Gy) to high doses (60 – 68 Gy), a significant reduction of severe telangiectases was observed after two years, compared to the No-ERB group (Table 3). This might be caused by an increased

tolerance of the Rwall mucosa for development of severe late changes in patients treated with an ERB. This increased tolerance might either have a physical origin: dose build-up in the superficial Rwall due to the presence of an air cavity (12), or a radiobiological origin: stretching of the Rwall leading to hypoxia.

Before definitive conclusions can be drawn on the possible beneficial effects of an ERB in prostate cancer 3D-CRT and IMRT, longer follow-up and thorough assessment of late symptoms and effects is necessary. As we have shown, the ERB can still be further improved (14). Also this study has shown that an ERB can be advantageous in prostate cancer radiotherapy. Therefore, and to further increase its acceptability, we are currently in the process of developing a more patient- and therapist-friendly ERB for daily usage.

CONCLUSION

This study prospectively investigated the differences in late rectal wall (Rwall) mucosal changes in prostate three-dimensional conformal radiotherapy (3D-CRT) with or without an endorectal balloon (ERB), by periodical endoscopic assessment. The ERB reduced significantly the Rwall volume exposed to intermediate and high doses and significantly less severe late mucosal changes were seen at one and two years. Acute toxicity was mild in both groups. Although longer follow-up is warranted, at 30 months late rectal toxicity was reduced in the ERB group. In intermediate and high-dose exposed Rwall mucosal areas less high-grade telangiectases (T 2-3) were seen after two years in the ERB group compared to the No-ERB group. These observations suggest an ERB-induced increased tolerance for late Rwall damage.

REFERENCES

1. Peeters ST, Lebesque JV, Heemsbergen WD, et al. Localized volume effects for late rectal and anal toxicity after radiotherapy for prostate cancer. Int J Radiat Oncol Biol Phys 2006;64(4):1151-1161.

2. Kupelian PA, Thakkar VV, Khuntia D, et al. Hypofractionated intensity-modulated radiotherapy (70 Gy at 2.5 Gy per fraction) for localized prostate cancer: long-term outcomes. Int J Radiat Oncol Biol Phys 2005;63(5):1463-1468.

3. Huang EH, Pollack A, Levy L, et al. Late rectal toxicity: dose-volume effects of conformal radiotherapy for prostate cancer. Int J Radiat Oncol Biol Phys 2002;54(5):1314-1321.

4. Storey MR, Pollack A, Zagars G, et al. Complications from radiotherapy dose escalation in prostate cancer: preliminary results of a randomized trial. Int J Radiat Oncol Biol Phys 2000;48(3):635-642.

5. Tucker SL, Zhang M, Dong L, et al. Cluster model analysis of late rectal bleeding after IMRT of prostate cancer: a case-control study. Int J Radiat Oncol Biol Phys 2006;64(4):1255-1264.

6. Tucker SL, Dong L, Cheung R, et al. Comparison of rectal dose-wall histogram versus dose-volume histogram for modeling the incidence of late rectal bleeding after radiotherapy. Int J Radiat Oncol Biol Phys 2004;60(5):1589-1601.

7. Jackson A, Skwarchuk MW, Zelefsky MJ, et al. Late rectal bleeding after conformal radiotherapy of prostate cancer. II. Volume effects and dose-volume histograms. Int J Radiat Oncol Biol Phys 2001;49(3):685-698.

8. Skwarchuk MW, Jackson A, Zelefsky MJ, et al. Late rectal toxicity after conformal radiotherapy of prostate cancer (I): multivariate analysis and dose-response. Int J Radiat Oncol Biol Phys 2000;47(1):103-113.

9. D'Amico AV, Manola J, McMahon E, et al. A prospective evaluation of rectal bleeding after dose-escalated three-dimensional conformal radiation therapy using an intrarectal balloon for prostate gland localization and immobilization. Urology 2006;67(4):780-784.

10. Bastasch MD, Teh BS, Mai WY, et al. Tolerance of endorectal balloon in 396 patients treated with intensity-modulated radiation therapy (IMRT) for prostate cancer. Am J Clin Oncol 2006;29(1):8-11.

11. Ronson BB, Yonemoto LT, Rossi CJ, et al. Patient tolerance of rectal balloons in conformal radiation treatment of prostate cancer. Int J Radiat Oncol Biol Phys 2006;64(5):1367-1370.

12. Teh BS, Dong L, McGary JE, et al. Rectal wall sparing by dosimetric effect of rectal balloon used during intensity-modulated radiation therapy (IMRT) for prostate cancer. Med Dosim 2005;30(1):25-30.

13. Woel R, Beard C, Chen MH, et al. Acute gastrointestinal, genitourinary, and dermatological toxicity during dose-escalated 3D-conformal radiation therapy (3DCRT) using an intrarectal balloon for prostate gland localization and immobilization. Int J Radiat Oncol Biol Phys 2005;62(2):392-396.

14. van Lin EN, Hoffmann AL, van Kollenburg P, et al. Rectal wall sparing effect of three different endorectal balloons in 3D conformal and IMRT prostate radiotherapy. Int J Radiat Oncol Biol Phys 2005;63(2):565-576.

15. Patel RR, Orton N, Tome WA, et al. Rectal dose sparing with a balloon catheter and ultrasound localization in conformal radiation therapy for prostate cancer. Radiother Oncol 2003;67(3):285-294.

16. Wachter S, Gerstner N, Dorner D, et al. The influence of a rectal balloon tube as internal immobilization device on variations of volumes and dose-volume histograms during treatment course of conformal radiotherapy for prostate cancer. Int J Radiat Oncol Biol Phys 2002;52(1):91-100.

17. Teh BS, Mai WY, Uhl BM, et al. Intensity-modulated radiation therapy (IMRT) for prostate cancer with the use of a rectal balloon for prostate immobilization: acute toxicity and dose-volume analysis. Int J Radiat Oncol Biol Phys 2001;49(3):705-712.

18. O'Brien PC. Radiation injury of the rectum. Radiother Oncol 2001;60(1):1-14.

19. O'Brien PC, Hamilton CS, DenhamJW et al. Spontaneous improvement in late rectal mucosal changes after radiotherapy for prostate cancer. Int J Radiat Oncol Biol Phys 2004;58(1):75-80.

20. Wachter S, Gerstner N, Goldner G, et al. Endoscopic scoring of late rectal mucosal damage after conformal radiotherapy for prostatic carcinoma. Radiother Oncol 2000;54(1):11-19.

21. van Lin EN, van der Vight LP, Witjes JA, et al. The effect of an endorectal balloon and off-line correction on the interfraction systematic and random prostate position variations: a comparative study. Int J Radiat Oncol Biol Phys 2005;61(1):278-288.

22. D'Amico AV, Manola J, Loffredo M, et al. A practical method to achieve prostate gland immobilization and target verification for daily treatment. Int J Radiat Oncol Biol Phys 2001;51(5):1431-1436.

23. Wu Q, Mohan R, Niemierko A, et al. Optimization of intensity-modulated radiotherapy plans based on the equivalent uniform dose. Int J Radiat Oncol Biol Phys 2002;52(1):224-235.

24. Denham JW, O'Brien PC, Dunstan RH, et al. Is there more than one late radiation proctitis syndrome? Radiother Oncol 1999;51(1):43-53

25. van Lin EN, Futterer JJ, Heijmink SW, et al. IMRT boost dose planning on dominant intraprostatic lesions: gold marker-based three-dimensional fusion of CT with dynamic contrast-enhanced and 1H-spectroscopic MRI. Int J Radiat Oncol Biol Phys 2006;65(1):291-303.

26. Andreyev HJ, Vlavianos P, Blake P, et al. Gastrointestinal symptoms after pelvic radiotherapy: role for the gastroenterologist? Int J Radiat Oncol Biol Phys 2005;62(5):1464-1471.

27. Zelefsky MJ, Cowen D, Fuks Z, et al. Long term tolerance of high dose three-dimensional conformal radiotherapy in patients with localized prostate carcinoma. Cancer 1999;85(11):2460-2468.

28. Teshima T, Hanks GE, Hanlon AL, et al. Rectal bleeding after conformal 3D treatment of prostate cancer: time to occurrence, response to treatment and duration of morbidity. Int J Radiat Oncol Biol Phys 1997;39(1):77-83.

29. Feigenberg SJ, Hanlon AL, Horwitz EM, et al. Long-term androgen deprivation increases Grade 2 and higher late morbidity in prostate cancer patients treated with three-dimensional conformal radiation therapy. Int J Radiat Oncol Biol Phys 2005;62(2):397-405.

30. Cho KH, Lee CK, Levitt SH. Proctitis after conventional external radiation therapy for prostate cancer: importance of minimizing posterior rectal dose. Radiology 1995;195(3):699-703.

31. Lee WR, Hanks GE, Hanlon AL, et al. Lateral rectal shielding reduces late rectal morbidity following high dose three-dimensional conformal radiation therapy for clinically localized prostate cancer: further evidence for a significant dose effect. Int J Radiat Oncol Biol Phys 1996;35(2):251-257.

9

Summary

Conclusions

Future Perspectives

SUMMARY

For localized prostate cancer (Pca) evidence is growing for improved tumour control (PSA-relapse free survival) with higher radiotherapy doses (1-3). But if this improved biochemical control can be translated into survival gain, remains to be answered (4,5). This needs to be clarified in randomized trials with long follow-up, such as the ongoing RTOG 0126 trial comparing two dose levels; 70.2 Gy and 79.2 Gy. This study is designed to test for an overall survival end point and will need an accrual of 1520 patients. But, as recently shown in a large Scandinavian randomized trial, local treatment can positively influence survival (6). Overall survival after prostatectomy was superior over watchful waiting, in men < 75 years and localized favourable Pca. The cost of dose escalation is an increase of late toxicity (2,3,7). This is recently summarized in a comprehensive review on outcome and toxicity in Pca 3D-CRT (5). Before offering Pca patients a higher dose, the physician has to be aware of the potential risks and has to inform the individual patient. One of the challenges of the future Pca radiation treatment is to fully explore the technical possibilities and tools for reducing toxicity in this growing patient population with, in general, a long life expectancy.

The aim of this thesis was to describe the steps we took in Nijmegen to improve the radiation treatment for localized Pca. We focused on narrowing the size of the radiation fields, by margin reduction, or avoidance of irradiating the surrounding normal tissues (e.g. rectum and bladder). The ultimate goal will be targeted deliverance of a high tumor dose, with a minimum of expected damage leading to considerable impairment of quality of life (8).

In **chapter 2**, an improvement of patient positioning (set-up) was achieved with the implementation of the couch height set-up method and a technologist-driven off-line correction protocol. The patient position was assessed on bony landmarks with a camera-based portal imaging system. The couch height set-up resulted in reduction of the systematic position deviations in the ventro-dorsal direction and reduced the number of corrections within the correction protocol. On average, 10 position measurements were performed and 0.6 corrections per patient were needed. The systematic positioning errors were reduced to 1.3-1.6 mm (1 SD), while the daily random errors were 1.7-2.2 mm (1SD). As a result of this study, we reduced our treatment margins around the prostate and seminal vesicles to 8 mm and 9 mm, respectively.

Since 2002, the bony landmarks are not used as surrogate for prostate position anymore, because the prostate moves independently from the bony structures (9). Now, in all patients the urologist implants transrectally, under ultrasound guidance, gold markers into the prostate. As described in **chapter 3,** the implantation is a simple and safe procedure. In

209 men, a 6.2% moderate complication rate, defined as pain requiring analgesics, fever, nausea/vomiting or an allergic reaction on the antibiotics, was observed. Hematuria, lasting longer than 3 days, hematospermia and rectal bleeding (average duration 2.5 days) occurred in 3.8%, 18.5% and 9.1% of the patients, respectively. It was concluded that marker implantation did not differ from diagnostic prostate biopsies in terms of experienced complaints and complications.

In 2002, the endorectal balloon (ERB) was used only in a few centers worldwide for Pca radiotherapy. Early reports suggested improved prostate immobilization resulting in reduced daily position variation. In **chapter 4**, we have shown that the prostate position variations, measured on implanted gold markers, were comparable in patients irradiated with ERB or without ERB. Especially, the daily prostate motion in the anterior-posterior direction remained relatively high; 4.7 mm (1 SD). Stool and gas besides the ERB could be an explanation for this. Also, the motion of the prostate relative to the bones was not reduced by the ERB. With regard to the implanted markers, our data confirmed that migration of the markers within the prostate is negligible. This study also showed the effectiveness of the applied marker-based correction protocol in reducing the systematic prostate position variations.

In **chapter 5,** the issue of the generally recommended full bladder Pca irradiation was addressed. A full bladder is advantageous in terms of reduced bladder toxicity and could effect, comparable to the variable filling of the rectum, the prostate position variation during daily treatment. The daily bladder filling was measured with a bladder ultrasound scanner. Although patients were instructed to have a full bladder, a very high daily bladder volume variation (47 % (1 SD)) was found. Applying a scanner-based biofeedback protocol did not change the average bladder filling or reduce the daily filling variation. In this study, no significant correlation between bladder filling and daily prostate motion could be observed.

After our first positive ERB experiences, in terms of patients' tolerance and staff acceptance, it was decided to test and compare the so-far known different types. The three investigated ERBs were quite different in shape, volume and manual handling. In **chapter 6**, we have shown the different resulting spatial dose distributions over the inner rectal wall (Rwall mucosa) for high-dose (78 Gy) three-dimensional conformal radiotherapy (3D-CRT) and intensity-modulated radiotherapy (IMRT). Based on calculations of the expected late rectal toxicity and radiation exposed volumes of Rwall, it was concluded that, for both 3D-CRT and IMRT, a reduction of the relative inner Rwall surface exposed to intermediate and high-doses was found, which may lead to reduced late rectal toxicity. The two ERBs with larger volumes were superior over the smaller one. We concluded that none of the three

ERBs had the ideal design, and therefore the development of a more user- and patient-friendly ERB is warranted.

Advanced magnetic resonance (MR) imaging techniques were introduced into our Pca treatment preparation and planning. An in-house developed CT-MR image fusion tool, based on gold markers and an ERB, resulted in a highly accurate matching of these images (10). Simultaneously, IMRT treatment planning became available in our department. In **Chapter 7**, a concept of a biological target volume in Pca RT was tested. It was shown that it was technically feasible to integrate two functional prostate MR imaging techniques (dynamic contrast-enhanced MR imaging (DCE-MRI) and [1]H-MR spectroscopic imaging (MRSI), into IMRT treatment planning. The DCE-MRI and MRSI were able to define the dominant tumor bearing regions within the prostate (the so-called intra-prostatic lesion (DIL)). Next, this DIL was used for high-dose intra-prostatic boosting with IMRT (DIL-IMRT). DIL-IMRT (90 Gy on the DIL and 70 Gy on the other part of the prostate) resulted in reduced expected late rectal toxicity, compared to homogeneous (78 Gy) prostate irradiation. It was hypothesized that the typical Rwall spatial dose distribution, as a result of the DIL boosting, may indicate a further reduced actual rectal toxicity.

In **chapter 8** acute and late toxicity rates for patients treated with an ERB are compared to patients irradiated without an ERB. This was not a randomized study, but these data suggested a reduced late rectal toxicity in the ERB-group after a moderate dose of 67,5 Gy. It was possible for each patient, to calculate and display the dose over the inner rectal wall (Rwall) as Rwall surface dose maps. This spatial dose distribution was compared to the radiation-induced mucosal changes, as observed in repeated rectosigmoidoscopy. After a follow-up of 30 months, 146 scopies were performed in 48 patients. The ERB clearly reduced the Rwall volume exposed to high doses, resulting in decrease of late rectal mucosal changes. Interestingly, in Rwall areas exposed to doses > 40 Gy, less severe Rwall damage was seen in the ERB group, compared to the No-ERB patients. This observation may suggest an ERB-induced increased tolerance for late Rwall damage.

CONCLUSIONS AND FUTURE PERSPECTIVES

For the future the following issues are of major importance:

1. PROSTATE POSITION VERIFICATION AND CORRECTION STRATEGIES

Control of prostate position is essential in high-dose Pca radiotherapy, because large systematic shifts of the prostate relative to the irradiation field can cause considerable underdosage and loss of local tumour control (11). Position verification based on implanted gold markers is superior to the usage of bony landmarks, because the prostate moves independently form the pelvic bones (12). We have shown that the gold markers are safe and a simple tool for portal imaging based correction procedures. In our setting, one dedicated urologist is responsible for the implantation and it takes about 10 minutes per patient in an outpatient setting.

During the radiotherapy treatment the prostate position is checked and corrected by trained technologists, under supervision of the physician. As described, the off-line correction protocol reduces the position variation, enabling to use smaller treatment margins (13). Recently, we have started an on-line correction protocol for the anterior-posterior direction (towards the rectum) and re-position the patient, if necessary, before the daily treatment has been given. As a result, we have reduced the treatment margin towards the rectum to 5 mm. We continue to improve our portal imaging based correction procedures in close collaboration with our technologists, who are responsible for executing these protocols. Another method of prostate position verification is the so-called kilovoltage Cone-beam CT. This imaging system is integrated into the lineair accelerator and is able to construct volumetric CT images of the area to be irradiated after a single gantry rotation. Preliminary results look promising, but the usage for prostate position verification is hampered due to image distortion when bowel gas is present (14). With a cheaper portal imaging system and gold markers, image quality is constantly good and either off-line or on-line correction protocols can be executed fast and in a reliable way.

As the bladder concerns, despite a laborious bladder scanner based biofeedback protocol, we did not observe a reduction of bladder filling variation. In our study, the amount of bladder filling did not influence the prostate position. As a consequence, we continue to instruct patients to be treated with a comfortable full bladder but no extra checks on bladder filling are being performed.

2. ENDORECTAL BALLOON

As demonstrated, the endorectal balloon is expected to be advantageous in reducing late rectal toxicity in high-dose radiotherapy. So far, we have treated 50 patients with an ERB at a moderate dose level (67.5 Gy) with 3D-CRT. Based on our clinical experience and planning studies, we are now developing a dedicated single-use Pca ERB for daily treatment use. Patients treated with this ERB will be followed closely, and the acute and late toxicity profile will be monitored. More late Rwall damage data, derived from repeated rectosigmoidoscopies, will be collected to confirm if the ERB is associated with an increased tolerance of the Rwall for late rectal damage. Work in progress is to study the role of the ERB in reducing the incidence of fecal incontinence, as preliminary planning study data have suggested a reduction of the dose onto the anal wall. Peeters *et al*. (7) have indicated a clear dose volume effect for the anal wall and the presence of fecal incontinence.

3. HIGH DOSE RADIOTHERAPY

As proven in a large Dutch randomized trial, a higher radiotherapy dose yields a better tumour control in a subset of patients with localized Pca (1). This higher dose also resulted in higher late rectal toxicity. This can raise an interesting question if patients really prefer a better tumour control at the cost of increased toxicity. This issue was recently investigated at our department and it was concluded that the majority of the Pca patients is reluctant to accept these higher toxicities (15).

These results emphasize the importance of a well-informed patient and the necessity to be careful to elevate the treatment dose without taking measures to prevent increased late toxicity (4). Besides the gold markers and the endorectal balloon, we have integrated anatomical MR imaging for better definition of the prostatic gland and the normal surrounding tissues, which lead to smaller irradiated volumes, as studied by the group of the Netherlands Cancer Institute (16). Advanced DCE-MRI and MRSI techniques will be used for further exploration of the DIL-IMRT concept, as a measure of decreasing the Rwall volume to be irradiated. It is certain, that the role of MR imaging will be expanding in the near future. Pre-treatment staging will be more accurate, resulting in tailor-made treatment decisions (17, 18) and perhaps CT-based planning will be replaced by MR-based planning systems (19). This staging is particularly important to discriminate between localized or locally advanced disease and decide whether radiotherapy should be combined with hormonal therapy. Although beyond the scope of this thesis, the role of hormonal therapy in combination with high-dose Pca radiotherapy has not been established yet (20, 21). The adverse effects of this systemic treatment are well known and long term androgen deprivation increased late

rectal toxicity in Pca radiotherapy (22). In the literature it has been suggested that, for certain subsets of Pca patients, high dose radiotherapy (> 74 Gy) would result in comparable tumour control as the combination of hormonal treatment and conventional doses (≤ 70 Gy) (23, 24).

A relatively novel approach in high-dose Pca radiotherapy is hypofractionation. There is evidence from clinical studies that the a/b ratio for Pca may be low, which would correspond to an increased fractionation sensitivity, i.e. a biological equivalence in outcome can be achieved by giving a higher radiation dose per fraction at a lower total dose. For example, 76 Gy in 2 Gy daily fractions may be equivalent to 70.2 Gy in 2.7 Gy daily fractions (26). Kupelian *et al.* (23) conducted a hypofractionation study, prescribing 70 Gy in 28 daily fractions of 2.5 Gy. They presented an excellent 5-years PSA-relapse free survival of 85% in this group with localized Pca. Persistent late rectal and urinary toxicity rates at 5 years were low, 5% and 8% respectively. In this study, no impact of hormonal therapy on biochemical relaps free survival was noted. In Nijmegen we have adopted this scheme for the intermediate and high-risk Pca patients, in combination with gold marker based correction and daily ERB.

REFERENCES

1. Peeters ST, Heemsbergen WD, Koper PC, van Putten WL, Slot A, Dielwart MF et al. Dose-response in radiotherapy for localized prostate cancer: results of the Dutch multicenter randomized phase III trial comparing 68 Gy of radiotherapy with 78 Gy. J Clin Oncol 2006;24:1990-6.

2. Zietman AL, DeSilvio ML, Slater JD, Rossi CJ, Jr., Miller DW, Adams JA et al. Comparison of conventional-dose vs high-dose conformal radiation therapy in clinically localized adenocarcinoma of the prostate: a randomized controlled trial. JAMA 2005;294:1233-9.

3. Pollack A, Zagars GK, Starkschall G, Antolak JA, Lee JJ, Huang E et al. Prostate cancer radiation dose response: results of the M. D. Anderson phase III randomized trial. Int J Radiat Oncol Biol Phys 2002;53:1097-105.

4. Sandler HM. Exploring dose-intensity: carefully comparing high-dose with low-dose external-beam radiotherapy for prostate cancer. J Clin Oncol 2006;24:1975-7.

5. van Tol-Geerdink JJ, Stalmeier PF, Pasker-de Jong PC, Huizenga H, van Lin EN, Schimmel EC et al. Systematic review of the effect of radiation dose on tumor control and morbidity in the treatment of prostate cancer by 3D-CRT. Int J Radiat Oncol Biol Phys;64:534-43.

6. Bill-Axelson A, Holmberg L, Ruutu M, Haggman M, Andersson SO, Bratell S et al. Radical prostatectomy versus watchful waiting in early prostate cancer. N Engl J Med 2005;352:1977-84.

7. Peeters ST, Lebesque JV, Heemsbergen WD, van Putten WL, Slot A, Dielwart MF et al. Localized volume effects for late rectal and anal toxicity after radiotherapy for prostate cancer. Int J Radiat Oncol Biol Phys 2006 March 15;64(4):1151-61.

8. Denham JW, O'Brien PC, Dunstan RH, Johansen J, See A, Hamilton CS et al. Is there more than one late radiation proctitis syndrome? Radiother Oncol 1999;51:43-53.

9. Langen KM, Jones DT. Organ motion and its management. Int J Radiat Oncol Biol Phys 2001;50:265-78.

10. Huisman HJ, Futterer JJ, van Lin EN, Welmers A, Scheenen TW, van Dalen JA et al. Prostate cancer: precision of integrating functional MR imaging with radiation therapy treatment by using fiducial gold markers. Radiology 2005;236:311-7.

11. de Crevoisier R, Tucker SL, Dong L, Mohan R, Cheung R, Cox JD et al. Increased risk of biochemical and local failure in patients with distended rectum on the planning CT for prostate cancer radiotherapy. Int J Radiat Oncol Biol Phys 2005;62:965-73.

12. Schallenkamp JM, Herman MG, Kruse JJ, Pisansky TM. Prostate position relative to pelvic bony anatomy based on intraprostatic gold markers and electronic portal imaging. Int J Radiat Oncol Biol Phys 2005;63:800-11.

13. van Herk HM, Remeijer P, Lebesque JV. Inclusion of geometric uncertainties in treatment plan evaluation. Int J Radiat Oncol Biol Phys 2002;52:1407-22.

14. Smitsmans MH, de BJ, Sonke JJ, Betgen A, Zijp LJ, Jaffray DA et al. Automatic prostate localization on cone-beam CT scans for high precision image-guided radiotherapy. Int J Radiat Oncol Biol Phys 2005;63:975-84.

15. van Tol-Geerdink JJ, Stalmeier PF, van Lin EN et al. Do patients with localized prostate cancer really want more aggressive radiation treatment? J Clin Oncol 2006;24:4581-4586

16. Rasch C, Barillot I, Remeijer P, Touw A, Van Herk M, Lebesque JV. Definition of the prostate in CT and MRI: a multi-observer study. Int J Radiat Oncol Biol Phys 1999;43:57-66.

17. Harisinghani MG, Barentsz J, Hahn PF et al. Noninvasive detection of clinically occult lymph-node metastases in prostate cancer. N Engl J Med. 2003;348:2491-2499

18. Futterer, JJ. Prostate cancer; comparison of local staging accuracy of pelvic phased array coil alone versus integrated endorectal pelvic phased array coils. Radiology (accepted for publication).

19. Chen L, Price RA, Jr., Nguyen TB, Wang L, Li JS, Qin L et al. Dosimetric evaluation of MRI-based treatment planning for prostate cancer. Phys Med Biol 2004;49:5157-70.

20. Lee AK. Radiation therapy combined with hormone therapy for prostate cancer. Semin Radiat Oncol 2006;16:20-8.

21. Chodak GW, Keane T, Klotz L. Critical evaluation of hormonal therapy for carcinoma of the prostate. Urology 2002;60:201-8.

22. Feigenberg SJ, Hanlon AL, Horwitz EM, Uzzo RG, Eisenberg D, Pollack A. Long-term androgen deprivation increases Grade 2 and higher late morbidity in prostate cancer patients treated with three-dimensional conformal radiation therapy. Int J Radiat Oncol Biol Phys 2005;62:397-405.

23. Kupelian PA, Thakkar VV, Khuntia D, Reddy CA, Klein EA, Mahadevan A. Hypofractionated intensity-modulated radiotherapy (70 gy at 2.5 Gy per fraction) for localized prostate cancer: Long-term outcomes. Int J Radiat Oncol Biol Phys 2005;63:1463-8.

24. Speight JL, Roach M, III. Radiotherapy in the management of clinically localized prostate cancer: evolving standards, consensus, controversies and new directions. J Clin Oncol 2005;23:8176-85.

25.Pollack A, Hanlon AL, Horwitz EM, Feigenberg SJ, Konski AA, Movsas B et al. Dosimetry and preliminary acute toxicity in the first 100 men treated for prostate cancer on a randomized hypofractionation dose escalation trial. Int J Radiat Oncol Biol Phys 2006;64:518-26.

SAMENVATTING

Meerdere studies hebben laten zien dat bestraling met hogere dosis voor niet gemetastaseerd prostaatkanker betere resultaten geeft. Hiermee blijft de prostaatkanker merkstof in het bloed, het zogenaamde prostate specific antigen (PSA) langere tijd laag. Of deze langere periode van laag PSA zich vertaalt in een langere prostaatkankeroverleving moet nog blijken omdat deze patiënten nog niet zo lang onder controle zijn en we moeten wachten op de resultaten 10-15 jaar na deze behandeling.

Een hogere dosis op de prostaat geeft ook een hogere dosis op de omgevende organen zoals de blaas, de darm en de anus. Het is gebleken dat de patiënten die met een hogere dosis bestraald zijn ook een grotere kans op complicaties hebben zoals bloedverlies uit de endeldarm en toename van incontinentie voor ontlasting, vaak pas onstaan jaren na de radiotherapie. Onderzoek door de groep van Dr. Van Tol-Geerdink, van onze afdeling, liet zien dat patiënten bevreesd zijn voor deze verhoogde kans op late bijwerkingen. In deze studie hadden ze de keuze voor een lagere of iets hogere bestralingsdosis. De meerderheid koos voor de lagere bestralingsdosis uit vanwege de toename van verwachte late bijwerkingen.

Eén van de uitdagingen voor de toekomst voor bestraling van prostaatkanker om een behandeling te geven met de minste kans op bijwerkingen, maar waarbij wel een goede kans op genezing kan bestaan. Doel van dit proefschrift was om de diverse technische hulpmiddelen te testen, die ervoor zouden zorgen dat de bijwerkingen kunnen worden verminderd.

In **hoofdstuk 2** wordt een nieuwe methode van patiënt positionering op de bestralingstafel beschreven. Een patiënt wordt 25-35 keer bestraald en de bedoeling is dat hij elke dag op dezelfde wijze wordt gepositioneerd aan de hand van de inktlijnen die op zijn huid zijn getekend tijdens de CT scan, als voorbereiding op de behandeling. Tijdens de bestraling kunnen foto's worden gemaakt (de zgn. portal images) waarop de botstructuren van het bekken te zien zijn. Aan de hand van deze botstructuren kan gecontroleerd worden of de patiënt goed gepositioneerd is. Met een zogenaamd off-line portal imaging correctieprotocol kan zo nodig een verschuiving van de bestralingstafel worden uitgevoerd zodat de bestraling nog preciezer kan worden uitgevoerd. Met de zogenaamde digitale tafelhoogte in combinatie met een off-line correctieprotocol was het mogelijk om de patiënten nog nauwkeuriger te positioneren en bleek het aantal correcties per patiënt te worden gereduceerd. Dit resulteerde in een verkleining van de

veiligheidsmarge om de prostaat tot 8 mm in plaats van 1 cm zodat minder darm en blaas bestraald hoefden te worden.

Sinds 2002 worden bij alle patiënten goudmarkers in de prostaat ingebracht. Deze goudstaafjes van 1 bij 7 mm worden door de uroloog via de darm in de prostaat ingebracht. Het voordeel van de goudmarkers is dat ze goed zichtbaar zijn op de portal images. Het blijkt namelijk dat het corrigeren op de bekken-botstructuren geen betrouwbare methode is, omdat de prostaat onder invloed van met name de darmvulling en ademhaling kan verschuiven onafhankelijk van de botstructuren.

In **hoofdstuk 3** wordt de procedure van het inbrengen van de goudmarkers beschreven in 209 patiënten. In slechts 6 % van de gevallen traden geringe bijwerkingen (m.n. pijn en koorts) op als gevolg van de goudmarkerimplantatie. Het inbrengen duurt slechts 10 minuten en patiënten ervaren gemiddeld minder pijn van het inbrengen dan bij het nemen van prostaatbiopten t.b.v. de diagnose prostaatkanker.

In hetzelfde jaar 2002 is begonnen met het testen van de zogenaamde endorectale ballon bij prostaatkankerbestraling. De endorectale ballon bestaat uit een flexibel staafje met aan het uiteinde een ballon dat in de endeldarm ter hoogte van de prostaat wordt opgeblazen tot een volume van 80 of 100 cc. Het voordeel van deze ballon is dat de achterwand van de darm wordt weggeduwd van de prostaat en daarmee kan een deel van het slijmvlies van de endeldarm buiten het bestralingsgebied gehouden worden. Eerdere onderzoeken uit de USA en Oostenrijk hebben laten zien dat het gebruik van een dergelijke ballon leidt tot minder bijwerkingen, met name minder rectaal bloedverlies. Een ander voordeel van deze ballon zou zijn het fixeren van de prostaat tussen de darm en het schaambeen. In **hoofdstuk 4** is getest of de endorectale ballon de prostaat inderdaad kan immobiliseren. Bij twee patiëntengroepen (bestraald met of zonder ballon) is de dagelijkse positievariatie van de prostaat vergeleken aan de hand van de goudmarkers en portal images. Er was geen verschil tussen de beide groepen. Met name de positievariatie richting de endeldarm bleef onveranderd hoog. Ondanks de endorectale ballon bleek er toch lucht en darminhoud naast de ballon te zitten die de verandering van prostaatpositie kon verklaren.

In **hoofdstuk 5** is het nut van een volle blaas tijdens prostaatbestraling onderzocht. Een volle blaas is een voordeel omdat daarmee het grootste deel van de blaaswand buiten het bestralingsgebied ligt en daardoor minder blaasirritatie op kan treden. Over het algemeen worden patiënten geadviseerd om tijdens de dagelijkse bestraling een goed gevulde blaas te hebben door vlak vóór de bestraling nog extra te

drinken. Uit ons onderzoek bleek dat, ondanks deze strikte voorschriften, de variatie in blaasvulling over de bestralingsdagen zeer groot was. Ook het dagelijks meten van de blaasvulling mbv een blaas-echo bleek geen verbetering of vermindering van de blaasvullingsvariatie op te leveren. Verder werd er geen relatie gevonden tussen de mate van blaasvulling en de positie van de prostaat. Sindsdien gebruiken wij de blaas-echo niet meer voor het controleren van de blaasvulling.

Na onze eerste klinische ervaringen met de endorectale ballon, is er een planningsstudie (**hoofdstuk 6**) uitgevoerd waarbij drie verschillende typen endorectale ballonnen werden getest en vergeleken op de mate van rectumwandsparing tijdens hoge doses radiotherapie. Voor zowel de meer conventionele 3-D conformatieradiotherapie als voor de meer geavanceerde intensiteits-gemoduleerde radiotherapie (IMRT) bleek dat de endorectale ballon een duidelijke bescherming zien van het darmwand. De ballonnen met het grootste volume gaven een groter rectumwandsparing. Verder kwam naar voren dat eigenlijk geen van de drie geteste ballonnen patiëntvriendelijk was en is besloten om een eigen endorectale ballon te ontwerpen.

In samenwerking met de afdeling Radiologie van het UMC St Radboud is de rol van de magnetische resonantie afbeelding (MRI) van de prostaat onderzocht. Uit eerder onderzoek bleek dat de MRI een scherpere afbeelding van de prostaat geeft in vergelijking met de CT-scan zoals die wordt gebruikt voor bestralingplanning. Het vaststellen van het bestralingsvolume met behulp van een MRI leidt tot een kleiner bestraald volume omdat de CT het prostaatvolume tot wel 30% kan overschatten. Met behulp van de goudmarkers bleek het mogelijk te zijn om met hoge precisie de MR- en CT-beelden samen te voegen (fuseren) in het radiotherapie planningssysteem.

In **hoofdstuk 7** is een relatief nieuw concept getest voor prostaatkanker bestraling. Met geavanceerde MRI-technieken is het mogelijk om binnenin de prostaat de eigenlijke prostaattumor goed te lokaliseren. Voor een aantal patiënten is een IMRT-bestralingsplan gemaakt waarbij het kankerdeel van de prostaat bestraald wordt tot een extra hoge dosis en de rest van de gezonde prostaat tot een gemiddelde dosis. Uit deze theoretische planningsstudie kwam naar voren dat met deze bestralingstechniek eenzelfde tumorcontrole kon worden bereikt, met een lagere verwachte darmbeschadiging in vergelijking met de standaard bestraling waarbij de hele prostaat een gelijke bestralingsdosis krijgt.

In **hoofdstuk 8** wordt aangetoond dat na 30 maanden bestraling met de endorectale ballon minder darmbijwerkingen geeft. Twee patiënten groepen (met en zonder ballon bestraald) werden vergeleken. Bij al deze patiënten zijn over een periode van twee jaar regelmatig darmonderzoeken (sigmoïdoscopieën) verricht. De patiënten, bestraald met ballon, hadden duidelijk minder darmschade. Uit dit onderzoek komen aanwijzingen dat de endorectale ballon wellicht een extra beschermende werking zou hebben op de darmwand tegen hoge doses bestraling. Oorzaken hiervoor zijn nog niet bekend.

De komende jaren zal ons onderzoek van de prostaatbestraling zich richten op een drietal onderwerpen.

1. Nog verdere verbetering van de procedures om de positie van de prostaat tijdens de bestraling te kunnen controleren en corrigeren. Inmiddels zijn we al gestart met een correctieprotocol waarbij de bestralingslaboranten voorafgaande (zgn on-line) aan de bestraling controleren wat de positie van de prostaat is en waarbij, voordat de echte bestraling gegeven wordt, een correctie van het bestralingsveld kan worden uitgevoerd. De uitkomsten hiervan zijn veelbelovend en inmiddels hebben is de veiligheidsmarge rondom de prostaat richting de darm nog verder verkleind naar 5 mm.

2. De endorectale ballon zal in een grotere groep patiënten worden toegepast. Deze mannen zullen nauwkeurig gevolgd, tot jaren na de bestralingsbehandeling. Ook zullen regelmatig darmonderzoeken worden uitgevoerd om te kijken wat de eventuele schade aan de darmwand zal zijn. We hebben een eigen "Nijmeegse ballon" ontworpen in samenwerking met Hospimed International B.V. te Dalfsen, die nu door ons dagelijks

RectalPro©, www.hospimed.nl
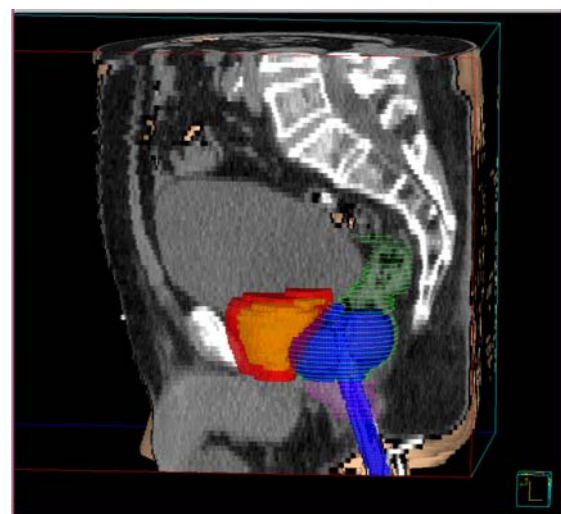
wordt gebruikt. .Inmiddels is ook een onderzoek gestart om te zien of de endorectale ballon ook een mogelijke beschermende werking zou kunnen hebben op het anale

kanaal. Er zijn aanwijzingen dat met de endorectale ballon een lagere bestralingsdosis op de anus en de omringende spieren komt. Hierdoor zou de kans op incontinentie voor ontlasting kunnen afnemen. Dat is dan van voordeel, met name wanneer er in de toekomst met een hogere bestralingsdosis bestraald zal gaan worden.

3. Onlangs heeft een Nederlandse studie laten zien dat een hogere bestralingsdosis een betere kans op tumorcontrole geeft. Inmiddels wordt ook in Nijmegen deze hoge bestralingsdosis gegeven. Tot nu toe wordt de gehele prostaat een hogere bestralingsdosis bestraald. De verwachting is dat we in de nabije toekomst, op basis van de MRI-beelden, het concept van een deelbestraling van de prostaat, met extra hoge dosis, klinisch kunnen gaan testen. Verder zijn er aanwijzingen in de literatuur dat het geven van een extra hoge dosis op de prostaat zou kunnen volstaan en dat hiermee de hormonale behandeling (in combinatie met bestraling) zou kunnen vervallen, voor bepaalde groepen patiënten.

Een verdere nieuwe ontwikkeling binnen de prostaatbestraling is de zogenaamde hypofractionering. Bij prostaatkanker is het mogelijk is om een goede tumorcontrole te krijgen als de bestralingsdosis per dag wordt opgehoogd en waarbij dan in minder behandelingsdagen eenzelfde biologische tumordosis kan worden gegeven. Dit heeft grote voordelen voor de patiënt, die hoeft dan minder bestralingsbehandelingen te ondergaan, en voor de bestralingsafdeling in verband met de bezetting van de bestralingstoestellen en de eventuele wachttijden. De eerste onderzoeken vanuit andere instituten hebben laten zien dat deze aanpak ook goede resultaten geeft met zeer acceptabele bijwerkingen op langere termijn. Inmiddels is in Nijmegen gestart met een dergelijk hypofractioneringsschema in combinatie met de geïmplanteerde goudmarkers en de endorectale ballonnen.

DANKWOORD

Ik ben trots en blij met dit resultaat.

Dit had ik niet durven dromen toen ik 12 jaar geleden in Nijmegen aan de opleiding tot radiotherapeut begon maar het is zover, het "boekje" is geschreven en ligt voor u.

Dit proefschrift is tot stand gekomen door samenwerking met meerdere afdelingen en vele enthousiaste en gedreven collega's en ik wil iedereen bedanken die heeft bijgedragen aan de totstandkoming ervan. Enkelen wil ik in het bijzonder noemen

Zonder de medewerking van mijn patiënten die ik nog regelmatig zie op de polikliniek Radiotherapie, was dit proefschrift er niet geweest. Mijn oprechte dank voor jullie vertrouwen en durf.

Professor dr. J.W.H. Leer, mijn promotor. Beste Jan Willem, jij hebt me aangenomen als staflid in 1998. Ik wil je bedanken voor je vertrouwen en de kans die je me hebt gegeven om de bestraling van prostaatkanker in Nijmegen om te vormen naar zijn huidige vorm, met alle "toeters en ballonnen".

Ook mijn co-promotor dr. A.G. Visser verdient alle lof. Beste Andries, jouw deur stond altijd open en ik kon uitgebreid al mijn plannen met je delen. Je hebt me bijgestuurd waar nodig en zonder jouw inbreng was dit niet mogelijk geweest.

Professor dr. J.A. Witjes, beste Fred. Ik voel me vereerd om samen met jou onze plannen voor de toekomst uit te werken. Al jaren sta je op maandagochtend klaar om de goudmarkers bij onze patiënten in te brengen; dat was de basis van dit proefschrift. Ook de andere leden van de afdeling Urologie wil ik danken voor hun enthousiaste medewerking.

Lisette van der Vight, "onze" research laborante. Jij vormt de rode draad door het hele proefschrift en je bent nauw betrokken geweest bij de totstandkoming en verwezenlijking van alle gepubliceerde onderzoeken. Dank voor je tomeloze inzet en accuratesse. We zullen je missen.

Dr. J.J. Fütterer, beste Jurgen. Vooral door jouw enthousiasme is het gelukt om een solide brug te slaan tussen de afdelingen Radiologie en Radiotherapie. Ook onze samenwerking is nog lang niet voorbij. Onder de bezielende leiding van professor dr. Jelle Barentsz en professor dr. Arend Heerschap is de rol van de MR prostaat imaging voor de prostaatbestraling vastgelegd in mooie publicaties. Mijn dank gaat ook uit naar dr. ir. Henkjan Huisman en drs. Stijn Heijmink.

Dr. D.J. de Jong, beste Dirk. Ook jij bent onbevangen en met groot enthousiasme de samenwerking met onze afdeling aangegaan. De gegevens die we aan het verzamelen

zijn, zijn van grote waarde en een eerste publicatie is een feit. Ik dank ook drs. Mariëlle E.P. Philippens voor haar bijdrage aan deze publicatie.

Drs. M.R. Stam, beste Marcel. Samen hadden we een idee over een blaasvullingsonderzoek. Binnen korte tijd is het je gelukt om er een mooie publicatie van te maken, hiervoor mijn oprechte bewondering.

Drs. J.F. Langenhuijsen, beste Hans. Samen is het ons gelukt om een mooie publicatie over de goudmarkers te schrijven. Dank voor je inzet.

Edwin Nijenhuis en dr. Henk Huizenga. Dank voor jullie belangrijke hulp bij het opzetten van de eerste portal imaging studies.

Peter van Kollenburg, dank voor je enthousiasme, je prachtige ideeën en allermooiste figuren voor dit proefschrift.

Aswin L. Hoffmann, jouw rol in dit alles is groter dan je wellicht vermoedt. Jij hebt me geïnspireerd en aangemoedigd om verder te gaan. Met grote vreugde denk ik terug aan onze "studie-weekenden" in de Eifel. Mijn dank voor al je steun en een luisterend oor.

Professor dr. J.H.A.M. Kaanders, beste Hans. Jij hebt me de eerste stapjes geleerd op het wetenschappelijk gebied. Met groot geduld heb je me, in de vroege ochtenden, begeleid bij de plannen voor een KNO-IMRT studie. Deze is echter niet doorgegaan. Ik dank je voor je hulp bij het schrijven van dit prostaat proefschrift. Dankzij jouw aanvullingen en correcties zijn het mooie artikelen geworden. Dr J. Bussink, beste Jan. Onder het genot van een paar biertjes, met het zweet nog op ons voorhoofd van het sporten, heb ik van jou en Hans veel opgestoken over het werken in een academische omgeving, dank voor jullie lessen en tips.

De overige stafleden van de Radiotherapie, dank dat jullie mij de tijd en ruimte hebben gegeven om ook een deel van dit proefschrift binnen kantooruren te kunnen maken.

Drs T. Rozema, beste Tom. Het laatste jaar van de promotie was het zwaarste en het drukste. Jij hebt mij ontzettend geholpen op velerlei manieren.

Alle medewerkers van de afdeling Radiotherapie die op hun wijze een bijdrage hebben geleverd aan dit proefschrift, bedankt.

Simone Meeuwsen, dank voor je secretariële ondersteuning. We hebben de deadlines gehaald.

Marian Bax, dank voor je geduld bij het ontwerpen van dit digitale proefschrift, het resultaat mag er zijn.

Jeroen Jansen en Mark Glaap, mijn fietsvrienden. Tijdens onze tochten op de mountainbike zijn de mooiste ideeën voor het onderzoek ontstaan.

Mijn ouders, schoonouders, familie en vrienden wil ik danken voor hun steun.

Lieve Ellen, Dirk, Vera en Roos. Ik houd van jullie

CURRICULUM VITAE

Emile van Lin werd geboren op 26 december 1963 te Overasselt. In 1982 behaalde hij het Gymnasium diploma aan het St. Dominicus college te Nijmegen. Aansluitend startte hij met de studie geneeskunde aan de Katholieke Universiteit Nijmegen. In 1989 en 1990 heeft hij als arts-onderzoeker van het levertransplantatieproject op het instituut maatschappelijke gezondheidszorg van de Erasmus Universiteit Rotterdam. In die periode kwam hij in contact met de afdeling Radiotherapie van het Academisch Ziekenhuis te Groningen. Tot 1994 heeft hij daar als arts-assistent niet in opleiding zeer prettig gewerkt. Tot 1 september 1998 volgde hij de opleiding tot radiotherapeut-oncoloog op de afdeling Radiotherapie van het Universitair Medisch Centrum St. Radboud te Nijmegen, toen onder leiding van Prof. dr.W.A. van Daal. Aansluitend is hij door het huidige hoofd Prof. dr. J.W.H. Leer opgenomen in de staf.

Emile van Lin is getrouwd met Ellen van Kuppeveld en ze hebben een zoon (Dirk) en twee dochters (Vera en Roos).

OVERIGE PUBLICATIES

van Lin, E. Het gebruik van een personal computer als enquête-medium bij patiëntenonderzoek. *Tijdschrift Soc Gezondheidszorg 1989;67: 49.*

Arnold W, van Lin E, van de Kerkhof P. Angiosarcoom van het behaarde hoofd en psoriasis capitis: een verraderlijke combinatie. *Ned. Tijdschrift Dermatol Venerol 1996;6:33-34.*

van Lin E, van der Vight L, Huizenga H, Kaanders J and Visser AG. Set-up improvement in head and neck radiotherapy using a 3D off-line EPID-based correction protocol and a customized head and neck support. *Radiother Oncol 2003;68:137-48*

Huisman HJ, Fütterer JJ, van Lin EN, Welmers A, Scheenen TW, van Dalen JA, Visser AG, Witjes JA, Barentsz JO. Precision of integrating functional magnetic resonance in radiotherapy treatment of prostate cancer using fiducial gold markers registration methods. *Radiology 2005;236:311-317.*

van Tol-Geerdink J, Stalmeier P, Pasker-de Jong P, Huizenga H, van Lin E, Schimmel E, van Daal W, Leer J. Systematic review of the effect of radiation dose on tumor control and morbidity in the treatment of prostate cancer by 3D-CRT. *Int J Radiat Oncol Biol Phys 2006;64:534-43.*

van Tol-Geerdink J, Stalmeier P, van Lin E, Schimmel E, Huizenga H, van Daal, Leer J. Do prostate cancer patients want to choose their own treatment? *Int J Radiat Oncol Biol Phys (in press)*

van Tol-Geerdink J, Stalmeier P, van Lin E, Schimmel E, Huizenga H, van Daal, Leer J. Do patients with localized prostate cancer really want more aggressive radiation treatment? *J Clin Oncol 2006;24: 4581-4586.*

Paintings used on cover and CD by: Marian Bax   www.marianbax.nl

Fantasiebloem
100x100 cm

Detail used on cover
Chapter 1

Winterviooltjes
100x100 cm

Chapter 6

Nieuwsgierige
toeschouwers
100x100 cm

Chapter 2

Ridder te paard
60x60 cm

Chapter 7

Stemmingswisselingen
100x100 cm

Chapter 3

Boeket van rijpe
zomervruchten
50x70 cm

Chapter 8

Ontluikend zelfbewustzijn
100x100 cm

Chapter 4

Het oog
100x100 cm

Chapter 9

Als bloemen een verhaal
konden vertellen
90x120 cm

Chapter 5